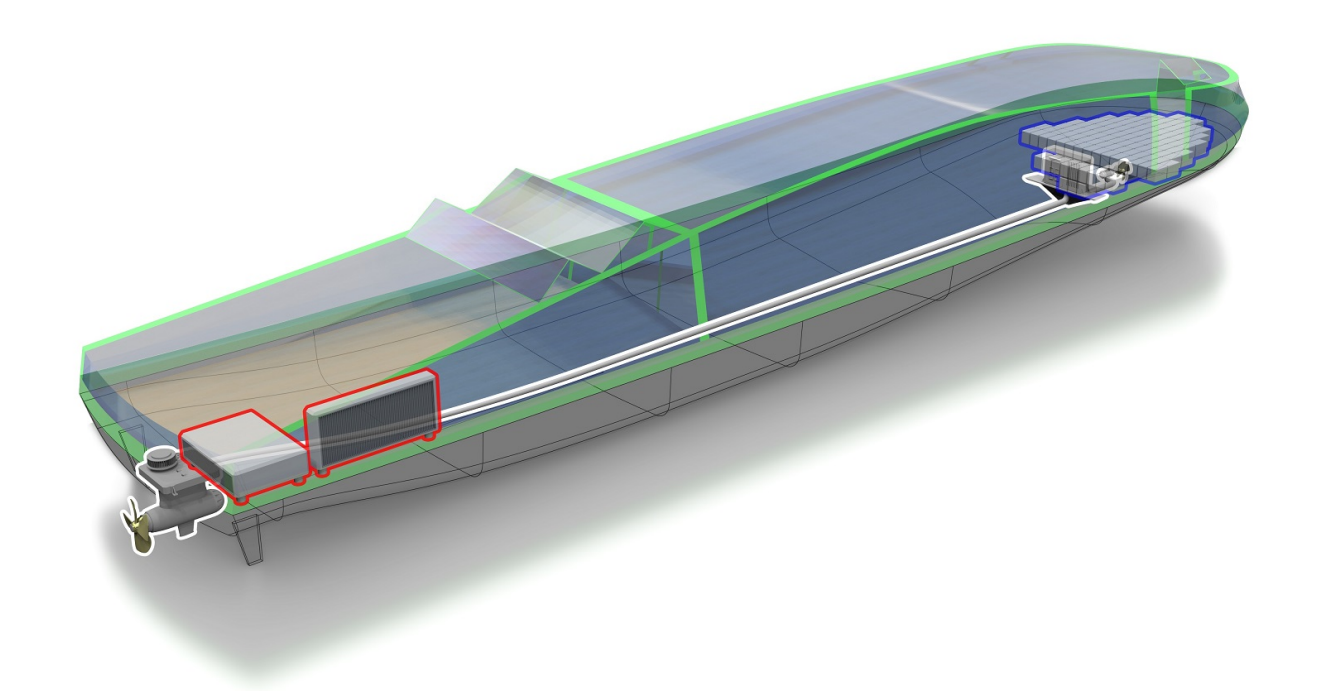
Zero emission concept of a future Amsterdam canal boat

Energy reduction and system integration coupled with an operational profile and environmental comparison method

F.A.G. Jacobs





ZERO EMISSION CONCEPT OF A FUTURE AMSTERDAM CANAL BOAT

ENERGY REDUCTION AND SYSTEM INTEGRATION COUPLED WITH AN OPERATIONAL PROFILE AND ENVIRONMENTAL COMPARISON METHOD

by

F.A.G. Jacobs

in partial fulfilment of the requirements for the degree of

Master of Science

in Mechanical Engineering

Specialization Mechanical Systems and Integration

at the Delft University of Technology, to be defended publicly on Tuesday April 30, 2015 at 10:00 AM.

Document number: SDPO.15.015.m

Student number: 1536540

Thesis committee: Prof. Ir. J.J. Hopman, TU Delft

Ir. K. Visser, TU Delft

Dr. Ir. A. Vrijdag, Damen Shipyards B.V.

Dr. Ir. H.J. de Koning Gans, TU Delft

An electronic version of this thesis is available at http://repository.tudelft.nl/.



ABSTRACT

Due to new regulations starting from 2025 all commercial canal boats have to be zero local emission in Amsterdam. The goals of this MSc. thesis are: 1) To optimize energy consumption in canal boats using zero emission components to reduce polluting emissions in Amsterdam and 2) The creation of a calculation method which can quantify emissions, energy and fuel usage, and can compare the concept(s) with a baseline. The first goal is achieved by creating a model of a full electric Amsterdam canal boat. The model consists of a battery, heat pump, electric motor and ship model, together defining the complete system concept. Analyses have been made with regards to energy consumption, amount of required energy storage, two types of batteries and auxiliary energy usage. These results are projected onto three different full electric concepts: 1) A fixed propeller coupled with a gearbox and bow thruster, 2) Pod propulsion without gearbox with a bow thruster and 3) Same as (2), but with a larger capacity for batteries. These configurations are compared in terms of energy and environmental impact to a typical diesel boat.

Results favour concept 1 in terms of energy efficiency and energy storage size, due to a higher open water efficiency. Total chain efficiency from energy storage to effective energy is, depending on battery type and charge current, as follows: 1) 35-40% 2) 26-30% and 3) 26-29%. Typical diesel boats have a chain efficiency of 17%. Size of battery energy storage is calculated for each concept as 160, 182 and 220 [kWh] respectively when only overnight charging is applied. Values of battery energy storage with intermittent charging after each trip are 65, 72 and 91 [kWh] for a charging power of 1C with an lithium-metal-phosphate battery for concepts 1, 2 and 3 respectively, and 42, 60 and 49 [kWh] for 2C charging with a lithium-titanate battery. Important observations from the simulations include the recommendation to assess the charging strategy carefully as a result from the simulations was that a lower charging current can prolong the battery lifetime and state of charge significantly.

The second goal is achieved by conceiving a calculation method consisting of environmental performance indicators. These indices are able to estimate (non-dimensional) energy, power and emissions, including part load operation and auxiliaries, per 'benefit of society' of different vessel types in a simple and cohesive manner. This is achieved by using several operational modes for the calculation of the indices, contrary to the currently proposed Energy Efficient Design Index which is a point index at 75% of installed power. The conclusion from this environmental comparison is that the full electric concepts do not have local emissions. Global emissions for the concepts depend on the method of power generation and definition of the boundary. An energy efficiency of at least 42% from fossil fuelled land-based power plants to the crossing from quay to boat must be achieved for the electric concepts to be more energy efficient than the diesel reference.

Recommendations include a more thorough hydrodynamic analysis including hull optimization, better estimation of hydrodynamic forces and the modelling of a geared thruster to aid in the manoeuvrability analysis. Recommendations to aid the accuracy of the battery model are given, including the recommendation to obtain more data with respect to lifetime and charging characteristics.

PREFACE

This MSc. thesis is the result of a year-long graduation process carried out at the Technical University of Delft and Damen Shipyards Gorinchem. The topic is the creation of a future concept of an all-electric canal boat in Amsterdam, and the creation of a comparison method to compare emissions and energy consumption between the full electric concepts and a diesel reference boat. I would like to express my thanks to the following persons:

From Damen Shipyards: Wouter Joosten, for helping me, reading the enormous amounts of text I produced and his feedback and enthusiasm during my graduation process. Arthur Vrijdag, for his feedback and interest he showed during the meetings that I attended. Bart Smit, for the artist rendering on the front. Furthermore all the colleagues and other interns and graduation students that made my time at Damen a very pleasant one, and a extensive thank you for Damen Shipyards for having me and providing all the necessary resources to complete this project successfully.

From the TU Delft: Klaas Visser, for his guidance, networking skills in the Boeggolf project and transparent supervision during this project. Hans Hopman, for his supervision and useful feedback during this thesis, and for being my MSc. professor.

From Boeggolf: Each member from Boeggolf, but especially Pim van Mensch and Ruud Verbeek, for the nice discussions we had about batteries and the operational profile of the canal boats.

From BlueBoat company: A huge thanks to Vincent Geljon and Ramon van der Storm, without their help the measurements would not have taken place. Furthermore, their encouragement and kindness during my visits were admirable. I hope this thesis will help your business go forward in the future.

Furthermore I would like to thank Henk Jan Bosman, for the long discussions about difficulties in both our theses and useful sparring sessions. My parents and family, for always believing and supporting me. My friends, for lending an ear or a beer when required and last but certainly not least my girlfriend, for putting up with me during this time and helping and encouraging me when I needed it.

F.A.G. Jacobs Delft, April 24, 2015

"There are three important points in matching a propeller, ship and engine. Operational profile, operational profile and operational profile."
— Peter de Vos

CONTENTS

1	Introduction	1
	1.1Motivation	3
	1.2Methodology	5
	1.3Background	9
2	Baseline and concepts	11
	2.1Baseline	13
	2.2Measurements	15
	2.3Concept approach	23
	2.4Concept overview	31
3	Modelling	35
	3.1 Resistance modelling	37
	3.2Ship and system modelling	45
	3.3Auxiliary modelling	51
	3.4Battery modelling	59
	3.5Environmental Performance Indicator method	81
4	Simulations and results	89
	4.1 Simulation methodology	91
	4.2Verification simulation results	97
	4.3Simulation results	101
	4.4Application of results	117
5	Conclusions and recommendations	123
	5.1Discussion	125
	5.2Conclusions	129
6	Appendices	137
	A Example energy conversions	139
	B Flywheel and super capacitor	141
	C Motor efficiency plot	143
	D Openprop propeller calculation	145
	E Alternative propulsion multiple criteria analysis	147
	F Water temperature 1990-2010	149
	G Propeller optimization	151

Н	ECI calculation results for concepts	161
I	Sailing hours per day	163
J	Battery parameters for temperature fit	165
K	Lifetime calculation	167
L	Static energy and power calculation	169
M	Glossary	173
Bi	bliography	179
List of Figures		185
Li	st of Tables	189

1

INTRODUCTION

This chapter starts with a short thesis statement explaining the purpose of this thesis. This is followed by an introduction detailing the scientific and social relevance. The methodology is presented, including two main research goals. The research goals are succeeded by main research questions that lead to two main hypotheses. The scope boundaries are established after which the outline and structure of the thesis is explained

1.1

MOTIVATION

1.1.1. SHORT THESIS STATEMENT

The Technical University of Delft is, together with Damen Shipyards, the Netherlands Organization for Applied Scientific Research (TNO) and Waternet, engaged in project Boeggolf. Project Boeggolf aims to develop zero emission (ZE) Waternet boats and ZE commercial canal boats for use in the Amsterdam canals. The project focuses on new technologies and optimization of energy and power consumption. Rules and regulations regarding water, canals and water in and around Amsterdam are made by Waternet, which is operating on behalf of the municipality of Amsterdam. The requirement for these ZE vessels follows from rules and regulations, as from 2025 onward Waternet has conceived ZE regulations for the complete commercial Amsterdam canal boat industry, see Table 1.1.1. Ship owners can aim for two objectives before 2025, either objective 2015 or objective 2020, where objective 2020 gives previously clean vessels an advantage. After 2025 the boats have to be fully ZE, and the problem is that the emissions of the current canal boats are too high by the regulations set in this statutory definition. Therefore alternative solutions need to be found. The goals of this thesis are therefore: 1) To optimize energy consumption in canal boats using zero emission components to reduce polluting emissions in Amsterdam and 2) The creation of a calculation method which can quantify emissions, energy and fuel usage, and can compare the concept(s) with a baseline.

Table 1.1.1: Emission regulations according to Waternet [1]

Segment	Objective 2015	Objective 2020	Objective 2025
Vessels up to	Either: Meet Phase IIIB re-	Or: Weighing on emissions	ZE^2
20 meters	quirements before 1 Jan-	in 2020, large benefits for	
	uary 2015. New built ships:	clean vessels	
	minimum of Phase ${ m IIIB}^1$		

1.1.2. MOTIVATION AND TARGET OF THE WORK

The design of future ZE canal boat concept(s) is socially and academically relevant. The social relevance follows from the ever increasing awareness of reducing fossil fuel usage and emissions, partially accelerated by the nowadays common available electric or plug-in hybrid cars. The maritime industry always seems to be ten to fifteen years behind the automotive market, and it can be seen that full electric alternatives are now beginning to emerge for ships. As there is little experience in the design of small passenger boats like the canal boats in this thesis, the academically relevant part is also included. This is signified in a thorough analysis and optimization of the required power, energy and propulsion train. Modelling of the complete drive train, including heating facilities, energy storage and propulsion, based on a realistic operational profile is carried out. Furthermore this text includes an analysis and a comparison of the current diesel situation regarding canal boats with a possible future situation. This way, main obstacles (like the amount of energy storage and required power for propulsion and auxiliary load) in the transition to ZE canal boats can be tackled.

 $^{^1}$ Phase IIIB: maximum of 3.3 [g/kWh] NO_x, 0.19 [g/kWh] non-methane hydrocarbons (NMHC), 0.025 [g/kWh] particulate matter (PM) 2 as well as 'zero noise', but this is not analysed in this thesis

CHAPTER 1.1. MOTIVATION

Additionally, a calculation method needs to be constructed which can be used to rank ships on environmental emissions and energy usage. This is useful for the inland shipping (passenger) industry, as it can be quickly seen what the environmental footprint of certain vessels will be.

In order to achieve the aforementioned goals, information must be gathered. To obtain crucial (validation) information such as power, energy and resistance of the canal boats, measurements should be carried out on a typical diesel canal boat if this data is not available. Furthermore, in cooperation with BlueBoat company and TNO, measurements should be conducted on the Barlaeus, a lead-acid powered hybrid³ canal boat. The advantage of this measurement is the opportunity to have a reference with respect to electric propulsion in the Amsterdam canals. To achieve these goals, the following information and tools are required:

- Information to give insight in the Amsterdam canal boats, by conducting measurements on the boats. The data obtained from these measurements will be used to optimize the propulsion system.
- A tool to optimize and minimize required energy storage on board to be able to deploy the most energy efficient concept(s).
- The creation of a tool to analyse operational profiles. This tool will be used to simplify the operational profile and make it possible to construct different trips. For these trips the tool can be used to estimate power and energy requirements, as well as the efficiencies of the electric system.
- The creation of a model of the ZE propulsion system containing motor, energy storage and heating.
- To present a tool or framework that can be used to rank different types of (canal) boats based on environmental indices.
- To provide recommendations regarding the transition to ZE sailing in 2025 for the Amsterdam situation.
- To provide recommendations regarding energy storage and propulsion systems on canal boats.

1.1.3. SCIENTIFIC CONTRIBUTIONS

This thesis aims to offer a scientific as well as a practical background that will help the transition to the ZE future. The scientific contributions are, in global order of appearance in this text:

- · Results of measurements of canal boats.
- An analytical model to analyse energy usage for a given operational profile of a canal boat, taking into account auxiliary loads and environmental indices.
- A comparative study on battery energy storage options for the Amsterdam canal situation.
- A model of a heat pump based on thermodynamic principles.
- Analytical models of lithium-ion batteries and an electric motor.
- · Results of simulations of canal boat concepts.
- A comparative lifetime and cost assessment of chosen energy storage options.
- A future proof and optimized ZE concept.
- Verification and validation of used models wherever possible.

³It is an electric boat with a range extender (diesel generator charging the batteries), for simplicity called hybrid boat throughout this text

1.2

METHODOLOGY

As stated in Chapter 1.1.1, 'Short thesis statement', two main goals are distinguished. Because these two main goals differ significantly, there are two different main hypotheses established. The first main goal is about the detailed conceptual design of the future canal boat. The second main goal is about a generic environmental comparison calculation method that will be applied to the concepts and baseline. To keep these two very different goals separated, there are two main research questions derived. The main goal, along with the main hypothesis and research questions will be presented for each goal.

1.2.1. ZERO EMISSION CONCEPT

The first main goal states the zero emission concept:

To optimize energy consumption in canal boats using zero emission components (G.1)

For this main goal a corresponding main research question is formulated:

How can energy consumption in canal boats be optimized using zero emission components? (Q.1)

By answering this main research question, the methodology to obtain energy efficient zero emission concepts will be explained in a structured way. For each main question the hypothesis, together with the reasoning behind it, is given:

A zero emission energy efficient canal boat concept can be designed by using an integrated model of onboard energy consumers by using an operational profile (H.1)

Design of ships is often carried out by using models to predict certain characteristics of the specified boat. By modelling the important consumers and systems on board of the canal boat, a clear and complete picture arises about the requirements in terms of energy and power. Coupling these requirements to a model that simulates a typical sailing day will give a tailored solution in terms of energy requirements. Based on these model results, the most energy efficient concept can be chosen.

1.2.1.1. DEFINITION, RESEARCH QUESTIONS

The research questions for the first main goal are divided in three main sections: Definition, concept and model.

With the definition section, the problem is defined and outlined. The scope will be defined and current information about canal boats is distilled into workable knowledge. Missing information is identified and options are given to fill these knowledge gaps. With the collection and analysis of all available data, including added data from the knowledge gaps, a typical boat is constructed which will serve as a baseline throughout this text. This is done by answering three research questions:

What parameters determine energy consumption?	(Q.1.1)
What is known about the canal boat systems in Amsterdam?	(Q.1.2)
How can the baseline be set?	(Q.1.3)
What are possible improvement points of the baseline, in terms of energy and power usage?	(Q.1.4)

1.2.1.2. CONCEPT, RESEARCH QUESTIONS

With the concept section the baseline is extended into the concept design phase. The scope of the concepts is given along with the focus and goal of each concept. Options are discussed, dismissed or accepted. Finally, the concepts are presented. This is done by answering three research questions:

What are the considerations, requirements and limitations of the concepts?	(Q.1.5)
--	---------

What are the most viable concept options?

(Q.1.6)

(0.1.7)

(Q.1.12)

1.2.1.3. MODEL, RESEARCH QUESTIONS

How can the concepts be modelled?

With the model section, the concepts are extended into the modelling phase. Models are presented, built and integrated. When the models are completed, they are simulated according to the simulation methodology. This is done by answering the following research questions:

	(2.11)
How should components be connected to each other?	(Q.1.8)
What is the simulation strategy?	(Q.1.9)
There are two smaller sub-questions defined with respect to the simulation strategy:	
How can the energy storage system be kept in a safe operating condition?	(Q.1.9.1)
Is charging with intervals possible?	(Q.1.9.2)
Are the obtained model results realistic and do they agree with the baseline?	(Q.1.10)
What are the lifetime and costs of the energy storage?	(Q.1.11)

1.2.2. Environmental comparison method

What infrastructure is necessary to make zero emission possible?

The second main goal is:

The creation of a calculation method which can quantify emissions, energy and fuel usage and can compare the concept(s) with a baseline. (G.2)

For this main goal a corresponding main research question is formulated:

How can a fair comparison be made between the baseline and zero emission concepts? (Q.2)

When answering this question, the methodology behind the comparison method is given, which allows a clear comparison including limitations of the methodology.

A fair energy and emission comparison between the baseline and zero emission concepts can be conducted by conceiving an 'Environmental Performance Indicator' methodology (H.2)

By using energy and emission indices to calculate the emissions and energy usage the hypothesis is that a fair comparison can be conceived between the baseline and the concepts. 'Fair' is defined here as an equal starting point for the comparison, where special care has to be taken with regards to the index boundary where the indices are defined.

Apart from the secondary main research question Q.2 there are other research questions that need to be answered in order to complete the goal set by G.2. With respect to the Environmental Performance Indicator (EPI) calculation method the following research questions are created:

1.2.2.1. Environmental comparison research questions

What are existing methods to rate ships?	(Q.2.1)
How can current rating methods be used to evaluate canal boats?	(Q.2.2)
How can diesel propulsion be compared with electric propulsion?	(Q.2.3)

1.2.3. Scope boundaries 7

1.2.3. SCOPE BOUNDARIES

The items in this thesis that are briefly analysed are listed. Some of these points were analysed in cooperation with one of the Boeggolf partners.

- Artist impression of the proposed ZE canal boat. This is designed in cooperation with Damen.
- Extensive business/cost analysis of the ZE canal boat. Cost analysis is conducted for energy storage only.
- A basic performance optimization for propellers and turning characteristics, keeping in mind practical constraints. Propeller diameter is assumed fixed at 0.65 [m].

The items that this thesis will not incorporate are:

- Advanced hydrodynamics, such as hull shape optimization (Hydrodynamic, fouling, ageing) and cavitation. The hull dimensions are strictly bound [1] and will not be analysed.
- Analysis of non-zero emission alternatives such as Liquid Natural Gas (LNG) or Diesel-Electric (DE) propulsion systems. This is because the boats have to be *fully* ZE after 2025.
- Alternating current (AC) to direct current (DC) conversion, switchboard and gearbox efficiencies are not taken into account (see section 2.3.2.4)
- Detailed onshore efficiency and emission calculations and analysis of emissions of power plants (No complete life cycle emission analysis).
- There is also a demand for 'zero noise'. This is not further specified by Waternet. After consultation, the explanation of zero noise by Waternet is given as 'whisper quiet' and 'should not approach the noise level of a diesel boat'. It is assumed that the concepts will adhere to this noise regulation automatically, as electric propulsion is usually more quiet than diesel propulsion. Therefore noise is neglected.

1.2.4. THESIS OUTLINE

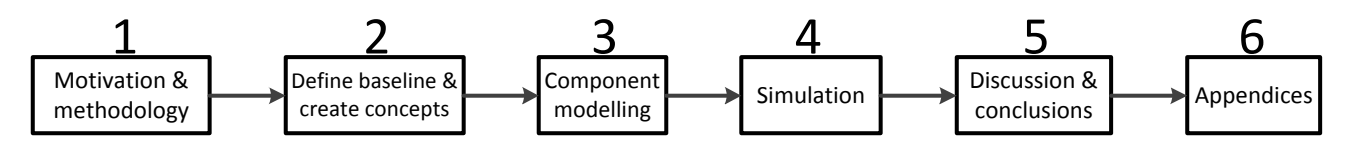


Figure 1.2.1: Thesis chapters overview

The structure and order of the six chapters will be explained here:

- 1. In the first chapter the motivation for this text was given, along with the methodology and a short introduction about canal boats and the canal boat industry. Also an outline of the thesis was given.
- 2. This chapter starts with an assessment of known and missing data and the description of typical canal boats in Chapter 2.1, 'Baseline'. With the required information known, measurements were conducted that are explained in Chapter 2.2, 'Measurements. This chapter is followed by Chapter 2.3, 'Concept approach' where the requirements for the concepts are stated, and Chapter 2.4, 'Concept overview', where the detailed concepts are developed.
- 3. With the concepts known, the resistance and power requirements for the baseline hull types is calculated in Chapter 3.1, 'Resistance modelling'. Modelling and coupling of the ship, electric motor and propeller is detailed in Chapter 3.2, 'Ship and system modelling'. Detailed auxiliary modelling succeeds the ship modelling chapter in Chapter 3.3, 'Auxiliary modelling', followed by the battery modelling in Chapter 3.4, 'Battery modelling'. When this is completed the calculation method for the environmental and emission comparison is presented in Chapter 3.5, 'Environmental Performance Indicator method'. At this point, all required models and theory is known to start simulations.
- 4. The simulations part of this thesis starts with Chapter 4.1, 'Simulation methodology', followed by a comparison simulation that gives insight in the power at different speeds of the concepts, as well as electric motor efficiency and open water efficiency during different speeds of the canal boats. This simulation is used as a verification and is detailed in Chapter 4.2, 'Verification simulation results'. A complete simulation during a typical sailing day is carried out in Chapter 4.3, 'Simulation results' which

- results in information about daily energy usage, energy storage size, efficiencies, charge strategy and the environmental comparison. These results are applied and quantified in the form of a practical analysis of the simulation results in Chapter 4.4, 'Application of results'.
- 5. In Chapter 5.1, 'Discussion' the improvement points, recommendations and remarks are given. This chapter poses as a feedback chapter. The conclusions are presented in Chapter 5.2, 'Conclusions', summarizing all results and findings and answering the research questions and hypotheses.
- 6. The last part of this thesis consists of an addendum including appendices (A to M), including a glossary. This is followed by the bibliography and lists of figures and tables.

1.3

BACKGROUND

What do Winston Churchill (Figure 1.3.2(b)), the Beatles and Nelson Mandela have in common? They have all been on a canal cruise through the Amsterdam canals. The very first canal boat tour in Amsterdam took place in 1621, for Queen Elisabeth Stuart of Bohemen, see Figure 1.3.2(a). Since then, it became a tradition to treat important guests to a canal boat tour [2].



Figure 1.3.1: Aerial photograph of the Amsterdam canals (Roger Wollstadt, public license)

Nowadays, the Amsterdam canals are widely known throughout the world. The city is known as the "Venice of the North" [3, 4]. The 17^{th} -century centre ring is on the United Nations Educational, Scientific and Cultural Organization (UNESCO) World Heritage List [5]. It is therefore no wonder that there is a lively industry built around these canals. Apart from 2 million tons of cargo transported each year and 2 500 house-boats, more than 3 million passengers are transported each year by official canal boats [6, 7]. This makes a tour of the canals in a canal boat the most popular tourist attraction in Amsterdam, with more than twice the amount of people than the runner-up (The Van Gogh Museum, with 1.4 million visitors) [6, 8]. 35% of all foreign tourists went on a canal boat tour while they were on vacation in the Netherlands [9]. It is clear that the canal boat tours form a significant part of the tourist industry in Amsterdam and in the Netherlands.

1.3.1. ELECTRIC VESSELS

There are already many full electric vessels built in the world. Most of these are electric ferries, operating in the Nordic countries. However, there is not a lot of scientific data known about these ships, as most studies aim to develop detailed first principle models of the ship network and components, instead of focussing on the design and concept phases, as this study aims to do.

1.3.2. CURRENT INDUSTRY SIZE

Due to the enormous popularity of the canal boat tours, a lot of business owners started canal boat tour companies. This has led to a total of around 330 operating permits to exploit this tourist attraction in 2012 [6, 10]. These permits vary from pedal boats for two persons to vessels of more than 20 meters that can transport 140 people [11]. The industry is responsible for the employment of around 1 000 Full-time Equivalent (FTE) employees [12]. To ensure successful and safe exploitation of the canals, the Amsterdam municipality is engaged



(a) A drawing of the first canal boat tour in 1621 (Amsterdam.info)



(b) Winston Churchill enjoying his Amsterdam canal tour, 1946 (Geheugenvannederland.nl)

Figure 1.3.2: Historical canal boat trips

in setting up regulations, legislation and rules regarding the canals. This is done through Waternet. Waternet maintains the waterways, enforces regulations, cleans waste water, operates water facilities and purifies and supplies water in the Amsterdam region [6, 13].



Figure 1.3.3: Typical canal boat (Tripadvisor.com)

1.3.2.1. DEFINITION OF A CANAL BOAT

As the size of the industry is now known, a canal boat will be defined. First of all, a canal boat is also called a sightseeing boat, tourist boat, tour boat or cruise boat. For the sake of clarity, in this report the name "canal boat" will be maintained. There are numerous definitions of a canal boat. Four are given below [14]:

- Aquo-lex dictionary: Boat which is used to sail past sights and thereafter returns to the starting point.
- General Dutch dictionary: Boat which is used for a tour through a city or a different limited area, mainly for tourists
- Inland shipping dictionary (1): Vessel destined or used for short tours with passengers.
- Inland shipping dictionary (2): Motorized vessel with low creep height and an almost full glass structure on a low, broad hull with a plane mirror.

For this thesis, a combination of the definitions is used:

A canal boat is a boat that sails through a limited area such as a city or certain canals. This is done on the basis of a business model, which can include the transportation of tourists along (1.3.1)sights, among other activities. It has a low creep height and an almost full glass structure on a low, broad hull.

Canal boats are also used for parties, anniversaries, dinners or even as taxis; the usage is not only limited to sightseeing tours [15]. In this thesis, only canal boats that can carry 80 persons or more are considered.

2

BASELINE AND CONCEPTS

This chapter starts with the known information about the Amsterdam canal boat industry. This information lacks energy and power data and is therefore not enough to design concepts, so measurements are described in the following chapter. An outline of the trips where measurements were conducted on both a diesel as well as a hybrid boat is followed by a discrete operational profile and the accompanying speed blocks which help to create a generic operational profile. With the operational requirements known in the form of the operational profile the concept approach is explained, defining global design requirements. With the requirements known, the detailed methodology to choose the concepts is analysed, finally arriving at the defined concepts in the concept overview chapter.

2.1

BASELINE

In this chapter the baseline will be constructed from known information and measurements on canal boats. Information will be given with respect to industry requirements and scope of this thesis. This chapter is used as a summary of background and measurement data, and starts with the answer to research question Q.1.1:

What parameters determine energy consumption?

(Ref. Q.1.1)

Energy consumption on ships can be broken down in six main groups:

- Power train configuration
- Heating and auxiliary requirements
- · Percentage of cargo load
- Hull shape and ship resistance
- Weather and current influences
- · Captain influence

In this thesis the focus is on the first two points: Power train configuration, heating and auxiliary requirements. The hull shape is not taken into account. Ship resistance is required to calculate power requirements, but no analysis of fouling of the hull or hull improvements has been carried out. This thesis focusses on the systems on-board the ship. The influences from the captain, weather and current are neglected. Influences of different cargo loads are not taken into account. Throughout this text (except for the measurements) a fully loaded boat is assumed. This thesis tries to reduce energy consumption by altering the configurations. There are dozens of configurations possible. Some are analysed, but with the restraint that the results and modelling must be able to be verified and validated where possible, the configurations will be based as much as possible on the current boats in Amsterdam. In order to know the power consumers and system lay-out, a study into the systems on-board of the canal boats is conducted in Jacobs [16]. From this report, the following information is extracted:

14 Chapter 2.1. Baseline

2.1.1. KNOWN INFORMATION

What is known about the canal boat systems in Amsterdam?

(Ref. Q.1.2)

The fleet of interest is defined as canal boats with a capacity of \ge 80 persons or more. This fleet in Amsterdam consists of \pm 70 boats. Average installed engine power is 91 [kW] and average length of the vessels is about 20 [m]. The auxiliary power requirements are for marine systems about 600 [W] and the diesel heaters used in canal boats have a typical power range of around 20 [kW] and an efficiency of 90% [16, 17]. A linesplan of a harbour canal boat is given in Figure 2.1.1. Up to 10 hours of sailing per boat per day is possible during peak

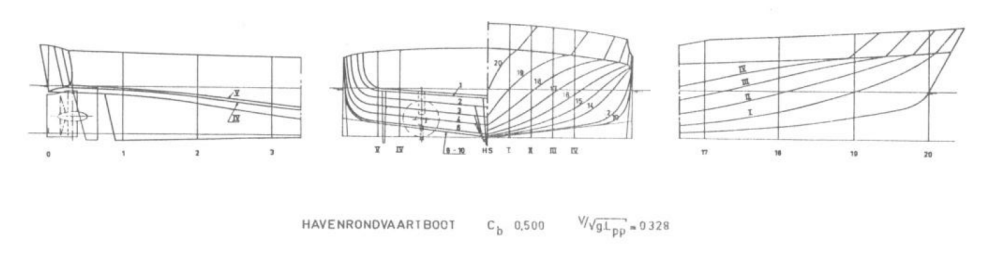


Figure 2.1.1: Linesplan of a harbour tourist boat

days. Typical hours of sailing are in the range of 6 to 8 hours per boat per day. With respect to hydromechanics no information could be obtained. Because this information is not known, measurements are conducted to be able to set the baseline with respect to power, energy and operational profile.

MEASUREMENTS

How can the baseline be set?

(Ref. Q.1.3)

The baseline will be set by conducting measurements on two types of canal boats. The reason to conduct measurements is to be able to give a baseline with power and energy requirements, as this information is so far not known.

2.2.1. MEASURED BOATS

Two different types of canal boats are measured. One is a diesel/hydraulic boat with an fixed propeller (FP), powered by a diesel engine, the other an electric boat powered by a pod. Starting with the FP boat:

2.2.1.1. FIXED PROPELLER BOAT

A fixed propeller boat has an rigid shaft attached to the prime mover, in this case a diesel/hydraulic system. A schematic view of a FP is given in figure 2.2.1. Manoeuvring is done by giving pressure on the rudder, creating a force. See Figure 2.2.2 for the Energy Flow Diagram (EFD). The used abbreviations are:

- ES energy storage
- · M mechanical link
- H hydraulic link
- M propulsion method (fixed pitch propeller)
- E electric link or consumer

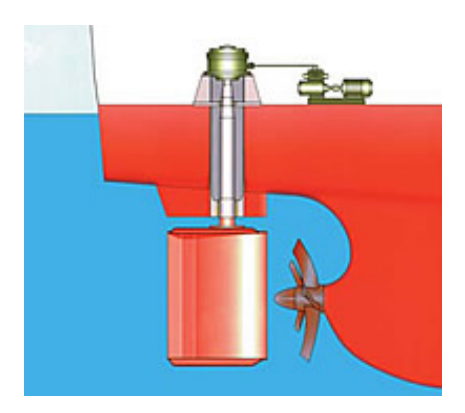


Figure 2.2.1: Fixed propeller, schematic view

2.2.1.2. POD BOAT

The second measured boat is an electric boat. This boat is powered by a pod drive. The pod drive is shown in Figure 2.2.3. This pod can turn and therefore a rudder is not needed. This improves manoeuvrability, as

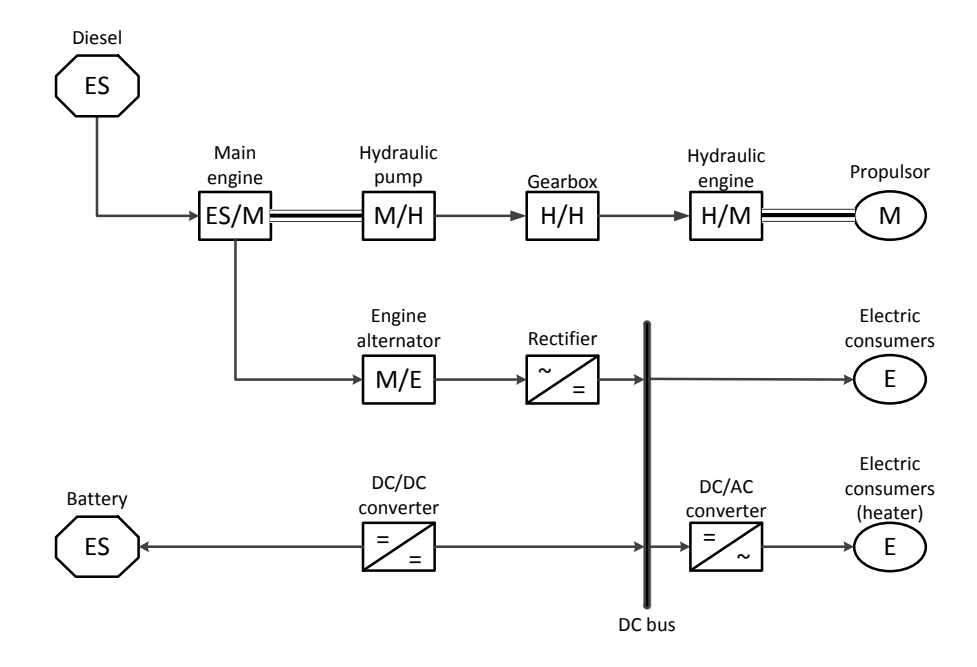


Figure 2.2.2: Energy Flow Diagram of the measured diesel hydraulic vessel

there is no pressure against a rudder required to manoeuvre. The boat that was measured has a keel with 250 [kWh] lead-acid batteries stored. These batteries weigh about 7.5 [t], and still extra ballast is required to be able to sail under the low bridges in Amsterdam. The boat is also equipped with a 8 [kW] bow thruster, BT in Figure 2.2.4. Key specifications of these boats are given in Table 2.2.1.



Figure 2.2.3: Pod with four blade propeller under a canal boat $\,$

Table 2.2.1: Main specifications of the measured boats

	Main propulsion power [kW]	Auxiliary power [-]	Top speed [m/s]	Passenger capacity [-]
Fp	80	20 kW heater	3.6	100
Pod	55	20 kW heater	3.3	100

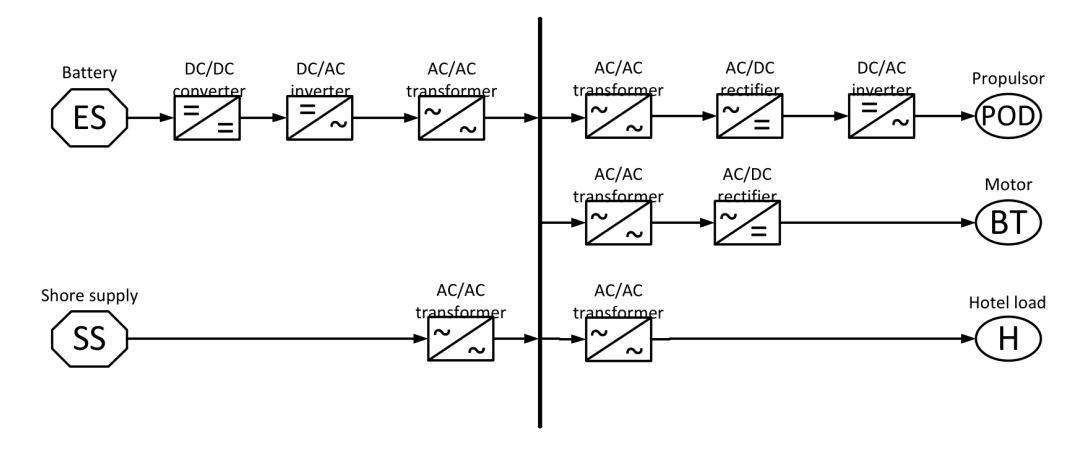


Figure 2.2.4: Energy Flow Diagram of the measured pod/hybrid vessel

2.2.2. REQUIREMENTS

Measurements have taken place in cooperation with BlueBoat company, a canal boat operator with a fleet of fifteen large canal boats. Requirements from these measurements are:

- Speed
- Rpm
- Power
- Energy
- Trip of the vessel

Because the trips of the vessels can change per trip, first the route must be chosen. As the boats are committed by BlueBoat, their standard route is chosen. The standard route as sailed by BlueBoat company is depicted in Figure 2.2.5 with a blue line. The standard route takes about 75 [min] depending on traffic on the water, detours and weather. After these 75 [min] the boats are moored for 15 [min] to unload and load passengers.

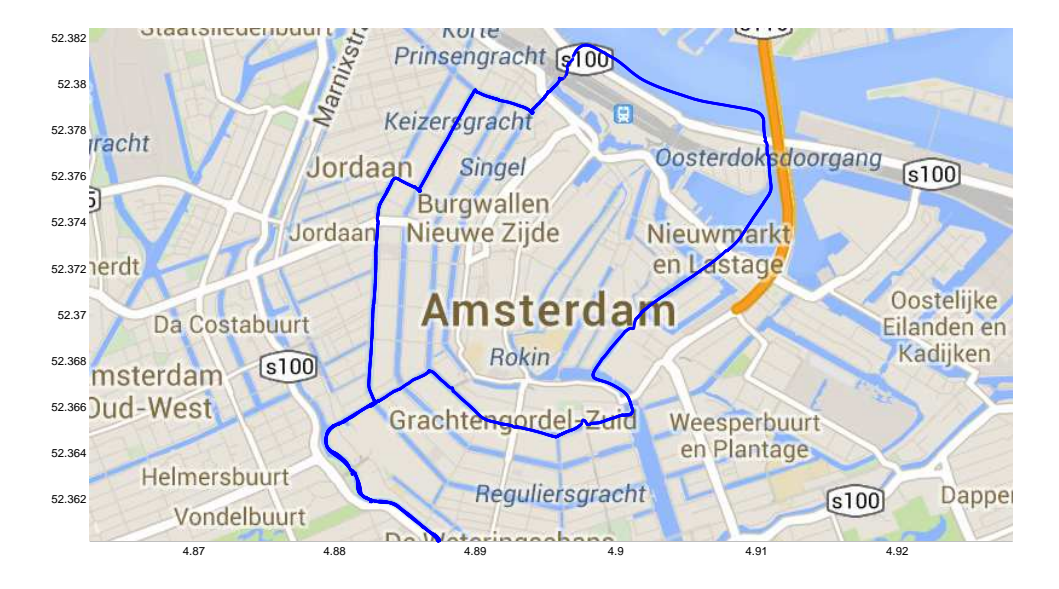


Figure 2.2.5: Standard sailing route

2.2.2.1. APPROACH

For the diesel boat the torque of the propeller shaft is measured with the use of strain gauges. This torque, together with the revolutions per minute (RPM), gives the power, see Equation 2.2.1 [18]. The RPM of the diesel engine and propeller shaft is measured with a digital stroboscope. By sailing the trips with a Global Positioning System (GPS), speed of the vessel is known. From this data all requirements can be concluded. Using time and power the energy can be calculated, Equation 2.2.2. Details about the diesel measurements can be found in Jacobs, [16].

$$P = 2\pi \cdot Q \cdot n \tag{2.2.1}$$

Where Q is torque, n is the propeller shaft RPM and P is the power.

$$E = P \cdot t \tag{2.2.2}$$

Where t is time and E is energy.

The hybrid boat is more difficult to measure, as it has a pod drive with the electric motor in the housing, under the water line. Therefore the voltage and currents at the battery output are measured. Removing all auxiliaries will therefore give the propulsion power and energy, keeping in mind motor and conversion efficiencies. The RPM is read from the electronic display, and again a GPS is used to obtain speed data. The measurements were carried out by sailing two different scenarios with both boats. The first scenario consisted of 'mini-trials', conducting run-up, top speed, turning and crash stop tests. The second scenario consisted of typical trips through the canals.

2.2.2. RESULTS

Average values for the standard route are a distance of about 7.5 [km] and an average speed of ± 2 [m/s]. The measurement results are divided into discrete blocks which specify different operational modes. In Table 2.2.2 the power required for these blocks is displayed. The powers are averaged over the blocks at the drive shaft. For the hybrid pod boat an efficiency of converters and electric motors of 0.9 is assumed in Table 2.2.2. The total energy for one trip is given as well in this table.

Block [-]	Fp [kW]	Pod [kW]
Moored	0.0	0.0
Manoeuvres	13.1	12.8
Nominal speed	6.0	10.7
Min attainable speed	13.6	14.4
Maximum speed	44.0	30.6^{1}
90° turns	18.0	16.2
Block	Fp	Pod
[-]	[kWh]	[kWh]
Total energy per trip	14.5	16.1

Table 2.2.2: Measured average brake power requirements per block

What are possible improvement points of the baseline, in terms of energy and power usage? (ref. Q.1.4)

From Figure 2.2.7 it can be seen that manoeuvring and 90° turns are using about 60% of the energy during a trip, whilst only 40% of the time the boat is manoeuvring or turning. This means that there is a lot of energy lost which is explained by the fact that maximum power against the rudder is required to obtain sufficient pressure to turn in a short distance. The downside is that this pressure against the rudder will result in movement forward, hence the thrust will be reversed and maximum power will be directed backwards [11]. This is the most common way to get through the narrow corners. Turning as described here will be analysed to see if energy and power consumption can be lowered. Furthermore the highest amount of power measured at the

 $^{^1}$ This is probably a measurement error and should be higher, as this was higher (± 40 -45 [kW] during the top speed test during trials

2.2.2. REQUIREMENTS 19

TIME PROFILE

DISTANCE DISTRIBUTION

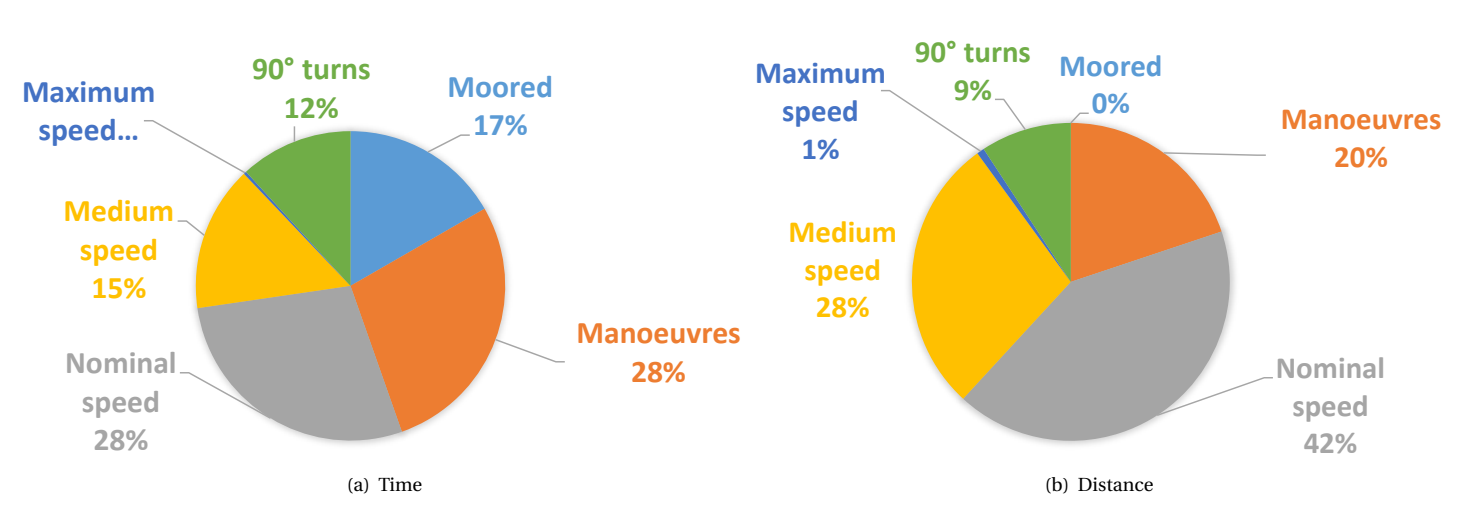
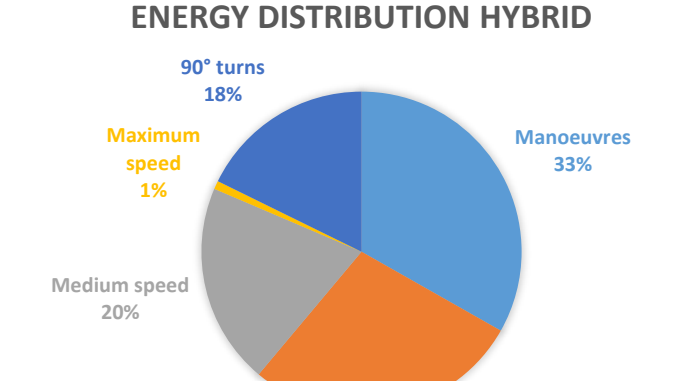


Figure 2.2.6: Discrete time and distance distributions



(a) Measured hybrid

Nominal speed

28%

ENERGY DISTRIBUTION DIESEL

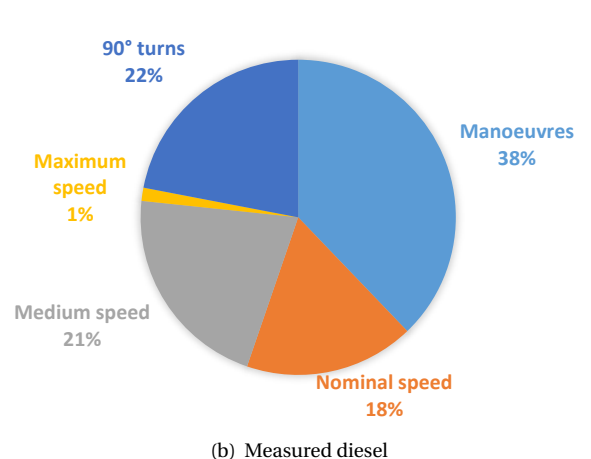


Figure 2.2.7: Energy distributions

propulsion shaft was 51 [kW] when the diesel was running at maximum power (80 [kW]). This gives rise to the idea that the propeller is not operating optimally. This must be further analysed.

2.2.3. CONCLUSIONS

It is clear that the hybrid boat is less economical with respect to energy. Only during manoeuvres and the 90° turns energy usage is around that of the diesel boat. The reason for this is probably because there is a keel welded underneath the hybrid boat that is used as battery storage room. This keel is adding resistance, hence requiring larger powers to obtain the required speed. During manoeuvring the added versatility of the pod motor gives it an advantage. As can be seen the manoeuvres require about 13 [kW] for both vessels, and the 90° turns require more than 16 [kW]. Analysis of these results indicates that speed during these manoeuvres is very low (in the range of 1 [m/s]). Possible optimizations might be carried out in the propeller and in the manoeuvring of the ships, as lowering these powers will decrease energy usage drastically.

2.2.3. DISCRETE TRIPS

As there are many more possibilities in trips in the Amsterdam canals, the measurement results from the standard BlueBoat route are divided into discrete blocks, from which every trip can be constructed, see Figure 2.2.8:

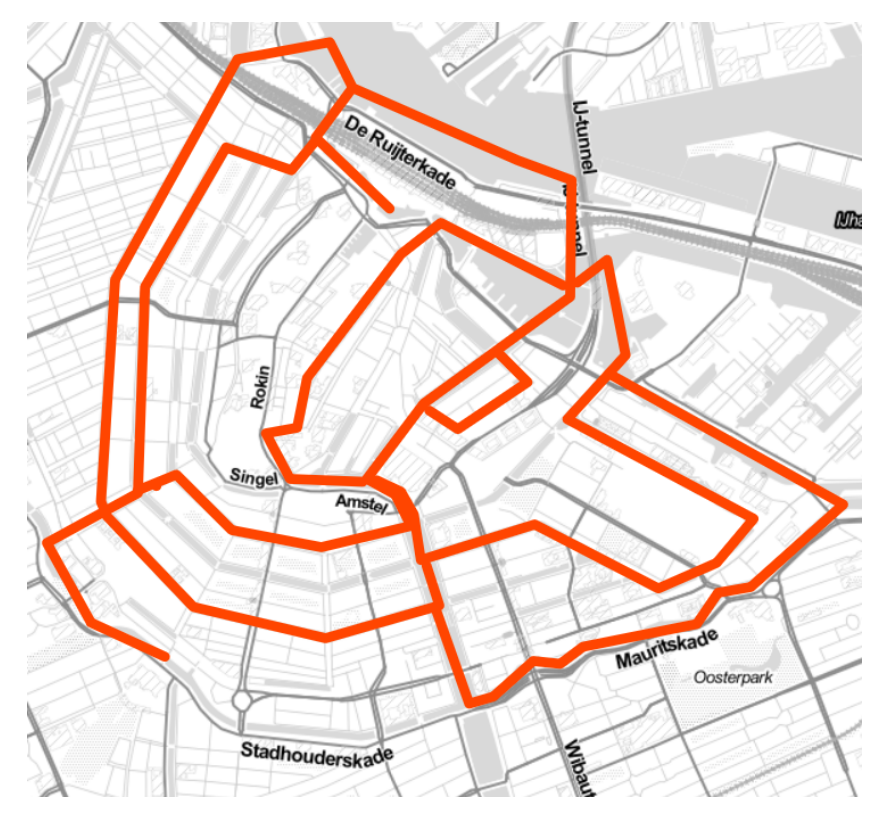


Figure 2.2.8: Possible sailing passages in the city centre

2.2.3.1. BLOCKS

Based on the standard route and the maximum and minimum speed requirements in the canals and at the Ij lake, seven different blocks are developed. Together they represent a simplified route based on the measurements. The blocks are depicted in Table 2.2.3. The moored block is explained by the fact that the canal boats are moored for 15 [min] between each trip [19]. This will be used later on, when charging in short intervals will be analysed. The manoeuvres block covers the low speed manoeuvres of the canal boat, stops, accelerating, overtaking and fast turns, up to a speed of 1.9 [m/s]. The nominal speed block is generated to capture the nominal speed in the canals, varying between 1.9 and 2.3 [m/s] (2.1±10% [m/s]). The medium speed refers to the speed faster than nominal, but as high as the minimum speed that the canal boat must be able to sail. This medium speed, or also called minimum attainable speed, is 13 [km/h] [20] or 11 [km/h] with a special permit. This speed is used at the Ij lake and is sometimes used to overtake other vessels or make up for lost time. The maximum speed, faster than the minimum attainable speed, is only rarely used and captures the remaining time that the canal boat sails fast. Caution is required with this data, as sometimes it gives a skewed view due to the bridges over the canals. They sometimes inhibit the GPS signal, after which the speed of the canal boat is suddenly larger due to the gap in distance travelled.

In addition to these standard blocks for the route, there is an auxiliary block developed for the 90° turns. Regarding the 90° turns, they require the most instantaneous power so they are categorized in their own block [16].

2.2.4. GENERIC OPERATIONAL PROFILE

Because the operational profiles can differ significantly, a generic operational profile is constructed that consists of averages with regards to mission requirements, see Table 2.2.4. The operational profile of a ship is

Table 2.2.3: Blocks for the route

Block [-]	Average speed [m/s]
Moored	0.0
Manoeuvres	Varies
Nominal speed	2.1
Medium speed	2.6
Maximum speed	3.3
90° turns	Varies
Crash stop	Varies

constructed from the amount of time the vessel spends at a certain speed [21]. The operational profile of a canal boat is required for the design of the concept, as it gives information about the sailing parameters of the ship, such as speed, time sailing and time moored, power consumption and motor RPM. This profile gives speed values which will be used later on to model the canal boats. As can be seen, distance and average time (and consequently average speed) is in the range of the typical values for the standard route of BlueBoat.

Table 2.2.4: Simplified generic operational profile

Block [-]	Time [min]	Distance [km]	Average V _s [m/s]
Moored	15	0.0	0.0
Manoeuvres	25	1.5	Varies ²
Nominal speed	25	3.2	2.1
Medium speed	14	2.1	2.6
Maximum speed	0.3	0.1	3.3
90° turns	11	0.7	1.0
Total	90	7.6	-

²Taken as average 2.35 [m/s]

2.2.4.1. ASSUMPTIONS AND VALIDATION

For the blocks method as depicted in Table 2.2.3, a few assumptions are made. The most important one is that the energy and power numbers are averaged over the blocks' speed interval. When looking at the manoeuvres block the *used* average speed for modelling is quite high (2.35 [m/s]). This is because later in the modelling the power will be derived from the speed the ship sails. To emulate the high power required for manoeuvring, a higher block speed is taken. From this block speed the power is calculated. Note that in real life this block speed should have an average of about 1.1 [m/s]. When the power would be calculated with this speed this gives a required propeller power of ± 1 [kW], where it was shown in Table 2.2.2 that the power during manoeuvring for the partially or empty boats is already more than ten times as high (about 13 [kW] depending on configuration). Therefore adjusting the speed profile is required. In section 3.2.1 of chapter 3.2, 'Ship and system modelling', an justification is given why the speed should be the controlled variable and not the power.

To check if the blocks method works sufficient, a validation is carried out, see the results in Table 2.2.5. Here the FP continuous measurement data³ is compared to the corresponding measurement data in block form. this results in a maximum error of 2% for the travelled distance. For the pod configuration the energy at the battery output according to the blocks and measurements is given, resulting in an error of maximum 4%. These errors are due to rounding the distances of the blocks. From the distance error, smaller errors in energy and time are also present. As both these measurements compared to the blocks have an error of less than 5% it is assumed that the blocks give a satisfactory estimation of energy, distance and time for a trip. Depending on the captain, amount of emergency stops and manoeuvres that are required (heavy or light traffic for example), these blocks can differ.

	Time [min]	Distance [km]	Energy [kWh]
FP - total blocks	96	8.6	17.4
FP - total measured	97	8.8	17.2
FP - difference [%]	1	2	1
	Time [min]	Distance [km]	Energy [kWh]
Pod - total blocks		_	0.5
Pod - total blocks Pod - total measured	[min]	[km]	[kWh]

Table 2.2.5: Validation of blocks method

2.2.5. FORTHCOMING METHODOLOGY

For each block, the appropriate average power is extracted from the measurements. As the canal boat during the measurements was empty, a higher resistance and hence a higher required power needs to be calculated for each block. This is done in Chapter 3.1, 'Resistance modelling. Then, each block will be optimized in this average power using a program that applies the Wageningen B series open water equations in Appendix G, 'Propeller optimization'. From these optimizations, the energy reduction with respect to the baseline from this chapter can be found.

³This is data that uses the specific route sailed when measuring, not the generic operational profile

2.3

CONCEPT APPROACH

As the goal, background and operational profile are now known, in this chapter different ZE configurations will be created that will be used in the simulations. Using the knowledge from chapter 2.1, 'Baseline', global design requirements will be developed. Secondly, the global design requirements are translated to possible configurations. Third, a more detailed choice of configurations and how they differ from each other is presented. Finally, an overview of the concepts is given.

2.3.1. GLOBAL DESIGN REQUIREMENTS

The design selection process entails choosing the general concept of the systems on board. The scope of the design of the concepts must be narrowed, as there are virtually unlimited possibilities to design a zero emission canal boat concept. In this thesis, focus will be on the systems optimization in and around the canal boat. For the conceptual design in this thesis, the dimensions such as length, width, height and draught of the boat will not be changed. These are restricted by Waternet [1]. The passenger capacity may not be lower than current boats and is assumed to be 100 throughout this text. Motor power and auxiliary power must be minimized where possible to obtain the most energy efficient design. In this chapter a global breakdown of options will be made and these will be detailed to three different definite concepts. Detailed key points and why these key points are important will be discussed next. Global design requirements for the functional design (in this thesis) are given by answering research question Q.1.5:

What are the limitations and scope of the concepts?

(Ref. Q.1.5)

- The concepts must have the same or a larger people transporting capability within the same size boat (≥ 100).
- The concepts must be able to be deployed 365 days per year. This means adequate passenger comfort year-round (sufficient heating).
- The concepts must be able to obtain a minimum speed of 3.3 [m/s] which is the minimum speed that a boat must be able to sail in the centre of Amsterdam with a permit.
- The concepts must have an independent back up propulsion system to safely reach the quay in case of an emergency must be available (see Section 2.3.2.1).

Important points that must be kept in mind, but are not top priority:

- Space in the boat, this is directly linked with the minimum people transporting capacity that must stay the same. If the system is too large, this will require space that could have been used for passengers.
- Cost of components, as this is an conceptual design made for 2025. Cost is included for the energy storage but no full cost/benefit analysis will be conducted.

Global limitations of the concepts are already mentioned in Chapter 1.2.3, 'Scope boundaries'. Added to these limitations is the fact that the propeller diameter will stay the same (0.65 [m]) due to the shallow water in the canals. Validation and verification are important in scientific documents, hence in all steps this has to be kept in mind.

2.3.2. DESIGN METHODOLOGY

In this section different design options will be discussed to answer research question Q.1.6:

What are the most viable concept options?

(Ref. Q.1.6)

The design options are discussed per type, starting with the propulsion options. This is followed by the motor, heating and electrical network options. Subsequently the possibilities of different energy storage possibilities are analysed, after which the accepted possibilities are summarized and the concepts are presented

2.3.2.1. PROPULSION

Requirements from the propulsion are as follows:

- Possible lower energy consumption compared to reference
- Possible lower power consumption compared to reference
- Possible better (manoeuvring) performance

Possible options that are common are:

- FP configuration, as used in the diesel baseline
- · Pod or thruster configuration, as used in the hybrid baseline
- Twin screw configuration
- Contra rotating propeller configuration
- Waterjet configuration

A trade-off process for more exotic and not so common propulsion options is shortly discussed in Appendix E, 'Alternative propulsion multiple criteria analysis'.

FP

A FP combined with a rudder gives adequate performance when straight sailing. It is the most simple form of a propeller, which makes it cheap and reliable. As this is a simple form of propulsion, and the measurements showed that it could be optimized with respect to the propeller, the FP will be considered as an alternative.

Pod

As the manoeuvring performance of the baseline should be improved, a pod propulsion system is proposed. The reason that this is considered is that it can deliver thrust in an 180 degree arc. This will enable better manoeuvring performance, as there is no rudder and subsequent maximum pressure against this rudder required. Interesting to see will be the difference in energy efficiency between the pod and the FP. As the hybrid baseline has a pod configuration the conceptual pod drive can be compared to this baseline.

BOW PROPULSION

A bow thruster is required in Amsterdam for canal boats and other newly built keels from 2006 onward [6]. Furthermore, there are regulations that state that when the main propulsion fails, the ship must be equipped with an independent second propulsion system that can manoeuvre the ship on its own [20]. Therefore, it is interesting to add a bow thruster to the equation to see if this can improve manoeuvring performance. The regulation above greatly reduces the potential for a second thruster or pod propulsion at the bow, as this would require a large redundancy in electrical systems and energy storage. This is the reason that a standard bow thruster (which operates mostly on 24 [V]) or a small water jet operating at 24 [V] will be considered.

CRP

Contra Rotating Propeller (CRP) is a technology that improves efficiency of the propeller(s) and manoeuvrability. However, for the Amsterdam canal boats CRP is not optimal. Looking at Figure 2.3.1 it can be seen that an extensive installation is required for the CRP. This will decrease the available room on the ship significantly, something that is not wanted. The shaft-in-shaft construction will also require more maintenance, which is undesirable.

TWIN SCREW PROPULSION

Twin screw propellers, or two fixed pitch propeller (FPP) propellers offer improved manoeuvrability but the downside is that it requires a lot more space in the vessel. The same arguments hold here as for the CRP. Furthermore, two drive lines will require more maintenance.

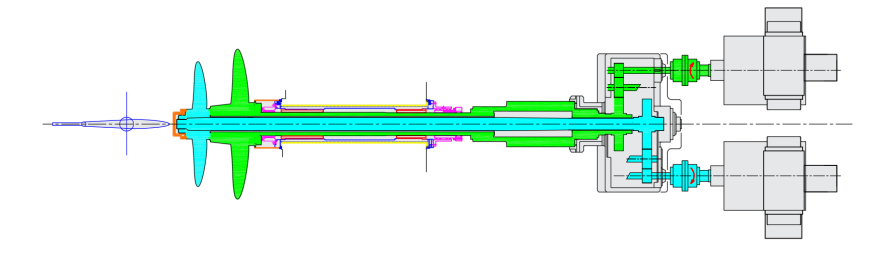


Figure 2.3.1: CRP lay out (Wärtsila)

WATERJETS

Waterjets for main propulsion are only efficient at high speeds and have very low efficiency at the speeds of the canal boats, see Figure 2.3.2 [22, 23]. Therefore they are not seen as a viable alternative in the Amsterdam situation.

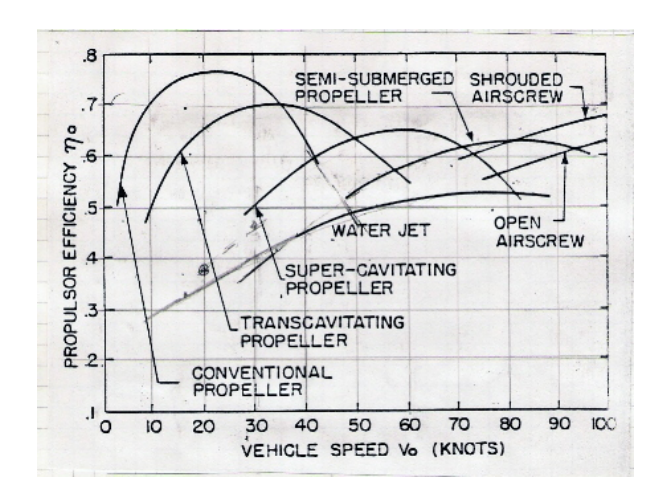


Figure 2.3.2: Propulsion efficiencies, including waterjets (Boatdesign.net)

2.3.2.2. ELECTRIC MOTOR

The choice of the electric motor is important in the energy optimization process of the boat. When resistance and required power are known, the propeller can be optimized. When the propeller is known, an electric motor can be modelled to find an optimum solution for the propulsion part of the boat. In this thesis, a Permanent Magnet Synchronous Machine (PMSM) electric motor of 55 [kW] is modelled and used in the concepts. This motor is chosen because it is compact, delivers sufficient performance, has high efficiency (77-93%) and detailed information with regards to efficiency was available from the manufacturer, which aids in the accuracy of the model. It has to be kept in mind that the data that is used to create the model used in this thesis is obtained from the manufacturer. It is assumed that this data is correct.

PERMANENT MAGNET SYNCHRONOUS MACHINE

The used PMSM is an alternating current (AC) driven motor. A permanent magnet (magnetic excitation) motor has significant advantages compared to a commuted (electromagnetic excitation) motor. It requires less maintenance as there is no commutator or slip ring required. There are no excitation losses because there is no electrical energy absorbed by means of field excitation. This increases efficiency. Finally, AC motors are generally smaller and lighter than their DC counterparts. As size plays an important role in the Amsterdam situation, this is an important reason to choose an AC machine. The chosen PMSM is vector controlled, which gives high speed and fast torque response. Vector control controls the motor by defining magnetic flux and torque and calculating the required current from these values.

2.3.2.3. HEATING

In current canal boats it is common to use a diesel heater to heat the boat [16]. They operate by burning diesel oil to generate heat. As these diesel heaters are not allowed after 2025 due to their emissions [24], an alternative to heat the boat has to be found. The alternative must be more energy efficient if possible. Possible options include heated seats, electric (ohmic) heating, a hot water boiler and a heat pump. A typical hot water boiler has a low efficiency of 78% [25] and requires a lot of space. It is therefore not considered. The other options will be compared to the current diesel heaters that are installed, as these will be more efficient than the electric heating. The heating will be analysed with these key parameters in mind:

- Give energy efficient zero emission options to heat the canal boat
- Estimate the required energy capacity for heating during different weather scenarios

2.3.2.4. ELECTRICAL NETWORK

An choice to make in the case of an electric system is whether the distribution system should be operating on AC or DC power. Both have certain advantages and disadvantages.

AC

AC networks use three phase sinusoidal alternating currents which reverses direction. Traditionally most vessels and ships have an AC distribution system and, if applicable, AC thrusters or pods. This is because at the end of the 20th century, the AC machines were easier and cheaper to control than their DC counterparts. The AC motor efficiency is also slightly higher [26]. The main advantage of using an AC network with AC systems is that they are generally a lot smaller than their DC counterparts.

DC

The advantage of using DC lies in the application of energy storage systems. Batteries, photovoltaic cells and fuel cells all deliver DC power. As this thesis will apply zero emission alternatives, which deliver DC, it is an obvious choice to choose a DC network. There are other reasons as well. An on-board DC network will require less power conversions. As power conversions are not ideal, less conversions mean fewer losses and a higher overall system efficiency. Refer to figures 2.4.4, 2.4.5 to see the required conversions in an EFD. A typical amount of energy conversions and a comparison is shown in Appendix A, 'Example energy conversions'.

NETWORK ASSUMPTIONS

In this thesis the following parts of the electrical system are assumed to have an efficiency of 1. Key figures for these electrical systems are given [27, 28].

- DC to AC inverter, $\eta = 0.94-0.98$
- DC to DC converter, $\eta = 0.98-0.99$
- Switchboard, $\eta = 0.999$

There are three reasons why these electrical systems are not taken into account. First of all, their efficiency is high, so not including them will give a negative deviation of only maximum 8%. Second, no usable data has been found or measured for a ship with a main propulsion power of around 50-100 [kW]. Larger electric systems [27, 29] are modelled, but it is unknown if this performance is equal when power is downscaled. Third, the optimum efficiency point of the inverter and converters can be optimized by choosing a larger or smaller maximum power that the system can handle, hence the efficiency will have a lower impact than the calculated 8%.

NETWORK VOLTAGE

The network voltage on board will be decided by the combined battery voltage. As battery voltage decreases when the battery is discharging, a bus voltage that is higher than the maximum battery voltage is the most safe and easy choice for the network voltage. The reason for this is because of possible over- voltage transients that can occur in the electric system. If the network devices are all specified for a higher voltage, these transients pose less of a threat to the survivability of the hardware [30]. Higher voltage mean lower currents in the system due to Ohm's law. As a higher current means (heat) losses, the lower the current (and the higher the voltage) the lower the losses are in the network. In chapter 4.3, 'Simulation results', the network voltage will be determined. As a converter from battery to bus voltage, an Insulated Gate Bipolar Transistor (IGBT) is proposed, as it is a cheap and adequate option to maintain a steady bus voltage [31].

2.3.2.5. ENERGY STORAGE

When the energy that is required for propulsion and auxiliary consumers is known the energy storage can be chosen. This is an important part of the design concept as this includes energy storage efficiency, availability, infrastructure, cost, size limitations and feasibility. The concepts will be shaped by this choice. Requirements from the energy storage are as follows:

- The option has enough power and energy to fulfil requirements
- Is energy efficient
- Has an infrastructure nearing 2025
- · Is feasible in terms of volume, safety and cost

Possible options that will be discussed here are:

- Batteries
- · Hydrogen (fuel cell)

In Appendix B, 'Flywheel and super capacitor' the super capacitor and flywheel are very briefly discussed. They are omitted in the rest of the concept design, mainly due to inadequate size, performance and cost.

BATTERY

Batteries as energy storage (ES) are ideal in the Amsterdam situation because of a few unique settings in the canals. First of all, batteries are often not feasible for ships because they are heavy and have a low energy density, a low [kWh/kg] value. Second, most ships travel long distances without mooring, which requires a larger available capacity of batteries. Larger required capacity means higher initial costs. In the Amsterdam situation, weight is not an issue. The current hybrid boat has 250 [kWh] of lead-acid batteries, around 7.5 [t], laying in its keel. However, still extra ballast is added in the hull, because the boat needs to be able to pass under the low bridges in Amsterdam. Hence, weight is not an issue at all.

Choosing a battery type Size is contrary to weight an issue in Amsterdam, as explained in Section 2.3.1, 'Global design requirements'. The larger the size of the energy storage, the less size there is for other systems and passengers. The shipbuilders want the same amount of passengers to fit in the boat as the current situation permits. When considering batteries, it is important to note that they can be charged. So what if they could be charged after each trip, reducing the energy storage requirements and hence size of the energy storage? The canal boats sail for 1 or 1.5 [hr] before letting the passengers off and new passengers on. This mooring time could be used to charge the batteries. Such short sailing times also lead to low energy requirements compared to other types of ships, and this might even make an electric battery powered canal boat feasible cost-wise.

Battery types Having established that charging could reduce the required size, it is time to look at battery technologies. A few will be described in Table 2.3.1

Based on these *generalized* values, and the knowledge that fast charging is required to reduce the size, it seems clear that lithium ion is the most corresponding options. The amount of (theoretical) cycles determines the lifetime of the battery, and in this comparison lithium ion phosphate and titanate score the best. An added bonus is the high peak load and nominal load currents. Because of these reasons, two types of batteries are chosen. These are of the lithium-ion type, lithium metal phosphate (LMP) and lithium-titanate (LTO). Lead-acid batteries are a mature technology which will not improve a lot in the coming years. As the specifics, efficiencies and dynamics of lead-acid batteries are widely known, required ES values can be applied to a static calculation and give a reasonable accuracy if lead-acid battery storage is required. Furthermore, lithium ion is a battery type that is relatively new compared to for example lead-acid. LTO batteries are only on the market since ± 2003 . This makes it an interesting technology to put research into. Lots of new innovations and cost reductions could take place between now and 2025, which makes a concept with one of these battery types future proof.

COMBINATION OF BATTERY PACKS

A possible option that has not been mentioned so far is the possibility to combine the different types of battery technology to obtain the best of two worlds: relatively cheap LMP batteries and fast charging times due to LTO. The downside of such a configuration is that there is a lot of extra hardware required to match

	Lead-acid	NiCd	NiMH	Lithium ion			
				Cobalt	Manganese	Phosphate	Titanate
Specific cell energy	30-50	45-80	60-120	150-190	100-135	90-120	50-90
density [Wh/kg]							
Cycle life (0-80%	200-800	1 000	300-500	500-1 000	500-1 000	1 000- 3 000	8 000 - 20 000
discharge)							
Fast-charge time	8-16h	1h	2-4h	2-4h	<1h	<1h	<1h
Self discharge per	5%	20%	30%	<10%	<10%	<10%	<5%
month							
Cell voltage	2V	1.2V	1.2V	3.6V	3.8V	3.3V	2.3V
Peak load current	5C	20C	5C	>3C	>30C	>30C	>4C
Nominal load cur-	0.2C	1C	0.5C	<1C	<10C	<10C	<2C
rent							
Charge tempera-	-20 to 50	0 to 45 $^{\circ}$ C	0 to 45 $^{\circ}$ C	0 to 45 $^{\circ}$ C	0 to $45^{\circ}\mathrm{C}$	0 to $45^{\circ}\mathrm{C}$	0 to 45 $^{\circ}$ C
ture	°C						
Discharge tempera-	-20 to 50	-20 to 65	-20 to 65	-20 to 60	-20 to 60 °C	-20 to 60 °C	-20 to 60 °C
ture	°C	°C	°C	°C			
Maintenance inter-	3-6	1-2	1-2	not re-	not required	not required	not required
val (months)				quired			
In use since	>1800s	1950	1990	1991	1996	1999	2003

Table 2.3.1: Battery types and specifics

the battery packs. Double Battery Management System (BMS), double voltage regulators and a system to control when which battery must be used. As the voltage drop of the two technologies is not equal charging will be difficult to accomplish and require extra equipment, such as two different charging outlets. All in all it would give only a small benefit compared to a huge extra investment in equipment and installation costs. This option is therefore not analysed.

HYDROGEN (FUEL CELL)

The most competitive alternative to battery propulsion is hydrogen propulsion. This entails a fuel cell coupled with a battery that produces only water as an emission. One such a boat is already built in Amsterdam, and was successfully deployed. This technology however, has some disadvantages. First of all, the generation of hydrogen is polluting and in some cases only about 70% efficient [32]. Secondly, infrastructure is not yet available. The built canal boat is now not used anymore because the ships fuel tank has to be refilled by a hydrogen delivery truck. This is expensive. For batteries, infrastructure is possible on a shorter notice, for example by using tram lines or existing electrical networks. After a discussion with Alewijnse, it was found that maintenance is expensive due to all the supporting systems, see Figure 2.3.3. Rules and regulations in Amsterdam are not on par with the technological standard of using hydrogen (for example, allowed pressure versus possible pressure).

Technical disadvantages Zooming in on the technical side of a fuel cell boat additional disadvantages arise. A few will be mentioned here:

- When the bonding between hydrogen and oxygen occurs and electrons are transferred to the electrodes in the fuel cell, a lot of heat is generated. This heat requires an extensive cooling system.
- Bad throttling times so when accelerating or when a crash stop is required a battery stack is still needed.
- When filling the tank, there are considerable losses when compressing the gas. It requires cooling after compression as well, and filling without an automatic filling station is dangerous due to possible blowback, leaks, freezing and/or burning.

Because of the given reasons, technical as well as operational and functional, hydrogen is not analysed in this thesis.

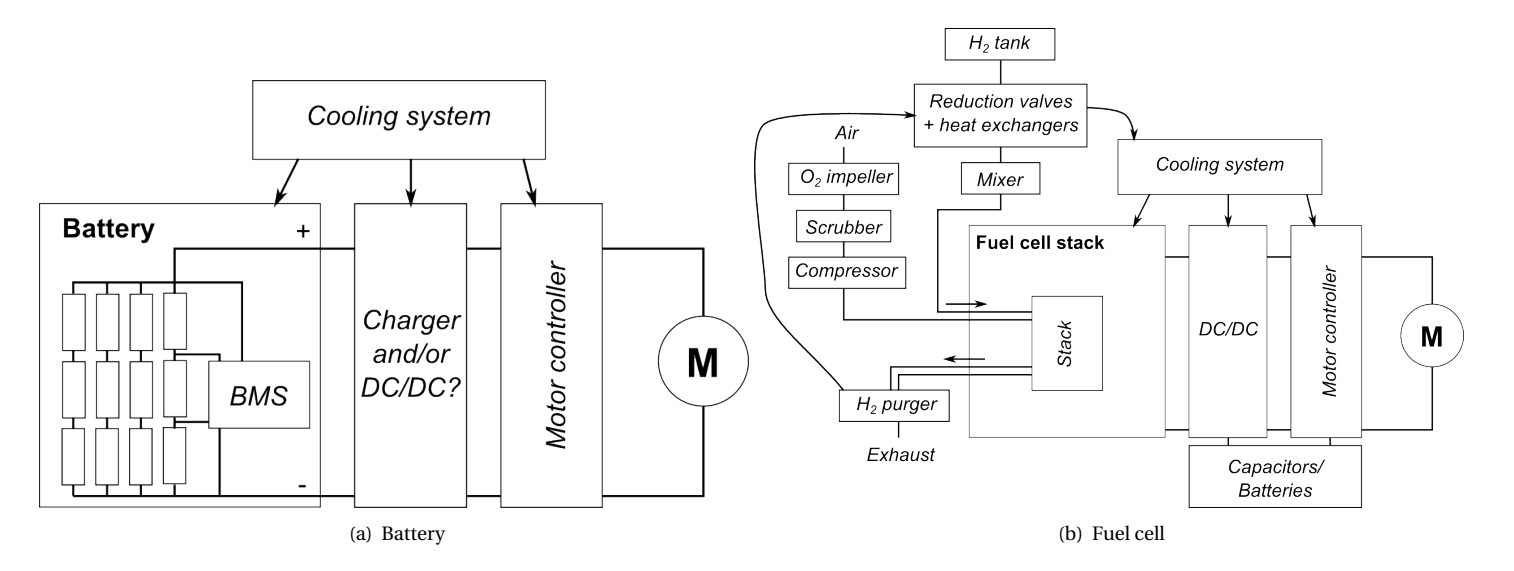


Figure 2.3.3: Systems comparison between battery and fuel cell (Mux, Tweakblogs.net)

2.3.2.6. SUMMARY OF GLOBAL DESIGN CONCEPTS

Summarizing all of the outcomes of this chapter so far, the concepts will be lithium ion battery powered, by a 55 [kW] electric PMSM. The propeller will be optimized and propulsion will originate by either a FP or pod main propulsion coupled with a bow thruster to aid in manoeuvring performance. Heating will be in the form of electric seats or a heat pump. These concepts will be developed in more detail in the next section.

LIST OF FUNCTIONAL REQUIREMENTS

In Table 2.3.2 the requirements are translated to functional requirements. This table will be used later on to assess the configurations:

Table 2.3.2: List of functional requirements

	Requirements
Main propulsion	≥3.3 [m/s]
Bow thruster	Included
Heat pump	0-20 [°C]
Energy storage	6 trips per day
Passenger capacity	Equal to typical boat now
Chain efficiency	More efficient
Space in the boat	Ideally less space required
Cost, yearly (avg.)	Cost effective
Cost, 25 years (avg.)	Cost effective

CONCEPT OVERVIEW

2.4.1. DETAILED CONCEPT OVERVIEW

Summarizing the concepts is done in Figure 2.4.1. The schematic layout of the concepts is as follows:

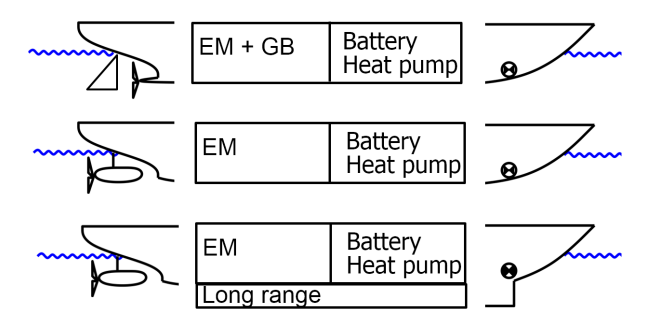


Figure 2.4.1: Schematic view of concepts, EM RF OPT, EM OPT and EM REF respectively

Here, EM is the electric motor, GB is a gearbox.

The concepts are displayed in detail in Figure 2.4.2 for simple reference. Three concepts are conceived and compared to each other regarding efficiencies and energy usage. Each concept is listed in Figure 2.4.2.

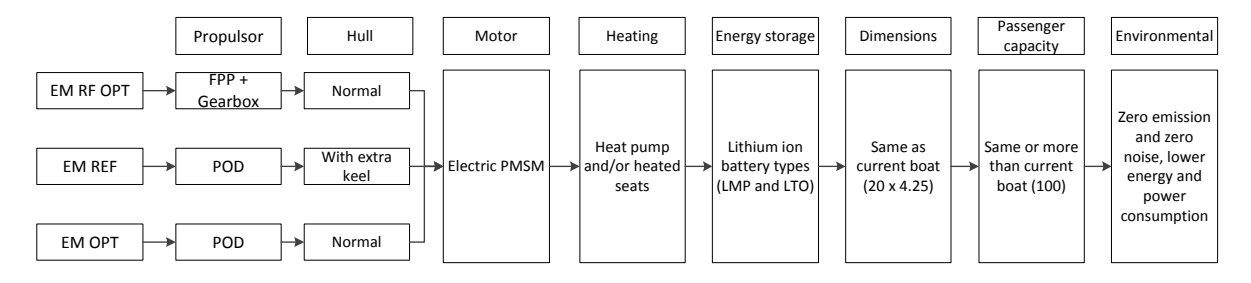


Figure 2.4.2: Overview of concepts

In the next sections the baseline boat and the concepts will be explained in further detail with the help of an EFD.

2.4.2. FIXED PROPELLER BASELINE

The reference diesel baseline boat consists of the hull of the diesel boat and a 80 [kW] diesel engine. The gearbox has a reduction ratio of 4.3. It is assumed ideal, η_{GB} =1 because there is already an efficiency of 0.9 taken for the hydraulic systems. The reference propeller is used. The resistance of the boat will be calculated for a full boat. This configuration will act as a reference baseline and validation of the model. Furthermore, Environmental Performance Indicators (EPIs) will be calculated for this boat, so that it serves as a baseline

for the electric concepts. The abbreviation to refer to this concept is DE REF which stands for Diesel Engine Reference. Current diesel canal boat specifications are listed in Table 2.4.1. For a more detailed overview the reader is referred to [16]. The EFD is given in Figure 2.4.3. In the EFD, depending on boat type and configuration, a diesel or diesel-hydraulic system is possible. Furthermore, both AC as well as DC networks are used on board.

Motor power (fossil fuels)	80-100	[kW]
Diesel heater power	20	[kW]
Length (max)	20	[m]
Width (max)	4.25	[m]
Draft	1.2-1.4	[m]
Passenger capacity	80-100	[-]
Fleet size	$\pm 70^{1}$	[-]

Table 2.4.1: Typical canal boat specifications

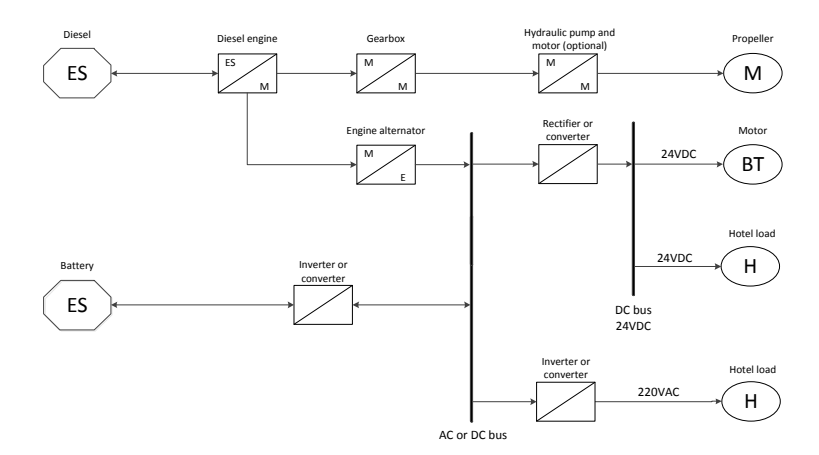


Figure 2.4.3: Energy Flow Diagram of the reference diesel boat

2.4.3. OPTIMIZED RETROFIT

This configuration represents a retrofit possibility of the canal boats. It is derived from the diesel boat and the goal is to make it as efficient as possible whilst using a gearbox and a FP in the boat. The diesel engine is replaced with the electric motor. It consists of a standard Wageningen B propeller that is matched with the electric motor. The gearbox ratio is optimized for the difference in RPM of the electric motor and diesel, keeping in mind common available reduction ratios. The same hull and hence resistance as the diesel is assumed. The abbreviation to refer to this concept is EM RF OPT which stands for Electric Motor Retrofit Optimized. The concept EFD is given in Figure 2.4.4.

2.4.4. POD BASELINE

This concept is derived from the measured hybrid boat. It is assumed that batteries are stored in a keel under the hull, to obtain a longer range conceptual design. This boat represents the baseline electric boat. As the hybrid boat does not have a gearbox, this one does not have one either. As the PMSM has a maximum rotational speed of 1500 [rpm] this could lead to cavitation. According to the installer of the motor, ARKA, this is not or very slightly the case. Cavitation will not be analysed in this thesis. The abbreviation to refer to this concept is EM REF which stands for Electric Motor Reference. The concept EFD is given in Figure 2.4.5.

¹ See [16] for more details

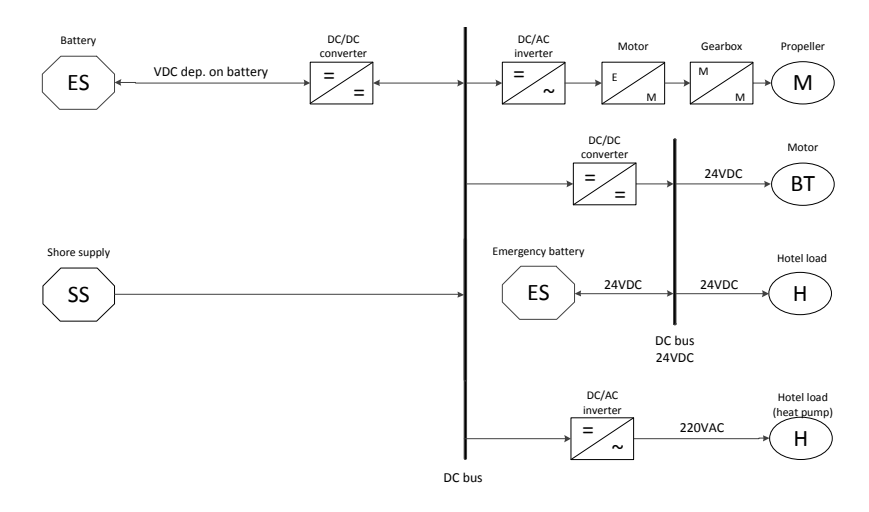


Figure 2.4.4: Energy Flow Diagram of EM RF OPT

2.4.5. OPTIMIZED ELECTRIC

The final concept is an optimized electric boat. It uses the diesel boat hull and resistance, as the batteries will be stored in the fore or aft of the vessel rather than underneath in a keel. To save space for batteries, a gearbox is not used. The abbreviation to refer to this concept is EM OPT which stands for Electric Motor Optimized. The concept EFD is given in Figure 2.4.5.

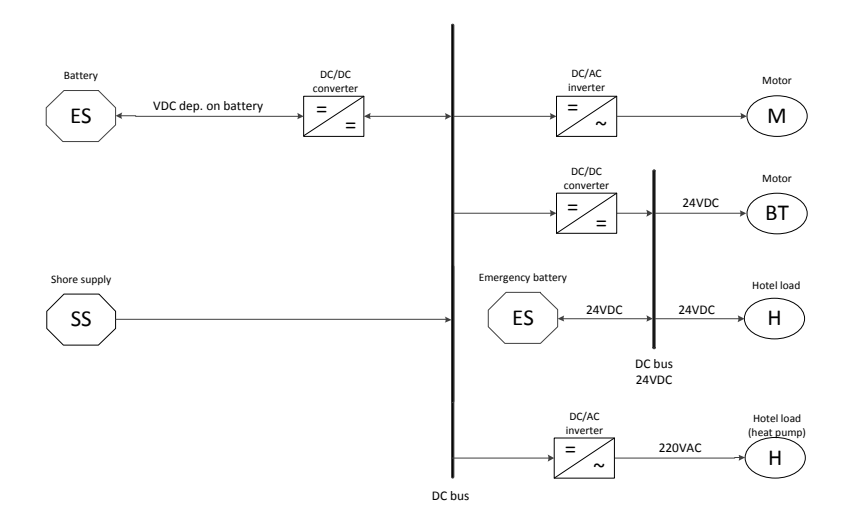


Figure 2.4.5: Energy Flow Diagram of EM REF and EM OPT

Table 2.4.2: Overview of concepts

Concept #	Name of concept	Hull type	Engine	Gearbox	Propeller
Ref	Reference diesel	diesel	diesel	standard	FP
1	Optimized retrofit	diesel	electric	standard	opt. FP
2	Reference electric	electric	electric	none	pod
3	Optimized electric	diesel	electric	none	pod ²

An explanation of the used terms in Table 2.4.2 follows below:

 $^{^2{\}rm This}$ propeller is already optimized for this electric motor

HULL TYPE

Hull type can either be 'diesel' or 'electric'. As will be explained in Chapter 3.1, 'Resistance modelling', the resistance of the hybrid boat is larger than that of the diesel boat due to the keel with the batteries. For concepts EM OPT and EM RF OPT, the optimized electric boats, it is assumed that this keel will not be present, hence the 'diesel' resistance curve will be used.

ENGINE

Compared engines can either be 'diesel' (only for the reference as a comparison) or 'electric'. Based on this choice, an electric concept or a diesel concept will be chosen.

GEARBOX

Gearbox choice is 'standard', a gearbox with a typical reduction ratio installed in the diesel boat. 'none', refers to a direct driven propeller with no gearbox.

PROPELLER

Either 'FPP', 'optimized FPP' or 'pod'. FPP refers to the standard propeller for the measured cases. 'pod' refers to the podded propulsion propeller, where 'optimized FPP' is the optimized standard Wageningen B series propeller matching with the electric motor using an optimized gearbox ratio.

3

MODELLING

This chapter starts with the detailed calculation of the resistance for both vessels, keeping in mind the added weight and therefore resistance of the passengers. The resistance chapter is completed with the validation of the resistance based on multiple methods, and an overview of the accompanying power at certain speeds for both the diesel and the hybrid boat. Ending this chapter is the approach of the modelling, explaining the integration of different required models. In the chapter that follows, the ship, propeller and electric motor models are linked to each other, succeeded with a chapter defining the auxiliary modelling strategy in the form of a seat heating analysis and the modelling of a heat pump model based on thermodynamics. The energy storage, in the form of batteries, is modelled in detail and coupled to the ship, propeller, electric motor and heat pump models, together defining the full ship model. The methodology behind certain modelling choices is substantiated. The environmental performance indication calculation method closes this chapter.

3.1

RESISTANCE MODELLING

The generic operational profile is defined in chapter 2.1, 'Baseline'. Because the measurements leading to the required power in Table 2.2.2 are conducted with empty canal boats, a correction needs to be made in the resistance of the boats to simulate a fully loaded canal boat correctly. Furthermore, by comparing the resistances of the hybrid boat and the diesel boat, the keel that is made under the hybrid boat can be decoupled from this resistance. When the battery pack is small enough, this keel is not required and in the simulation model the resistance curve of the diesel boat can be used instead of the hybrid boat. This is advantageous for the energy consumption. First the method to obtain the resistance and power requirements of the diesel boat will be extensively described. After this, the hybrid boat resistance and power will be calculated as well.

3.1.1. DIESEL BOAT RESISTANCE

From measurements conducted in [16] it was found that although the typical (diesel) engines are between 80 and 100 [kW] the maximum power the propeller could absorb was only 51 [kW]. This peak power is used only when manoeuvring in the 90° turns. In this section, the resistance of the FP configuration will be calculated. The resistance will be extrapolated to simulate a fully loaded canal boat, and to give room for a conservative value for the resistance. A conservative value is important, because the propulsion power will be slightly over-dimensioned that way, to be on the safe side.

3.1.1.1. MEASURED RESISTANCE

The known data for a typical canal boat propeller is stated in Table 3.1.1. Nominal speed is defined as $2.1 \, [\text{m/s}]$. The open water efficiency is calculated with Equation 3.1.1 and for the standard propeller equal to 0.43 at the nominal speed. This open water efficiency is based on calculation of Propeller Performance, a computer program used at DAMEN Shipyards to calculate propellers according to Wageningen B series data.

$$\eta_o = \frac{P_e}{P_p} \tag{3.1.1}$$

Table 3.1.1: Baseline propeller data at nominal speed for an partially loaded canal boat

Parameter	Value	Unit
D	0.65	[m]
z	4	[-]
$V_{s,nom}$	2.1	[m/s]
P_p	6.0	[kW]
P_e	2.6	[kW]
R_{nom}	1.25	[kN]
T_{nom}	1.45	[kN]
$\eta_{o,nom}$	0.43	[-]
RPM_{nom}	300	[rpm]

The propeller diameter is known to be 0.65 [m] with four blades and fixed pitch [29]. The highest η_o for the power range and Wageningen B series data is found to be 0.43. This is used in the calculation of the resistance as shown further in this chapter.

In this chapter η_R is taken as 1. Typical values for a canal boat are 1 for η_H , and a wake factor of w = 0.15 and a thrust deduction factor of t = 0.15.

MEASURED RESISTANCE RESULTS

Measured resistance is shown in Figure 3.1.1. The flat area in resistance around 2.3 [m/s] in Figure 3.1.1 can be explained by the fact that some data was obtained when sailing downstream and some when sailing upstream, thus changing the power requirements and ultimately the resistance of the vessel. Furthermore, the width of the canals changed a lot during the second run, which changes the resistance as well [33]. Due to time restrictions a complete one way run could not be conducted.

The values from Table 3.1.1 are for a partially loaded (48 people) canal boat. The shaft or propeller power (P_s or P_p , as they are assumed equal, η_s =1) can be obtained by taking the open water efficiency from Table 3.1.1 and applying Equation 3.1.2 [18].

$$P_e = P_n \cdot \eta_0 \tag{3.1.2}$$

The effective towing power, P_e , is now known. With Equation 3.1.3 the resistance of the canal boat can be calculated, as the speed of the boat is measured.

$$R = P_e \cdot V_s \tag{3.1.3}$$

Figure 3.1.1 displays the results for this method.

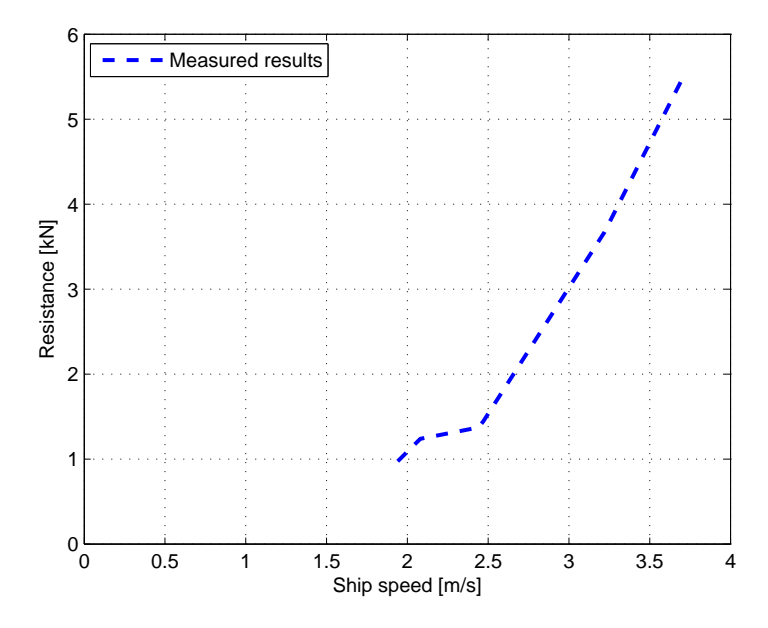


Figure 3.1.1: Measured resistance of the diesel/FP canal boat $\,$

As mentioned before, these measurement results are for a partly loaded canal boat. Because the resistance and required thrust will increase if the boat is completely loaded, the highest resistance point (at 3.7 [m/s]) from the measured resistance curve is taken. From this resistance point, a quadratic resistance curve of the form of Equation 3.1.4 is assumed [34]. Here, a is 0.4007.

$$R = a \cdot V_s^2 \tag{3.1.4}$$

This method is visualised in Figure 3.1.2. By calculating the quadratic resistance curve at the point of maximum measured required power (this is at maximum speed), an upper limit for the resistance and required propeller power is found. This is a conservative value for the resistance.

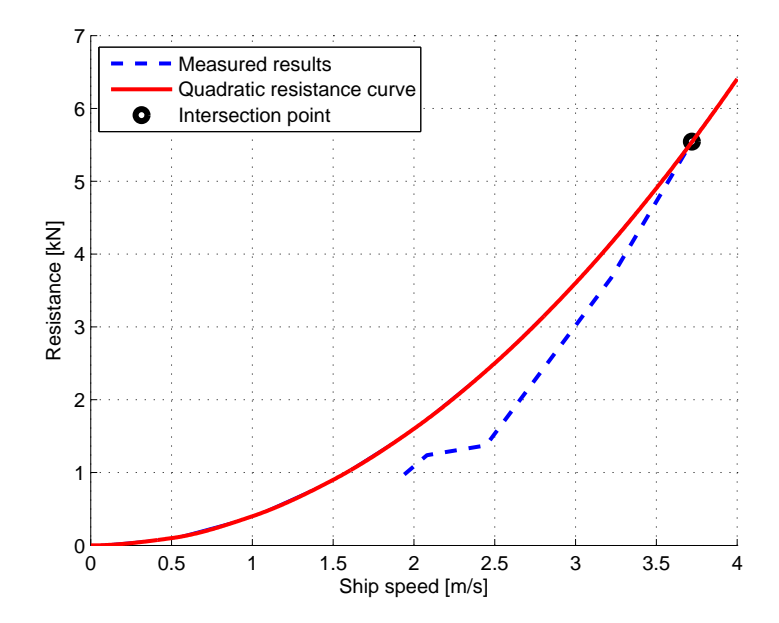


Figure 3.1.2: Method of acquiring the quadratic resistance curve

3.1.1.2. ASSUMPTIONS

Assumed is that the shaft power, P_s , is equal to the propeller power P_p , hence η_s is assumed 1. Furthermore, as earlier stated, η_R and η_h are assumed 1 as well. From this and Equation 3.1.5 it follows that P_d is equal to P_p as well.

$$P_e = P_D \cdot \eta_o \cdot \eta_R \cdot \eta_h \tag{3.1.5}$$

Further assumptions are:

- No cavitation
- · Shaft speed is linearly proportional to translating speed
- No shaft losses
- Constant thrust deduction factor and wake factor
- The difference in pod boat resistance compared to the FP baseline is due to the keel

3.1.2. CALCULATING PROPELLER POWER

Propeller power P_p for the quadratic resistance curve from Figure 3.1.2 can be calculated with the propeller law, Equation 3.1.6 [18, 34].

$$P_p = c_4 \cdot n_p^3 \tag{3.1.6}$$

Here, c_4 is taken at the highest resistance, at the intersection point of Figure 3.1.2. c_4 is assumed constant. It is defined as a function of torque coefficient and relative rotative efficiency η_R , which is assumed constant. Visualising this propeller law gives Figure 3.1.3. The relation between V_s and V_a is given in Equation 3.1.8 [18].

 P_e is equal to Equation 3.1.3 and can be calculated for the higher resistance case. At 2.1 [m/s] the resistance goes up from 1.25 [kN] to 1.77 [kN]. This can be seen in Figure 3.1.2. Using this resistance, P_e is calculated as 3.72 [kW]. If the same open water propeller efficiency is assumed, then P_p is 8.6 [kW], see Figure 3.1.3. From this nominal working point, the required thrust is calculated with Equation 3.1.7 [18]. The results of the preceding calculations are given in Table 3.1.2.

$$T = \frac{P_e}{V_a} \tag{3.1.7}$$

$$V_a = V_s \cdot (1 - w) \tag{3.1.8}$$

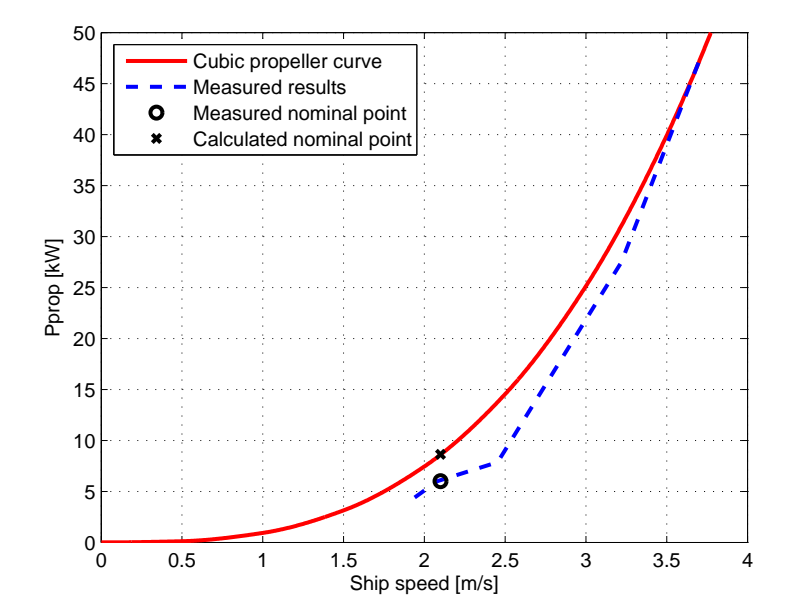


Figure 3.1.3: Calculated cubic propeller law curve for the quadratic resistance line of Figure 3.1.2

Table 3.1.2: Required performance from the propeller, for a fully loaded canal boat

Parameter	Value	Unit
$ ho_{water}$	1000	[kg/m ³]
V_{nom}	2.1	[m/s]
P_e	3.72	[kW]
R_{nom}	1.77	[kN]
T_{nom}	2.08	[kN]
t	0.15	[-]
w	0.15	[-]

$$\eta_o = \frac{P_e}{P_p} \tag{ref. 3.1.1}$$

Apart from the standard propeller operating at measured resistance, now a new propeller has been calculated. This new propeller has the same diameter as the standard propeller, but is calculated for a higher ship resistance and hence a different RPM at nominal speed.

3.1.3. DISCUSSION ON RESISTANCE METHOD

One could argue that the 'added' resistance is too large for only ± 50 -100 passengers. This might be the case, but it is the aim to give a conservative value here, as the propeller will be optimized further. Three different methods are used to see if they can give a better indication of resistance.

3.1.3.1. ADMIRALTY CONSTANT

The first method is using the Admiralty constant, see Equation 3.1.9.

$$C_{adm} = \frac{\Delta^{2/3} \cdot V_s}{P_D} \tag{3.1.9}$$

Where Δ is the displacement of the ship in tonnes, which can be rewritten to hull displacement volume with Equation 3.1.10 [18].

$$\Delta = \rho \cdot \nabla \tag{3.1.10}$$

Using this Admiralty constant method, the same resistance is found as for the quadratic resistance method when using a hull volume displacement of 60 [m^3], the same as in the specifications of the boat. If it is assumed that this displacement is for a fully loaded boat, the values coincide.

3.1.3.2. HOLTROP AND MENNEN RESISTANCE CALCULATION

The Holtrop and Mennen method can be found in [35, 36]. The input and output data are given in [16]. As can be seen from Figure 3.1.4, the values of Holtrop and Mennen are almost identical to those calculated by the quadratic resistance curve. This is probably due to the fact that the vessel is sailing at such low speeds. The method of Holtrop is mainly used for sea going vessels, therefore the lines will differ significantly at larger speeds [37]. Because at this speed the lines are comparable, no further correction (for example the method of Lackenby to correct for shallow water [38]) is applied.

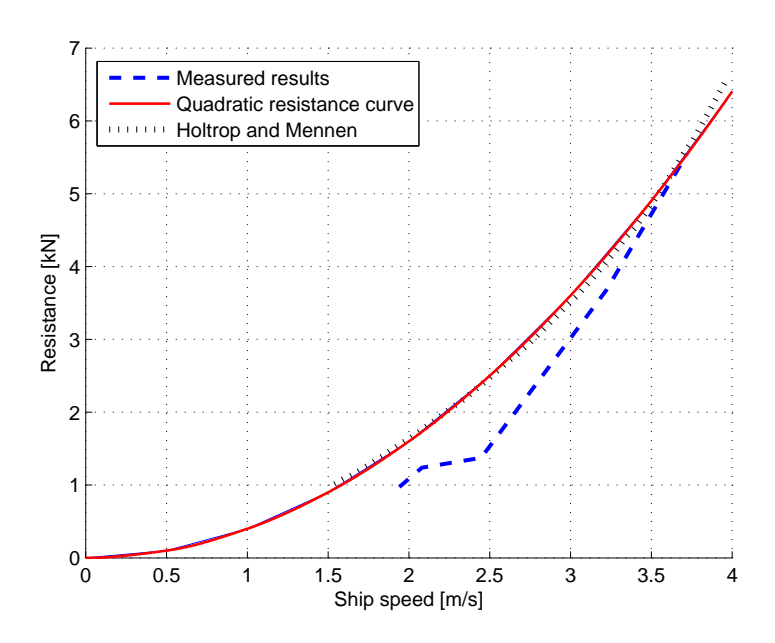


Figure 3.1.4: Measured resistance according to Holtrop and Mennen method

3.1.3.3. Effective power and displacement relation

Passengers are equal to a change in displacement. This can be expressed as Equation 3.1.11 [18].

$$P_e = \left(\frac{\Delta}{\Delta_{nom}}\right)^{2/3} \cdot P_{e,nom} \tag{3.1.11}$$

If 60 $[m^3]$ again is taken as the upper displacement volume limit, the resistance according to the displacement method can be calculated by subtracting passengers with their weight from the displacement weight. Volume to weight can be translated into each other with Equation 3.1.10. To be able to smoothen the flat part at 2.3 [m/s] a quadratic fit for the measurements is obtained, see Equation 3.1.12.

$$0.348 \cdot V_s^2 \tag{3.1.12}$$

Results are given in Figure 3.1.5. This fit has a R^2 value of 0.92, overestimating resistance between 2 to 2.5 [m/s] and underestimating resistance above 3.4 [m/s]. It can be seen that this resistance is lower (9% to be precise) than the assumed quadratic curve. To allow for foul weather and a possible heavier load (here passengers with an average weight of 80 [kg] are taken) the quadratic method is assumed substantiate.

3.1.4. Hybrid boat resistance

The same method as used in the previous section can in this case *not* be used to calculate the resistance of the measured hybrid boat. The problem with the calculation of the resistance of the hybrid boat is that it is

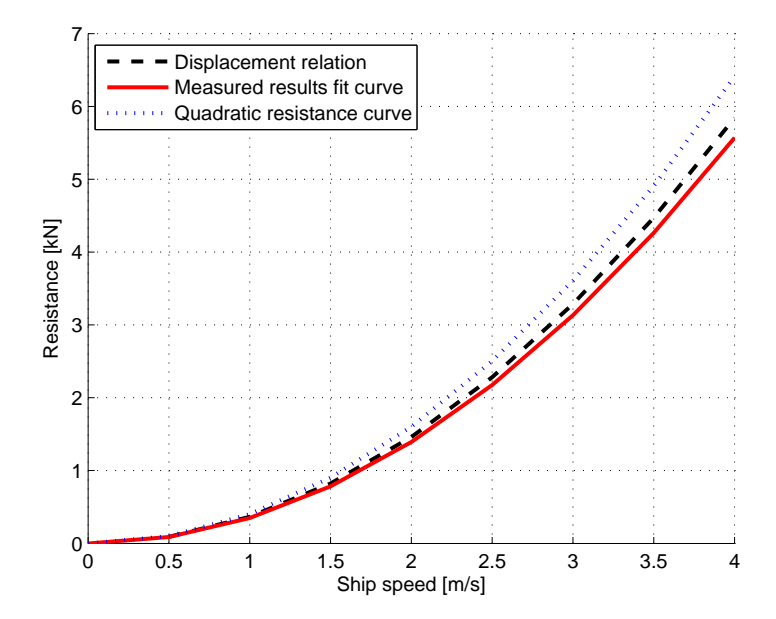


Figure 3.1.5: Resistance for a fully loaded canal boat according to displacement method

unknown what P_p is, as only the battery output power is measured. Electric motor efficiency and converter efficiencies are only known in the peak point of operation. The resistance is nevertheless important to compare, as this hull is many years younger, but there is a keel used to store the batteries in added to the underside of the ship that is probably increasing resistance substantially.

USING OPENPROP TO CALCULATE THRUST

The maximum power that is measured at the discharge side of the battery is 58 [kW]. It is assumed that this is at 1500 [rpm]. Using the electric motor efficiency map, shown in Appendix C, 'Motor efficiency plot', Figure C.1, it can be seen that the efficiency of the electric motor in the working point of maximum RPM and maximum torque is equal to 0.93. The maximum power output of the electric motor is assumed to be in this point, and is hence equal to 54 [kW] (of a theoretical 55 [kW]). Maximum *effective* propeller power P_e at this point is 28.3 [kW] according to the specification sheet. This leads, when using Equation 3.1.1, to a maximum theoretical open water efficiency of 0.51. When putting these specifications into OpenProp, an open water efficiency of 0.34 effective is calculated. For a short explanation about OpenProp the reader is referred to Appendix D, 'Openprop propeller calculation'. The maximum power is 54 [kW] with a torque of 340 [Nm]. This is in accordance to the electric motor specification sheet. From these data, as this is again the maximum working point as with the diesel boat, the resistance of the boat can be calculated with a slightly different method. Using Equation 3.1.13 to calculate propeller RPM as a function of ship speed:

$$n_p = c_3 \cdot V_s \tag{3.1.13}$$

From the measurement at 1500 [rpm], c_3 is assumed constant at 448. For every electric motor speed, the speed of the boat can now be calculated. $P_{e,max}$ with the current propeller is $0.34 \cdot P_{prop,max}$, 18.3 [kW]. This results in a resistance of 5.6 [kN] at 3.3 [m/s]. Compared to the diesel boat, this is significantly higher. Using Equation 3.1.6, c_4 is found to be $1.58 \cdot 10^{-5}$. With this value, the propeller power as function of the RPM can be calculated. An overview of the preceding data is given in Table 3.1.3. The resistance parameter a, when assuming that c_1 is constant, can now be calculated by combining equations 3.1.3 and 3.1.4, where a is equal to 0.511.

The resistance compared to the diesel boat is shown in Figure 3.1.6(a). Propulsive power is shown in Figure 3.1.6(b). Naturally due to the higher resistance, propulsive power is higher for the hybrid boat. As can be seen the resistance is significantly higher. This is probably due to the aforementioned keel. Note that the propeller power for the hybrid boat is already at its calculated maximum, because the measurements did not include propeller or shaft torque. Because this is not known, the open water efficiency for the hybrid case is already optimized with respect to P/D ratio.

Maximum point of operation	n	
Speed	3.3	[m/s]
Propeller power P_{prop}	53.4	[kW]
Propeller torque M_p	340	[Nm]
RPM	1500	[rpm]
Effective power P_e	18.3	[kW]
Resistance	5.6	[kN]
c_1	509.7	[-]
c_3	448	[-]
c_4	1.58E-05	[-]

Table 3.1.3: Calculated data for point of maximum operation

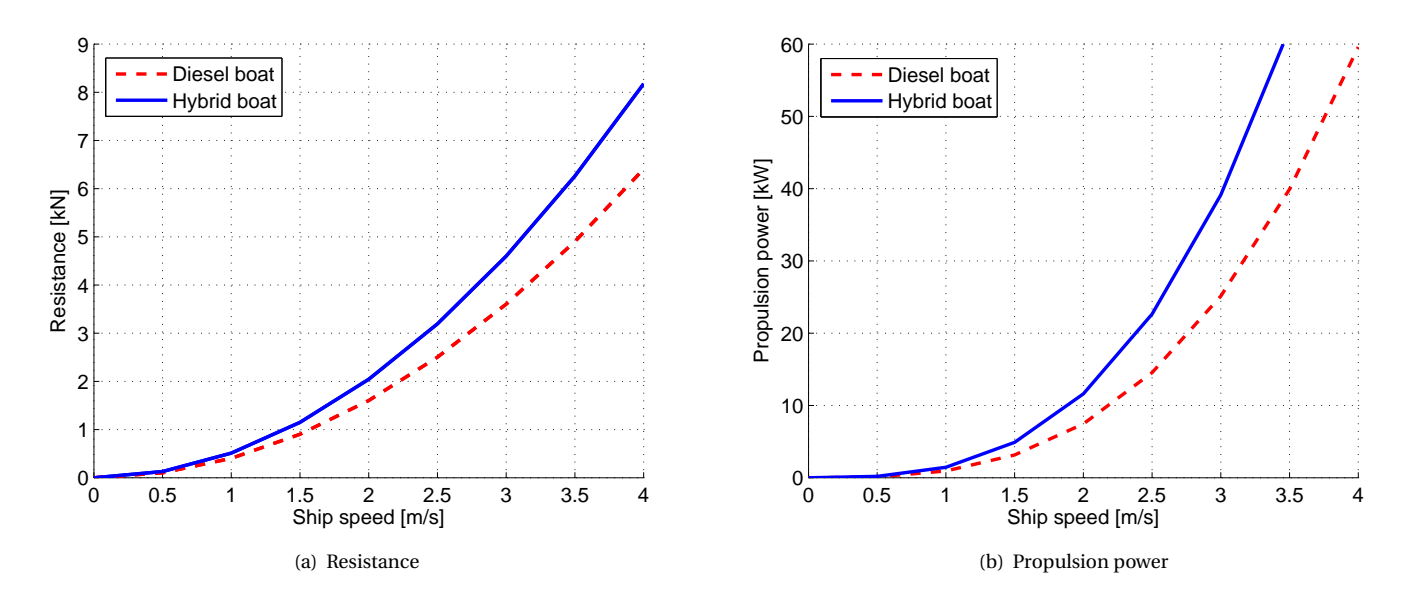


Figure 3.1.6: Resulting ship resistance and power curves for a fully loaded hybrid and diesel canal boat

3.1.5. Integration of models

In the following chapters the modelling and background, using the calculated data from this chapter, for the used models in this thesis is explained. For clarity, an overview of the models is given in Figure 3.1.7, where the links between the different models are visualised. The text on the arrows between the model 'rectangles' is the interface or variable which serves as the input.

The integration of the models must occur to create a fully working dynamic environment which is able to simulate the operational profile.

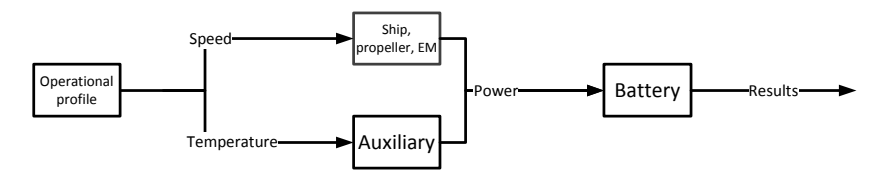


Figure 3.1.7: Integration of the models

SHIP AND SYSTEM MODELLING

This and the two forthcoming chapters will answer research question Q.1.7:

How can the concepts be modelled?

(Ref. Q.1.7)

The modelling starts with the coupled ship, propeller and motor model which are presented. In Figure 3.2.1 the light green block shows the model that will be described in this chapter: the ship, propeller and electric motor models. Modelling is done in a MATLAB/Simulink environment. In Figure 3.2.2 the global lay out of

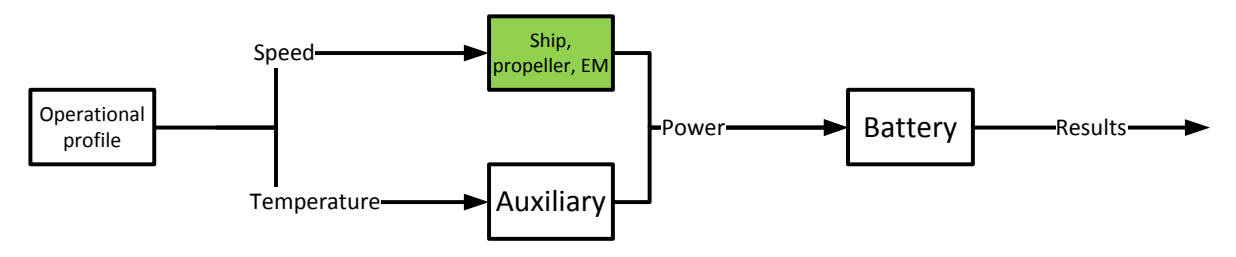


Figure 3.2.1: Model overview

the ship model is visualised. Starting from left to the right every block from Figure 3.2.2 will be explained in the next paragraphs. First the PI controller will be explained.

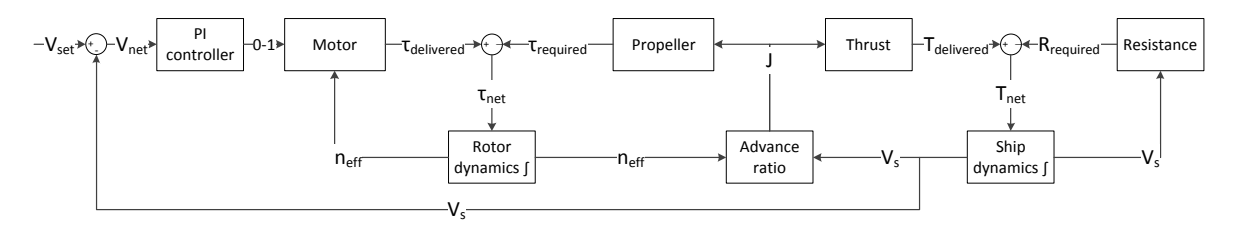


Figure 3.2.2: Ship, motor and propeller modelling

3.2.1. PI CONTROLLER

The motor controller uses the vessel speed as an input (V_{set} in Figure 3.2.2). This required speed comes from the (generic) operational profile that is defined by the user. The motor is controlled by the Proportional-Integral (PI) controller, what this essentially means is that the motor will have a feedback loop that works towards producing the power that is required for the required speed. The motor controller is equipped with a PI regulator. This PI regulator recalculates the difference between the set speed and the required speed into a signal from 0 to 1. This way, the motor will be controlled by the non-dimensional difference between set speed (required speed) and delivered speed.

The proportional part P of the controller will minimize the present error between the V_{set} and V_s . The integral part I of the controller will be used to minimize the accumulated past errors. The integral action is required, because with only a proportional part there will always be an error between the desired and delivered value. Integral action will minimize this error. No derivative action D is implemented in the controller, because the derivative is a prediction of the future error based on the current rate of change [39]. As this current rate of change can change very suddenly, decreased performance was noted when the derivative action was implemented.

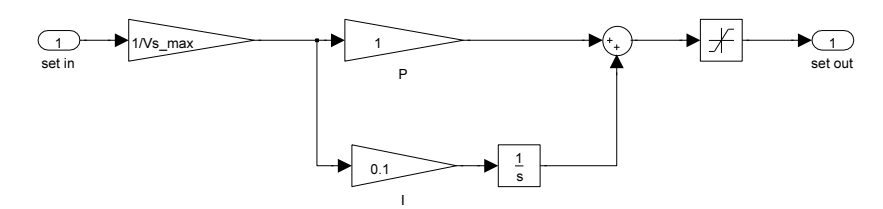


Figure 3.2.3: PI Controller model, P = 1 and I = 0.1

3.2.1.1. Considerations for feedback loop

As stated in the preceding paragraph, V_s , effective ship speed is chosen as the controlled motor variable. This is done to be able to compare the concepts based on their net output power. One of the goals of this thesis is to see how the battery energy storage options perform. By using V_s rather than P_{batt} as an input this can be visualised, as the differences in open water efficiency can now be included as well, whereas setting power as the controlled variable will require a different operational profile for each configuration, as the power is dependent on resistance and efficiencies in the system.

3.2.2. MOTOR

Electric motors have high efficiencies. Used in this thesis is an efficiency curve for a 55 [kW] permanent magnet synchronous machine. This motor is currently used in the hybrid canal boat and measurements have been conducted on this boat and motor. The RPM, efficiency and torque plot is given in Figure 3.2.4. The indicated torque line is the maximum nominal torque (torque without overloading) that the motor can deliver. A larger version of this figure can be found in Appendix C, 'Motor efficiency plot', Figure C.1.

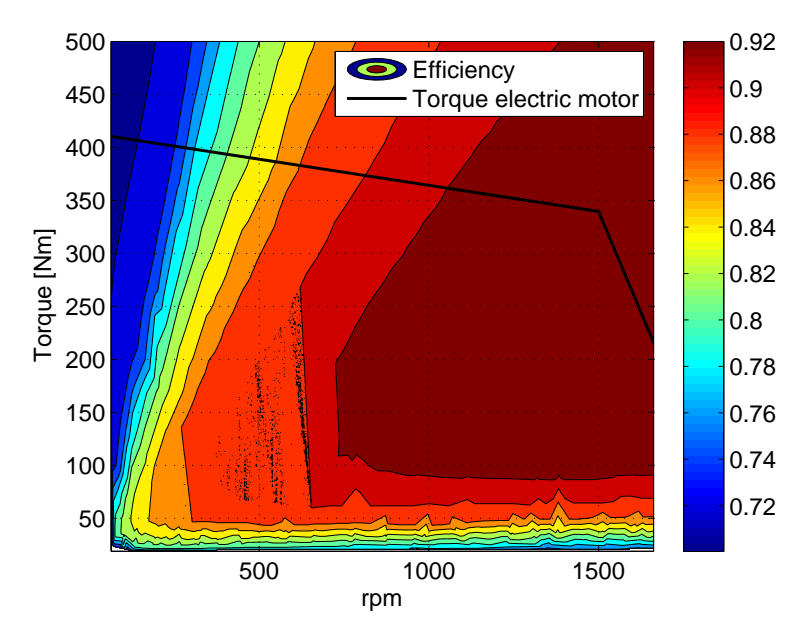


Figure 3.2.4: Torque - rpm - efficiency contour plot

The maximum continuous torque is visualised as well in Figure 3.2.4. This torque line follows these equa-

3.2.3. ROTOR DYNAMICS 47

tions:

When the RPM is below or equal to 1500:

$$\tau_{normal} = 410 - n_e \cdot \left(\frac{410 - 340}{1500}\right) \tag{3.2.1}$$

When the RPM is above 1500 (flux weakening region):

$$\tau_{weak} = 340 - n_e \cdot \left(\frac{340}{1920 - 1500}\right) \tag{3.2.2}$$

3.2.2.1. COUPLING CONTROLLER AND MOTOR

Variable n_{eff} is the engine or motor RPM. The n_{eff} in Figure 3.2.2 is fed into the torque equations of the motor, see Equations 3.2.1 and 3.2.2. This gives a maximum torque. The signal from the PI controller is fed into the motor block, see Figure 3.2.2, and this calculated maximum torque is then multiplied with the 0-1 value from the controller. An 'usable torque' value can now be calculated. The usable torque value is then fed through the torque map (either the diesel or the electric motor torque map), see Figure 3.2.4, to obtain the motor efficiency. The output is the torque that is effectively used for propulsion, $\tau_{delivered}$.

$$P = 2\pi \cdot n \cdot \tau \tag{3.2.3}$$

3.2.3. ROTOR DYNAMICS

The rotor dynamics in Figure 3.2.2 is the shaft inertia of the motor driven by the (un)balance of delivered and required torque [34]. The block rotor dynamics calculates the effective RPM that the motor should obtain based on the difference between the required propeller torque and the delivered motor torque. Using the definition of torque, inertia (I) multiplied with angular acceleration (α), gives Equation 3.2.4:

$$\tau = I \cdot \alpha \tag{3.2.4}$$

This can be rewritten using Equation 3.2.5 to Equation 3.2.6:

$$\alpha = \frac{d\omega}{dt} \tag{3.2.5}$$

$$\tau = I \cdot \frac{d\omega}{dt} \tag{3.2.6}$$

As the effective RPM is required, the rotational term, ω , is taken to the left side of the equation and integrated. This gives Equation 3.2.7:

$$\omega = \int \frac{d\omega}{dt} = \int \frac{\tau_{in} - \tau_{out}}{I}$$
 (3.2.7)

Here τ is in [Nm], I is in [kg/m²] and ω in [rad/s]. The moment of inertia I is not known for this motor, therefore it is taken as 1% of the weight of the pod. The total pod weighs 240 [kg], I is taken as 2.4 [kg/m²]. The torque term τ in Equation 3.2.7 is known from the motor (τ_{in}) and propeller (τ_{out}), hence ω can be calculated. This term will be divided by $60/2\pi$ to get from [rad/s] to [rpm], obtaining n_{eff} .

3.2.4. ADVANCE COEFFICIENT

 n_{eff} will be used to calculate advance coefficient *J* according to Equation 3.2.8. This advance coefficient is used to calculate the propeller thrust and torque according to the data from the propeller characteristics.

$$J = \frac{V_s \cdot (1 - w)}{n \cdot D} \tag{3.2.8}$$

3.2.5. SHIP DYNAMICS

The ship dynamics give the ship inertia that is driven by the (un)balance between thrust and resistance. Resistance calculation was covered in chapter 3.1, Resistance modelling. A short summary can be found in the next paragraph. The ship dynamics block consists of Newtons' second law of motion, $F = m \cdot a$. This can be rewritten into Equation 3.2.9:

$$F = m \cdot \frac{dv}{dt} \tag{3.2.9}$$

And this can be rewritten to solve for speed v, 3.2.10:

$$V_s = \int \frac{F_{in} - F_{out}}{m} \tag{3.2.10}$$

With V_s the ship speed in [m/s]. Both forces F are in [N] and mass m in [kg]. Mass is taken as the mass of the ship, calculated with Equation 3.2.11:

$$m = V \cdot \rho_w \tag{3.2.11}$$

Here, ρ_w is the density of water, 1 000 [kg/m³] and V the water displacement of the vessel, taken as constant 60 [m³]. This value is taken from the sailing letter. Filling in the values gives a mass of 60 [t] or 60 000 [kg]. A better value of 40 [t] (40 000 [kg]) however is obtained in chapter 3.2.9, Validation of ship model.

3.2.6. RESISTANCE

The resistance curve of the hybrid boat is calculated in Chapter 3.1, 'Resistance modelling'. The associated equations are reiterated here:

$$R = a \cdot V_s^2 \tag{ref. 3.1.4}$$

For the hybrid canal boat, α was found to be 0.511, hence:

$$R_{hybrid} = 0.511 \cdot V_s^2 \tag{3.2.12}$$

For the diesel canal boat, α was found to be 0.4007, hence:

$$R_{diesel} = 0.4007 \cdot V_s^2 \tag{3.2.13}$$

This difference in resistances will be used in the concepts later on.

3.2.7. PROPELLER AND THRUST

Thrust and propeller torque are included by integrating the calculated coefficients K_T and K_Q values in the model. Calculating thrust from K_T is done with Equation 3.2.14 and calculating propeller torque from K_Q is done with Equation 3.2.15 [18].

$$T = K_T \cdot \rho \cdot n_p^2 \cdot D^4 \tag{3.2.14}$$

$$Q = K_Q \cdot \rho \cdot n_p^2 \cdot D^5 \tag{3.2.15}$$

3.2.8. DIESEL SFC

Diesel efficiency will be calculated with the following equation, conceived in [18]:

$$\eta_e = \frac{3600000}{sfc \cdot LHV} \tag{3.2.16}$$

Here, Specific Fuel Consumption (SFC) is in [g/kWh] and the Lower Heating Value (LHV) is 43 400 [kJ/kg]. η_e gives the diesel efficiency from fuel to brake power. To get from RPM to SFC parametric fit equations 3.2.17 and 3.2.18 are taken from [16]:

$$z = \frac{(n_e - 1788.9)}{530.2} \tag{3.2.17}$$

$$sfc = -0.76803 \cdot z^4 - 1.2462 \cdot z^3 + 8.2403 \cdot z^2 + 4.9866 \cdot z + 208.84$$
 (3.2.18)

3.2.9. VALIDATION OF SHIP MODEL

The model of the ship is validated by comparing the speed from ± 0.5 [m/s] to ± 3.5 [m/s] of the model to the measurement. As can be seen from Figure 3.2.5(a), a 40 [t] value for ship inertia has a better similarity with the measurement baseline. The 40 [t] value for inertia is therefore taken. One could argue that the hybrid boat was empty during measurements, hence the acceleration will be slower for a fully loaded boat, but this is already incorporated in the calculated resistance used in the model. The electric model is validated by the speed comparison shown in Figure 3.2.5(b). The inertia here is lower, but the empty boat weighs less as well (25 [t]). The inertia values chosen here offer sufficient performance in comparison with the baselines.

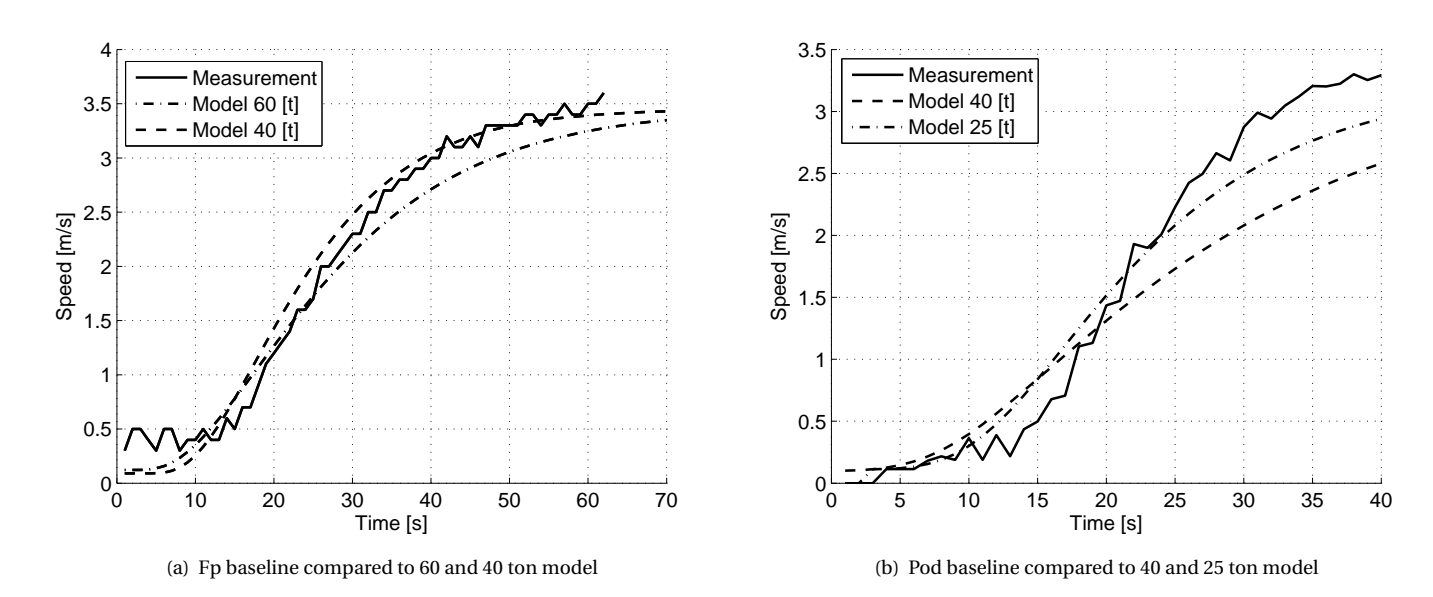


Figure 3.2.5: Acceleration comparisons for different ship inertia values

AUXILIARY MODELLING

In the Chapter 3.1, 'Resistance modelling' the resistance and power of the canal boats at different speeds was calculated. To get to know the whole picture of the energy usage of the canal boat the auxiliaries must be included in the equation. In this chapter the auxiliary energy users will be analysed and where required modelled. The auxiliary users on a canal boat can be divided into two main groups, maritime systems and heating. Both will be introduced after which the heating will be analysed in depth.

In Figure 3.3.1 the light green block shows the model that will be described in this chapter: the auxiliary models. The dark green models represent the models already defined in earlier chapters.

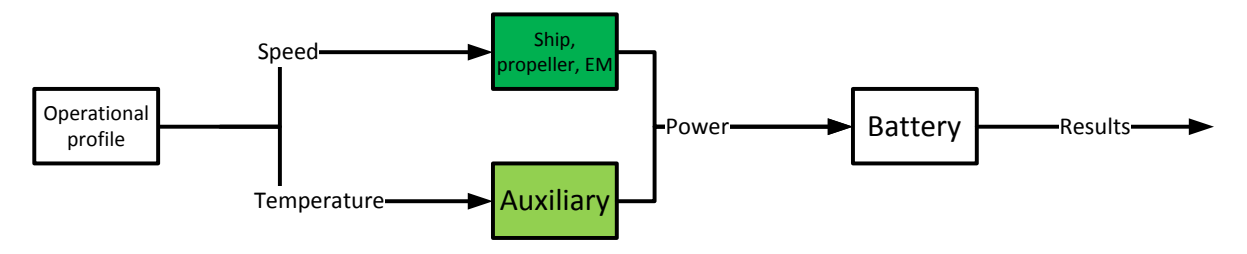


Figure 3.3.1: Model overview

3.3.1. MARITIME SYSTEMS

The maritime systems include things like the Automatic Identification System (AIS), GPS, lighting and sound system. In Jacobs [16] it was found that these systems draw a power of around 600 [W] continuously. This is therefore the amount that is used from here on when referring to the maritime systems.

3.3.2. HEATING

In current canal boats it is common to use a diesel heater to heat the boat [16]. They operate by burning diesel oil to generate heat. The diesel heaters used in canal boats have a typical power range of around 20 [kW] and an efficiency of 90% [17]. As these diesel heaters are not allowed after 2025 due to their emissions [24], an alternative to heat the boat has to be found. The alternative must be more energy efficient if possible.

3.3.2.1. LOWERING AUXILIARY ENERGY CONSUMPTION

To lower the auxiliary energy consumption, an alternative to the diesel heater must be found. This is done by looking at innovative solutions to reduce energy consumption. One such a solution could be a heat pump system, or (electric) seat heating.

3.3.2.2. SEAT HEATING

Seat heating could provide an economical way to reduce heating energy, because the heat source is directly in contact with the person. Furthermore, seat heating can be made in such a way that it is possible to switch on

or off per seat, hence saving energy when the canal boat is not full. When looking at commercially available seat heat options, typical power requirements are between 40 and 70 [W] per cushion. Used data for table 3.3.1 is taken from [40].

Table 3.3.1: Heated seats cost and energy breakdown, worst case scenario

Heating stance [-]	Power per seat [W]	# of seats [-]	Total power [kW]	Energy per trip ¹ [kWh]
Low heating	40	100	4	5.4
High heating	70	100	7	9.4

The downside of using heated seats is that only the posterior of the person is heated, hence leaving the rest of the body cold. This could be less comfortable on cold days. Furthermore, in recent canal boats the static benches are replaced with free-standing chairs. The cushions of these chairs are used as emergency floatation devices, hence it is difficult to implement seat heaters in this case. One last disadvantage of seat heating is that there will be electric heaters required to remove condensation moisture if it appears on the large glass surfaces of the canal boat. This condensation moisture will not disappear with heated seats. For completeness some key figures are given in table 3.3.1. The cost of the system is estimated around 250 $[\mathfrak{E}]$ per seat.

3.3.2.3. HEAT PUMP

A heat pump has the advantage of heating the interior completely. Heat pumps take heat from a source (ground, air or water) and use it to heat the destination (with air or water). When considering an water-to-water pump, a heated water reservoir is required. A water-to-water or a water-to-air system requires a water depth of at least 2 [m], and a required area of approximately 9 [m²/kW] [41]. This is difficult to realize in the Amsterdam situation, as canals are ≥ 1.8 [m] deep where canal boats are allowed [42]. Due to size limitation of the canal boat these types are therefore neglected. Only an air-to-air and air-to-water heat pump system will be analysed. This air-to-water heat pump operates by transporting heated water through a radiator, common practice in household heating systems. The downside of an air source heat pump is that the air temperature differs throughout the year. This is in contrast to a water source system, because the temperature in large bodies of water (such as the Amsterdam canal system) is not fluctuating a lot throughout the day. An upside of using an air-to-air system is that it can be used as an air conditioner as well, when it is installed with a reversing valve [43]. An air-to-water system is slightly more efficient than an air-to-air system, but is not able to cool the boat.

PRINCIPLE OF OPERATION

An air source heat pump consists of an evaporator coil that is filled with a liquid refrigerant (often R410-A). A fan draws in the outside air over this coil, see the evaporator in Figure 3.3.2. The refrigerant in the coil absorbs the heat from the air. It then passes through a compressor which increases its pressure and temperature. The refrigerant is then transported to the internal condenser unit where it delivers its heat to the internal canal boat duct (air) or pipe (water) system with the help of a second heat exchanger coil, see the 'heat sink' arrow in Figure 3.3.2. Finally, the refrigerant passes through an expansion valve which lowers temperature and pressure and the cooled refrigerant is returned to the external evaporator unit again. The 'P' in Figure 3.3.2 stands for pressure.

EFFICIENCY OF HEAT PUMPS

Efficiency of heat pumps is expressed in a Coefficient of Performance (COP), see Equation 3.3.1. The COP is basically the ratio of the heating effect to the net work required to achieve that heating effect [44]. For a COP of 2, there are two units of heating produced for one unit of electricity. Average heat pumps have a COP between 2 and 4 [45, 46], contrary to electric (resistive) heating, which has a COP of 1.

$$COP_{heating} = \frac{Q_{out}}{W_{cycle}} \tag{3.3.1}$$

¹Assuming a fully loaded canal boat, 100 passengers

3.3.2. Heating 53

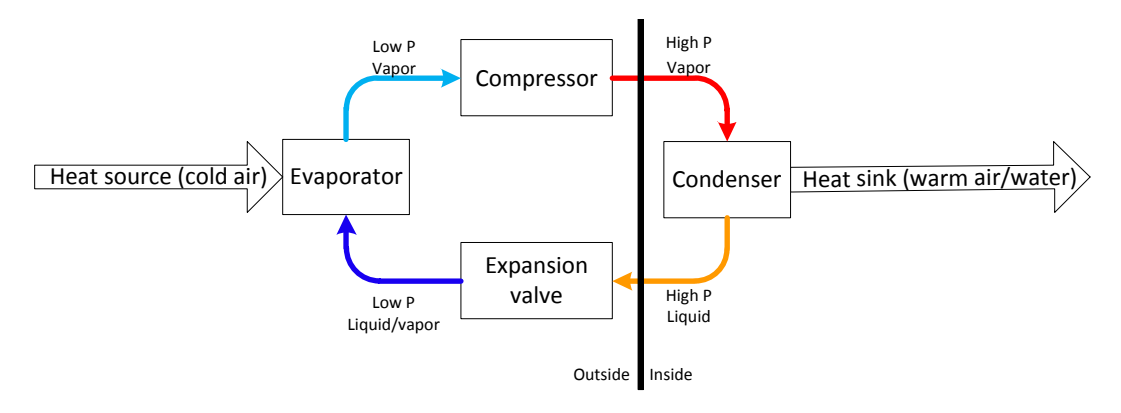


Figure 3.3.2: Air source heat pump operating principle

A problem with heat pumps is that the COP is dependent on the source temperature, in this case air, and that they do not operate well in source temperatures below 0°C. The *minimum* average minimum temperature in Amsterdam from 1951 to 2013 is 0.12°C, in February [16]. Therefore this is not viewed as critical for the Amsterdam situation. At 10°C, the COP of air-source heat pumps is typically about 3.3. At –8.3°C, the COP is typically 2.3 [47, 48]. There is a problem with part load operation though. At low heating load, the heat pump will cycle on and off, giving rise to losses. An empirical efficiency curve based on [48] and [49] incorporating the part-load capacity (PLC) and part-load factor (PLF) is shown in Equation 3.3.2. PLC is the ratio of heating or cooling load divided by the heat pump maximum capacity. PLF is the ratio for part-load to steady state heat pump efficiency, as shown in Equation 3.3.2.

$$PLF = \frac{1.44 \cdot (PLC^2 + 2.91 \cdot PLC)}{PLC^2 + 4.6 \cdot PLC + 0.0339} = \frac{\text{part-load efficiency}}{\text{steady-state efficiency}}$$
(3.3.2)

Plotting Equation 3.3.2 in a graph to obtain the efficiency curve for a typical heat pump gives Figure 3.3.3. It can be seen that below a PLC of 0.2, the performance deteriorates rapidly. It is therefore recommended to let the heat pump operate longer with less capacity (install a throttling valve on the compressor), than at full capacity (at the highest efficiency) and constant off/on switching.

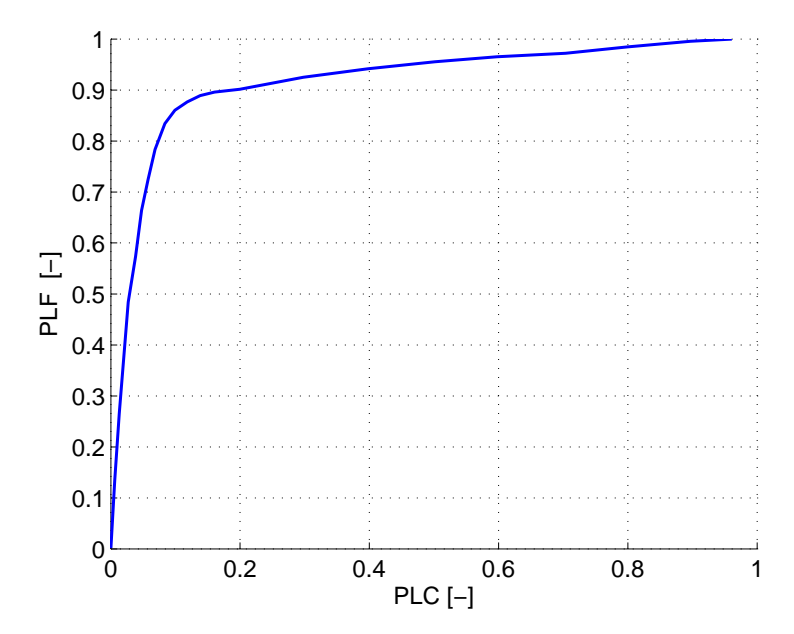


Figure 3.3.3: Part-load empirical efficiency curve for typical heat pumps ([48, 49])

3.3.3. MODELLING OF HEAT PUMP

A Simulink model is created which incorporates the heating time of the canal boat interior. The heat pump is modelled by taking a typical COP curve of an air-source heat pump. This is coupled to ventilation and convection losses. The heat energy is calculated by utilizing the COP and the outside temperature to calculate the heat input in the boat. The passenger space in the canal boat, shown in Figure 3.3.4, heats up and losses will begin to form due to the temperature difference between the inside and outside of the boat. The dynamic internal boat temperature can be controlled by setting the heat pump power and hereby setting the required steady state temperature in the boat. This model takes into account the ventilation and heat loss by convection, to obtain precise estimates of the required energy to heat the canal boat, and to see how long it takes to heat the canal boat to a specific temperature. It is assumed that the boat needs to be heated up from 0°C to 20°C, which makes it a worst-case scenario. The canal boat is modelled as a rectangle consisting of three different parts, see Figure 3.3.4 and Table 3.3.2. No insulation below the waterline is assumed.

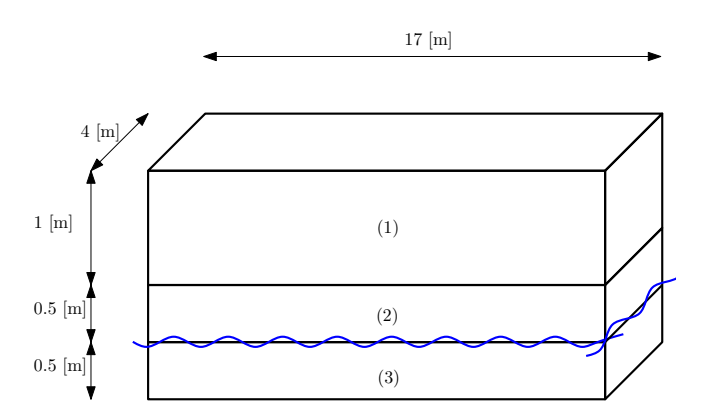


Figure 3.3.4: Schematic view of the modelled canal boat passenger compartment

Segment Material Heat transmission coeffi-Total surface [m²] Steady-state ΔT [K] cient $[W/(m^2 \cdot K)]$ 1.22 88 (1)80% glass 20 20% wood 0.64 22 20 (2)Steel 1.20 17 20 (3)Steel (under waterline) 1.20 85 8

Table 3.3.2: Overview of modelled segments of the canal boat

3.3.1. GOVERNING EQUATIONS

The water temperature is taken as uniform throughout the year at 12°C (see Appendix F, 'Water temperature 1990-2010', Figure E.1). Based on the COP and the set power requirements of the heat pump, Equation 3.3.3 applies. This calculates the temperature that the heat pump yields based on the outside temperature dependency of the COP.

HEAT PUMP ENERGY IN

$$T_{out,HP} = \frac{COP \cdot P_{el}}{\dot{m}_f \cdot c_{p,air}}$$
 (3.3.3)

Where P_{el} is the electric energy in [kW], \dot{m}_f is the flow in [kg/s] and $c_{p,air}$ is the specific heat of air in [J/kg·K]. Based on the yielded heat pump temperature the power that is transferred into the boat in [kJ/s] (or [kW]) is calculated with Equation 3.3.4. This is dependant on the temperature difference between the heat pump yield temperature and the temperature inside the boat (T_{boat}).

$$\dot{Q}_{in} = (T_{out,HP} - T_{boat}) \cdot \dot{m}_f \cdot c_{p,air} \tag{3.3.4}$$

With \dot{Q} in [kJ/s] or [kW]. The net power input is calculated with Equation 3.3.5.

$$\dot{Q}_{net} = \dot{Q}_{in} - \dot{Q}_{loss} \tag{3.3.5}$$

The net energy is divided as shown in Equation 3.3.6 to calculate the temperature rise per second [K/s].

$$\frac{dT_{boat}}{dt} = \frac{\dot{Q}_{net}}{V_{boat} \cdot \rho_{air} \cdot c_{p,air}}$$
(3.3.6)

Here V_{boat} is the volume of the passenger compartment in [m³] as specified by Figure 3.3.4. This is integrated to obtain the instantaneous boat temperature T_{boat} . This temperature is used in a feedback loop to calculate \dot{Q}_{in} and \dot{Q}_{loss} , see Figure 3.3.5.

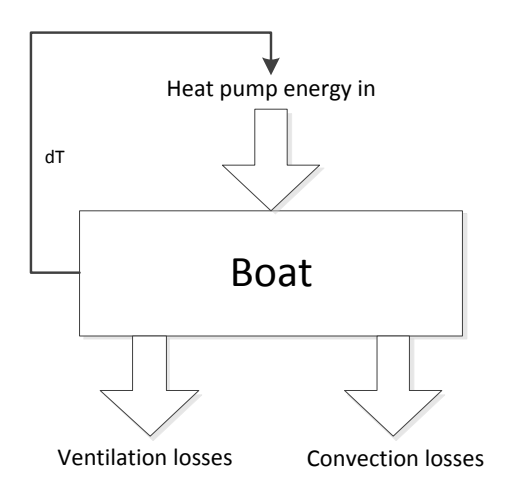


Figure 3.3.5: Schematic view of the input and output streams of the model

CONVECTIVE HEAT LOSS

 \dot{Q}_{loss} consists in this model of two parts, a part for convective heat transfer and a part for ventilation and infiltration. Equation 3.3.7 describes the convective heat loss.

$$\dot{Q}_{loss,conv} = A \cdot \alpha \cdot (T_{boat} - T_0) \tag{3.3.7}$$

Where A is the surface of the material in $[m^2]$ as specified in table 3.3.2, α is the convective heat transfer coefficient in $[W/(m^2 \cdot K)]$ and T_0 is the outside temperature in [K]. The values from table 3.3.2 are used. For the surface below the waterline, a steady-state temperature difference of 8°C is taken.

VENTILATION HEAT LOSS

Natural ventilation losses are estimated with Equation 3.3.8 taken from [50].

$$\dot{Q}_{loss,vent} = V_{boat} \cdot \rho_{air} \cdot c_{p,air} \cdot (T_{boat} - T_0) \cdot ACH \tag{3.3.8}$$

Where air changes per hour (ACH) is equal to Equation 3.3.9:

$$ACH = 3600 \cdot C_v \cdot A_{vent} \cdot \frac{v_{wind}}{V_{boat}}$$
(3.3.9)

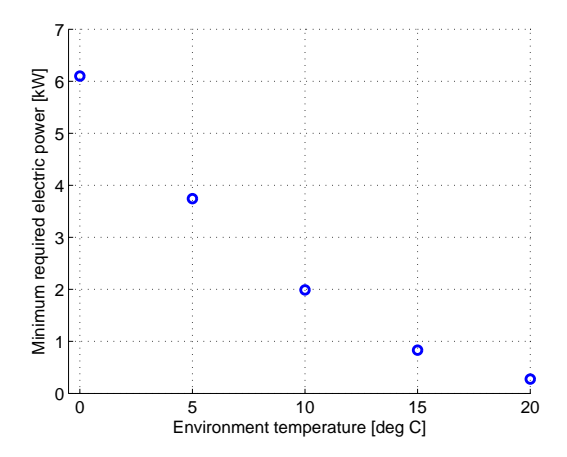
In this equation C_v [-] is a scale factor for the effectiveness of the openings, A_{vent} is the area of the ventilation opening in [m²], V_{boat} is the volume of the passenger compartment in [m³] and v_{wind} is the outside wind velocity in [m/s].

The ACH is thus i.a. dependent on the wind velocity and C_{ν} . For this estimation, a wind velocity of 2 [m/s] and a C_{ν} of 0.05 is taken. The ACH is 1.3 [1/hr], which means that the air in the canal boat is completely refreshed due to natural ventilation 1.3 times per hour.

3.3.3.2. ASSUMPTIONS

Assumptions of this model are:

- Corner effects are ignored
- Wind speed is ignored except for the ventilation losses
- Losses are only dependant on the temperature difference inside and outside the boat
- Temperature of object surface and interior is the same. Conduction and radiation are neglected
- No temperature dependency $c_{p,air}$
- Heat transfer through the underside of the vessel is steady-state
- · Little to no insulation at the under water side of the ship
- Assumed is that the heat pump operates near or on ideal conditions. Referring to Figure 3.3.3 this means that the efficiency is assumed around 1.



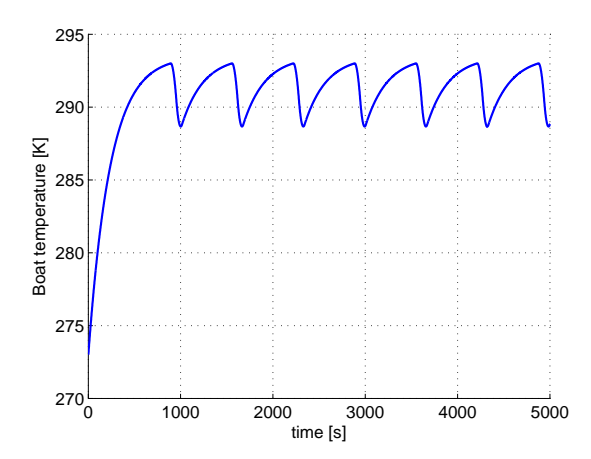


Figure 3.3.6: Minimum required electric power for different environmental temperatures

Figure 3.3.7: Temperature of the boat, starting at 273 [K] and the heat pump is shut off at 293 [K] for lower energy consumption

3.3.3. RESULTS

From Figure 3.3.6 it can be seen that for an outside temperature of 0°C an *electric* power of 6.1 [kW] is required to heat the boat. With this power it will take 15 [min] (900 [s]) to heat the canal boat from 0 to 20°C. With the 6.1 [kW] heat pump and a mean COP value of 2.4 a heat capacity of 14.9 [kW] is generated according to Equation 3.3.1. This is the worst case scenario. The inside boat temperature is visualised in Figure 3.3.7. To lower the energy consumption, the heat pump is switched off for 60 seconds when the desired temperature is reached. In real life, this would have a deteriorating effect on the lifetime and performance of the heat pump but it is included to see what the temperature graph would look like were a throttling valve applied. As can be seen, a steady state situation develops after some time.

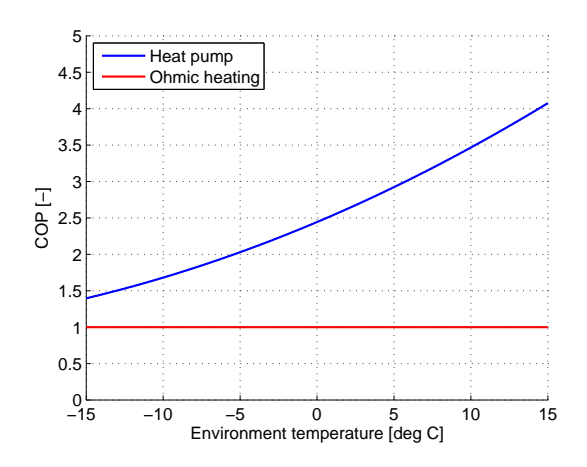
The COP values of both electric heating and the modelled heat pump are given in Figure 3.3.8. As can be seen, the heat pump is depending on the outside temperature but still has a better COP than normal electric heating, for temperatures that far exceed most maximum winter temperatures in the Netherlands. It can be seen that with an outside temperature above 0°C the time to heat the boat decreases rapidly. An economical analysis must be made to determine if this high capacity heat pump will be viable for the occasional low temperatures. A heat pump with less capacity coupled with electric heaters could be more efficient. For the rest of this thesis, as it is a worst case scenario, a heater power of 6.1 (electric) and 14.65 (effective) [kW] is used.

3.3.4. ENERGY OVERVIEW

Canal boats are averaging about 6 hours sailing time per day per boat [16].

If the worst case scenario is taken for heating this means that the canal boat will use 6.1 [kWh] during one hour of operation. For one cruise, a total auxiliary energy consumption of 7.0 [kWh] is required. This is lower than the heated seats option, which uses 9.4 [kWh] during one cruise, and a heat pump has the advantage of heating the whole interior instead of only the posterior. The heat pump is chosen as the most viable option.

3.3.5. Verification 57



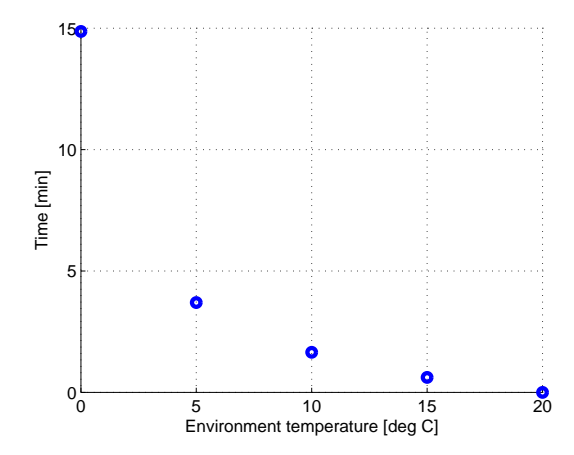


Figure 3.3.8: COP values for different environmental temperatures

Figure 3.3.9: Time required to heat the boat to 20° C with 6.1 [kW] electric power

3.3.5. VERIFICATION

The model is verified with personal communication with ARKA Electric Propulsion Systems. They stated that a ballpark figure to heat the canal boats due to the large surface of glass is $75 \, [W/m^3]$. The total volume of the canal boat is calculated to be $136 \, [m^3]$, and this calculates to a power requirement of $10.2 \, [kW]$. As the $14.9 \, [kW]$ in the model is the worst case scenario, this is in high agreement with the values that are used for the model here. The model is also verified with the Damen Tank Heat Balance Tool v1.05. This is a tool that can be used to calculate the heating of a fuel tank in a ship. It can be used to calculate the air heat requirements. The tool from Damen is based on free and forced convection equations [51]. The comparison between the tool and the model is shown in table 3.3.3. As it is not possible to stop the Damen tool at 20° C, the time to reach an equilibrium temperature is displayed. The results from the constructed model are taken as substantiate.

Table 3.3.3: Comparison between the two models

Variables 0-20 [deg C]	Units	DTHCT v1.05	Simulink model	Difference [-]
Equilibrium temperature	[K]	301.8	302.3	0.99
Time to equilibrium	[s]	1500	2000	0.75
Steady state convection losses	[kW]	4.5	4.9	0.92
Total heat transfer coefficient	$[W/(m^2 \cdot K)]$	2.5	3	0.83

Variables 5-20 [deg C]	Units	DTHCT v1.05	Simulink model	Difference [-]
Equilibrium temperature	[K]	306.6	313.4	0.98
Time to equilibrium	[s]	1500	2400	0.63
Steady state convection losses	[kW]	2.2	5.8	0.38
Total heat transfer coefficient	$[W/(m^2 \cdot K)]$	2.5	3	0.83

BATTERY MODELLING

In this chapter the working principle of a battery is explained. Two different batteries will be specified and modelled in detail.

In Figure 3.4.1 the light green block shows the model that will be described in this chapter: the battery. The dark green models represent the models already defined in earlier chapters.

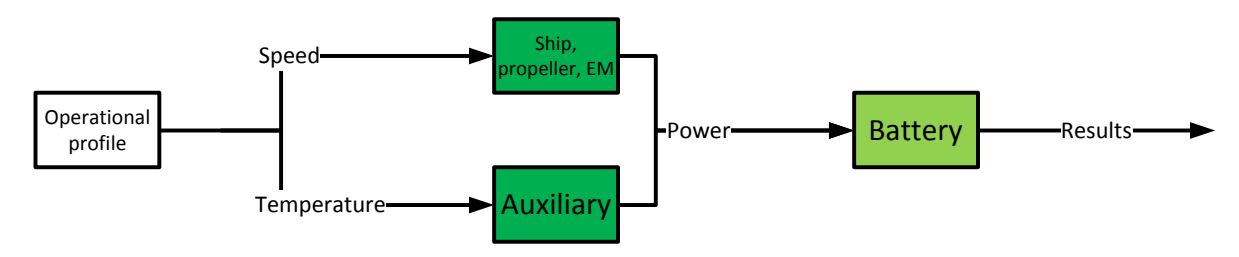


Figure 3.4.1: Model overview

3.4.1. BATTERY TECHNOLOGIES

There are lots of different battery types and technologies used nowadays. Lead-acid, nickel-metal-hydride and lithium-ion to name a few. Between these types, another differentiation can be made based on energy and power. In Table 3.4.1 a short overview of the analysed battery types LMP and LTO is given, with lead-acid as a base reference. The reason to choose lithium ion is given in Chapter 2.3.2.5, 'Battery'. Note that the values in Table 3.4.1 are obtained from manufacturers, whereas the table in Chapter 2.3.2.5, 'Battery' gives more generalized values.

Description	Unit	Lead-acid	LMP	LTO
Specific cost	[Eur/kWh]	150	700	1 400
Cycles 0-100% DOD	[-]	600-800	2 800-3 500	10 000-15 000
Specific weight	[kg/kWh]	35	11	16
Specific energy	[Wh/kg]	35	91	55
Specific volume	[Wh/L]	80	148	145
Nominal cell voltage	[V]	2.1	3.8	2.3

Table 3.4.1: Battery overview, values from manufacturer

3.4.2. BATTERY WORKING PRINCIPLE

A battery converts chemical energy to electrical energy during discharge. As cell voltage and capacity of a battery is often lower than required, it will be required to couple batteries in parallel and/or series to obtain

the required voltage and capacity; parallel connections increase capacity, series connections increase voltage. With a higher voltage, lower currents are required from the energy storage, which is beneficial for the temperature and losses in the energy storage system. The four major components of a lithium battery are the cathode, anode, electrolyte and separator. They are indicated in Figure 3.4.2. Lithium-ion LMP batteries generally produce an average cell voltage of around 3.7-3.8 [V] [52].

ANODE AND CATHODE

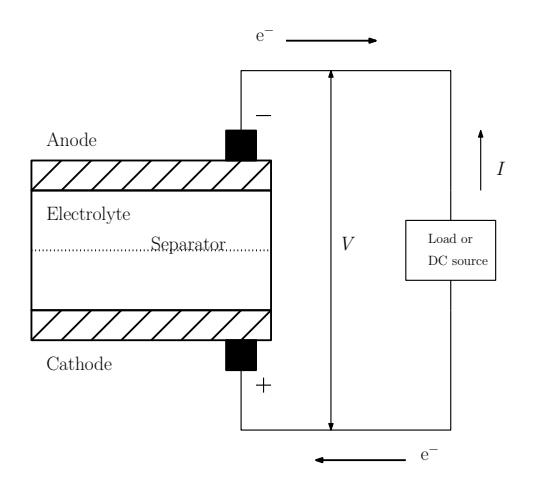
The positive electrode is defined as the cathode during discharging, and as the anode when charging. The negative electrode is defined as the anode during discharging and as cathode during charging [53].

SEPARATOR

The separator is a membrane placed between an anode and cathode. Its first function is to separate the anode and cathode to prevent a short circuit. The second function of the separator is to allow the anions (negatively charged atoms) and cations (positively charged atoms) to flow between anode and cathode. It is therefore a permeable membrane.

ELECTROLYTE

The function of the electrolyte is to act as a transport carrier for the anions and cations between anode and cathode. The electrolyte is ideally an electronic insulator (to prevent short circuits) and a good conductor of the working ion of the cell.



 $Figure\ 3.4.2:\ Main\ components\ of\ lithium\ battery\ cell\ (shown\ ion\ flows\ indicate\ discharging)$

DISCHARGING PROCESS

In Figure 3.4.3 both the discharge as well as the charging state is displayed. The left picture shows the discharging process. A load is applied between the anode and cathode. Electrons flow from the anode through the load to the cathode. The electric circuit is completed in the electrolyte, where the negative ions (anions) and positive ions (cations) flow to the anode and cathode respectively [52]. See Figure 3.4.3.

CHARGING PROCESS

During charging the current flow of the electrons is reversed due to an externally applied voltage. This converts the electrical energy from the power supply into chemical energy. The flow of anions and cations is reversed as well to complete the electric circuit. Notice in Figure 3.4.3 that due to the definitions, the cathode is now the negative electrode whereas the anode is the positive electrode.

3.4.3. BATTERY SPECIFICATIONS

The battery model in this thesis will be based on lithium-ion battery data from different manufacturers. Two battery types will be modelled. Specifications of the data is given in Table 3.4.2[54] and Table 3.4.6. The used Valence battery has a cathode that is made of lithium iron magnesium phosphate (LiFeMgPO₄)¹.

 $^{^1}$ Technically this makes the battery a 'LFMP' battery, but for the sake of clarity and simplicity, it will be abbreviated with LMP, where the M can refer to any metal

3.4.4. Modelling 61

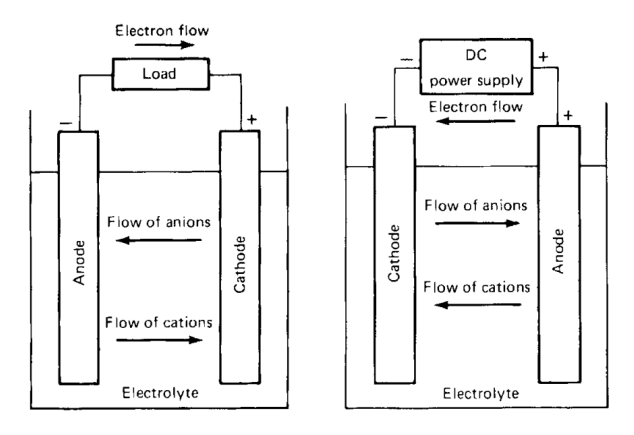


Figure 3.4.3: Electrochemical operation of a cell (left: discharge, right: charge) [52]

Table 3.4.2: Battery pack data from Valence

Manufacturer Type	Valence U27-12XP	
Specifications:		
Nominal module voltage	12.8	[V]
Nominal capacity (C/5, 23°C)	138	[Ah]
Weight (approx.)	19.5	[kg]
Specific energy	91	[Wh/kg]
Discharging current continuous load (25°C)	150	[A]
Discharging current peak load (25°C)	300	[A]
Cut-off voltage (25°C)	10	[V]
Maximum charge voltage	14.6	[V]
Float voltage (recommended current C/2)	13.8	[V]
Charge time (C/2)	2.5	[h]
Maximum internal DC resistance	5.0	$[m\Omega]$

3.4.4. Modelling

Modelling is done in a MATLAB/Simulink environment. The battery model is based on a lead-acid model from Stapersma ([55]) and the theses from Versluijs ([56]) and van Deursen ([57]). Discharging is associated with a positive current, and charging is associated with a negative current. The model is a constant current model during the testing and validation purposes. This means that the current that is required from the battery will be the same as the current delivered by the battery. If the current input is constant, the voltage of the battery is *not*; the voltage is depending on state of charge (SOC), internal resistance, temperature, capacity and required current. These are the battery dynamics visualised in Figure 3.4.4. When the battery model is coupled to the operational profile and the motor the model is a constant power model. This means that the battery will have to deliver the power that the canal boat requires. From the operational profile and the ship model current requirements appear. This will be the input for the battery model. Depending on battery specifications (capacity, number of cells) and the battery dynamics, an output voltage will be generated. This output voltage will be combined with the current to generate the delivered power. The output voltage will be fed back to the operational profile, after which the current will be changed according to the performance of the batteries. As the voltage of the battery decreases in time, a higher current must be applied. This feedback loop, together with the general lay out of the battery model, can be seen in Figures 3.4.4 and 3.4.5.

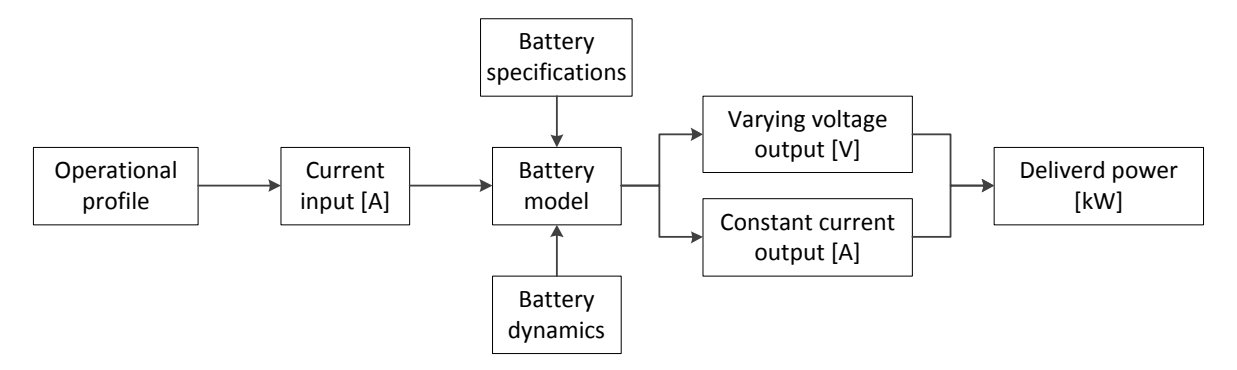


Figure 3.4.4: Battery model macro overview

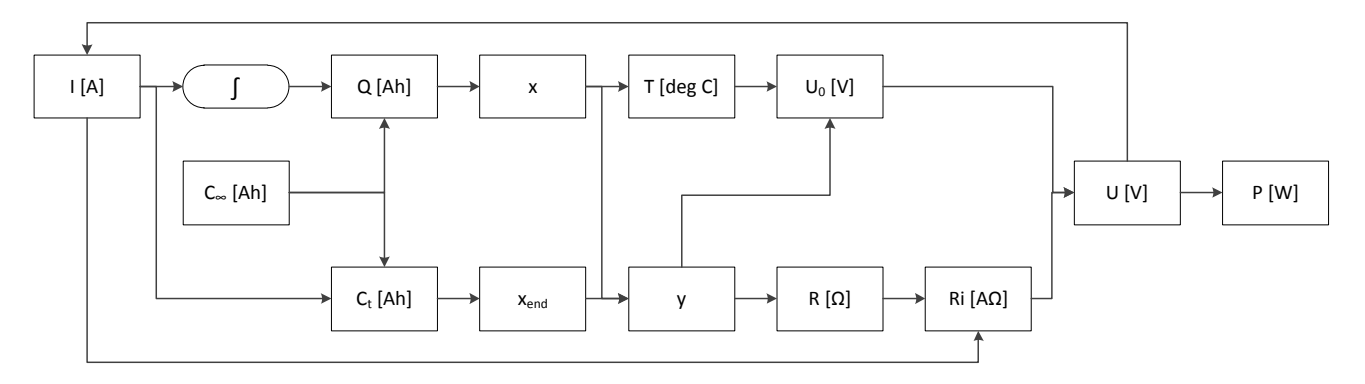


Figure 3.4.5: Battery model overview

The battery model consists of four main equations which define the (dis)charge characteristics:

- Capacity equation
- State of discharge equation
- Open cell voltage equation
- Internal resistance equation

These four equations describe the main battery model. Furthermore there is an ambient temperature model and a lifetime model included that will be discussed as well. Finally battery efficiency will be considered. The four main equations will be discussed next.

3.4.5. CAPACITY EQUATION

The capacity of a battery is defined as a theoretical energy value. This theoretical value is the maximum energy that can be delivered by the battery. Capacity can be defined as current capacity, with unit Amperehour [Ah] or as energy capacity, with unit Watt-hour [Wh]. Two types of capacity are defined in this thesis:

- $C_t(I)$ [Ah], instantaneous capacity dependent on current drawn from the battery.
- C_{∞} [Ah], theoretical maximum capacity at infinitesimal discharge current.

 C_{∞} will be an input for the model, see Figure 3.4.5. Note that in this thesis mostly current capacity will be used. Current capacity will therefore be called just 'capacity' from here on. Delivered charge or delivered capacity Q is defined in Equation 3.4.1. The unit of Q is [Ah]:

$$Q = \int I \cdot dt \tag{3.4.1}$$

From the capacity definitions, variables x, y and x_{end} can be defined. x gives the SOC. Because the discharge curve for a LMP battery is quite flat between 20 and 80% state of charge, it is difficult to determine the SOC in this region. The variable y, pseudo-discharge state is introduced. Pseudo-discharge state gives

the battery discharge at a certain current. The difficulty lies in the battery cell dynamics. When the pseudo-discharge state has reached 1, the battery is empty for that current only. When the current is decreased the battery will be able to continue with the discharge process. In the model y is used to calculate the resistance and open-cell voltage U_0 of the battery.

$$x = \text{real discharge state} = \frac{\text{delivered capacity}}{\text{maximum capacity}}$$
 (3.4.2)

$$x = \frac{Q}{C_{\infty}} = \frac{\int I \cdot dt}{C_{\infty}} \tag{3.4.3}$$

$$y = \text{pseudo-discharge state} = \frac{\text{delivered capacity}}{\text{instantaneous capacity}}$$
 (3.4.4)

$$y = \frac{Q}{C_t(I)} = \frac{\int I \cdot dt}{C_t(I)}$$
(3.4.5)

$$x_{end}$$
 = discharge factor = $\frac{\text{instantaneous capacity}}{\text{maximum capacity}}$ (3.4.6)

$$x_{end} = \frac{x}{y} = \frac{C_t(I)}{C_{\infty}} \tag{3.4.7}$$

C RATING

The C rate is a common applied method to indicate the (dis)charge current of a battery [58].

The C rating of a battery states how long a battery can discharge at a certain constant current. It is defined in Equation 3.4.8. For example, a C rating of 1C means that, whatever the capacity of the battery, will be discharged in one hour. The value of this constant current is dependant on the capacity of the battery. 0.5C means that the battery will be discharged in two hours, 0.1C that it is discharged in 10 hours. In chapter 4.3, 'Simulation results', often the term charge C rate is used. This definition can be approached from two sides: One, it can be defined as the time it takes for a battery to charge, 2C meaning that the battery will be charged in 30 minutes. Two, it can be defined as the appropriate charge power, meaning that when 2C is mentioned for a pack of 50 [kWh], it means that the pack will be charged with 100 [kW]. The latter definition will be used mostly in this thesis, although this is dimensionally incorrect, see Equation 3.4.8².

$$C_r = I \cdot C_n \tag{3.4.8}$$

Where C_r is the C rate, I is in [A] and C_n is the value of rated capacity in [Ah]

3.4.5.1. COEFFICIENTS

To calculate the capacity, some coefficients must be defined and used to calculate the battery characteristics for each type of battery. As stated before, the Valence data is used for the LMP battery. Four coefficients are defined, α , β , τ and τ_{char} . α shapes the minimum value for $C_t(I)$ that can be obtained. β is the 5 [hr] fraction of the total infinite discharge capacity. τ_{char} is the characteristic discharge time in [hr] for the 5 [hr] fraction. τ is the characteristic discharge time in [hr]. Their definitions can be found in equations 3.4.9, 3.4.10, 3.4.11 and 3.4.12, respectively. Table 3.4.3 displays used values. The lowercase c denotes c denotes c denotes capacity in [Ah/kg], where an uppercase c denotes capacity in [Ah]. This is not to be confused with the c rating, c.

$$\alpha = \frac{W_{cell} \cdot c_0}{W_{cell} \cdot c_{\infty}} = \frac{19.5 \cdot 6.7}{19.5 \cdot 7.6} = 0.88$$
 (3.4.9)

$$\beta = \frac{W_{cell} \cdot c_5}{W_{cell} \cdot c_\infty} = \frac{19.5 \cdot 7.1}{19.5 \cdot 7.6} = 0.93$$
 (3.4.10)

$$\tau_{char} = \left(\frac{1-\alpha}{\beta-\alpha}\right) = 2.25\tag{3.4.11}$$

$$\tau = t_5 \cdot \ln(\tau_{char}) = 5 \cdot \ln(2.25) = 4.05 \tag{3.4.12}$$

 $^{^2}$ See chapter 3.4 of the Handbook of Batteries, [58], for a more detailed explanation of the used C rate

With these previous equations the characteristic current in [A] can be calculated, see Equation 3.4.13.

$$I_{char} = \frac{W_{cell} \cdot c_5}{\tau} = \frac{19.5 \cdot 7.1}{4.05} = 34.15 \tag{3.4.13}$$

SPECIFIC CAPACITIES

Specific capacities for the used Valence cells are displayed in Table 3.4.3

Table 3.4.3: Specific capacities at different c levels

Specific capacity		
$-c_0^{\ 3}$	6.7	[Ah/kg]
c_5^4	7.1	[Ah/kg]
${c_{\infty}}^5$	7.6	[Ah/kg]
t_5	5.0	[h]
W_{cell}	19.5	[kg]

The capacity equation is taken from [55–57] and displayed in Equation 3.4.14. Note that C_{∞} is the capacity in [Ah], as stated previously. With Equation 3.4.14 the capacity in relation to installed capacity (C_{∞}) can be displayed for varying input currents. I_{in} is the input current from the operational profile. Note that the absolute value is used, this is required as for charging a negative current will be assumed.

$$C_t(I) = C_{\infty} \cdot \left(\alpha + \alpha \cdot e^{-\left(\frac{|I_{in}|}{I_{char}}\right)} \right)$$
(3.4.14)

In Figure 3.4.6 different I_{in} currents are used to visualize the relation between the capacity and the current. In the figure the current is increasing every second with 1 [A], from 0 to 300 [A]. It can be observed that the capacity remains constant when the current has reached a certain value of about 200 [A]. This means that the instantaneous battery capacity will not go down any further when an even larger current is required from the battery. Hence, if the battery is 100% charged, and is discharged with a constant current of 50 [A], it can be seen from Figure 3.4.6 that there is only about 91% of the battery capacity available. This is an important observation, as the available battery capacity is somewhere between the capacity at C_{∞} and this lower limit. These results are in accordance with [56]. Combining Equation 3.4.7 with Equation 3.4.14 gives Equation 3.4.15.

$$x_{end} = \frac{C_t(I)}{C_{\infty}} = \left(\alpha + \alpha \cdot e^{-\left(\frac{|I_{in}|}{I_{char}}\right)}\right)$$
(3.4.15)

3.4.6. State of discharge equation

x is defined as the real discharge state, also known as state of discharge (SOD). This means that when x is equal to 1, the battery is completely empty. The SOC and SOD are defined in Equations 3.4.16 and 3.4.17 respectively. State of charge is often expressed in a value between 0-1, or with a percentage (0-100%). The SOC displays how much charge is left in the battery, when it is equal to 0, the battery is empty.

$$1 - x_d = SOC \tag{3.4.16}$$

$$1 - SOC = SOD = x_d \tag{3.4.17}$$

Recalling Equation 3.4.3, it can be seen that both I and C_{∞} are known inputs, and hence x (and the SOC) can be calculated easily.

$$x = \frac{Q}{C_{\infty}} = \frac{\int I \cdot dt}{C_{\infty}}$$
 (ref. 3.4.3)

When *x* is known, the pseudo-(dis)charge state *y* can be calculated. When this pseudo discharge state is 1, it means that the battery cannot be discharged any further with the current drawn. (This current must

³infinite current

⁴C/5 current

 $^{^5}$ zero current

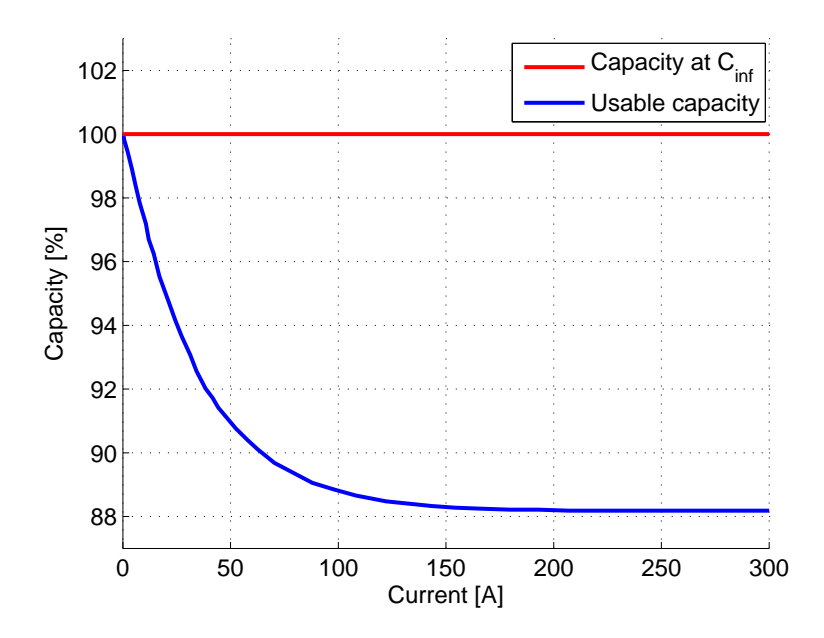


Figure 3.4.6: C_t as function of I_{in}

decrease, then y decreases as well and then there is some charge left again in the battery.) As can be seen from Figure 3.4.5, y is required to be able to calculate the open cell voltage and the internal resistance of the battery. However, both x and y have a different definition when charging or discharging, see Equations 3.4.19, 3.4.20 and 3.4.21. Subscripts d and d stand for discharging and charging, respectively.

$$x_{end} = \frac{x_d}{y_d} = \frac{C_t}{C_{\infty}} \tag{3.4.18}$$

$$y_c = 1 - y_d (3.4.19)$$

$$x_c = 1 - x_d = SOC (3.4.20)$$

Combining these equations:

$$x_{end} = \frac{x_d}{y_d} = \frac{(1 - x_c)}{(1 - y_c)} \tag{3.4.21}$$

3.4.7. OPEN CELL VOLTAGE EQUATION

To calculate open cell voltage U_o , a distinction needs to be made for the charging and discharging situations, as for these equations the voltage at zero discharge state (x=0) is required, which differs between the states. Looking at Table 3.4.2, the maximum charge voltage is 14.6 [V], whereas the maximum discharge voltage is taken as 13.45 [V].

3.4.7.1. OPEN CELL VOLTAGE DISCHARGING

The equation for the open cell voltage is given in 3.4.22 for discharging. Parameters a and b can be calculated with equations 3.4.23 and 3.4.24. A complete derivation of these equation can be found in Stapersma [55]. Parameter e is used to curve the 'tail' of the discharge curve after $\pm 80\%$ of (dis)charge. Here it is assumed as 10.

$$U_o(y) = U_o(0) \cdot (1 - a \cdot y - b \cdot y^e)$$
(3.4.22)

$$a = \frac{\left(1 - \frac{U_o(0.7)}{U_o(0)}\right) - (0.7)^e \cdot \left(1 - \frac{U_o(1)}{U_o(0)}\right)}{(0.7 - 0.7^e)}$$
(3.4.23)

$$b = \frac{0.7 \cdot \left(1 - \frac{U_o(1)}{U_o(0)}\right) - \left(1 - \frac{U_o(0.7)}{U_o(0)}\right)}{(0.7 - 0.7^e)}$$
(3.4.24)

For discharging, the following values are used:

- U(0) = 13.45 [V]
- U(0.7) = 13.00 [V]
- U(1)= 12.00 [V]

a is calculated as 0.0475 and b is 0.0603. e is assumed as 16.

3.4.7.2. OPEN CELL VOLTAGE CHARGING

The same equations apply as for the calculation of the open cell voltage during discharging, but now with the parameters and values used for charging. These are indicated throughout this report with a $'\sim'$ symbol. See equations 3.4.25, 3.4.26 and 3.4.27.

$$\tilde{U}_0(y) = \tilde{U}_0(0) \cdot (1 - \tilde{a} \cdot y - \tilde{b} \cdot y^{\tilde{e}}) \tag{3.4.25}$$

$$\tilde{a} = \frac{\left(1 - \frac{\tilde{U}_0(0.7)}{\tilde{U}_0(0)}\right) - (0.7)^{\tilde{e}} \cdot \left(1 - \frac{\tilde{U}_0(1)}{\tilde{U}_0(0)}\right)}{(0.7 - 0.7^{\tilde{e}})}$$
(3.4.26)

$$\tilde{b} = \frac{0.7 \cdot \left(1 - \frac{\tilde{U}_0(1)}{\tilde{U}_0(0)}\right) - \left(1 - \frac{\tilde{U}_0(0.7)}{\tilde{U}_0(0)}\right)}{(0.7 - 0.7^{\tilde{e}})}$$
(3.4.27)

For discharging, the following values are used:

- $\tilde{U}(0) = 13.40 [V]$
- $\tilde{U}(0.7) = 13.25 [V]$
- $\tilde{U}(1)=12.00 [V]$

 \tilde{a} is calculated as 0.0151 and \tilde{b} is 0.0894. \tilde{e} is assumed 14 for charging.

3.4.8. Internal resistance equation

The internal resistance of the battery cell can be estimated with Equation 3.4.28. Only the maximum resistance value (5 m Ω) at discharge is given by the manufacturer. The resistance at the pseudo-discharge state y is again dependant on charging or discharging state. As the voltage of the battery drops when a constant current is applied, a linear relation between internal resistance and voltage is assumed, Equation 3.4.28.

$$U(y) \approx I(y) \cdot R_{\text{int}}(y) + c \tag{3.4.28}$$

R(y) is defined as the pseudo resistance dependent on the pseudo-(dis)charge state y. Equation 3.4.29 is used to calculate the resistance as a function of y [57]. Here, the ' indicates pseudo-resistance (resistance as a function of y).

$$R'(y) = R(0) \cdot (1 + c \cdot y^d) \tag{3.4.29}$$

Where:

$$c = \frac{R'(1)}{R'(0)} - 1 \tag{3.4.30}$$

$$d = \frac{\ln\left(\frac{R'(0.7)}{R'(0)} - 1\right) - \ln(c)}{\ln(0.7)}$$
(3.4.31)

3.4.8.1. RESISTANCE DURING DISCHARGING

Using Equations 3.4.30 and 3.4.31 the following values for c and d are found: c is -0.42. d is 3.288. d > 1 implies a non-linearity in the internal resistance, as can be seen from Figure 3.4.7.

For discharging, the following values are used:

- $R'(0) = 5.00 [m\Omega]$
- $R'(0.7) = 4.35 [m\Omega]$
- $R'(1) = 2.90 [m\Omega]$

3.4.8.2. RESISTANCE DURING CHARGING

For charging, as the voltages are different, the resistance differs as well. $\tilde{R}(0)$ is here taken at zero current, as there is no data available from the manufacturer. The following values give the least error margin on the manufacturer data on charging:

- $\tilde{R}'(0) = 15.00 [m\Omega]$
- $\tilde{R}'(0.7) = 5.00 [m\Omega]$
- $\tilde{R}'(1) = 4.15 [m\Omega]$

For charging, using equations 3.4.30 and 3.4.31, \tilde{c} is found to be -0.7233 and \tilde{d} is 0.2287. Plotting the internal resistances as a function of y gives Figure 3.4.7.

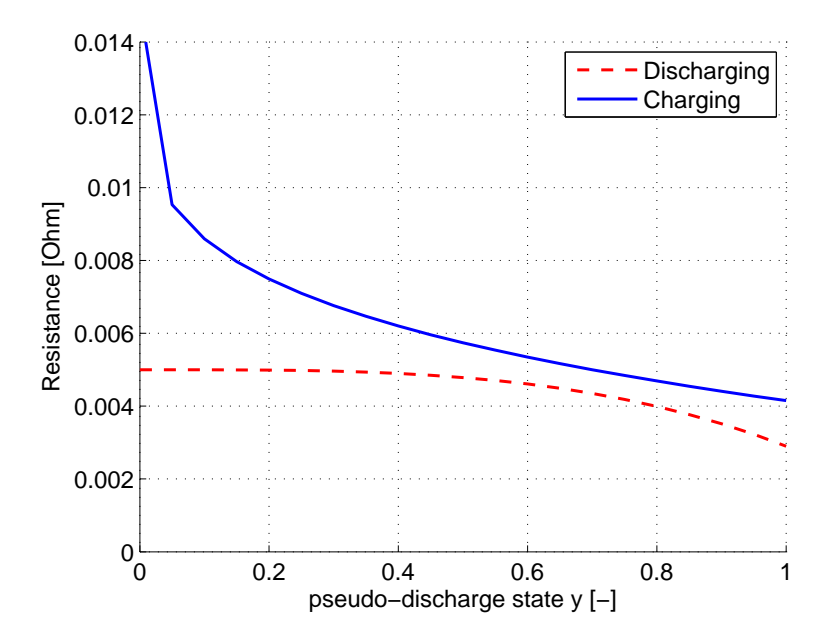


Figure 3.4.7: Resistance as a function of pseudo-discharge state y

3.4.8.3. INFLUENCE OF DIFFERENT C VALUES

In Figure 3.4.8 the influence of the C rating is visualised for a fixed temperature of 23°C. This is used to check whether the model can handle high and low C ratings. The C ratings displayed in Figure 3.4.8 differ from 0.1C to 2C. It can be seen that for low C values the battery has slightly more capacity than for higher C ratings. This is in accordance with the specifications of the manufacturer and can be explained by the fact that the capacity of the battery is lowered when larger currents are drawn. Higher C ratings mean higher currents, and thus lower available capacity.

3.4.9. Temperature dependency

Available from the manufacturer is the temperature graph as shown in Figure 3.4.9. In this section, this data will be used with new equations to generate a discharge curve that is similar to the data of the manufacturer. This temperature dependent discharge curve equation can then be altered to calculate different temperature influences.

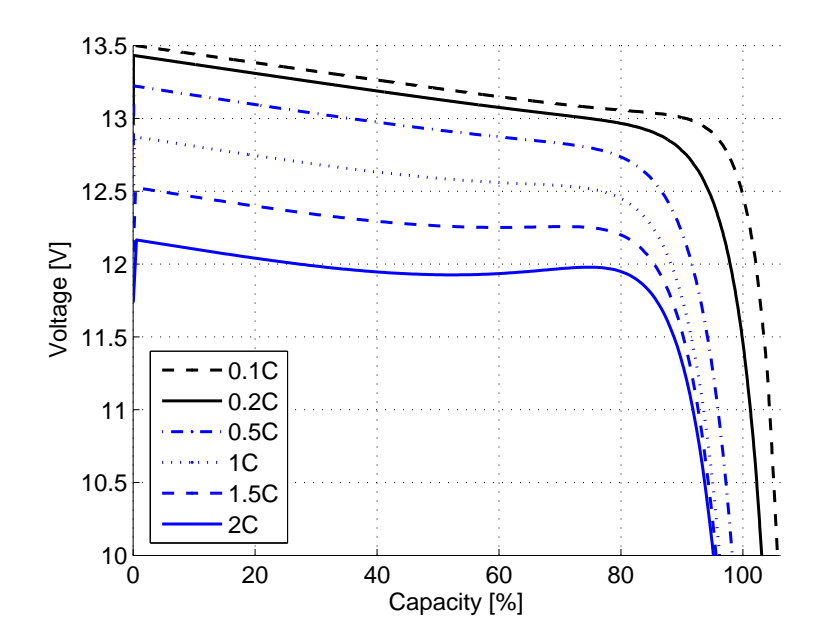


Figure 3.4.8: Modelled capacity curves for different C values

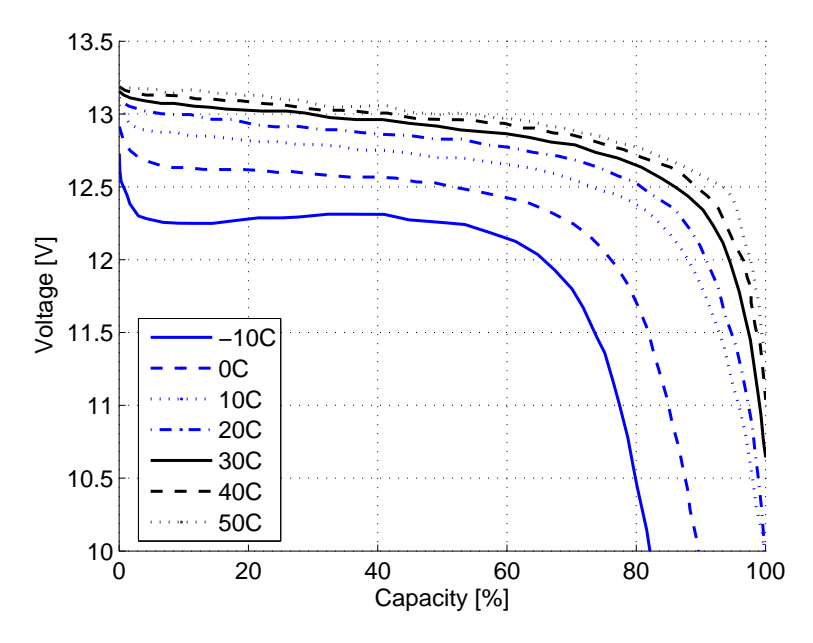


Figure 3.4.9: Temperature discharge curves from the manufacturer, as function of capacity and voltage

The discharge curves in Figure 3.4.9 are only valid for a discharge rate of 0.5C.

3.4.9.1. GENERAL TEMPERATURE EQUATION

To be able to incorporate temperature dependency into the model, an equation for temperature is constructed. In this thesis, a 2^{nd} order exponential function is conceived, see Equation 3.4.32.

$$U(x)_{T} = f \cdot e^{(g \cdot x)} + h \cdot e^{(i \cdot x)}$$
 (3.4.32)

Parameters f, g, h and i are fitted for each manufacturer curve and given in Appendix J, 'Battery parameters for temperature fit'. Parameter h is the starting voltage at x=0. The strong curved section of the discharge curve that can normally be found at the beginning of the discharge curve is neglected in this equation. It can

be seen from figures 3.4.10(a) and 3.4.10(b) that these modelled curves created with Equation 3.4.32 are in high accordance with the temperature discharge curves at 0.5C. It is therefore assumed that this is also the case with larger currents.

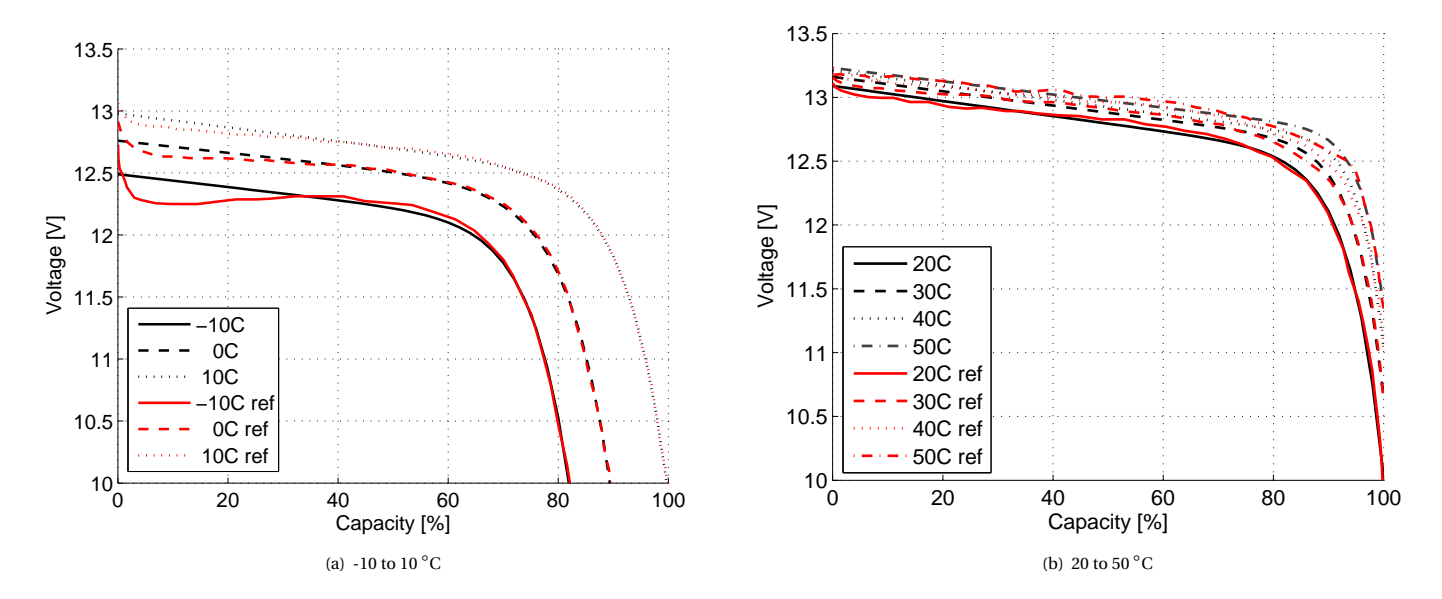


Figure 3.4.10: Valence and modelled discharge curves for different temperatures

3.4.9.2. TEMPERATURE EQUATION INCLUDED IN THE MODEL

The equations for each temperature curve are incorporated into the model. The influence of the temperature can now be visualised, see figures 3.4.11(a) and 3.4.11(b).

Note that figures 3.4.10(a) and 3.4.10(b) give the relation between the **manufacturers data** and Equation 3.4.32, whereas figures 3.4.11(a) and 3.4.11(b) give the relation between the **modelled** discharge curves and Equation 3.4.32.

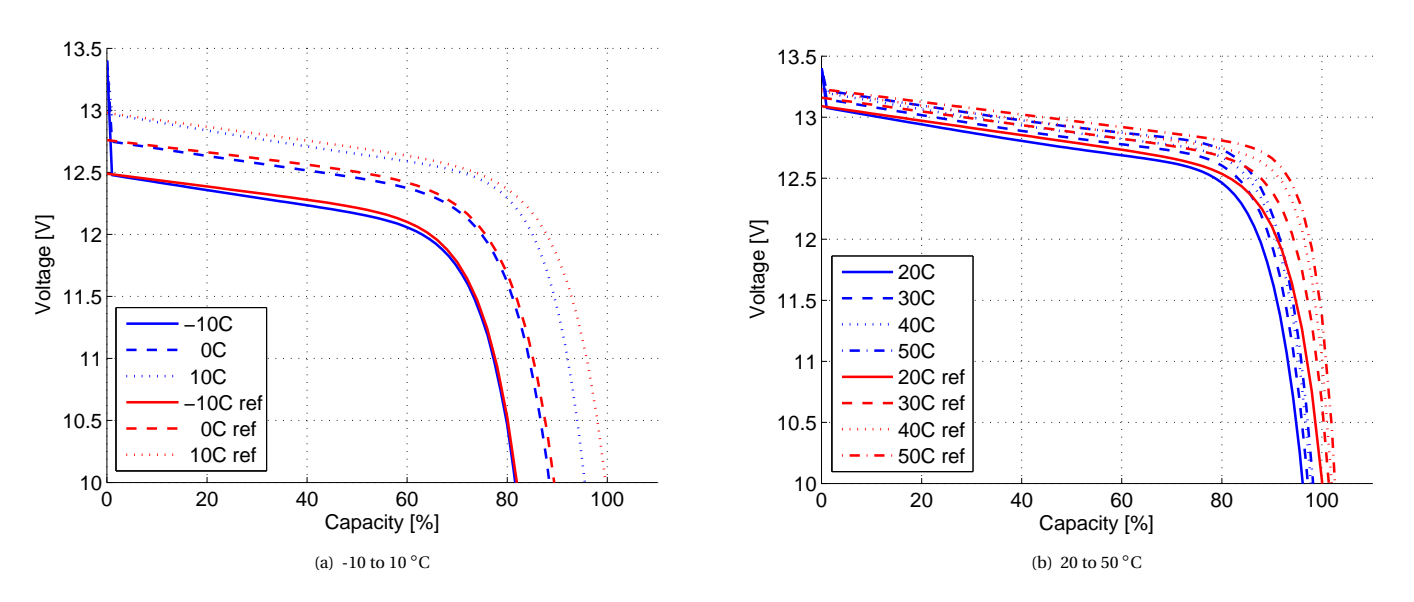


Figure 3.4.11: Modelled capacity curves for different temperature values compared to Equation 3.4.32

As can be seen from figures 3.4.11(a) and 3.4.11(b) the modelled curves compared to the temperature

curves differ less than 5% between each other. This is taken as adequately accurate.

3.4.9.3. TEMPERATURE FACTOR

The manufacturer only has public data about the 0.5C temperature curves. To be able to acquire satisfactory results when using different C factors in the model a new scaling factor γ is introduced.

As can be seen in Figure 3.4.9, the temperature dependency is incorporated in the calculation of the open cell voltage. Hence, Equation 3.4.33 is conceived:

$$\gamma(x,T) = \frac{U(x,T_{set})}{U_{23}(x)}$$
 (3.4.33)

Here, $U(x, T_{set})$ is the interpolated voltage from the discharge Equation 3.4.32 as a function of x and the ambient temperature T_{set} . It is divided by the reference voltage at a temperature of 23°C, U_{23} .

This factor γ is multiplied with the calculated cell voltage U_o , see Equation 3.4.34.

$$U = U_0(I, x) \cdot \gamma(x, T) - R(y) \cdot I \tag{3.4.34}$$

The underlying practical meaning is that the cell voltage is multiplied with some sort of 'temperature index', the factor γ . This γ is calculated for every timestep and x value, and scales the output cell voltage with a factor dependent on temperature information. It can be seen in Figure 3.4.12 that the capacity of the battery decreases slightly when the battery is discharged with 1C instead of 0.5C. This decrease in capacity seems small, but the voltage of the cell is also lower. For example the starting voltage is 12.5 [V] at -10°C for 1C and 12.6 [V] at -10°C for 1C. This means that the capacity of the cell is slightly lower, but that the current also has to increase for a larger C value to get the same power. An increase of current means a lower capacity, so when doing simulations, capacity for a higher C value will decrease more than the graphs in Figure 3.4.12 show.

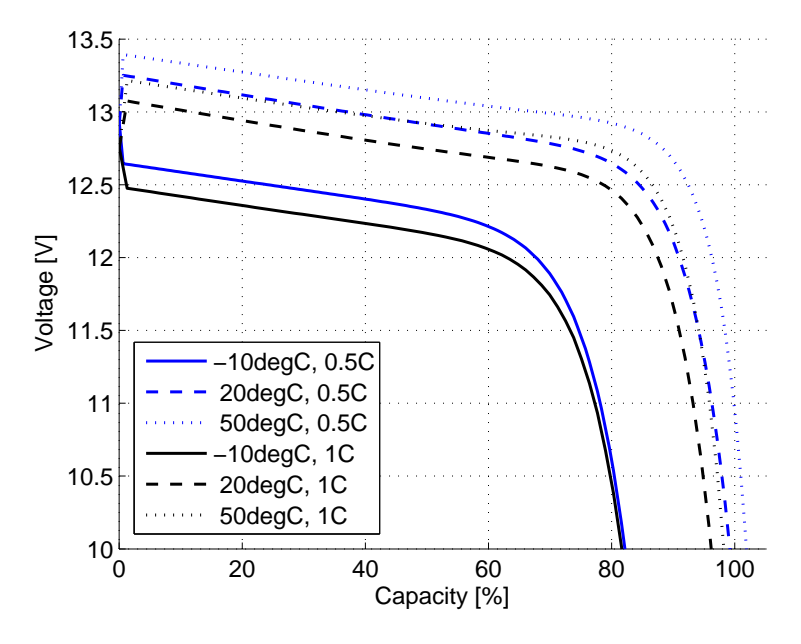


Figure 3.4.12: Temperature discharge curves from the model, dependent on C rate and temperature

3.4.10. BATTERY LIFETIME

Knowing the lifetime is one of the key parameters to be able to correctly size battery capacity. Capacity decreases over time dependent on temperature, cycles, current and state of charge the battery has been in. To be able to estimate the remaining life of the battery, a simple model is calculated based on data of the manufacturer and a linear approximation. The Valence batteries can be discharged from 100 to 0% for $2\,800$ cycles and still have 80% of their capacity left, according to the manufacturer. See Figure 3.4.13. The R^2 value of

3.4.10. Battery lifetime 71

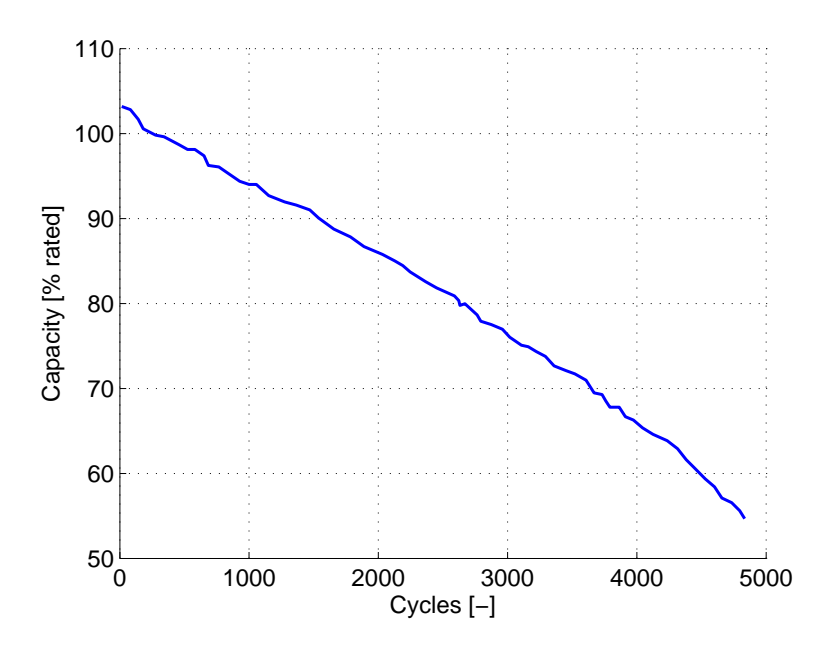


Figure 3.4.13: Capacity decrease with respect to applied cycles (Source: Valence)

a linear fit of this capacity decrease due to cycles is over 99%, so it is assumed that the capacity decreases linearly with the amount of cycles used.

The lifetime equation is divided in two parts, the maximum capacity the battery can deliver, and the cumulative delivered capacity. Together this gives an indication of the available life time and/or capacity of the battery. The complete equation is given in Equation 3.4.35. A detailed explanation will follow, first for the denominator and then the numerator.

$$C_{LC} = 100 - \left(\frac{Q_{LC}}{C_{LC,\text{max}}} \cdot 100\right)$$
 (3.4.35)

MAXIMUM LIFETIME CAPACITY

The maximum capacity is shown in Equation 3.4.36:

$$C_{LC,\text{max}} = C_{LC,100} - (f_{cap} \cdot n_{LC})$$
 (3.4.36)

 $C_{LC, {
m max}}$ is the maximum theoretical capacity that the battery can deliver. This is a function of $C_{LC, 100}$, the capacity at zero cycles multiplied with the amount of cycles until 80% capacity is reached, Equation 3.4.37. (In the case of the Valence LMP, 148 [Ah]).

$$C_{IC,100} = C_{\infty} \cdot n_{IC,max} \tag{3.4.37}$$

 C_{∞} defined as in section 3.4.5, Capacity equation. The variable $n_{LC,max}$ is the amount of cycles the battery is able to function between the maximum capacity $C_{LC,100}$ and the 80% capacity $C_{LC,80}$. f_{cap} is defined as the linear reduction of the capacity, up until 80% of original capacity is reached, Equation 3.4.38.

$$f_{cap} = \left(\frac{C_{LC,100} - C_{LC,80}}{n_{LC,max}}\right) \tag{3.4.38}$$

 $C_{LC,80}$ is the available capacity in [Ah] at 80% of the maximum capacity. The variable $n_{LC,max}$ is the amount of cycles the battery is able to function between the maximum capacity $C_{LC,100}$ and the 80% capacity $C_{LC,80}$.

 n_{LC} is defined as the cumulative sum of the depth of discharge (DOD). Phrased differently it gives the absolute amount of cycles depending on DOD, as not every cycle will be from 0 to 100% discharge. This variable scales the cycles with the amount of capacity that has left the battery, see Equation 3.4.39. Ideally n_{LC} will not exceed $n_{LC,max}$, but this is possible if a further decrease of capacity is allowed below 80%. The limit n in the summation sign indicates the cycle threshold, which for Valence is 2800.

$$n_{LC} = \sum_{n} x_{LC} \tag{3.4.39}$$

The resulting equation, Equation 3.4.36, hence gives the maximum capacity of the battery depending on amount of cycles that the battery has undergone. This amount of cycles takes into account that not all cycles are full cycles and corrects for this.

CUMULATIVE DELIVERED LIFETIME CAPACITY

The second part of the equation is the cumulative delivered lifetime capacity in the numerator. It is defined in Equation 3.4.40, where Q_{LC} is in [Ah].

$$Q_{LC} = C_{\infty} \cdot \sum_{n} x_{LC} \tag{3.4.40}$$

Combining Equation 3.4.40 with 3.4.39:

$$Q_{LC} = C_{\infty} \cdot n_{LC} \tag{3.4.41}$$

LIFETIME EQUATION

Combining numerator with the denominator gives the proposed lifetime equation:

$$C_{LC} = 100 - \left(\frac{Q_{LC}}{C_{LC,\text{max}}} \cdot 100\right) = 100 - \left(\frac{C_{\infty} \cdot n_{LC}}{\left(C_{LC,100} - \left(f_{cap} \cdot n_{LC}\right)\right)} \cdot 100\right)$$
(3.4.42)

Here, C_{LC} gives the percentage of capacity available.

CALCULATION EXAMPLE

To explain the method of calculation, a short example is introduced. If the battery is discharged *for the first time* and discharged until it is 30% empty (DOD of 0.3) before it was recharged again, n_{LC} is 0.3. This means that the battery has made 0.3 cycles during its life. When the next cycle is to a DOD of 0.9 it is added to n_{LC} . This gives a n_{LC} of 0.9 + 0.3 = 1.2, so 1.2 full cycles out of the possible maximum defined by $n_{LC,max}$.

Calculating an example and taking the Valence data and calculating for a n_{LC} value of 2000:

 $Table\ 3.4.4: Calculation\ example\ for\ the\ Valence\ battery\ and\ 2000\ out\ of\ 2800\ used\ cycles$

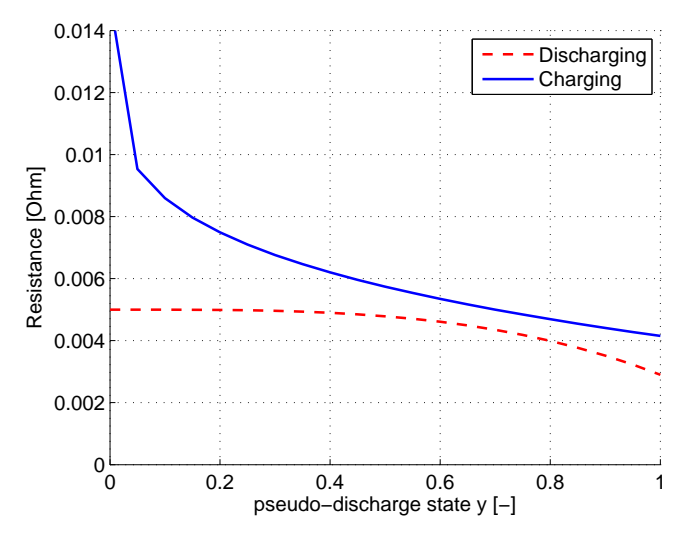
Description	Data source	Variable	Value	Unit
Amount of <i>full</i> cycles until 80% capacity remains	Manufacturer	$n_{LC,max}$	2800	[-]
Maximum capacity of one cycle (2 packs)	Manufacturer	C_{∞}	296	[Ah]
Total maximum life time capacity	Installed capacity	$C_{LC,100}$	828 800	[Ah]
Remaining life time capacity at 80%	Installed capacity	$C_{LC,80}$	663 040	[Ah]
Capacity decrease factor	Equation 3.4.38	f_{cap}	59.2	[Ah/cycle]
Used cycles	Equation 3.4.39	n_{LC}	2000	[-]
Total available capacity	Equation 3.4.36	$C_{LC,\max}$	710400	[Ah]
Used capacity	Equations 3.4.40 and 3.4.41	Q_{LC}	592 000	[Ah]
Remaining capacity [abs]	Q_{LC} minus $C_{LC,\max}$		118 400	[Ah]
Remaining capacity [%]	Equation 3.4.42	C_{LC}	17	[%]

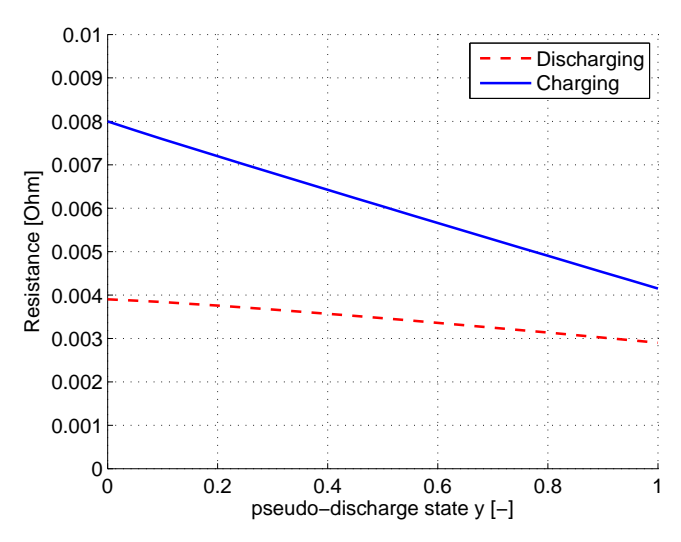
Note that the remaining capacity is 17%, instead of $(100-(2000/2800)\cdot 100)$ 29%. The usage of this lifetime calculations is limited by the low amount of available data from the manufacturer regarding lifetimes of the batteries. As can be seen from Figure 3.4.13, only one life time curve is available. This curve is at one discharge and charge current, at one temperature. Therefore caution is advised when using this linear model to assess battery life time, as influences like temperature, SOC per cycle and current peaks are not taken into account here.

3.4.11. VERIFICATION OF BATTERY MODEL

3.4.11.1. VERIFICATION OF RESISTANCE VALUES

No dynamic values of resistance as a function of the pseudo-discharge state y are known for the battery. Therefore, as a first estimate, the values from [57] were used. The results can be found in Figure 3.4.14(b),





(a) Resistance values that are used in the model, as function of pseudo-discharge state y

(b) Resistance according to [57] as a function of pseudo-discharge state y

When comparing Figure 3.4.14(a) to 3.4.14(b) it can be seen that they differ slightly, especially for values of y above 0.8 and below 0.2. It is unsure how the values from the thesis of Deursen (see [57]) are found for charging, but the values here presented give a higher consensus with the manufacturers data. The thesis of de Waard, [29], uses the SOC to fit the values to the data of Valence. As there is no pseudo-discharge state y defined (only the complement of the SOC, SOD=(1-SOC)) this method gives inaccurate or erroneous results for the model used in this thesis. A further observation is that the calculated resistance for charging has a maximum value of $14 \text{ [m}\Omega$], which is in accordance with the test results mentioned in the report of de Waard [29], whereas the method of de Waard gives results that differ a factor 6 [29].

3.4.11.2. Verification of discharge curve

The curve given by the manufacturer at 23° C and 0.5C should be equal to the modelled curve. In Figure 3.4.14(c) the two curves are shown. In Figure 3.4.14(d) the difference factor σ , defined as in Equation 3.4.43 is visualised.

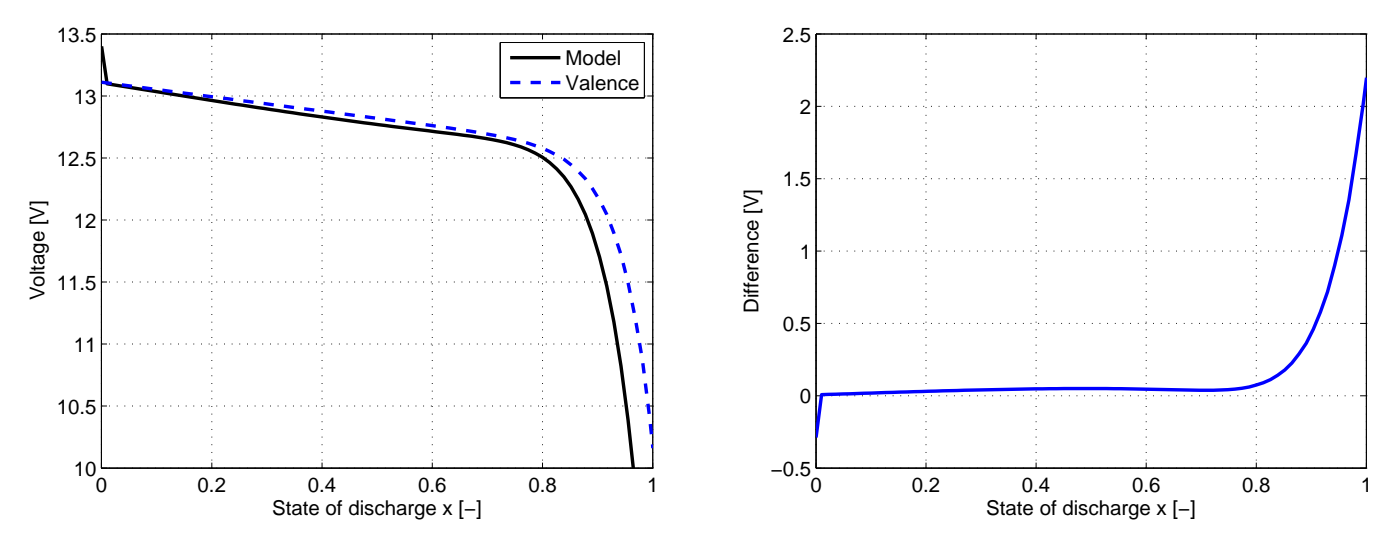
$$\sigma(x) = \frac{U_{valence}(x)}{U_{model}(x)}$$
(3.4.43)

 σ is clearly a non-linear function of the discharge state. The difference between the two functions rises steeply after $x \approx 0.8$. After a state of discharge larger then 0.8 the difference rises rapidly. It is noted that the model is not accurate in this region, as the difference is around 25 to 30%, see Figure 3.4.14(e). Zooming in on the region between 0.2 and 0.8 state of discharge, there is a high correlation between the model and the data from the manufacturer (difference is less than 0.6%). The small voltage drop in Figures 3.4.14(c) and 3.4.14(d) at x = 0 is the capacity drop that occurs between theoretical maximum capacity and the capacity that is available when there is a current drawn from the battery.

As a final check, the curves for pseudo discharge state y are visualised in Figure 3.4.15.

DISCHARGING COMPARED TO VAN DEURSEN MODEL

The difference between the model, manufacturers' data and the van Deursen model is depicted in Figure 3.4.16(a). σ , the factor that displays the error between the data from Valence and the model, is factors higher than the model with the parameters presented in this thesis, see Figure 3.4.16(b).



(c) Difference between the discharge curve given by Valence (blue) and calculated by the model (black) at $23^{\circ}\mathrm{C}$ at $0.5\mathrm{C}$

(d) Difference in voltage between the discharge curve of Valence and the model at 23°C

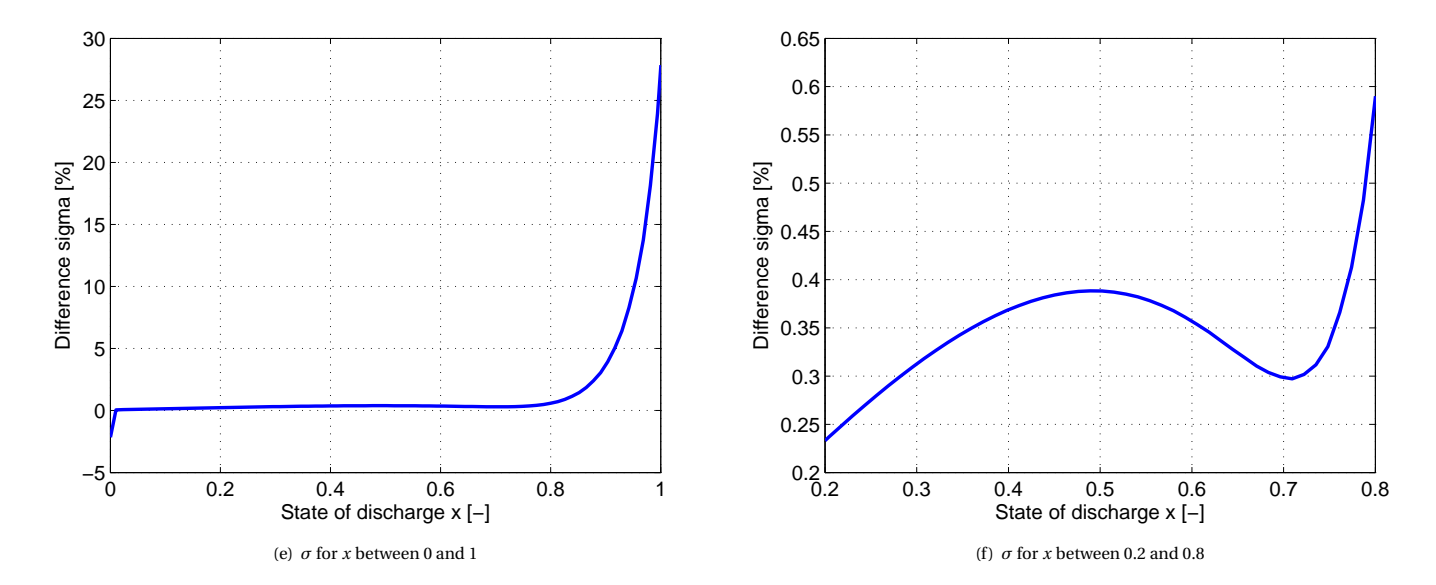


Figure 3.4.14: Difference factors σ

3.4.11.3. VERIFICATION OF CHARGE CURVE

The differences between the charge curve at 0.2C for the model and given data is given in Figure 3.4.17(a). There is high accordance between these curves, as can be seen from Figure 3.4.17(b) the difference throughout the whole charging process never exceeds 4%. This automatically means that the values chosen for the charge resistance are verified as well.

3.4.11.4. VERIFICATION OF TEMPERATURE DEPENDENCY

In the theses of Versluijs [56] and de Waard [29], temperature dependencies were included in a battery model in the form of a equation that compared the state of discharge of each temperature line at 10 [V] (empty battery) with the reference value at 23°C. This leads to an over- or underestimation depending on the ambient temperature. This error emerges because the manufacturers' discharge curves are clearly non-linear, as can be seen in Figure 3.4.9. The static method of temperature scaling used in Versluijs ([56]) and de Waard ([29]) is therefore less accurate than the method presented here, which calculates the difference between the reference and the ambient temperature for each time step.

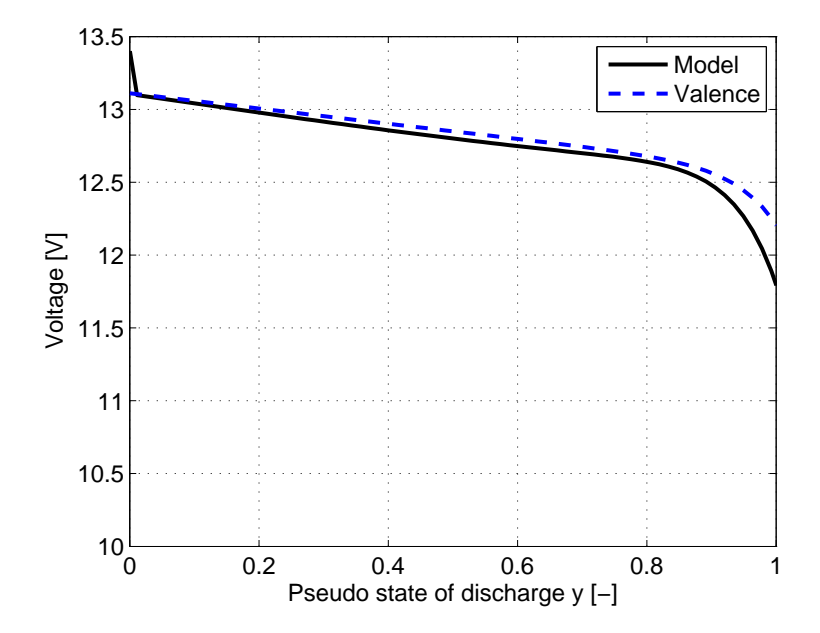


Figure 3.4.15: Modelled and Valence data for pseudo-discharge state y

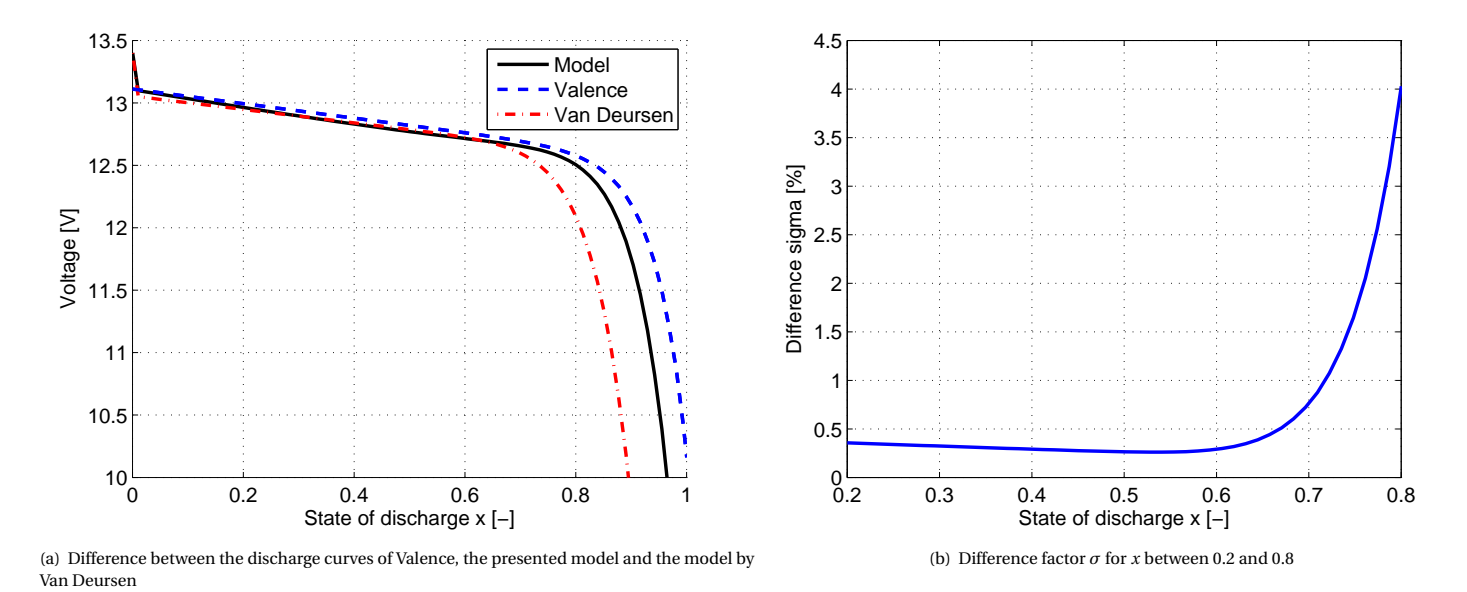


Figure 3.4.16: Different curves of Valence, the presented model and the model by Van Deursen compared

CHANGING TEMPERATURE VARIABLES

When raising voltage $U_o(0)$ to 12.30 [V] instead of 12.0 [V] better results for temperature discharge curves are obtained. This however has a degrading influence on the accuracy of the model when the temperature is not included. The values used in this thesis serve as an acceptable trade-off between the discharge curves with and without temperature influence. The discharge curve is taken as leading, as the temperature influence in this thesis will not be extreme (the canal boats operate in the 0-20°C region for the most part). This, together with the reason mentioned in 3.4.11.5, Battery data discussion is the reason that, for example, Figure 3.4.11(b) differs from the manufacturer data for capacity >80%.

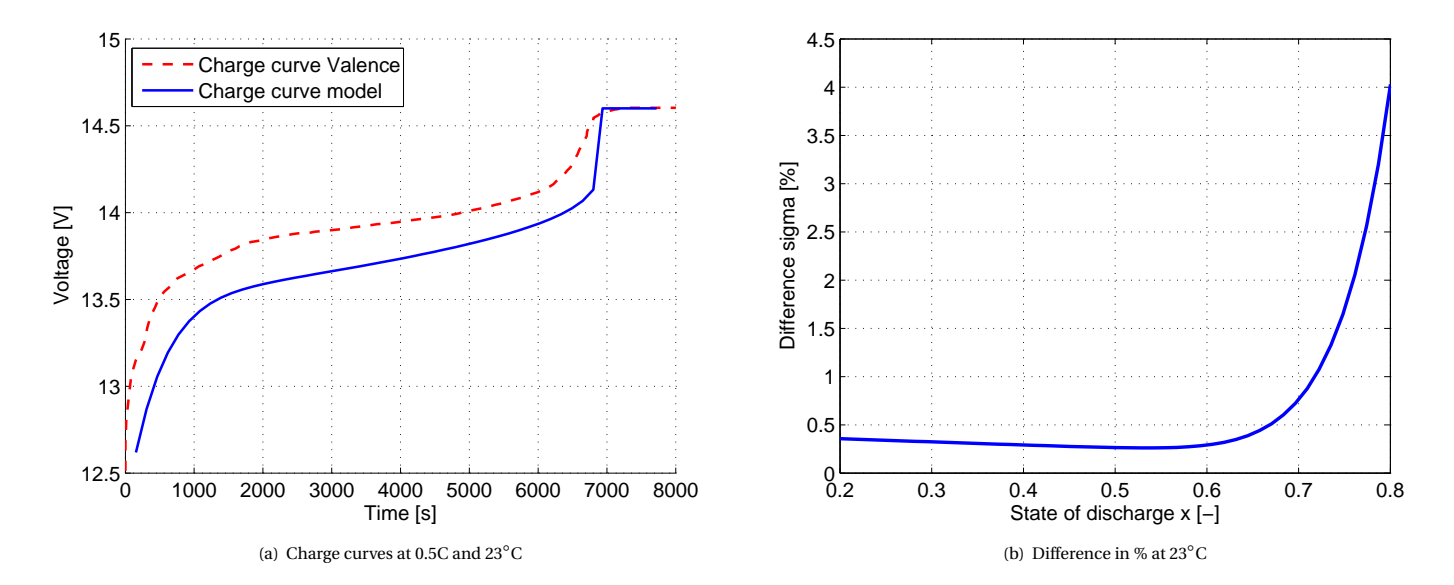


Figure 3.4.17: Charge curve comparison between model and Valence

3.4.11.5. BATTERY DATA DISCUSSION

When analysing the data from Valence, there was one small notable difference between two curves, see Figure 3.4.18. Shown here are two curves, both data from the manufacturer itself. However, the indicated Tcurve is the curve shown on the specification sheet as a temperature curve, whereas Dcurve is show in the discharge curve graph. If this data was correct, both should be equal, but this is not the case. Keeping this in mind, small errors due to this difference could have been made when fitting the parameters to the curves. Overall however the model shows great accuracy, especially in the region where capacity is between 20 and 80%.

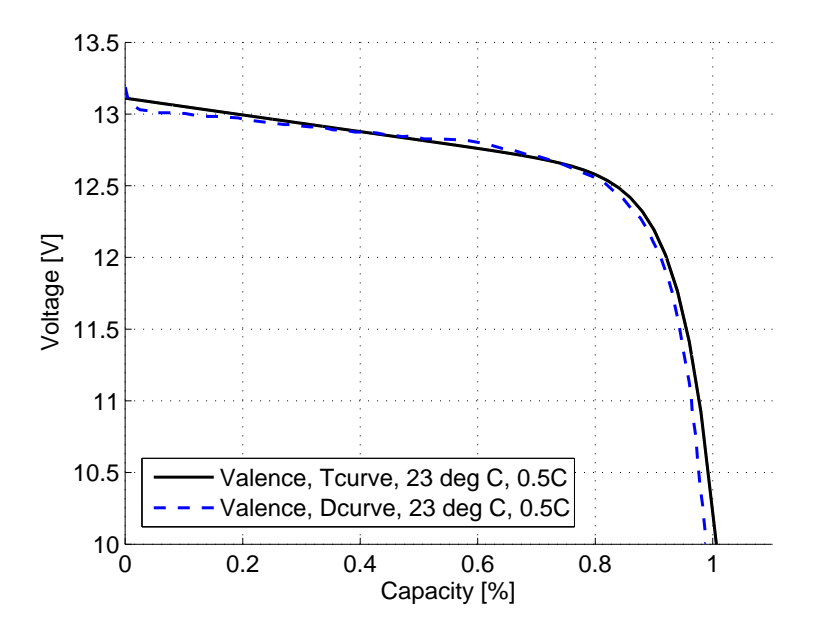


Figure 3.4.18: Difference between 0.1, 0.5 and 1C at 23°C

3.4.12. Overview of calculated variables and parameters

For easy reference, the used parameters and coefficients are given in Table 3.4.5.

3.4.13. LTO BATTERY 77

Discharging		Charging		
а	0.0475	ã	0.0151	[-]
b	0.0603	\tilde{b}	0.0894	[-]
c	-0.42	\tilde{c}	-0.7233	[-]
d	3.288	$ \tilde{d} $	0.2287	[-]
e	16	\tilde{e}	14	[-]
<i>U</i> (0)	13.45	$ ilde{U}(0)$	13.40	[V]
U(0.7)	13.00	$\tilde{U}(0.7)$	13.25	[V]
U(1)	12.00	$\tilde{U}(1)$	12.00	[V]
R(0)	5.00	$\tilde{R}(0)$	15.00	[mΩ]
R(0.7)	4.35	$\tilde{R}(0.7)$	5.00	[mΩ]
R(1)	2.9	$\tilde{R}(1)$	4.15	[mΩ]

Table 3.4.5: Calculated values and coefficients for LMP battery calculation

3.4.13. LTO BATTERY

Another type of battery, the LTO battery, is modelled. The advantage of the LTO battery is that it can have an extremely long lifetime with up to 20 000 cycles (3-5 times the amount of cycles of a similar LMP battery). The reason that this is possible is that there is an extremely small expansion and contraction during the charge and discharge phases of the battery. This is very important to achieve a high number of cycles [59].

3.4.13.1. LTO APPLICATION IN THE AMSTERDAM CANALS

This battery holds great promises for the canal boat industry, as it is capable of very high C rates when charging (up to 4C, see Table 3.4.6). It is not often used in a maritime environment due to its low specific energy that is about two thirds (63 [Wh/kg] versus [91 Wh/kg]) of a LMP battery. Practically, this translates to a high battery weight for the same energy compared to its lithium brethren. As the canal boats hulls are filled with lead to give them the depth able to sail underneath the low bridges in Amsterdam, weight is not an issue. In Table 3.4.6 the data regarding the LTO battery cell is given.

Manufacturer Type	Leclanché LecCell 30Ah	
Specifications:		
Nominal module voltage	2.3	[V]
Nominal capacity (C/10)	30	[Ah]
Weight (approx.)	1.1	[kg]
Specific energy	63^{6}	[Wh/kg]
Discharging current continuous load	30	[A]
(Dis)charging current peak load	120	[A]
Cut-off voltage	1.7	[V]
Maximum charge voltage	2.7	[V]
Maximum internal DC resistance	2.0	$[m\Omega]$

Table 3.4.6: Battery data from Leclanché

3.4.14. MODEL CONSTRAINTS

To compare the two lithium technologies, the model explained in the previous chapter is adapted via the parameters. This does not give a strictly precise model, as for discharge values over 1C the model will differ up to 10% with the discharge curves from the manufacturer, see Figure 3.4.19(a). This error is due to the following facts:

• The model is adapted to suit the LTO discharge curves and not specifically built for LTO. The LTO curve

⁶Cell level. Used is 55 [Wh/kg] as cell specific energy is always higher than maximum output energy

is less flat than the LMP.

• There is no information available about the internal resistance of the LTO batteries. This has to be estimated.

Furthermore all limitations of the LMP model still hold. For example, there are only two charging curves available. Keeping this in mind, the model will still give a fair estimate of the performance when it is discharged with less than 2C.

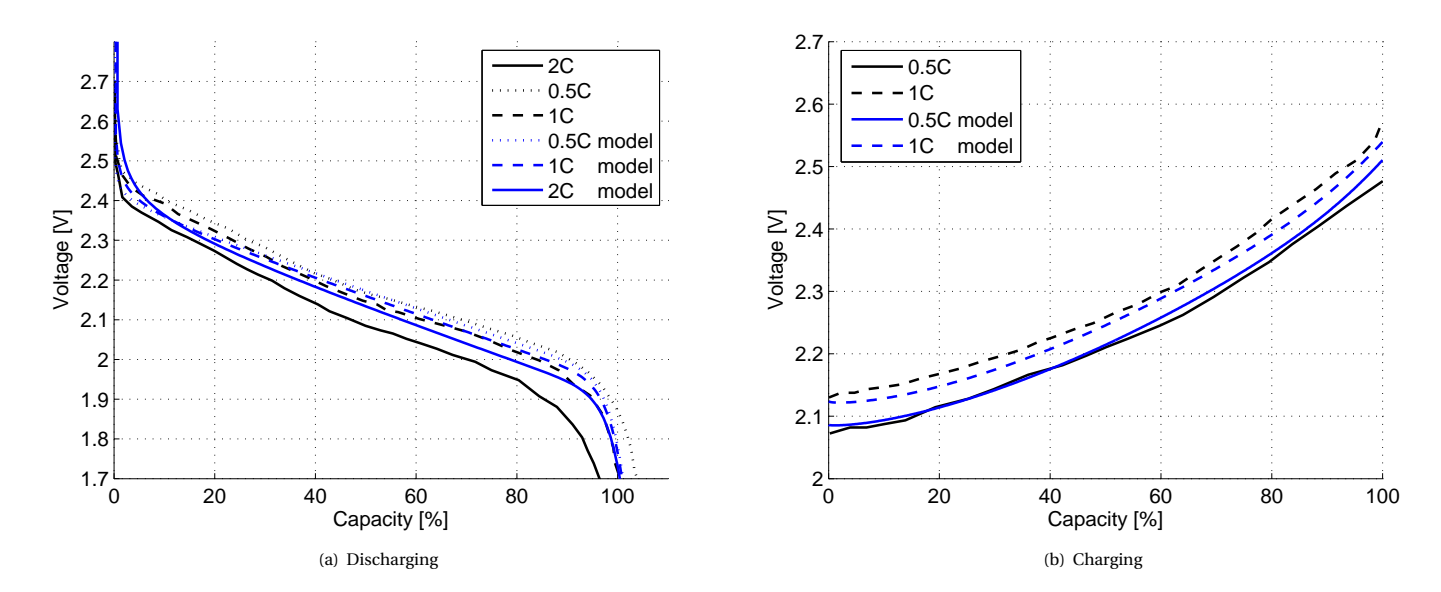


Figure 3.4.19: Modelled curves compared to data from Leclanché

3.4.15. PARAMETERS

The parameters for discharging and charging are summarized in Table 3.4.7. The same equations as for the LMP battery are used, hence they will not be repeated here. Note that the (voltage) values here are given for one cell as specified by the manufacturer, whereas the LMP battery was for a module pack.

Discharging		Charging		
a	0.1786	ã	0.0146	[-]
b	0.0714	$\mid ilde{b} \mid$	-0.2053	[-]
c	-0.4350	\tilde{c}	-0.2400	[-]
d	-0.3848	$\mid ilde{d} \mid$	0.5112	[-]
e	35	\tilde{e}	1.5	[-]
U(0)	2.40	$ ilde{U}(0)$	2.05	[V]
U(0.7)	2.10	$\tilde{U}(0.7)$	2.27	[V]
U(1)	1.80	$\tilde{U}(1)$	2.435	[V]
R(0)	2.00	$\tilde{R}(0)$	2.50	[mΩ]
R(0.7)	1.002	$\tilde{R}(0.7)$	2.10	$[m\Omega]$
R(1)	1.13	$\tilde{R}(1)$	1.90	$[m\Omega]$

Table 3.4.7: Calculated values and coefficients for LTO battery calculation

3.4.16. BATTERY EFFICIENCY

Battery efficiency can be divided in two definitions. The first is internal battery efficiency, giving the efficiency of internal reactions in the battery itself. The second is battery cycle efficiency, which takes into account the efficiency of charging and discharging as well as the internal battery efficiency.

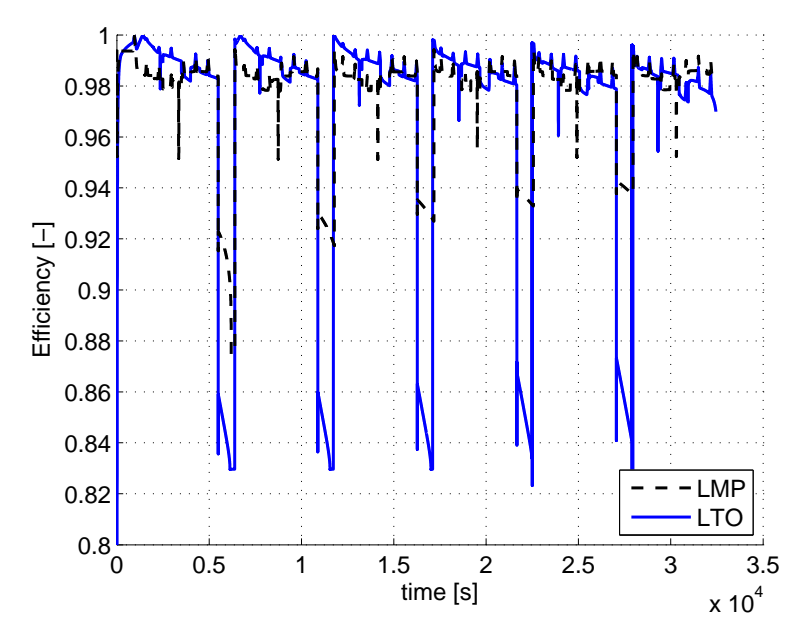
3.4.16.1. INTERNAL EFFICIENCY

This is defined as the efficiency due to the internal resistance. Internal battery efficiency is defined as the terminal voltage divided by the open cell voltage, Equation 3.4.44. The difference between the terminal voltage U and the open cell voltage U_0 is the IR loss due to the internal resistance, Equation 3.4.45.

$$\eta_{batt,internal} = \frac{U}{U_o} \tag{3.4.44}$$

$$U = U_o - I \cdot R \tag{3.4.45}$$

The internal battery efficiency is defined by Equation 3.4.44. The mean value of internal battery efficiency during one simulated day is for both types of batteries 0.97. See also Table 3.4.8 where the efficiencies for discharging and charging are given for both battery technologies during a typical day. Charging is done with 0.5C for LMP and 2C for LTO.



 $Figure~3.4.20: {\it Internal}~battery~efficiency~during~discharging~and~charging~for~a~typical~LTO~and~LMP~simulation~and~charging~for~a~typical~LTO~and~LMP~simulation~and~charging~for~a~typical~LTO~and~charging~for~a$

Table 3.4.8: Daily averaged internal battery efficiency

Combined LTO	0.97
Discharge LTO	0.99
Charge LTO	0.85
Combined LMP	0.97
Discharge LMP	0.98
Charge LMP	0.93
Charge LMP	0.93

3.4.16.2. CYCLE EFFICIENCY

The second definition of battery efficiency is battery cycle efficiency. It is defined as the efficiency regarding the whole battery cycle, including charging, discharging and internal resistance. It can therefore only be obtained when charging is applied in the simulation. Cycle efficiency arises when the fully charged battery is discharged with a certain energy. When charging with the *same* energy and power, the battery will not be fully charged again due to losses. This is visualised in Figure 3.4.21, where the battery is switched from discharging to charging at $t = 3\,000$ [s] but is not completely charged to $t = 0\,000$ [s]. This end value of SOD can be rewritten to an efficiency, see Equation 3.4.46:

$$\eta_{batt,cycle} = \frac{E_{discharged}}{x_{t,end} \cdot E_{nominal} + E_{charged}}$$
(3.4.46)

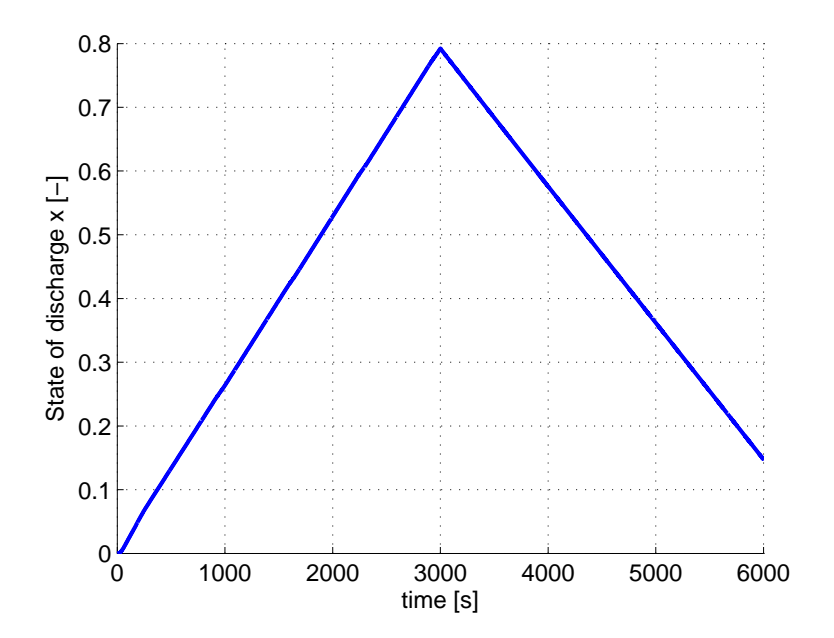


Figure 3.4.21: Visualisation of battery cycle losses during discharging and charging

In Equation 3.4.46, $E_{discharged}$ is the total discharged energy by the battery (excluding charging energy). $x_{t,end}$ is the DOD at the end of the simulation. This is multiplied with the nominal battery energy, $E_{nominal}$ to obtain the theoretical required energy that is required to charge the battery fully. Added to this value is the energy that is used for charging, $E_{charged}$. Dividing this by the discharged energy gives a factor. Using the nominal energy gives an indication of the efficiency, as the voltage is not constant during charging and/or discharging. However, this is a simple method that gives acceptable results. Charging LMP with 0.5C gives a cycle efficiency of 0.96, and for 1C this was 0.92. These values are in accordance with common values.

ENVIRONMENTAL PERFORMANCE INDICATOR METHOD

How can the environmental load of a ship be correctly defined? Environmental Performance Indicators (EPIs) give an indication of the environmental load of a person or platform on the direct surroundings. In the case of a vessel or boat they are a combination of design, sailing profile and maintenance. This indication of environmental loads can be done in dozens of possible ways. In this chapter, an overview of current EPI frameworks will be given, and it will be explained why they are not satisfactory for small passenger vessels such as canal boats in Amsterdam. For these vessels, a new 'Amsterdam canal index' must be defined.

3.5.1. BACKGROUND

Already in 1950 there was a so called 'coefficient of specific tractive force' introduced in a famous paper by Gabrielli and von Karman called 'What Price Speed?' [60]. This index forms the basis for the Energy Efficiency Design Index (EEDI) carbon dioxide (CO₂) index [61]. It consists of the power consumption of different modes of transport divided by the so-called 'transport capacity' that is defined as gross weight times velocity. The result of this division gives the 'coefficient of specific tractive force' [60], which is a non-dimensional quantity defined by the following equation:

Transport Efficiency =
$$\frac{P_{max}}{w \cdot V_s}$$
 (3.5.1)

In their article, Gabrielli and von Karman mention that the real measure of economy of a transportation mode should be the work necessary to transport certain useful load over a given distance, and not gross weight as in Equation 3.5.1. The general idea of Gabrielli and von Karman was used in [55, 62] to define a Specific Pollutant Index (SPI) according to operational profiles, and in Van de Ketterij et al., [61], to form a CO₂ design index based on different operational modes tailored for the dredging industry.

3.5.2. CURRENT INDICES

The idea of EPIs is not new. There are already many EPIs defined by different organizations. An overview and short description of the different EPIs follows. This section will answer the following research question:

What are existing methods to rate ships?

(Ref. Q.2.1)

3.5.2.1. EEDI

The EEDI was adopted during the Marine Environment Protection Committee (MEPC) 62^{nd} session [63–65] and is used as a design index. Measures to reduce emissions of Greenhouse Gases (GHGs) from international shipping are included in the International Convention for the Prevention of Pollution From Ships (MARPOL) Annex VI. They are mandatory since 1 January 2013 [63, 64] despite concerns of different parties [61, 66–70]. It focuses mainly on reducing CO_2 emissions, since CO_2 is the most important Greenhouse Gas (GHG) emitted by ships [71].

The fundamental EEDI equation is given in Equation 3.5.2.

$$EEDI = \frac{P \cdot SFC \cdot C_f}{DWT \cdot V_{ref}}$$
(3.5.2)

Where:

- P is installed power measured at 75% Mean Continuous Rating (MCR)
- SFC is the SFC of the engine(s)
- C_f is the CO_2 emission rate based on fuel type
- DWT is the Deadweight (DWT) tonnage
- V_{ref} is the vessel speed at the installed power measured at 75% MCR and DWT

There is some discussion about the EEDI, mainly about its effectiveness. It is pointed out by different sources that the EEDI might lead to an *increase* of CO₂ [61, 66, 67]. For ships with a fully integrated auxiliary system coupled with the main engine it is unclear how the value of the MCR is calculated [68].

Furthermore, speed reduction could be an 'easy' solution to lower the EEDI value. Finally, by minimizing the installed power, and making the lightest possible ship (thus increasing the loading capacity or DWT), the EEDI is lowered as well. This measure means that ships will be under-powered and compromised in strength and this will result in vessels that are prone to more safety risks [72].

For ships whose primary mission is not to transport a load or sail at a fixed speed (examples are dredgers, tugs or well intervention vessels), the EEDI formula does not express the ship index right, despite the EEDI being discussed for these vessels [61]. The EEDI index is based on a point value at 75% of the rated MCR [73]. The fact that this is a point value is the main concern when applying the EEDI to a canal boat because its operational profile varies a lot. Adding to this is the fact that the EEDI equation may not be able to be applied to diesel electric or hybrid propulsion plants [73], something that will become important after 2025 when canal boats in Amsterdam have to be ZE [16].

3.5.2.2. EEOI

The Energy Efficiency Operational Indicator (EEOI) is used to track the transport efficiency of a ship [69]. It is used to present the concept of an indicator for the energy efficiency of a ship *in operation*. The EEOI is used to evaluate and achieve a reduction of CO_2 emissions [74]. This is done by expressing the energy efficiency in CO_2 emitted per unit of transport work. A simplified version is shown in Equation 3.5.3 [72].

$$EEOI = \frac{\sum_{j} FC_{j} \cdot C_{Fj}}{\sum_{i} m_{cargo} \cdot d}$$
(3.5.3)

Where:

- FC_i is the mass of consumed fuel of type j
- C_{Fj} is the fuel mass to CO_2 mass conversion factor for fuel type j
- m_{cargo} is the *mean value* of cargo carried (tonnes) or work done (number of containers or passengers) or gross tonnes for passenger ships
- *d* is the distance in nautical miles
- The summation in the numerator indicates voyage amount or time

The EEOI is a voluntary index for seagoing ships. It is stated that for passenger ships the number of passengers or gross tonnes of the ship should be used [74]. The EEOI measures the energy efficiency during every voyage and evaluates the operational performance. It is therefore an operational Continuous Monitoring System (CMS). This is a useful feature, as it therefore can respond to a constantly changing operational profile [70].

3.5.2.3. THE SHIPPING KPI SYSTEM

The Shipping Key Performance Indicator (KPI) System uses a hierarchical and mathematical system which includes Shipping Performance Indexes (SPIs), Key Performance Indicators (KPIs) and Performance Indicators (PIs). It includes around 100 indexes that can be calculated [75], ranging from emissions to the experience rate of officers. Only the CO_2 index will be analyzed in this report. This CO_2 index is based on the EEOI

method. The calculation method is shown in Equation 3.5.4. It gives the accumulated emitted mass of CO₂ and divides this with the transported work during a set time frame.

$$KPI = \frac{\sum (\text{Bunkercons.} \cdot (\text{ton } CO_2 / \text{ ton fuel}))}{\sum (\text{Cargo loaded} \cdot \text{distance})} \cdot 10^6$$
(3.5.4)

The KPI value has units [g/transport work] where transport work can be defined as tonmile, passengermile, TEU mile or a different unit, depending on vessel type and mission statement [76]. The calculated KPI from Equation 3.5.4 is mapped to a rating based on a linear scale. This rating determines the non-dimensional performance of the vessels' $\rm CO_2$ production during (usually) one quarter of a year. Influencing factors for each vessel such as hull design, engine type and age and the load factor for a voyage are included in the KPI.

The state of the vessel and type of voyage (operational profile) hence influences the quantity of emitted CO₂ [77]. If the ship is sailed at a lower speed, or if the DWT is adjusted, a better KPI value can be achieved.

3.5.2.4. THE CO₂ DREDGING INDEX

A design index specifically targeted for the dredging industry was proposed in Van de Ketterij et al. [61]. Key points from this paper are that the 'benefit for society' of a dredging vessel cannot be displayed in 'DWT $\cdot V_{ref}$ ', as is the case in the proposed EEDI. Van de Ketterij et al. therefore proposed a standard dredging CO₂ operational cycle consisting of four phases: sailing empty, dredging, sailing fully loaded and discharging. Each phase has its average power consumption, taking into account the required (electric) power of the pumps and jets as well. The equation to calculate the energy index is given below:

$$I_{TSHD} = \frac{\sum_{i=1}^{4} \left(P_i \cdot \frac{t_i}{t_{cycle}} \right)}{DWT \cdot g \cdot V_{cycle}}$$
(3.5.5)

Where I_{TSHD} is the energy index value for a trailing suction hopper dredger (TSHD), V_{cycle} is the average speed of the vessel during one fully loaded trip, without taking into account sailing to the worksite. t_{cycle} is the cycle time. The CO₂ Dredging Index can be applied to every type of ship, if the standardized dredging cycle is replaced by the operational profile of the vessel that is analysed. It is an index that incorporates auxiliary energy consumption and electric consumers into a design index. It is comparable to the International Maritime Organization (IMO) test cycle for Nitrogen oxide (NO_x), which uses four different operational design points [78]. Why the IMO has chosen to incorporate a *point* design index method, the EEDI, as the CO₂ calculation method for ships instead of using the NO_x framework is therefore strange, to say the least.

3.5.3. THEORETICAL ASPECTS OF INDICES

Before defining the specific indices designed for small passenger vessels such as in the Amsterdam canals, a theoretical background is given on an important factor that has to be kept in mind: a Froude-like scale effect that influences the values of EPIs. This scale effect will be explained first, after which the requirements for the design index in Amsterdam will be detailed.

3.5.3.1. FROUDE LIKE SCALE EFFECT

Assuming a quadratic resistance curve, Equation 3.5.6 holds [18].

$$R_{ship} = A_w \cdot P = A_w \cdot \rho_w \cdot V_s^2 \tag{3.5.6}$$

Where R_{ship} is the ship resistance in [N], A_w is the wetted surface of the ship in [m²], ρ_w is the water density, taken as 1000 [kg/m³], and V_s is ship speed in [m/s]. Writing the equation for effective power P_e :

$$P_e = A_w \cdot \rho_w \cdot V_s^3 \tag{3.5.7}$$

Translating the required energy flow Φ_E to the effective power P_e is done by introducing partial efficiencies for all the losses in the power conversion chain [18]:

$$\frac{P_e}{\Phi_F} = \eta_o \cdot \eta_R \cdot \eta_h \cdot \eta_{TRM} \cdot \eta_{PM} \tag{3.5.8}$$

Here, η_{PM} is prime mover efficiency. Combining the open water propeller efficiency η_o , relative rotative efficiency η_R , hull efficiency η_h and transmission and shaft efficiency η_{TRM} into a single propulsive efficiency η_D :

$$\eta_D = \eta_o \cdot \eta_R \cdot \eta_h \cdot \eta_{TRM} \tag{3.5.9}$$

Then the total power chain efficiency is the product of the propulsive efficiency and the prime mover efficiency:

$$\eta_{tot} = \eta_D \cdot \eta_{PM} \tag{3.5.10}$$

Combining equations 3.5.7, 3.5.8 and 3.5.10 gives:

$$\Phi_E = A_w \cdot \rho_w \cdot V_s^3 \cdot \eta_{tot} \tag{3.5.11}$$

Defining an equation for the Energy Conversion Index (ECI) at *point* value, Equation 3.5.12:

$$ECI_{point} = \frac{\Phi_E}{W \cdot V_s} \tag{3.5.12}$$

and substituting Equation 3.5.11 in 3.5.12 gives:

$$ECI_{point} = \frac{A_w \cdot \rho_w \cdot V_s^2 \cdot \eta_{tot}}{W}$$
(3.5.13)

With W nominal payload weight in [N]. Introducing load factor z as mass of payload divided by ship displacement gives Equation 3.5.14:

$$W = \nabla \cdot z \cdot \rho_w \cdot g \tag{3.5.14}$$

Rearranging to obtain displacement ∇ gives Equation 3.5.15:

$$\nabla = \frac{W}{y \cdot \rho_w \cdot g} \tag{3.5.15}$$

The ship's volume displacement can also be expressed with a block coefficient C_b if breadth B, length of the water line L_{wl} and draught T are known [79]:

$$\nabla = \frac{C_b}{(L_{wl}/B)^2 \cdot (B/T)} \cdot L_{wl}^3$$
 (3.5.16)

Introducing a volumetric shape coefficient C_v :

$$\nabla = C_{\nu} \cdot L^3 \tag{3.5.17}$$

Following the same reasoning for the wetted surface A_w , which scales with L^2 , introduces a geometrical shape factor C_a :

$$A_{w} = C_{a} \cdot L^{2} \tag{3.5.18}$$

These scale factors give, when substituting equations 3.5.14, 3.5.17 and 3.5.18 in Equation 3.5.13, Equation 3.5.19. The efficiencies are grouped in η_{tot} (ref. 3.5.10).

$$ECI_{point} = \eta_{tot} \cdot \frac{C_a}{C_v \cdot y} \cdot \frac{V_s^2}{g \cdot L}$$
(3.5.19)

The last part of this equation is a Froude-like scale effect. This means that in general the energy conversion index value is proportional to speed squared and inversely proportional to ship size. This in turn means that the index can be lowered by sailing slower or building larger ships. The scale effect applies to canal boats as well. However, the length of canal boats in Amsterdam is regulated to have a maximum length of 20 [m]. Furthermore the speed during the canal boat trips does not differ extraordinary. Speed during trips is between 1 and 10 [km/h], with an average of about 6 [km/h]. Because of these reasons, the scale effect *in the Amsterdam canal boat analysis* will be neglected.

3.5.4. REQUIREMENTS AND DEFINITIONS OF THE DESIGN INDEX

In this chapter the requirements for the design indices will be considered. The chapter will end with a definition of the indices. Research question Q.2.2 will be answered:

How can current rating methods be used to evaluate canal boats?

(Ref. Q.2.2)

3.5.4.1. DETERMINING INFLUENCING FACTORS

The current EPIs are not flexible enough to allow for part load in a detailed manner during the *design phase* of the ship. The indices can be used to obtain an index value, but the issue with the current EPIs is that they are calculated at one point value instead of using mean values (the EEDI) or are not designed to be used in the design phase but rather are an operational index (Shipping KPI, EEOI). The $\rm CO_2$ dredging index could be adapted to suit the needs of a passenger design index. Required information to define an index or indices is given in the next section.

PRACTICAL CONSIDERATIONS

Vessels have constantly varying velocities and thus varying emissions. Therefore, when considering EPIs, the irregular operational character of vessels and in particular canal boats should be taken into account by taking mean values and weighing the most important operational modes. Factors that are important are power consumption, (part load) power requirements, efficiency, auxiliary power, track or time sailed, speed and people or cargo transported. EPIs must be defined in such a way that they can give an insight in the method to obtain environmentally friendly and efficient transportation. If one would like to compare vessels on a cost/benefit basis, the benefits can be defined as the useful cargo that is transported, whether this cargo is people, containers or bulk material. The cost can be defined by taking emissions, used fuel or required power values from the simulations.

3.5.4.2. INDEX REQUIREMENTS

There are four necessities to define a design index:

- An system boundary giving a fair comparison between different vessel configurations
- · A generalized representative operational profile based on the (typical) mission of the ship
- A ship model that is preferably based on measurements or real life practice, containing information about speed and (auxiliary) power consumption of the ship
- Knowledge about legislation and size and speed variations in the new design to see if the scale effect can be neglected or not

3.5.4.3. SETTING THE SYSTEM BOUNDARY

In this chapter research question Q.2.3 will be answered:

How can diesel propulsion be compared with electric propulsion?

(Ref. Q.2.3)

The boundaries of the indices are set in two different places, which are visualised in Figure 3.5.1: The

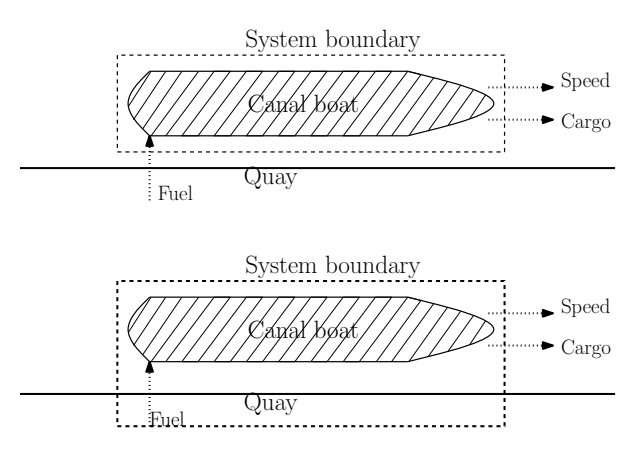


Figure 3.5.1: Definition of system boundary A (upper) and B (lower)

choice of power plant is important to decide whether the electric concepts do not have emissions at all, or do have emissions due to electricity generation. If the energy used by the concept is generated by renewable sources (solar panels, windmills, hydro) then indeed the electric canal boat concept is *globally* emission free and system boundary A can be used to calculate the environmental indices. system boundary A uses electricity from the grid and does not take into account power plant emissions and/or losses.

If the energy used is generated in a conventional land-based power plant which uses fossil fuels (oil, coal), there are emissions. To compensate for the unknown emissions of the power plant and electricity transport, system boundary B is used which calculates requirements from the power generation in terms of energy efficiency and emissions to compare this with the baseline.

The conclusion here is that it is important to specify *where* the energy is generated to be able to state whether an electric canal boat is local emission free or global emission free. The comparison will consequently be between three different concepts:

- · The baseline
- Full electric boat, powered by the grid using system boundary A
- Minimum efficiency required from the power plant to quayside crossing, using system boundary B, to obtain the same energy efficiency as the baseline.

DETERMINING INDICES

Combining the requirements from the preceding chapters gives the basis for the indices that will be used in the framework. The following indices are proposed:

- ECI This is the total energy flow across the set boundary (including auxiliaries) divided by the benefit for society. This is the energetic value of the arrow crossing system boundary A in Figure 3.5.1.
- Fuel Index (FI) Total fuel flow across a set boundary divided by benefit for society
- Energy Index (EI) Emission flow divided by benefit for society

$$ECI = \frac{\sum Required\ energy\ flow}{\sum Benefit\ to\ society}$$
(3.5.20)

$$Fuel Index = \frac{\sum Required fuel flow}{\sum Benefit to society}$$
 (3.5.21)

Emission Index =
$$\frac{\sum Emission flow}{\sum Benefit to society}$$
 (3.5.22)

'Benefit for society' can be defined from two perspectives, namely cargo and passengers. In view of the difference between carrying cargo or passengers the benefit could in general be defined as:

Benefit for society =
$$w \cdot n \cdot d$$
 (3.5.23)

In Equation 3.5.23, w is the average weight of the cargo in [N], or the average weight of passengers transported in [N]. n is the number of passengers transported. For container vessels, n can be the number of containers. For bulk cargo vessels, n is equal to 1, the weight will be defined with w in this case. w times n gives the defined mean nominal payload weight W in [N]:

$$W = w \cdot n = m \cdot g \cdot n \tag{3.5.24}$$

Here, g is gravitational acceleration equal to 9.81 $[m/s^2]$ and m is mean cargo or passenger mass in [kg].

3.5.4.4. ECI DEFINITION

The ECI is defined in Equation 3.5.20 and will be explained in detail in this section. The ES must be able to have capacity for both the main and the auxiliary energy requirements and total energy usage. The ECI is defined from the 'Energy flow' point in Figure 3.5.2 and is the energetic value that is required to be put into the energy storage each day.

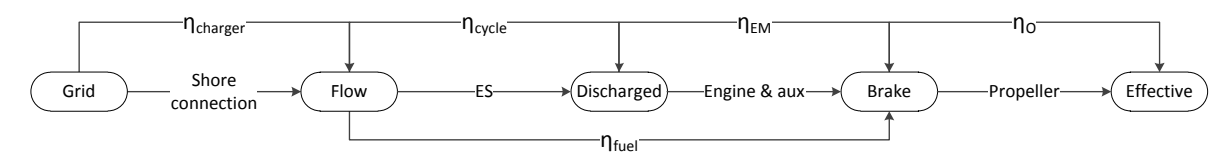


Figure 3.5.2: Definition of different energy flows and efficiencies

3.5.5. Summary 87

Equation 3.5.25 displays this relationship. Heating, communications, catering, secondary propulsion (bow thruster) and ship equipment all require an auxiliary energy flow.

$$\Phi_{E,total} = \Phi_{E,main} + \Phi_{E,aux} \tag{3.5.25}$$

 $\Phi_{E,total}$ is the required prime energy flow from the energy storage required for the main propulsion ($\Phi_{E,main}$) as well as auxiliaries ($\Phi_{E,aux}$). In case of a passenger vessel the dimensionless ECI is defined in Equation 3.5.26.

$$ECI = \frac{\sum_{i} E_{total,i}}{\sum_{i} (w_i \cdot n_i \cdot d_i)} = \frac{\int_{t} (\Phi_{E,main} + \Phi_{E,aux}) \cdot dt}{\int_{t} (w \cdot n \cdot V_s) \cdot dt}$$
(3.5.26)

The integral boundary t denotes the time of a certain operational mode. The integral boundary t denotes the amount of trips.

3.5.4.5. Fuel and emission indices definitions

To quantify emissions and fuel consumption definitions from equations 3.5.21 and 3.5.22 are used. This gives equations 3.5.27, 3.5.28, 3.5.29 and 3.5.30. m and m_i is the cargo mass in [kg]. The FI and the emission indices have the unit [g/(kg · km)]. Just like with the ECI, the subscript t denotes the time of a certain operational mode. The subscript t denotes the amount of trips.

$$FI = \frac{\sum_{i} E_{F,total,i}}{\sum_{i} (m_i \cdot n_i \cdot d_i)} = \frac{\int_{t} \left(\Phi_{F,main} + \Phi_{F,aux} \right) \cdot dt}{\int_{t} (m \cdot n \cdot V_s) \cdot dt}$$
(3.5.27)

$$CO_2 Index = \frac{\sum_{i} m_{CO_2, i}}{\sum_{i} (m_i \cdot n_i \cdot d_i)} = \frac{\int_{t} \Phi_{CO_2}}{\int_{t} (m \cdot n \cdot V_s)}$$
(3.5.28)

$$NO_x Index = \frac{\sum_{i} m_{NO_x,i}}{\sum_{i} (m_i \cdot n_i \cdot d_i)} = \frac{\int_{t} \Phi_{NO_x}}{\int_{t} (m \cdot n \cdot V_s)}$$
(3.5.29)

$$SO_x Index = \frac{\sum_{i} m_{SO_x, i}}{\sum_{i} (m_i \cdot n_i \cdot d_i)} = \frac{\int_{t} \Phi_{SO_x}}{\int (m \cdot n \cdot V_s)}$$
(3.5.30)

As the CO_2 and SO_x are directly coupled to the fuel consumption, they can be rewritten as follows:

$$CO_2 Index = \frac{\sum_{i} m_{f,i} \cdot f_{CO_2}}{\sum_{i} (m_i \cdot n_i \cdot d_i)}$$
(3.5.31)

$$SO_x Index = \frac{\sum_{i} m_{f,i} \cdot f_{SO_x}}{\sum_{i} (m_i \cdot n_i \cdot d_i)}$$
(3.5.32)

Where f_{CO_2} denotes the mass of CO_2 divided by total fuel mass m_f . The factor f_{CO_2} for (automotive) diesel is around 3.2 [kg/kg] [73]. The factor f_{SO_x} denotes the mass of Sulfur oxide (SO_x) divided by total fuel mass m_f and is 20 [g/kg] for (automotive) low-sulphur diesel.

3.5.5. SUMMARY

An Amsterdam canal environmental performance indicator index calculation method has been introduced that is able to estimate energy, power and emissions of different vessel types in a simple and cohesive manner. This is achieved by using i discrete operational blocks and hence i mean values for propulsion energy. This allows quick comparisons between vessels with different operational profiles. Furthermore, auxiliary power and energy are included in these indices as well, leading to a comprehensive comparison method that can be used to give insights in vessels' environmental footprint. A calculation example and simulation will be given in Chapter 4.3, 'Simulation results', based on the three concepts and the baseline.

4

SIMULATIONS AND RESULTS

This chapter of the thesis starts with the simulation methodology, defining two main simulations that need to be carried out. The first simulation, a validation and concept comparison simulation is carried out in the next chapter after which a simulation is carried out over the course of a full day. Simulation conclusions are followed by the applications of the results to the real world, along with a description of quayside requirements, battery cost analysis and quay infrastructure.

SIMULATION METHODOLOGY

Research question Q.1.9 will be answered here, along with subquestions Q.1.9.1 and Q.1.9.2.

What is the simulation strategy?

(Ref. Q.1.9)

In this chapter the methodology behind two simulations, one verification speed simulation and one full day simulation, is presented and explained. In Figure 4.1.1 the light green block shows the model that will be described in this chapter: the operational profile, or simulation methodology. The dark green models represent the models already defined in earlier chapters.

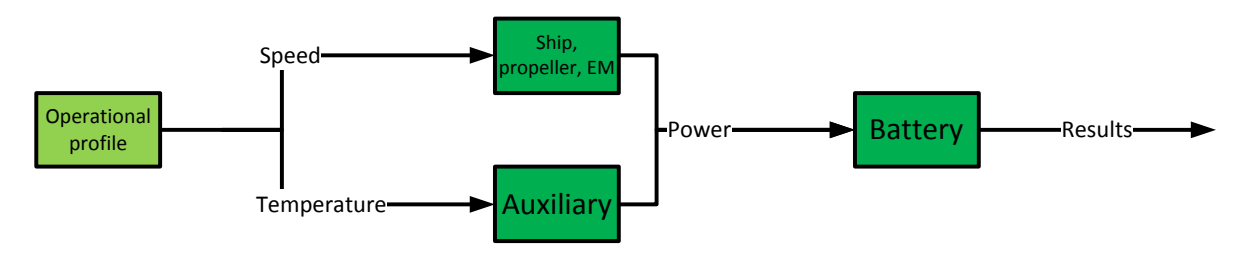


Figure 4.1.1: Model overview

4.1.1. Speed profile simulation

The speed profile that is used to compare the configurations with each other is given in Table 4.1.1. The first 500 seconds are used to remove any instability of the model at the start. After this, every 500 seconds 0.5 [m/s] is added to the required speed. The top speed is taken as 3.0 [m/s] as this was approximately the maximum speed that the hybrid boat could achieve. Auxiliary power such as the heat pump is not included in this profile.

The benefit of this speed profile simulation is that the brake power difference between the concepts can be seen immediately. This will give insight in the most efficient configuration. Furthermore it acts as a validation to see if each configuration is able to sail the speed that is required.

Table 4.1.1: Speed profile

Time per block [s]	Speed [m/s]
500	0
500	0.5
500	1
500	1.5
500	2
500	2.5
500	3

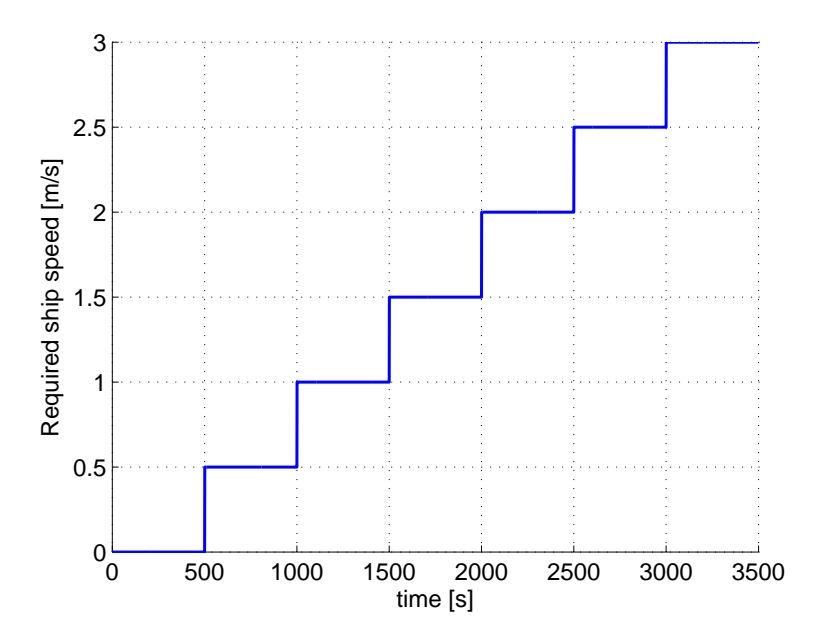


Figure 4.1.2: Speed profile used for simulations

4.1.2. DAILY SIMULATION

The main simulation will consist of a full day simulation. The details are given in this chapter, which starts with the trip profile. This trip profile is extended to a daily profile. When the daily profile is developed the simulation methodology for this main simulation will be clarified.

4.1.2.1. TRIP SIMULATION

The generic operational profile is formulated in Chapter 2.1, 'Baseline', Table 2.2.4. Refer to Table 2.2.4 for this generic operational profile and the measured distance and time input. For the simulations the according durations of the blocks are taken. As stated in Section 3.2.1 of Chapter 3.2, 'Ship and system modelling', the input and controlled variable in the models is ship speed. The power requirements per block, brake as well as at the energy storage, can be calculated by using this generic operational profile for each configuration. Due to the different resistance, efficiencies and propulsion systems of the configurations, each configuration will have different power and energy results.

4.1.2.2. Environmental indices

The EPIs will also be calculated during a trip simulation. Because all trips will be the same, the EPIs will not differ with values of a full day simulation. Values used in the denominator of the indices (the 'benefit for society') during this simulation are given in Table 4.1.3:

¹Taken as average 2.35 [m/s]

4.1.2. Daily simulation 93

Table 4.1.2: Simplified generic operational profile

Block [-]	Time [min]	Distance [km]	Average V _s [m/s]
Moored	15	0.0	0.0
Manoeuvres	25	1.5	Varies ¹
Nominal speed	25	3.2	2.1
Medium speed	14	2.1	2.6
Maximum speed	0.3	0.1	3.3
90° turns	11	0.7	1.0
Total	90	7.6	-

Table 4.1.3: Values used for benefit for society calculation

Parameter	Explanation	Value	Unit
m_i	mean passenger mass	80	[kg]
d_i	distance sailed	7.574	[km]
W_i	mean passenger weight	785	[N]
n_i	amount of passengers	100	[-]

4.1.2.3. Daily operational power profile

Expanding on the trip operational profile the daily operational profile can be set up as well. This will be the main operational profile used during simulations. The canal boats can be charged overnight, so they only need to last throughout the day. Simulations for the whole day (6 trips of 75 [min] each) are carried out. It is assumed that the canal boats start the day with a fully charged battery and that there is 15 [min] between each trip available to recharge.

How can the energy storage system be kept in a safe operating condition?

(Ref. Q.1.9.1)

The minimum charge remaining at the end of the day is taken as 20%. This is to make sure the batteries have a long lifetime and to have a buffer for when there is more energy used due to for example heavy traffic in the canals. The whole sailing schedule can be produced taking into account these variables, see Table 4.1.4:

Table 4.1.4: Sailing schedule for one day

State of charge [-]	Reference route [-]	Time [hr]
100% available	Trip 1	01:20
	Charge / quay	00:15
	Trip 2	01:20
	Charge / quay	00:15
	Trip 3	01:20
	Charge / quay	00:15
	Trip 4	01:20
	Charge / quay	00:15
	Trip 5	01:20
	Charge / quay	00:15
20% available	Trip 6	01:20
Total time sailing		08:00
Total time quay		01:15
Total time per day		09:15

Assumptions of this sailing schedule are:

- · Boats sail 8 hours per day
- 15 minutes quay time is 15 minutes possible charge time
- Fully loaded boat each trip
- · Ambient temperature and battery temperature is constant

The daily profile that is used for simulations is shown in Figure 4.1.3.

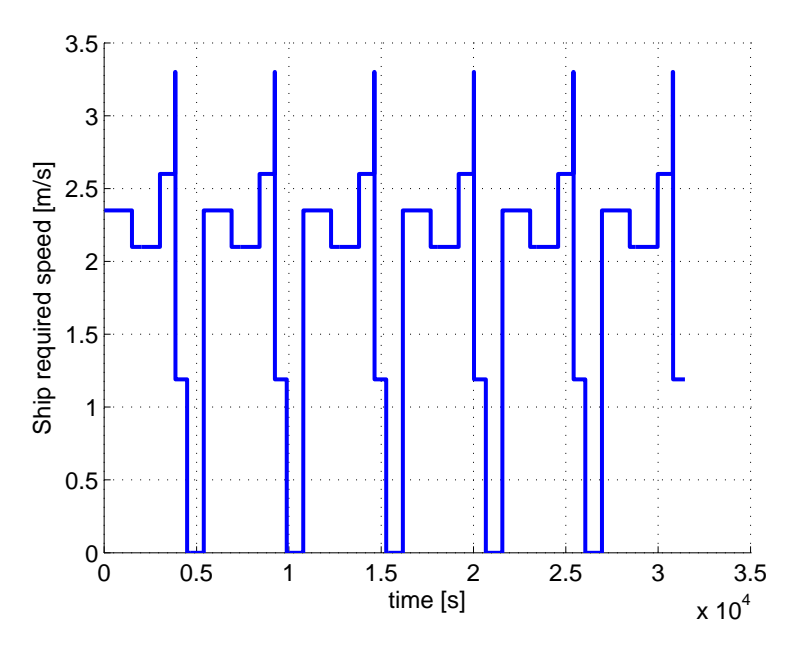


Figure 4.1.3: Randomized daily operational profile

4.1.2.4. SIMULATION METHOD DIESEL POWERED BOAT

The diesel boat will be simulated for one full day according to the schedule in Table 4.1.4. The canal boat is simulated for one full day without the (diesel) heater, as it is unknown how much fuel this heater uses. The heat pump is used as a heater. See Figure 4.1.4. It is assumed that the diesel boat has got enough fuel to be able to sail a full day.

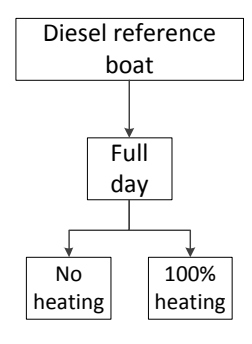


Figure 4.1.4: Diesel simulation tree

4.1.2.5. SIMULATION METHOD ELECTRIC POWERED BOATS

Two different operational modes will be tested:

- Full day simulation, only overnight charging
- Full day simulation, with intermittent shore charging and overnight charging

For the batteries the difference in required capacity when charging between trips will be visualised, as well as the difference between the LMP and LTO performance. Different heating profiles account for representative

4.1.2. Daily simulation 95

values all-year round. Figure 4.1.5 gives the simulation tree. Each configuration can be found in this picture, as each concept needs to pass through the whole simulation tree. This results in 24 different simulation configurations (three concepts multiplied with 8 possible options in the simulation tree).

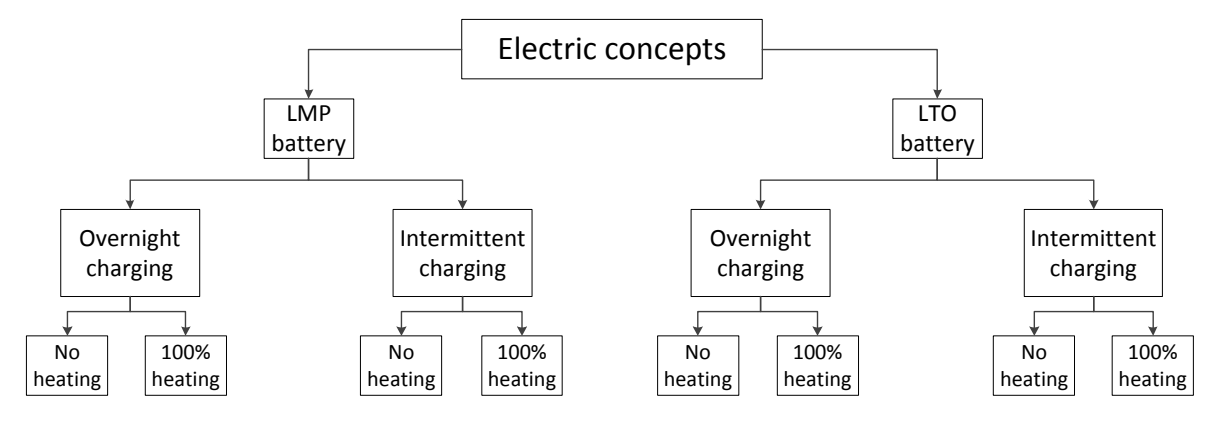


Figure 4.1.5: Electric concepts simulation methodology tree

4.1.2.6. INTERMITTENT CHARGING

Is charging with intervals possible?

(Ref. Q.1.9.2)

When intermittent charging is applied, the sailing schedule from Table 4.1.4 is used again, and after each trip the boat will be charged for 15 minutes. Time differences from these 15 minutes are neglected, it is assumed that there is always an opportunity to charge for a full 15 minutes. Initially the LMP battery is assumed to be charged with 0.5C and 1C, and the LTO battery is assumed to be charged with 2C and 4C. These are conservative values for these types of batteries, as for LMP it is possible to charge up to a maximum of 2C. For LTO charging with 10C is mentioned in literature [80].

4.1.2.7. REQUIRED RESULTS

The results that are needed from the simulations are summarized below:

- Energy values required from the energy storage
- Energy storage efficiency (battery efficiency)
- · Charging feasibility and influence on energy storage of intermittent charging
- Size of energy storage (in case of the batteries)
- Efficiency breakdown (open water efficiency, conversion efficiency, electric motor efficiency)
- Chain efficiency
- Values to calculate environmental indices
- The most energy efficient of the concepts

4.1.2.8. SOLVER

In the model a fixed step solver is used². This is done because the variables created by Simulink will be processed in Matlab and with a variable step size the variables cannot be mapped to the real-time clock directly. The fixed-step solver works by computing the next simulation step by adding a time step to the current time. At each time step numerical integration is used to calculate the variables of the model. This numerical integration uses the values from the previous time step. The time step in the simulations is 1 [s], to be able to easily plot the calculated data, and to have a high accuracy. Higher time steps gave less accurate results.

INTEGRATION TECHNIQUE

The model uses an ode-3 solver that applies the Bogacki-Shampine Formula integration method. The order is three. An ode-2 solver did not accelerate the simulation significantly, and an ode-1 solver did not give satisfactory results. Therefore the ode-3 is used, as it gives accurate results and adequate simulation speeds.

²The solver is chosen with the guide from Mathworks: http://nl.mathworks.com/help/simulink/ug/choosing-a-solver.html

VERIFICATION SIMULATION RESULTS

The aforementioned speed profile is simulated. This gives insight in the relative efficiency between the configurations, and poses as a verification for the models. Results are given below for each configuration.

4.2.1. BRAKE POWER

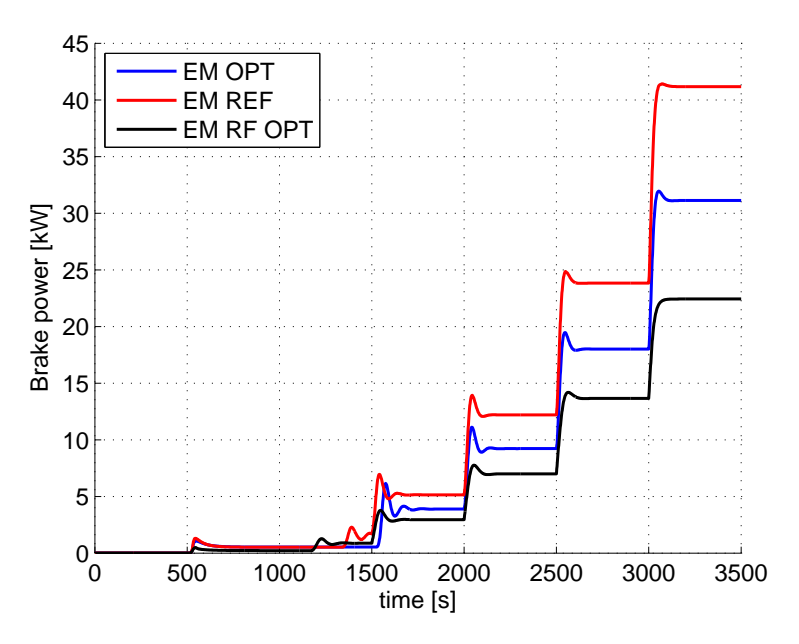


Figure 4.2.1: Brake power for the concepts

As can be seen from Figure 4.2.1 the reference electric configuration requires the largest brake power. When integrating these power requirements and ignoring the first 500 [s], the following figures for brake energy are found:

Electric reference: 12.2 [kWh]
Electric retrofit drive: 7.1 [kWh]
Electric optimized: 9.2 [kWh]

4.2.2. OPEN WATER EFFICIENCY

The open water efficiency is shown in Figure 4.2.2. Due to the optimization of the retrofit drive concept, this propeller has the highest efficiency. The pod propellers have a lower efficiency, this is due to the fact that there is no gearbox installed and due to their high RPM.

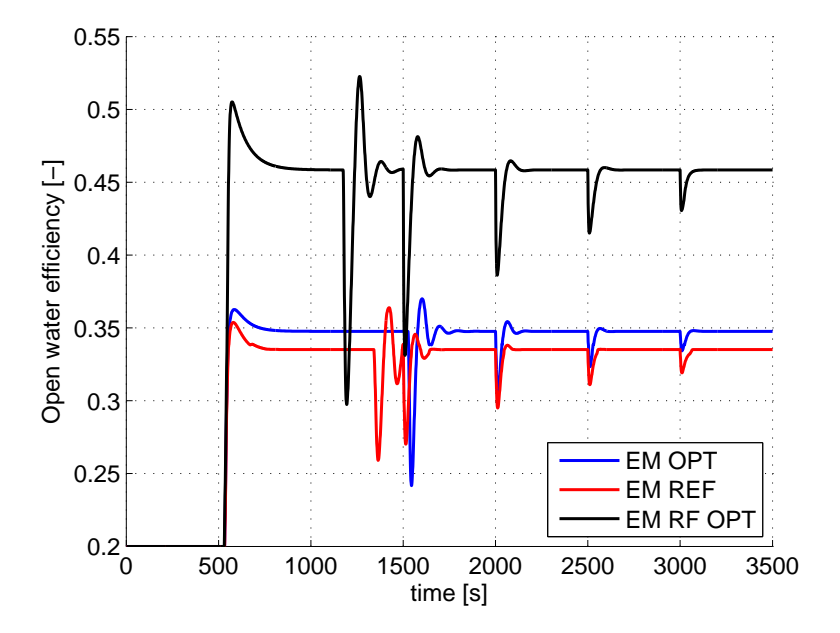


Figure 4.2.2: Open water efficiency for the electric concepts

4.2.3. ELECTRIC MOTOR EFFICIENCY

The efficiency of the electric motor is in all speeds higher than 77%, see Figure 4.2.3. This lowest efficiency is only at the lowest speeds below 1 [m/s]. From 1500 [s] onwards, vessel speeds > 1 [m/s], efficiency rises rapidly to values over 0.90. Due to the gearbox in the retrofit drive configuration, the required torque is higher, required RPM is lower and this gives the retrofit drive a slightly less engine efficiency.

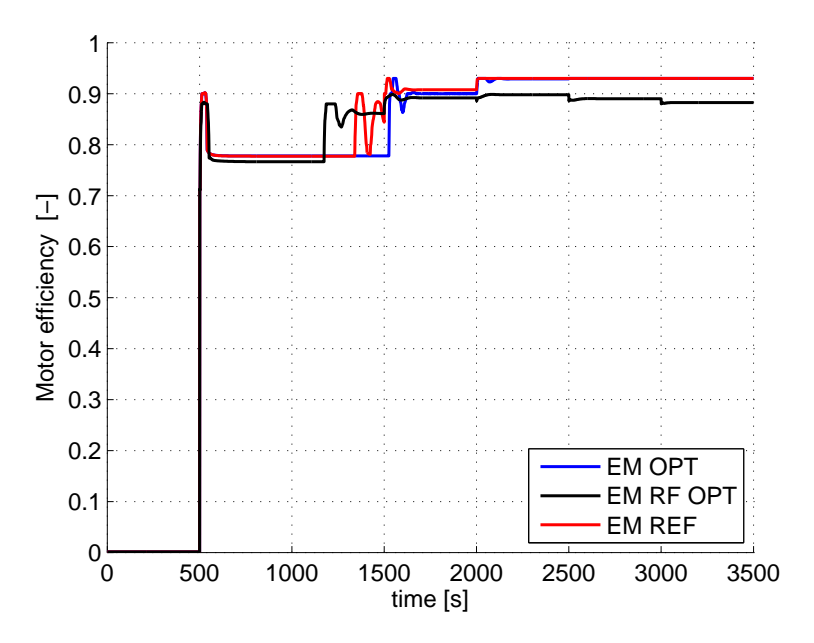


Figure 4.2.3: Efficiency of electric motors for the electric concepts

4.2.4. Brake energy 99

4.2.4. Brake energy

The brake energy is shown in Figure 4.2.4. Note that to find the energy in the tank, this still must be divided by the tank or battery efficiency and motor efficiency.

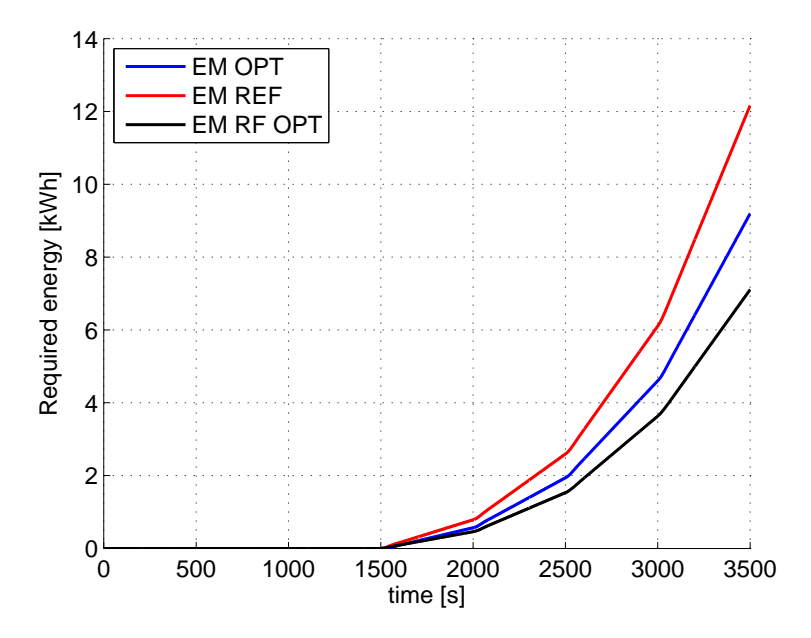


Figure 4.2.4: Energy usage of the electric configurations

4.2.5. ACCELERATION TIME

Acceleration from 2.0 to 2.5 [m/s] is shown in Figure 4.2.5. The retrofit drive configuration is the slowest, whereas the optimal without gearbox is the fastest but has the largest overshoot.

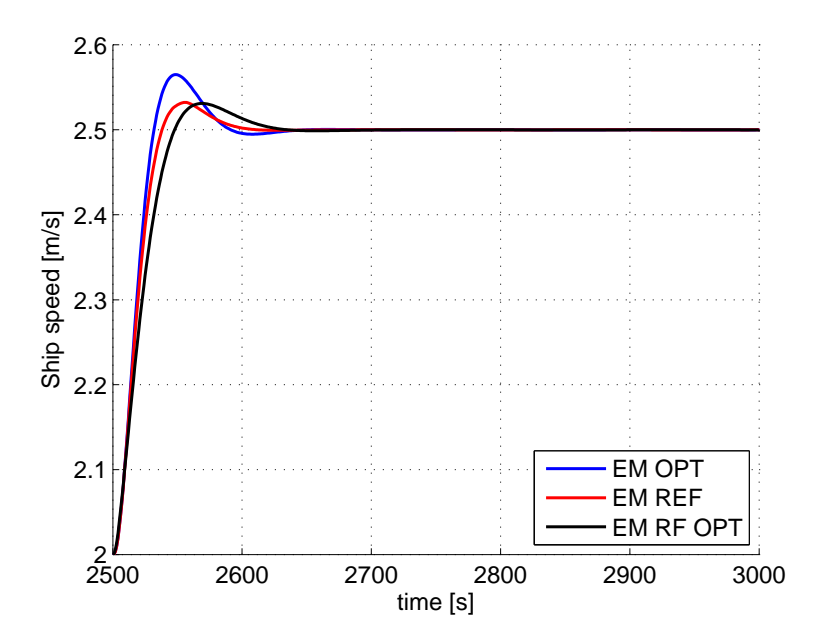


Figure 4.2.5: Acceleration from 2.0 to 2.5 [m/s]

4.2.6. CONCLUSION

When looking at the energy required by the propulsion, it is clear that EM RF OPT, electric drive coupled with a gearbox uses the least energy. Furthermore, it is clear that the model operates according to specifications with regards to power and responsiveness of the model. There are no odd outcomes or extreme values to imply that the model has faults. One conclusion that can already be made from this easy simulation is that addition of a gearbox will be decreasing the energy requirements.

SIMULATION RESULTS

Along with the simulation results of the trip and day, research objective Q.1.10 will be answered in this chapter:

Are the obtained model results realistic and do they agree with the baseline?

(Ref. Q.1.10)

4.3.1. SUMMARY OF RESULTS

The simulations of the concepts and diesel reference are carried out over the course of one trip and one day. The detailed methodology behind these simulations can be found in Chapter 4.1, 'Simulation methodology'. In this chapter the summary of results is presented, see Table 4.3.1. Succeeding this is a detailed analysis of these results, first for the diesel reference and then for the electric concepts. There will first be an energy storage and usage comparison. Second is a breakdown per efficiency, after which the total chain efficiency can be calculated for each concept. Important parameters that are found from the simulations are:

- Energy values required from the energy storage
- Energy storage efficiency (battery efficiency)
- · Charging feasibility and influence on energy storage of intermittent charging
- Size of energy storage (in case of the batteries)
- Efficiency breakdown (open water efficiency, conversion efficiency, electric motor efficiency)
- · Chain efficiency
- · Values to calculate environmental indices
- · The most energy efficient concept

In Table 4.3.1 the following data is given:

- **Charging:** If only overnight charging is applied or charging after each trip. If charging after each trip is applied, the C rating of charging is given as well.
- **ES/day:** Energy storage size. This is the required capacity of the batteries that needs to be installed to be able to sail one day, six trips, including all losses and at the end of the day a charge value of 20% or more. In the case of diesel, it is the energy value of diesel required to sail one day, with 20% capacity remaining after sailing.
- Flow. Energy flow across the system boundary. This is the energy that is coming from the quay required to sail one day. For the diesel reference, this is the amount of diesel converted to energy, including all losses. For the batteries this is the energy required for a full day including all losses. This is thus basically the refuelling or recharging energy from quay to boat at the end of the day. Brake, discharged and flow energies can be calculated with Equation 4.3.1:

$$E_{brake} = E_{batt,dis} \cdot \eta_{EM} = E_{flow} \cdot \eta_{EM} \cdot \eta_{batt,cycle}$$
(4.3.1)

- **Discharged**. Battery discharge energy. The amount of energy that the battery has discharged during the day.
- **Brake**. Brake energy usage per day. This is the energy required for the propulsion and heating systems from engine or motor shaft to the propeller and heating system. Energy usage whilst the canal boat is moored is also included.

Configuration	Charging	ES/day	Flow	Discharged	Brake	ES type	η_{batt}	η_e	η_o	η_{chain}
[-]	[-]	[kWh]	[kWh]	[kWh]	[kWh]	[-]	[-]	[-]	[-]	[-]
Baseline, excluding HP:										
Fp	No	456	45.1	-	16.7	Diesel	-	0.37	0.41	0.15
Pod	Overnight	250	24.6	19.7	17.7	Lead acid	0.80	0.90	0.33	0.24
Baseline, including HP:										
Fp opt.	No	456	61	-	15.5	Diesel	-	0.37	0.45	0.17
Pod	Overnight	250	33.3	26.7	17.7	Lead acid	0.80	0.90	0.33	0.24
Concepts including HP:										
EM RF OPT	Overnight	159	20.9	20.5	11.8	LMP/LTO	0.98	0.88	0.46	0.39
EM RF OPT	Yes, 0.5C	87	21.3	20.5	11.8	LMP	0.96	0.88	0.46	0.39
EM RF OPT	Yes, 1C	64	22.2	20.5	11.8	LMP	0.92	0.88	0.46	0.37
EM RF OPT	Yes, 2C	42	23.9	20.5	11.8	LTO	0.86	0.88	0.46	0.35
EM RF OPT	Yes, 4C	53	25.6	20.5	11.8	LTO	0.80	0.88	0.46	0.32
EM REF	Overnight	220	30.3	29.7	20.6	LMP/LTO	0.98	0.91	0.33	0.29
EM REF	Yes, 0.5C	125	30.9	29.7	20.6	LMP	0.96	0.91	0.33	0.29
EM REF	Yes, 1C	91	32.2	29.7	20.6	LMP	0.92	0.91	0.33	0.28
EM REF	Yes, 2C	60	35.1	29.7	20.6	LTO	0.85	0.91	0.33	0.26
EM REF	Yes, 4C	75	37.3	29.7	20.6	LTO	0.80	0.91	0.33	0.24
EM OPT	Overnight	182	24.6	24.1	15.4	LMP/LTO	0.98	0.90	0.34	0.30
EM OPT	Yes, 0.5C	102	25.1	24.1	15.4	LMP	0.96	0.90	0.34	0.30
EM OPT	Yes, 1C	72	26.1	24.1	15.4	LMP	0.92	0.90	0.34	0.29
EM OPT	Yes, 2C	48	28.5	24.1	15.4	LTO	0.84	0.90	0.34	0.26
EM OPT	Yes, 4C	62	30.5	24.1	15.4	LTO	0.79	0.90	0.34	0.25
Concepts excluding HP:										
EM RF OPT	Overnight	159	13.7	13.5	11.8	LMP/LTO	0.98	0.88	0.46	0.39
EM RF OPT	Yes, 0.5C	87	14.0	13.5	11.8	LMP	0.96	0.88	0.46	0.39
EM RF OPT	Yes, 1C	64	14.6	13.5	11.8	LMP	0.92	0.88	0.46	0.37
EM RF OPT	Yes, 2C	42	15.7	13.5	11.8	LTO	0.86	0.88	0.46	0.35
EM RF OPT	Yes, 4C	53	16.8	13.5	11.8	LTO	0.80	0.88	0.46	0.32
EM REF	Overnight	220	23.2	22.7	20.6	LMP/LTO	0.98	0.91	0.33	0.29
EM REF	Yes, 0.5C	125	23.7	22.7	20.6	LMP	0.96	0.91	0.33	0.29
EM REF	Yes, 1C	91	24.6	22.7	20.6	LMP	0.92	0.91	0.33	0.28
EM REF	Yes, 2C	60	26.8	22.7	20.6	LTO	0.85	0.91	0.33	0.26
EM REF	Yes, 4C	75	28.5	22.7	20.6	LTO	0.80	0.91	0.33	0.24
EM OPT	Overnight	182	17.4	17.1	15.4	LMP/LTO	0.98	0.90	0.34	0.30
EM OPT	Yes, 0.5C	102	17.8	17.1	15.4	LMP	0.96	0.90	0.34	0.30
EM OPT	Yes, 1C	72	18.5	17.1	15.4	LMP	0.92	0.90	0.34	0.29
EM OPT	Yes, 2C	48	20.2	17.1	15.4	LTO	0.84	0.90	0.34	0.26
EM OPT	Yes, 4C	62	21.6	17.1	15.4	LTO	0.79	0.90	0.34	0.25

 $Table\ 4.3.1: Overview\ of\ baseline\ and\ simulation\ results\ per\ trip,\ and\ required\ energy\ storage\ per\ day.$

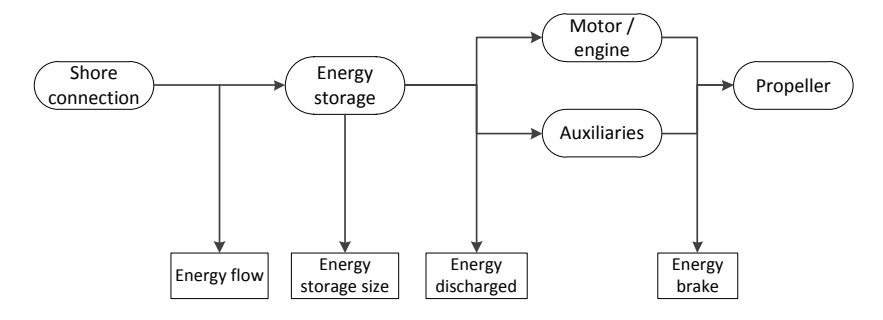


Figure 4.3.1: Definition of different energy names

4.3.2. FIXED PROPELLER BASELINE

Simulating energy and energy storage requirements for one day, six trips, using the generic operational profile it can be seen that the diesel uses 135 [kWh] per day for the propulsion, heating and auxiliary requisites. Dividing this by the found fuel to power efficiency mean value of 0.37 gives an energy storage size of ± 365 [kWh]. This value assumes that the auxiliaries are powered by the diesel engine as well. The trip values are 15.5 [kWh] per trip, without the auxiliaries. This equals about 22.5 [kWh] for propulsion, heating and maritime systems, see Table 4.3.3. Diesel brake power during the day is shown in Figure 4.3.2. In Figure

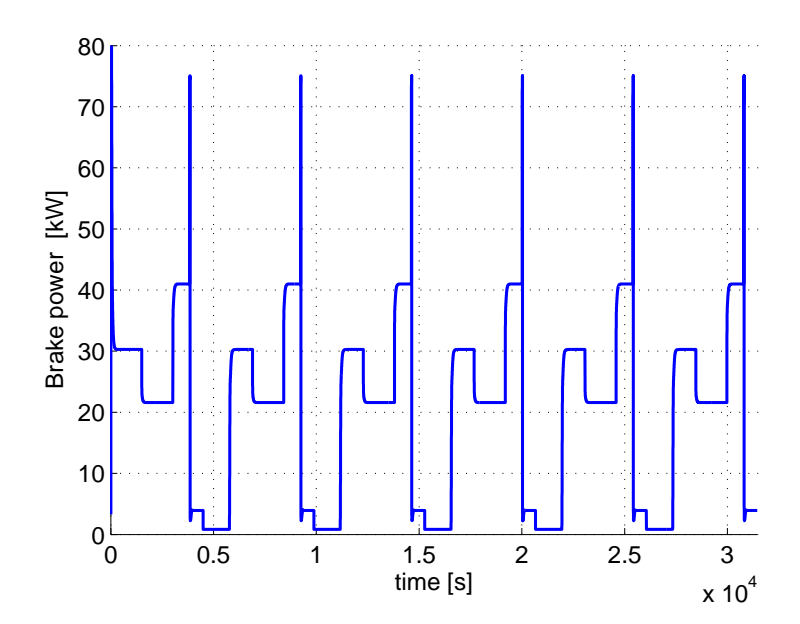


Figure 4.3.2: Diesel brake power

4.3.3 the speed results of the simulation are shown for one simulated day of about 9 hours. The required operational speed profile is found in Figure 4.1.3. It can be seen that the EM RF OPT electric boat accelerates faster after the stopping period. Furthermore the top speed of 3.3 [m/s] is not reached due to the short time per trip that this speed is required.

4.3.2.1. BASELINE EFFICIENCY CHAIN

The efficiency of the diesel engine and fuel to power conversion efficiency can be calculated with Equation 3.2.16. The average value during one day for this efficiency is 0.37 and it is shown in Figure 4.3.4. The average diesel open water efficiency is 0.45 due to the optimizations in Appendix G, 'Propeller optimization'.

4.3.2.2. BASELINE DIESEL MEAN VALUES

Diesel mean values for SFC and emissions per day are given in Table 4.3.2. See also Figure 4.3.5 for the NO_x variations throughout the day.

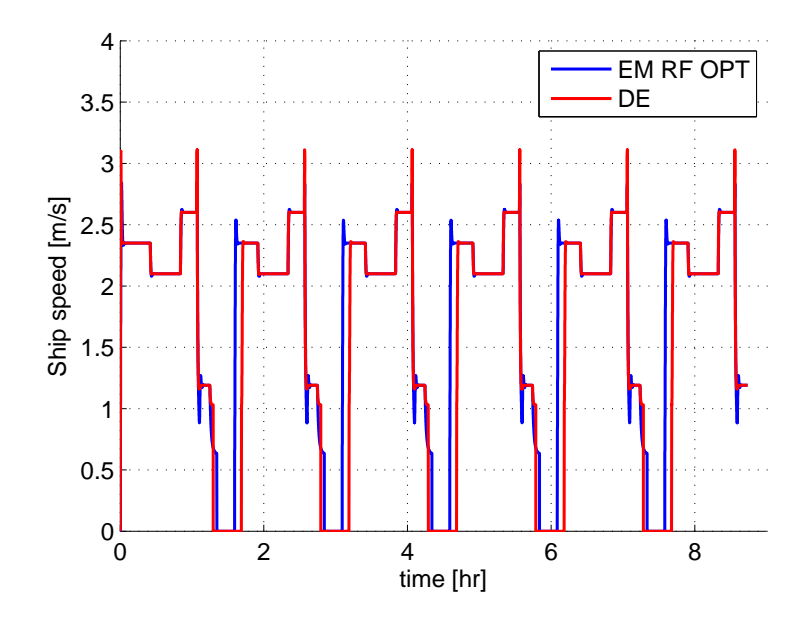


Figure 4.3.3: Ship speeds obtained during simulation

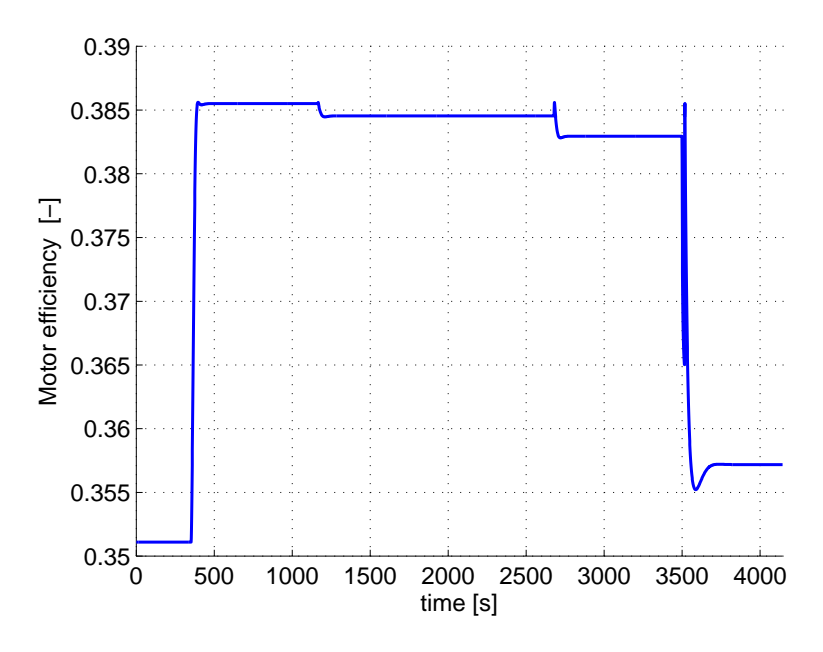


Figure 4.3.4: Diesel energy conversion efficiency

Table 4.3.2: Mean value in [g/kWh] emission and fuel results for the diesel daily simulation

	Mean value	Unit
Diesel fuel	224	[g/kWh]
CO_2	718	[g/kWh]
NO_x	7.3	[g/kWh]
SO_x	20	[g/kg fuel]

4.3.3. CONCEPTS - ONE TRIP RESULTS

The trip results for the electric concepts are given in Table 4.3.3.

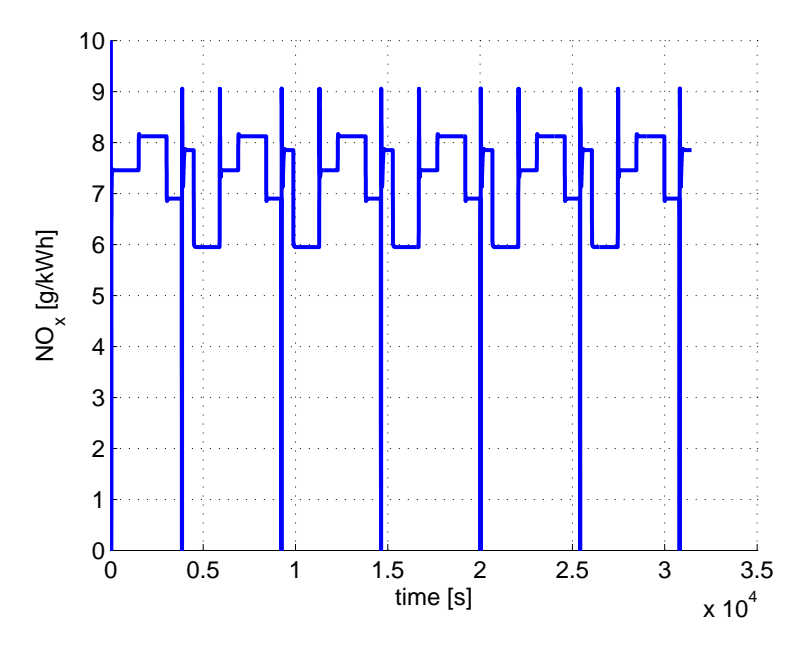


Figure 4.3.5: NO_x emission during full day

Table 4.3.3: One trip energy breakdown for concepts

	Discharged (battery) [kWh]	Auxiliaries [kWh]	Propulsion (brake) [kWh]
DE REF	22.5	7.0	15.5
EM RF OPT	20.5	7.0	11.8
EM REF	29.7	7.0	20.6
EM OPT	24.1	7.0	15.4

4.3.4. CONCEPTS - FULL DAY RESULTS

4.3.4.1. OVERNIGHT CHARGING

The required energy with only overnight charging is given in different forms. This is to be able to calculate the EPIs later on in a simple manner. The different energy properties are listed below. Each energy property is listed with its simulated result in Table 4.3.4. The energy required from the energy storage for the heaviest condition, heating with the heat pump and no intermittent charging, is displayed in Table 4.3.4. Figure 4.3.6(a) displays the brake energy usage. Figure 4.3.6(b) gives the battery discharge energy whereas Figure 4.3.6(c) gives the results of the energy flow. To calculate the total energy storage, the simulation is run including all losses. For diesel, the 365 [kWh] is divided by 0.8 to account for the 20% energy buffer. The results are given in Figure 4.3.7. The results in Table 4.3.4 and Figure 4.3.7 are rounded.

Table 4.3.4: Energy breakdown for the worst case, with heat pump, during the day

	Brake [kWh]	Discharged [kWh]	Flow [kWh]	ES size [kWh]
DE REF	135	-	365	456
EM RF OPT	107	123	125	160
EM REF	154	173	176	220
EM OPT	126	142	144	182

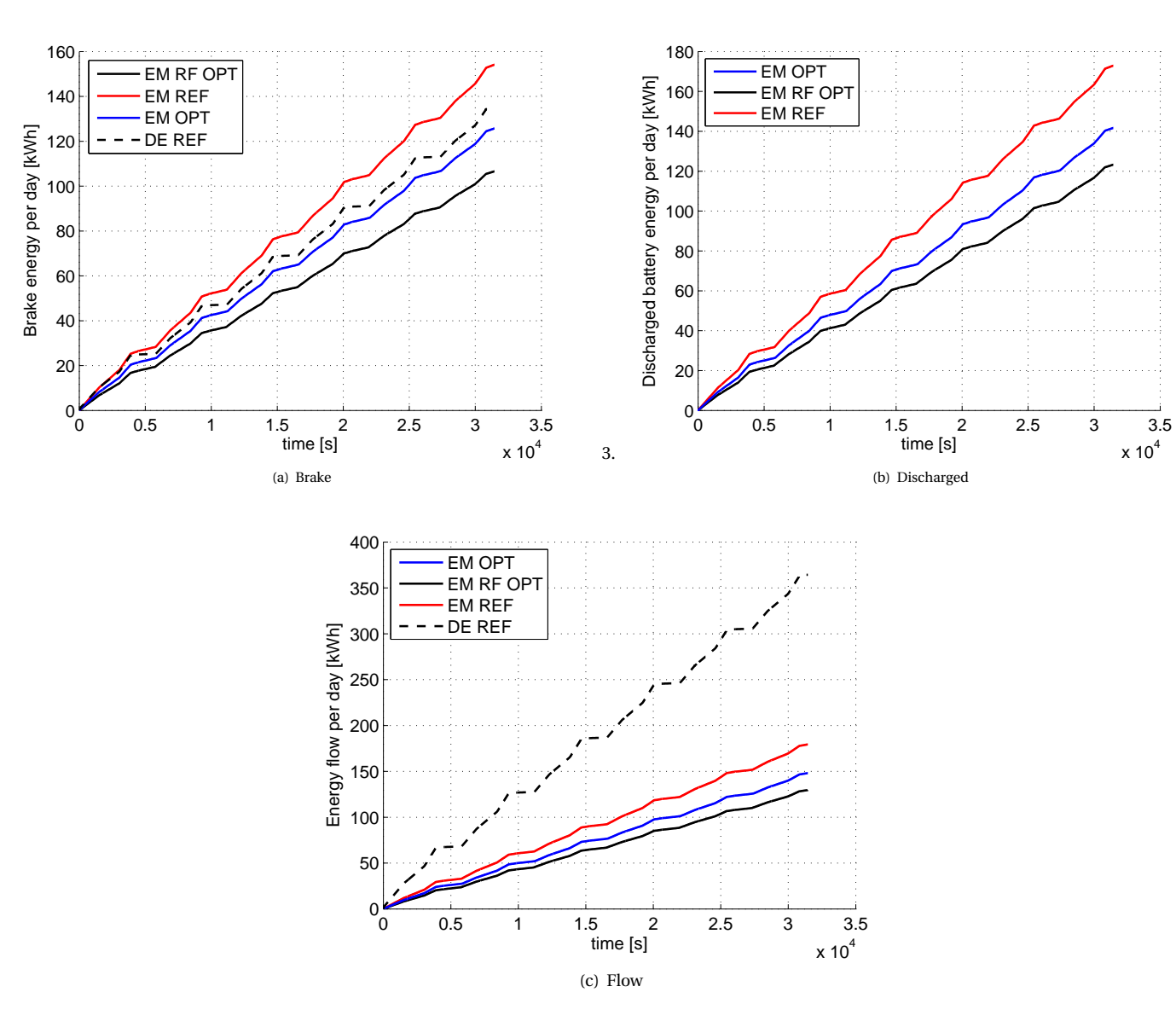


Figure 4.3.6: Energy results from full day simulation, no charging, full heat pump

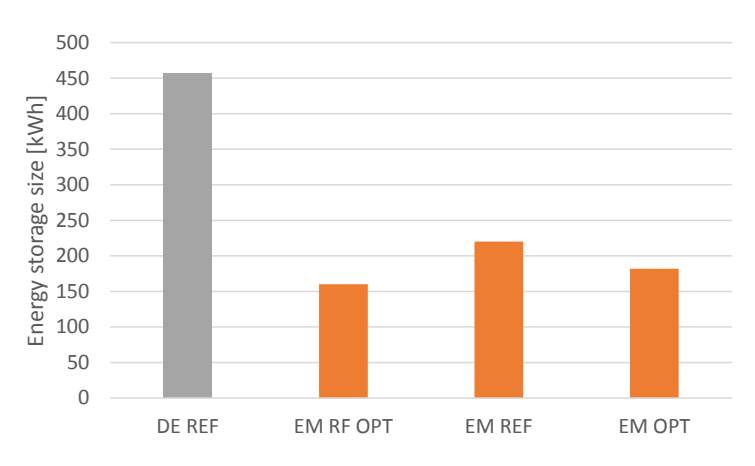


Figure 4.3.7: Storage size required per day when only overnight charging and 20% buffer size

It can be seen that the addition of the gearbox between EM RF OPT and EM OPT lowers the energy consumption with ± 20 [kWh] per day. This is mainly due to the higher open water efficiency of the EM RF OPT propeller, see Figure 4.3.8.

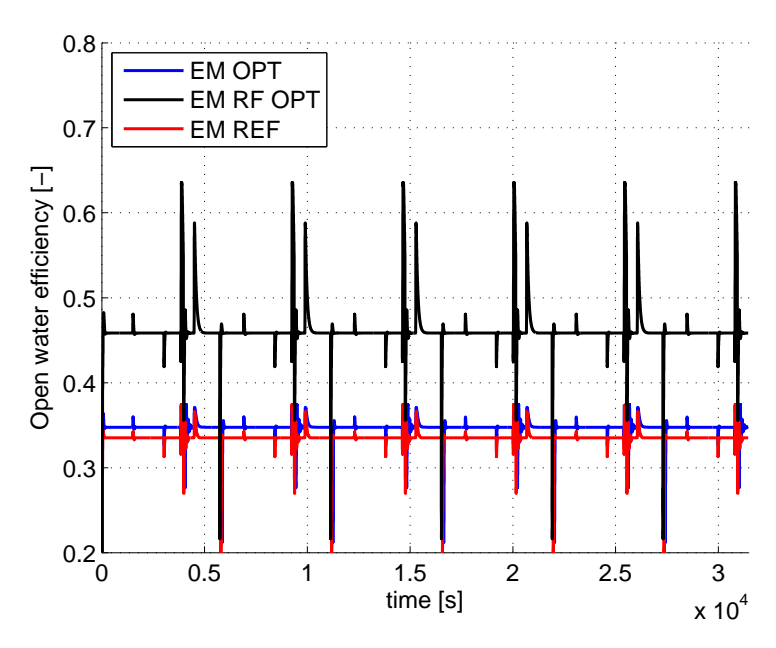


Figure 4.3.8: Open water efficiency of the concepts

4.3.4.2. Intermittent charging, full heat pump

Recalling the definitions for C charging rate, 3.4.5, 'C rating', C charging rate is here defined as the accompanying charge power, meaning that when 2C charge rate is mentioned for a pack of 50 [kWh], it means that the pack will be charged with 100 [kW]. In figures 4.3.9(a) and 4.3.9(b) the results of the simulations with the 6.1 [kW] heat pump are given for the LMP and LTO battery respectively. Both are charged with 1/2 of the maximum charge power according to the manufacturer. This improves life time compared to the maximum charging rate. In Figure 4.3.10 the comparison is made between the 1/2 charging C and the maximum recommended charging C by the manufacturer. As can be seen, this is useful for the LMP battery but not really improving for LTO. 1C is taken for LMP charging and 2C for LTO. The required energy *storage* capacity de-

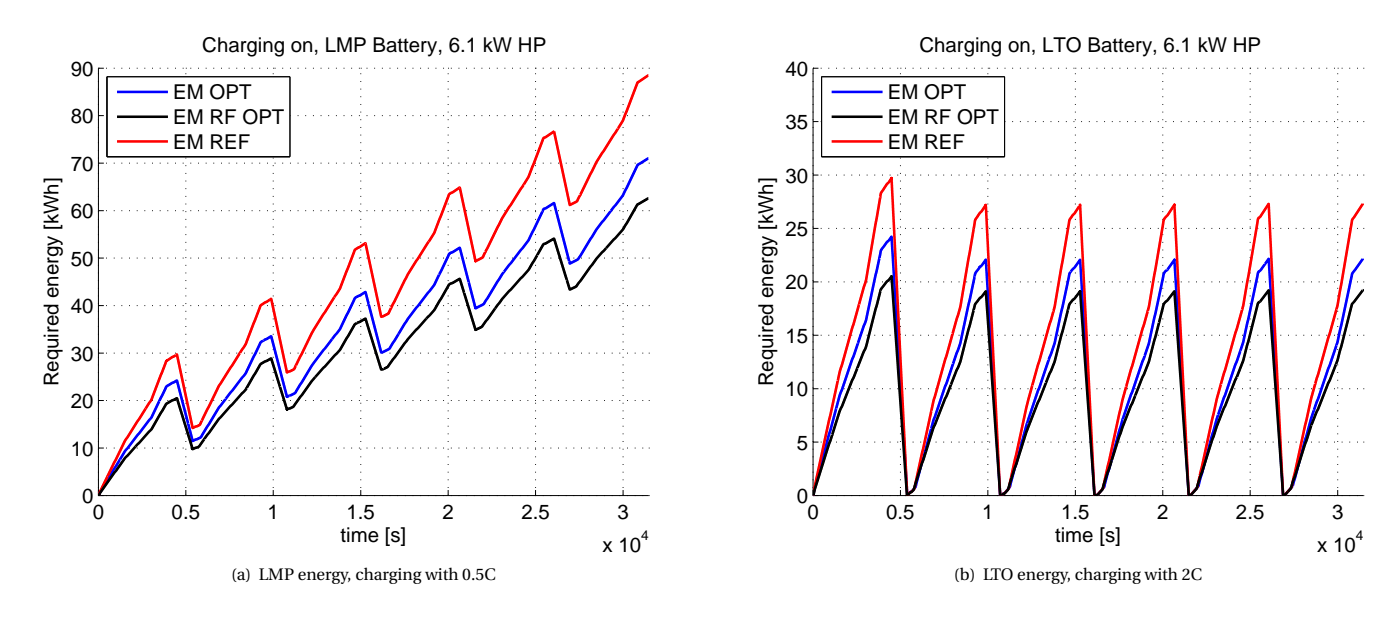


Figure 4.3.9: Required discharge energy from battery for battery types with 1/2 of maximum charging C

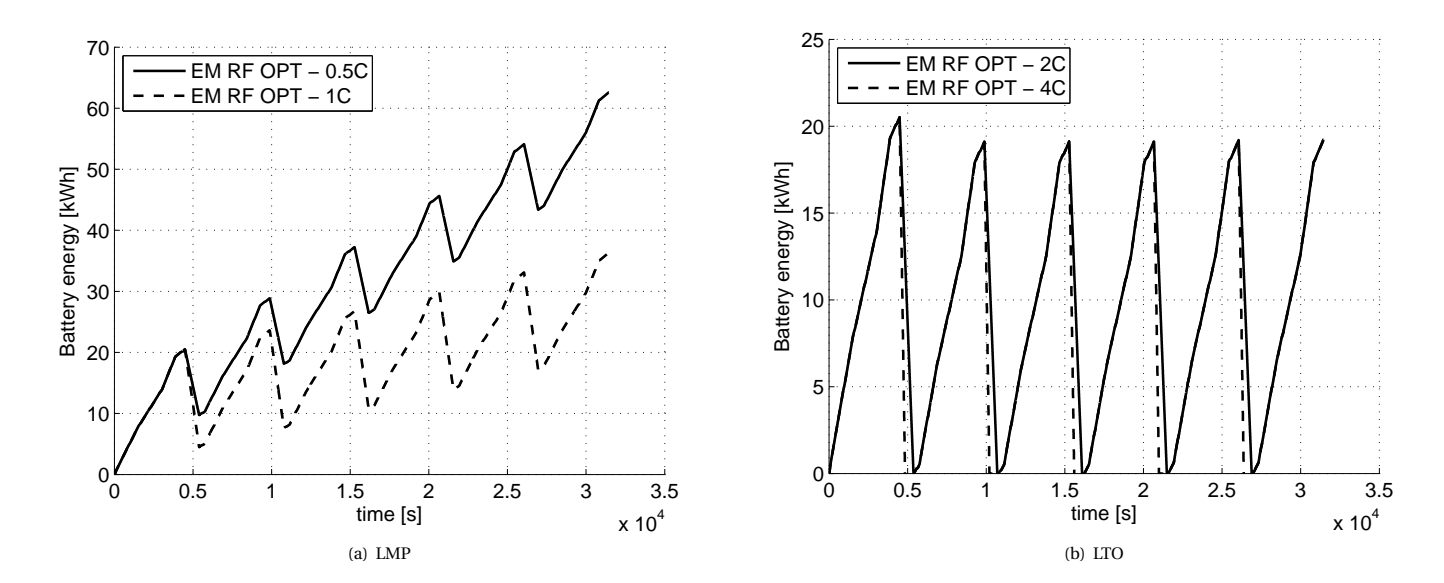


Figure 4.3.10: Comparison of battery energy for different charging C rates, for the EM RF OPT concept

creases with about 30% for LMP when charging with 1C instead of 0.5C, see Table 4.3.6. This is a trade-off though, as battery cycle efficiency decreases from 0.96 to 0.91, and a higher charge current means a faster decreasing life time [58]. As can be seen from Figure 4.3.10(b) and Table 4.3.7 there is no advantage noted when charging with 4C with LTO, as both charge rates can charge the battery within the assigned mooring

time. However, because at 4C there must be a larger power available to sustain the higher currents, required energy storage *goes up instead of down*, from 42 [kWh] to 53 [kWh], see Table 4.3.7.

4.3.4.3. SIMULATION COMPARED TO STATIC METHOD

Using the values from the block method and the measurements, Table L.2.: The results in Table L.2 for the hybrid static case are obtained with an electric efficiency between discharged energy and brake power of 0.90. As can be seen from Table 4.3.5 the modelled equivalents of diesel requires less energy whilst the electric (REF) case requires more energy:

Table 4.3.5: Overview of required energy

Data	Energy
[-]	[kWh]
Diesel static	16.7
Diesel modelled	15.5
Hybrid static	17.7
Hybrid modelled	18.7

The diesel case can be explained by the fact that the mean open water efficiency during static analysis is 0.33 whilst during the dynamic simulation this is 0.46. Higher open water efficiency means less brake power. This difference in mean open water efficiencies is explained in Chapter 5.1, 'Discussion'. For the hybrid case the open water efficiencies are much more alike, for both cases they round to 0.34. Therefore the energy increase for the hybrid boat can be allotted to the added dynamics of the vessel, mainly accelerating and decelerating between operational modes, which costs more energy than in a static calculation where this is not taken into account.

4.3.5. EFFICIENCY RESULTS

4.3.5.1. BATTERY EFFICIENCY

If the battery capacity is enlarged, this automatically means a higher charge power if the same C rating is applied, as can be shown by applying Equation 3.4.8. Battery efficiency is an important result of the simulations, as cycle efficiency plays a large role in the Amsterdam canals; the boats will be charged after every trip or every evening. Optimizing this charging process can improve total efficiency. Looking at tables 4.3.6 and 4.3.7 at the cycle efficiency it can be seen that the lower the C rate of charging, the more efficient the process is. This can be explained by the fact that a higher C rate is essentially a higher current which the battery is charged with. Higher currents mean higher heat losses. Compare it to a car: when driving faster you get there in less time but you will not be as economical compared to driving slower. Battery efficiency during overnight charging is found to be around 98% efficient when charging with 0.1C.

Table 4.3.6: Size of energy storage (rounded), LMP $\,$

Table 4.3.7: LTO (rounded)

Concept	Abbreviation	LMP [kWh]	0.5C charging η _{batt,cycle}	LTO [kWh]	2C charging η _{batt,cycle}
Concept 1	EM RF OPT	87	0.96	42	0.86
Concept 2	EM REF	125	0.96	60	0.85
Concept 3	EM OPT	102	0.96	48	0.84
Concept	Abbreviation	LMP [kWh]	1C charging η _{batt,cycle}	LTO [kWh]	4C charging η _{batt,cycle}
Concept 1	EM RF OPT	64	0.92	53	0.80
Concept 2	EM REF	91	0.92	75	0.80
Concept 3	EM OPT	72	0.92	62	0.79

4.3.5.2. ELECTRIC MOTOR EFFICIENCY

The motor efficiency will be used in the total chain calculation later on. In Figure 4.3.11 the efficiency for one trip is displayed. During the day the motor efficiency does not change hence it is only shown for one trip. It can be seen that the direct driven concepts have a higher motor efficiency than the concept with the gearbox. The oscillations at 3600 [s] in Figure 4.3.11 can be tuned by adjusting the PI controller variables.

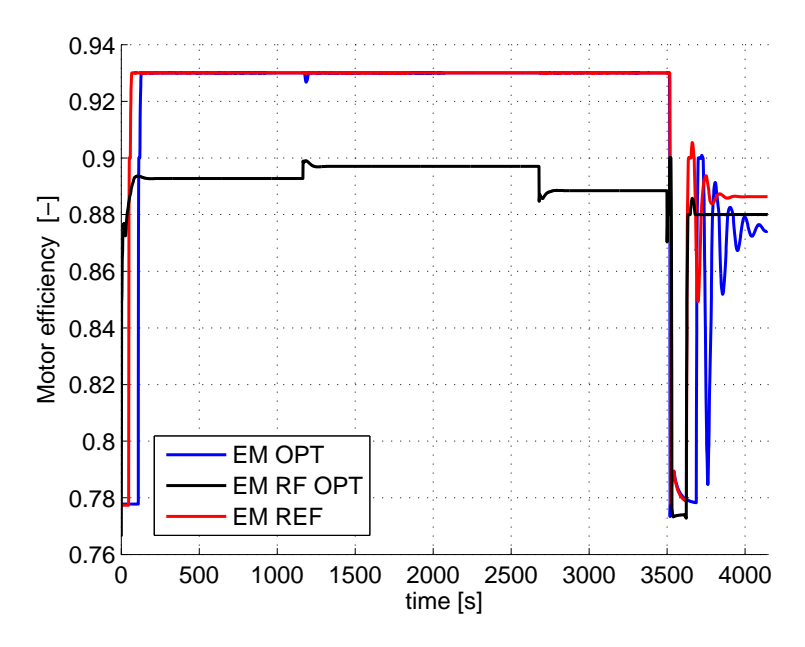


Figure 4.3.11: Electric motor efficiency of the concepts

4.3.5. EFFICIENCY RESULTS

4.3.5.3. TOTAL CHAIN EFFICIENCY

Chain efficiency is defined in Equation 4.3.2. The chain efficiency gives the total efficiency from energy storage to delivered power. In Figure 4.3.12 the different efficiencies are given for each concept with the heat pump on and the reference diesel.

The reference diesel has the lowest chain efficiency, Figure 4.3.12(a), only 0.17. This is mainly because of the poor conversion efficiency between diesel fuel and brake power which has a mean value of 0.37. Concept 1 has the highest chain efficiency, with 0.39 for LMP and 0.35 for LTO. This is due to the higher open water efficiency. For concept 2 the mean chain efficiency is 0.28 and 0.26 for LMP and LTO respectively. For concept 3, Figure 4.3.12(d), the mean value of chain efficiency is 0.30 for LMP and 0.26 for LTO.

$$\eta_{chain,EM} = \eta_{batt} \cdot \eta_{motor} \cdot \eta_o \tag{4.3.2}$$

$$\eta_{chain,DE} = \eta_e \cdot \eta_o \tag{4.3.3}$$

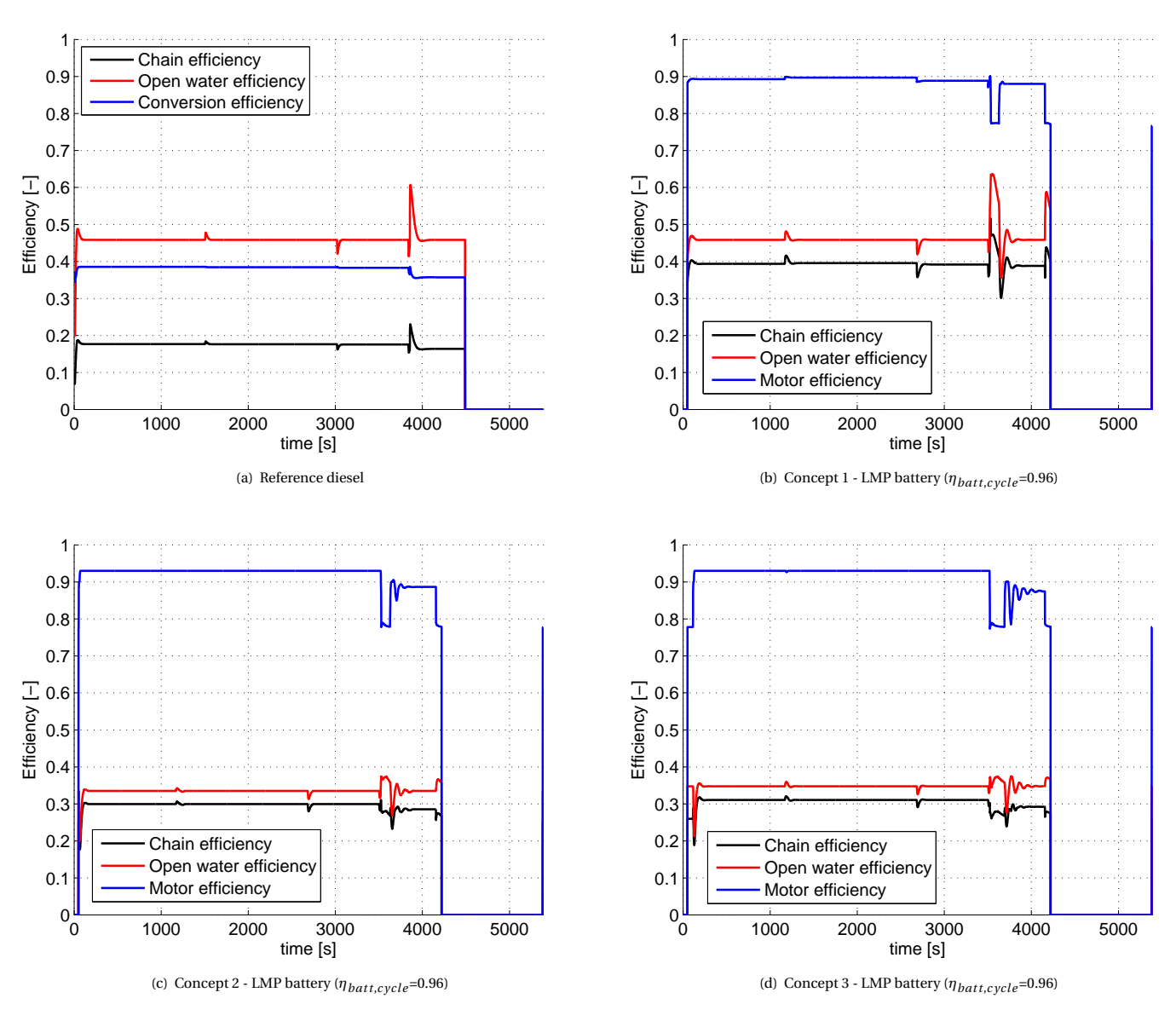


Figure 4.3.12: Breakdown of efficiencies and total chain conversion efficiency during one trip

When opting for the LTO battery instead of the displayed LMP in Figure 4.3.12 the battery efficiency is lower, refer to Table 4.3.7. This has influence on the total chain efficiency. For both battery types the total

chain efficiency is given in Table 4.3.8. The efficiency during mooring is not included in this chain efficiency as it is assumed that the motor is not running during that time.

Table 4.3.8: Mean chain		

Abbreviation	Diesel	LMP	LTO
DE REF	0.17	=	-
EM RF OPT	-	0.39	0.35
EM REF	-	0.29	0.26
EM OPT	-	0.30	0.26
	DE REF EM RF OPT EM REF	DE REF 0.17 EM RF OPT - EM REF -	DE REF 0.17 - EM RF OPT - 0.39 EM REF - 0.29

4.3.6. CHARGE STRATEGY

Looking at the electric concepts a LTO battery gives the least required battery capacity due to the ability to fast charge. In essence the LTO battery is capable to have an energy storage of only ± 20 [kWh] when concept 1 is used, see Figure 4.3.9(b). This is however not possible due to the large charge currents. As can be seen from Figure 4.3.13(a), when the energy reaches 0, this means that the battery should be full, the SOC is not yet at 1. This can only be achieved when the battery is slowly charged during a longer time. The reason behind this behaviour is that the voltage drop due to the cycle efficiency inhibits the model to go to a SOC of 1 during such a short time. This is due to the combined internal resistance and cycle efficiency in this model. The internal resistance consists of the complete resistance of the cell (including for example polarization resistance and electrolyte resistance). The solution is twofold. First, installing a larger capacity or charging with lower current can solve this problem. Second, a correct charging strategy must be implemented. The amount of energy charged during the mooring time is dependent on C rating. A higher charging rate is not always better, as Figure 4.3.13(b) shows. The best strategy is to be able to charge with the lowest C rating for the full mooring period. In the case of the LTO battery a charge power of 2C gives the best results, namely the highest SOC and acceptable cycle efficiency (84%).

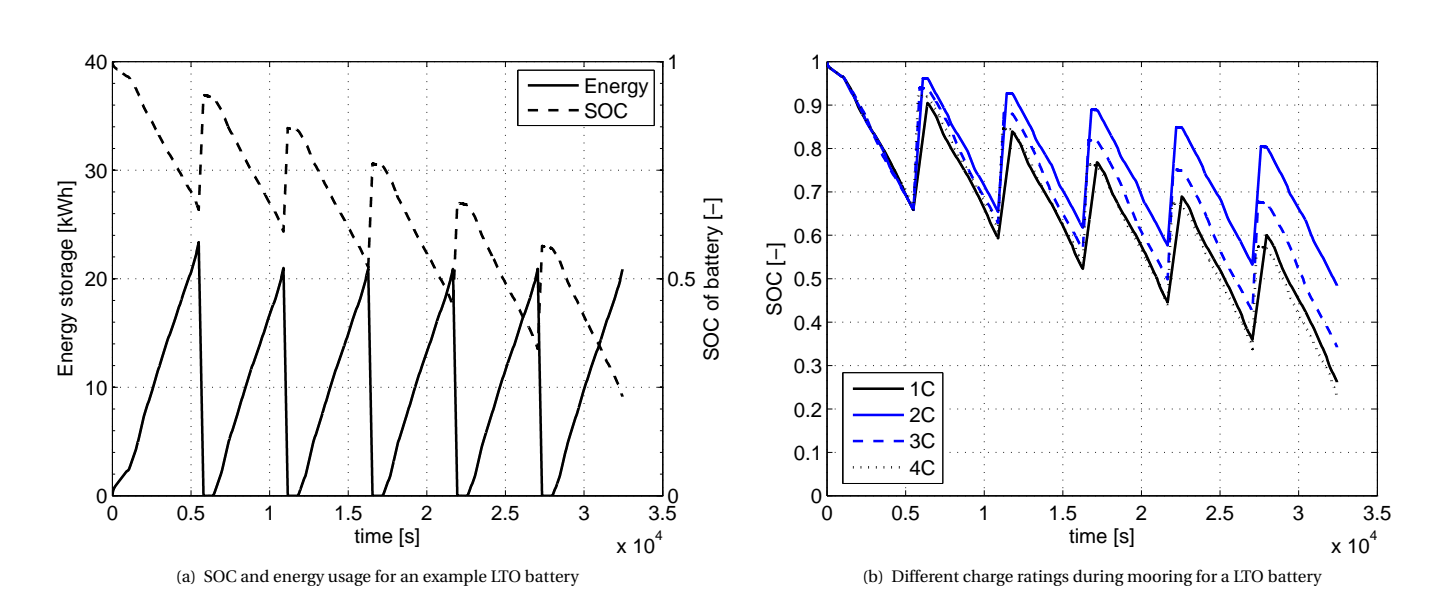


Figure 4.3.13: Charging strategy for LTO batteries

4.3.7. Environmental comparison

Using the emission values obtained from the simulation and using the method to calculate the environmental indices described in Chapter 3.5, Environmental Performance Indicator method, the environmental comparison results will be presented here. Using the values detailed in Chapter 4.1.2.2, 'Environmental indices' along with the obtained energy and emission values from the simulations. The EPIs are averaged over the charging possibilities, so that an average EPI value per concept is created.

4.3.7.1. EPI RESULTS

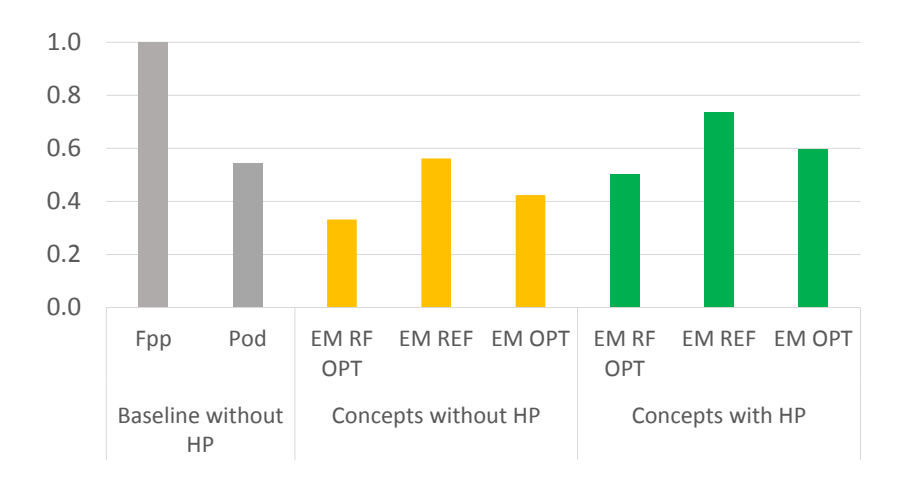


Figure 4.3.14: Relative difference of the electric configurations (averaged) compared to the diesel (=1) situation

The full electric concepts do not have *local* emissions, therefore their emission indices are zero if system boundary A is assumed. The emission indices for the baseline FP (diesel) is shown in Table 4.3.9.

Table 4.3.9: Fuel and emission indices for the diesel baseline

	Index values [g/(kg·km)]
FI	0.06200
CO_2	0.19800
NO_x	0.00201
SO_x	0.00123

MINIMUM REQUIREMENTS

Energy efficiency: When looking at system boundary B and applying the minimum requirements the land-based power plants must achieve to be equal to the diesel emissions and energy usage the value is averaged 46% for each concept configuration in Table 4.3.1. When looking at the most energy efficient concepts, overnight charging with an efficiency of 98%, the minimum required efficiency is 42%. A power generation method will therefore require an efficiency of at least 42% *including* transportation and conversion losses to be able to compete with the diesel boat in terms of energy efficiency. To compare, the energy efficiency in the Netherlands looking at all energy production methods (fossil fuels and renewable) for 2012 was 50.4%. Looking only at fossil fuels, this was 42.1% [?].

Emissions: The minimum attainable emission values are the same as the values calculated in Table 4.3.2:

To compare, values from a coal generation power plant are shown in Table 4.3.11 [81]. Note that values are SO_2 instead of SO_x .

Table 4.3.10: Minimum mean emission values for land-based power plants

	Mean value	Unit
CO_2	718	[g/kWh]
NO_x	7.3	[g/kWh]
SO_x	20	[g/kg fuel]

Table 4.3.11: Emission values for a coal power plant

	Mean value	Unit
CO_2	743	[g/kWh]
NO_x	0.7	[g/kWh]
SO_2	8.0	[g/kg fuel]

4.3.8. SIMULATION CONCLUSIONS

4.3.8.1. CONCEPT CONCLUSIONS

- EM RF OPT with gearbox uses the least energy and energy storage.
- EM RF OPT due to the gearbox and henceforth higher open water efficiency, has the highest chain efficiency.
- Combining optimization techniques and using the most efficient concept, a reduction in brake energy usage of 20% compared to the fixed propeller baseline is feasible. Note that there is also a reduction in energy usage possible if the bow thruster is used for the baselines.
- The usage of a gearbox improves open water efficiency with at least 10%. Furthermore the possibility of cavitation is greatly reduced.
- The usage of a gearbox reduces drive train efficiency. This is not taken into account. Chain efficiency will be 2-3% lower due to gearbox losses. However, this will give EM RF OPT still a better chain efficiency compared to the other concepts.

4.3.8.2. Energy storage conclusions

- Charging strategy is important in sizing the energy storage. The highest charging C rate does not always deliver the best result in terms of energy storage size and charging times.
- A minimum energy storage of 41.8 [kWh] of LTO batteries is required.
- A minimum energy storage of 64.4 [kWh] of LMP batteries is required.
- Intermittent charging reduces the energy storage requirement with 43-60% compared to only overnight charging for LMP, depending on configuration .
- Intermittent charging reduces the energy storage requirement with 66-74% compared to only overnight charging for LTO, depending on configuration .
- It is beneficial for energy usage to reduce the amount of energy storage as much as possible to refrain from having to use a keel to store the batteries.
- The cycle efficiency of the batteries is dependant on charge current (and hence C rate). Between the battery types, about 5% efficiency difference is noted for the same C *factor* (1/2 or 1 of the maximum).
- Batteries are a valid choice for the daily operational profile in the Amsterdam canals.
- For the C rates simulated, the LTO batteries are less efficient than the LMP batteries.
- Looking at the long range concept, a sailing time of 18 hours is possible for the long range concept, if the same keel that the baseline uses is assumed:

4.3.8.3. Energy flow and EPI conclusions

- Energy flow and EPI values are depending heavily on the ES method and the index boundaries
- The electric concepts are local emission free
- It depends on the method of power generation if the electric concepts are global emission free
- EPI wise, there is little difference between overnight charging and intermittent charging with 0.5C for the LMP battery

¹depending on keel size & battery amount

Table 4.3.12: Sailing hours

	Est. sailing hours per full charge
Baseline fp (diesel)	100+
Baseline pod	8-10
EM RF OPT	1-2
EM OPT	1-2
Long range concept	18^{1}

- The most environmentally friendly way of charging is with low currents
- For the C rates simulated, the LMP batteries are more environmentally friendly than LTO
- When a quayside generator with real life efficiency is assumed, chain efficiency for the diesel boat and quayside generator boat are almost the same
- The EPI method is able to predict environmental performance in a correct way, using the required energy divided by the benefit for society over a time range consisting of discrete modes in a generalized operational profile
- The conclusion from the created environmental calculation method is that the indices give a mean value based on operational profile and deployment of the ship. When green energy is assumed for the full electric boats there are no emissions. The analysis of power plant emissions must take place in case the energy is not fully renewable. As a quick comparison shows, it is not a given that electric boats reduce global emissions. A power plant will require an efficiency of at least 42% including transportation and conversion losses to be able to compete with the diesel boat in terms of energy efficiency. Power plant efficiency is about 50%, including renewable methods, and CO₂ emissions could be higher based on the fossil fuel used. Nevertheless, this calculation method will be of great importance once the canal boats and other vessels in the Amsterdam canals have to be fully zero emission in 2025.

4.3.9. FINAL CONFIGURATION

The configuration that uses the least amount of energy and requires the least amount of energy storage is EM RF OPT, the retrofit optimized concept. The gearbox in the concept lowers the energy consumption at the propeller with about 20 [kWh] per day compared to the next most efficient configuration. This gearbox will presumably have a high efficiency, as it will not require a clutch because the electric motor can be rotated forward and backward. The gearbox can be a simple 'reduction sprocket'.

A bow thruster or tunnel thruster helps reducing peak power in the 90° turns. The broad torque curve and high efficiency of the electric motor reduces propulsion energy compared to the typical diesel powered boats with $\pm 40\%$. This is achieved by optimizing the propeller (pitch and RPM), hull resistance (small battery pack, hence no keel), and turning capability of the canal boats. The downside is that the maximum speed is lowered to 3.3 [m/s]. Higher ship speeds are of course possible with a larger electric motor or a different propeller. With respect to ES, the consideration is made between a LTO 2C pack greater or equal to 42 [kWh] or the LMP pack greater or equal to 65 [kWh]. Due to the extended lifetime and lower costs, LTO is preferred, although its cycle efficiency is lower than the LMP pack. The EFD of the final configuration is given in Figure 4.3.15, where BT stands for bow thruster.

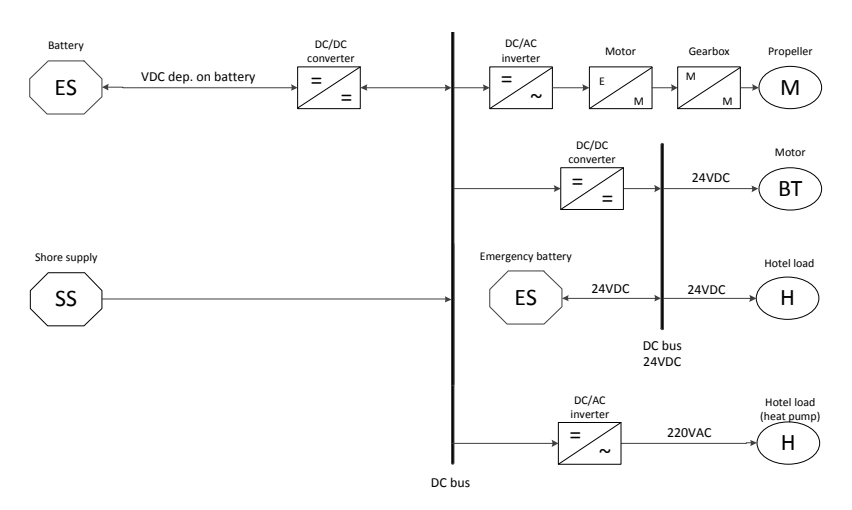


Figure 4.3.15: Energy Flow Diagram of the chosen configuration

Expanding Table 2.3.2 from Chapter 2.3, 'Concept approach', to include the solutions to the requirements gives Table 4.3.13. This table is used to give an overview of the key functional requirements used for concept 1 utilizing a LTO battery pack of 42 [kWh].

Table 4.3.13: Requirements, minimal requirements based on measurements and analysis, and used values in the simulations and
calculations, LTO 42 [kWh] pack

	Requirements	Minimal required	Used in sim.	Unit
Main propulsion	≥3.3 [m/s]	≥40	55	[kW]
Bow thruster	Included	≥8	8	[kW]
Heat pump	0-20 [°C]	≥6.1	6.1	[kW]
Energy storage	6 trips per day	≥42	42	[kWh]
Passenger capacity	Equal to typical boat now	100	100	[-]
Chain efficiency	More efficient	AHARP ²	0.35	[-]
Space in the boat	Ideally less space required	≤ than current ³	±1	$[m^3]$
Cost, yearly (avg.)	Cost effective	ALARP ⁴	12 150	[€/year]
Cost, 25 years (avg.)	Cost effective	ALARP	305	[k€]

²As High As Reasonably Possible

³3 [m³] for 200 [kWh] lead acid

⁴As Low As Reasonably Possible

APPLICATION OF RESULTS

The simulation results from the previous chapter will be used in this chapter to analyse practical constraints regarding the choice of concept. In this chapter lifetime and cost of the batteries is estimated, as well as volume and mass. In all comparisons, EM RF OPT, the concept that is the most energy efficient, will be used in the LMP and LTO intermittent charging configurations.

- · Life cycle analysis
- · Dilemma of battery (compromises, risks)
- · Volume and mass of components
- Cost analysis
- Final configuration

4.4.1. LIFETIME OF BATTERIES

The first part of research question Q.1.11 will be answered first:

What are the lifetime and costs of the energy storage?

(Ref. Q.1.11)

When looking at the lifetime of the batteries it was stated in Table 3.4.1, chapter 3.4, 'Battery modelling', that the average manufacturer given amount of cycles from 0-100% DOD was 2 800 - 3 500 for LMP and 10 000 to 15 000 for LTO. When analysing the lifetime of these batteries the lowest of these values will be used in the comparison.

4.4.1.1. LMP LIFETIME

The smallest energy storage size is assumed, 64.4 [kWh] for LMP. The DOD per trip is: $(19.1 / 64.4) \cdot 100 = 0.297$. Multiplying this value times six to obtain total cycles per day gives 1.78 cycles per day. Using the equations from chapter 3.4.10, 'Battery lifetime', to calculate the battery life time until there is 80% left gives an estimated lifetime of 3.6 years. Details of this calculation can be found in Appendix K, 'Lifetime calculation'.

4.4.1.2. LTO LIFETIME

The smallest energy storage size is assumed, 41.8 [kWh] for LTO. The DOD per trip is: (19.1 / 41.8) = 0.457. Multiplying this value times six to obtain total cycles per day gives 2.74 cycles per day. Using the equations from chapter 3.4.10, Battery lifetime to calculate the battery life time until there is 80% left gives an estimated lifetime of 8.3 years. Details of this calculation can be found in Appendix K, 'Lifetime calculation'.

4.4.1.3. LIFETIME DISCUSSION

Using the methodology described in this thesis to obtain lifetime does not take into account the current that is drawn from the battery, temperature, shelf time or usage of the battery (charging/discharging depth). This all influences lifetime of the battery. A higher installed capacity will lower the currents and this will result in a longer lifetime. If capacity is doubled, due to the linear nature of the method to calculate the lifetime, the lifetime will also double. This is highly unlikely, as lifetime is not linear with the amount of installed capacity.

Therefore this estimated lifetime is just an indication, and for this reason a variation study is conducted. In Table 4.4.1 the number of cycles is varied to give insight in the relative costs and lifetime of the batteries. The lifetime is varied with a deviation of 25% of the amount of cycles specified by the manufacturer. As these specifications differ between the manufacturers in discharge current, temperature and amount of cycles, the cycles are varied 25% both ways (25% less cycles and 25% more cycles).

4.4.1.4. BATTERY DILEMMA

There are two dilemmas when sizing the battery packs. The first one is if it is not better to choose a larger battery pack. In the application of the results little attention is given to the possibility of a larger energy storage. This is because this will increase initial costs and required volume on the boat. The goal is to give a minimum energy storage option that can be adapted for each specific case as required. For example, if the canal boat needs to operate 2 hours independently, more energy storage is required. However, taking into account every possibility is time consuming and therefore only the minimum required energy storage during a typical trip is analysed. There is a safety margin, the battery pack is sized in such a way that there will be at least 20% charge left at the end of the day. This is to take into account deviations in the operational profile and decreasing capacity during the lifetime of the battery pack, as has been shown in the lifetime chapter, 3.4.10, 'Battery lifetime'. The second dilemma is cost versus environmentally friendliness. As could be seen from the results, a larger battery pack and slower charge rate have a higher efficiency and therefore a lower environmental impact and lower energy usage. This trade-off process between cost and time versus energy usage, environmental footprint and reduced energy costs is something that the shipowner must carefully assess.

4.4.1.5. COST OF BATTERIES

The second part of research question Q.1.11 will be answered here:

What are the lifetime and costs of the energy storage?

(Ref. Q.1.11)

Using cost estimations based on personal correspondence with Leclanché and TNO the average prices per kWh (the highest prices in Table 4.4.1) are given in Table 4.4.1. Estimating a conservative decline of 20% in cost in 2025 with respect to current prices a basic variation study is conducted. Both prices per battery type are coupled to each number of cycles. From this, the costs per year are calculated, Figure 4.4.1(a), on the basis of 25 years of hull usage. Furthermore the expected lifetime of the battery pack is calculated, Figure 4.4.1(b).

Battery type [-]	Price per kWh [€/kWh]	Size of pack [kWh]	Cycles [-]
LMP	540, 675	65	2 100, 2 800, 3 733
LTO	1 120, 1 400	42	7 500, 10 000, 13 333
Lead - acid	120, 150	250 ¹	600, 800, 1 067

Table 4.4.1: Battery price and cycle variations

From Figure 4.4.1(a) it can be seen that the LTO battery is in most cases the cheapest choice. This is due to the small pack, low initial costs, and high amount of possible cycles. Based on availability of the LTO batteries and systems, the recommendation is to choose this technology, as it will require less replacements of batteries. The environmental footprint however is slightly larger than the LMP batteries, as the cycle efficiency is about 5% lower.

¹250 [kWh] is the current electric canal boat battery size

4.4.2. Network voltage 119

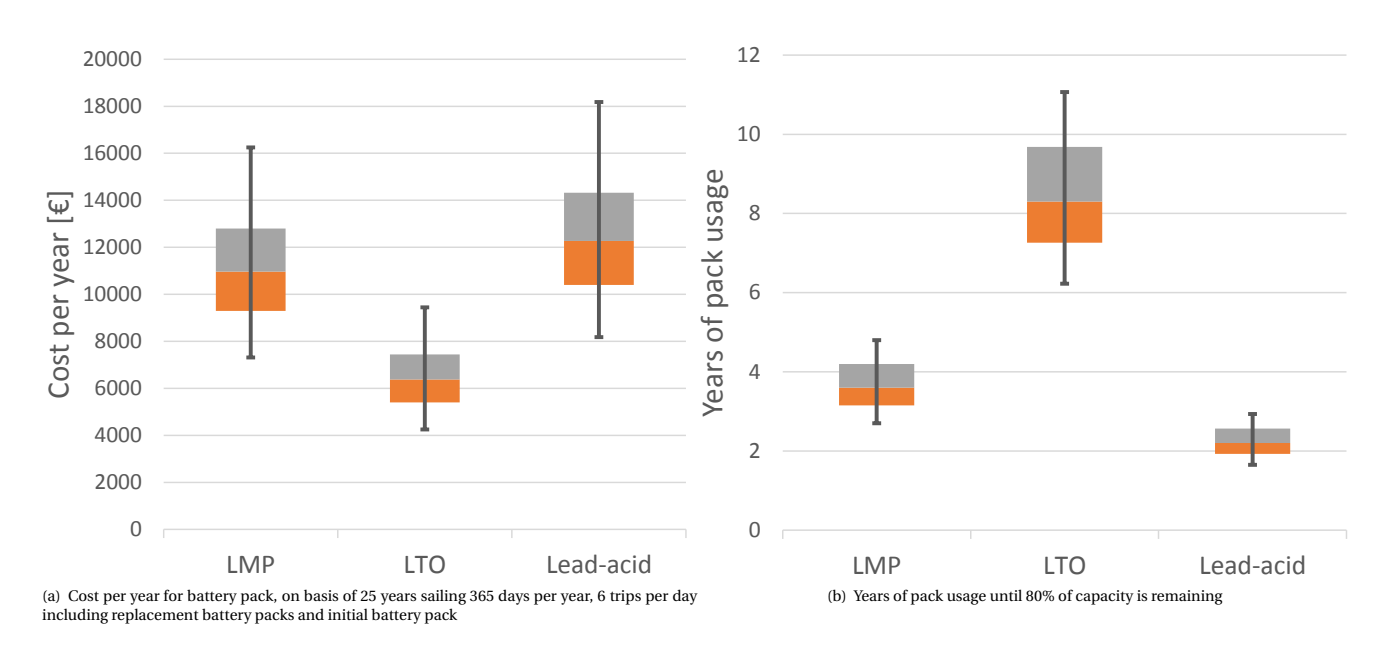


Figure 4.4.1: Variation study in battery pack initial parameters (cost and lifetime), not including other equipment and/or installation costs

4.4.2. NETWORK VOLTAGE

The voltage outputs are given by the simulation as well. The configuration parallel/series differs for each configuration and therefore the voltage differs a bit as well in each configuration. Typical values are shown in Figure 4.4.2 for the open cell voltage and delivered voltage. These values are well below the high voltage boundary of 1 000 [V] and plenty of power electronics can be found in this voltage range. Overall the configurations differ between 280 and 450 [V] (not including charging voltage) and therefore the specific configuration of battery pack, type and parallel/series combinations dictates the bus voltage.

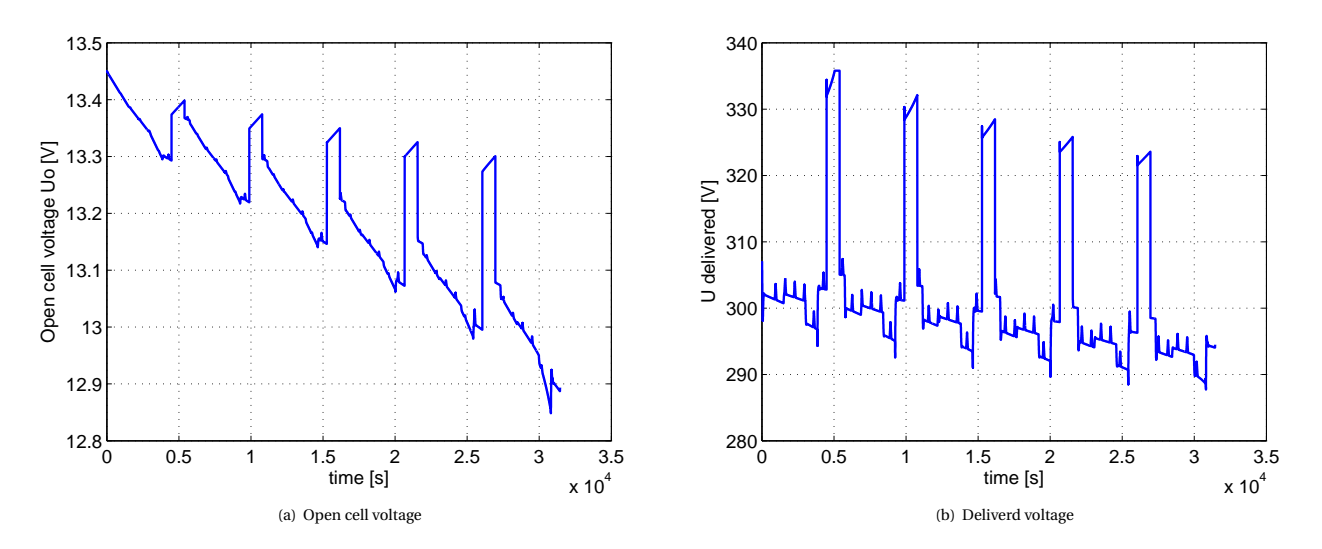


Figure 4.4.2: Typical voltage levels obtained from simulation

4.4.3. VOLUME AND MASS OF COMPONENTS

As stated before in chapter a smaller size battery pack is beneficial for numerous reasons:

• Batteries can be placed in the nose or at the aft of the ship, not requiring a keel that gives the ship a higher resistance

- A small battery pack is easier to replace and to do maintenance on. The lower the amount of cells to check, the faster an error can be found
- The battery pack can be placed in one place and does not need to be divided in the boat

Mass and volume is given in Table 4.4.2 where lead-acid is added to compare it to the current boat. As can be seen, mass of the lithium packs is about 10% of the mass of the lead-acid pack. Volume is about 13% of the lead-acid volume.

Battery type [-]	Volume [m ³]	Mass [kg]	Size of pack [kWh]
LMP	0.4	708	64.4
LTO	0.4	760	41.8
Lead-acid	3.0	7 500	250

Table 4.4.2: Battery volume and mass for the minimum required energy storage

The volume of the heat pump is estimated as $0.6~[m^3]$ in total (indoor and outdoor unit). This is the volume of an industrial heat pump with a heating capacity of $\pm 20~[kW]$. In total about $1~[m^3]$ is required for the energy storage and heating system when choosing a LTO energy storage system. This is about the size of the current diesel engine plus heater, so the train of thought is that this configuration will fit.

4.4.4. CHARGING AND QUAY INFRASTRUCTURE

Research question Q.1.12 is answered here:

What infrastructure is necessary to make zero emission possible?

(Ref. Q.1.12)

As can be calculated from Chapter 4.3, 'Simulation results', using LTO the charge power is 82 [kW]² for the LTO pack of 42 [kW] at 2C charging power. When this pack is charged with 4C, which sometimes might be required, the charging power is about 170 [kW]. The quayside infrastructure must be able to deliver this power. As the canal boat network will be a DC infrastructure, it is required that the quay delivers DC to be able to keep the conversion from AC to DC on the quay. The most simple solution on the quayside is the use of Electric Vehicle (EV) chargers. Nowadays, there are readily available chargers that can deliver about 50 [kW] per connection [82]. Using the latest standardization technique, J1772 level 3, a DC voltage up to 600 [V] and a current of 550 [A] is possible on a fast charging station. This translates to a maximum of 330 [kW] of power. These power levels are unfortunately not yet implemented, as practical power levels are nowadays between 60 to 150 [kW] [83]. This is therefore already almost enough to be able to charge the LTO configuration at 4C.

4.4.4.1. ALTERNATIVES

An alternative to the EV charger could be charging from the overhead wire of the tram and/or metro in Amsterdam. The tramlines in Amsterdam have a voltage of 600 [VDC] and a maximum power requirement of 960 [kW] [84]. The overhead tram line voltage is exactly the same as the J1772 level 3 standard. This might be useful in creating an infrastructure in the future. The metro in Amsterdam uses 750 [VDC] and metro carriages draw a maximum of 3.2 [MW] [84]. To put things in perspective, the extra power load on the metro line will be equivalent to almost four of these trams, if all 70 canal boats are charged with 170 [kW] (4C) *simultaneously*.

4.4.4.2. GRID CONSEQUENCES

A question that remains is if the grid can handle such extra powers required to charge the canal boats. Luckily, charge powers are relatively small due to the low amount of canal boats. A more in depth study into the details of the daily schedules and charging requirements of the canal boats must be conducted to be able to estimate or calculate grid impact. For this thesis, the uncontrolled charging strategy is assumed, a situation where boats are charged as needed, and no coordination between the charging of the boats is applied. Introducing this coordination could prove to lower grid impact in the future [85]. Calculating the total impact on the grid if all canal boats are made full electric in 2025 gives insight in the amount of extra energy required per year. This gives a preliminary estimation about the grid impact. Assumptions in this energy calculation are:

²Using nominal values

- Energy flow per day is taken for concept 1 from Table 4.3.4, for the overnight charging (125 [kWh] per boat per day) and LTO 2C intermittent charging configurations (147 [kWh] per boat per day).
- Charging station efficiency is 95%[86]
- Total fleet is 70 canal boats

Calculating total energy consumption per year:

$$E_{grid,yearly,overnight} = \frac{125}{1\,000 \cdot 0.95} \cdot 70 \cdot 365 \approx 3\,400 \text{ [MWh]}$$

$$E_{grid,yearly,intermittent} = \frac{147}{1\,000 \cdot 0.95} \cdot 70 \cdot 365 \approx 4\,000 \text{ [MWh]}$$

4.4.4.3. COST PER BOAT PER YEAR

Using an electricity price between 0.06 and 0.11 [€/kWh] [87], the electricity costs for overnight charging, LMP 1C and LTO 2C configurations are calculated, see Figure 4.4.3. These values are per boat per year.

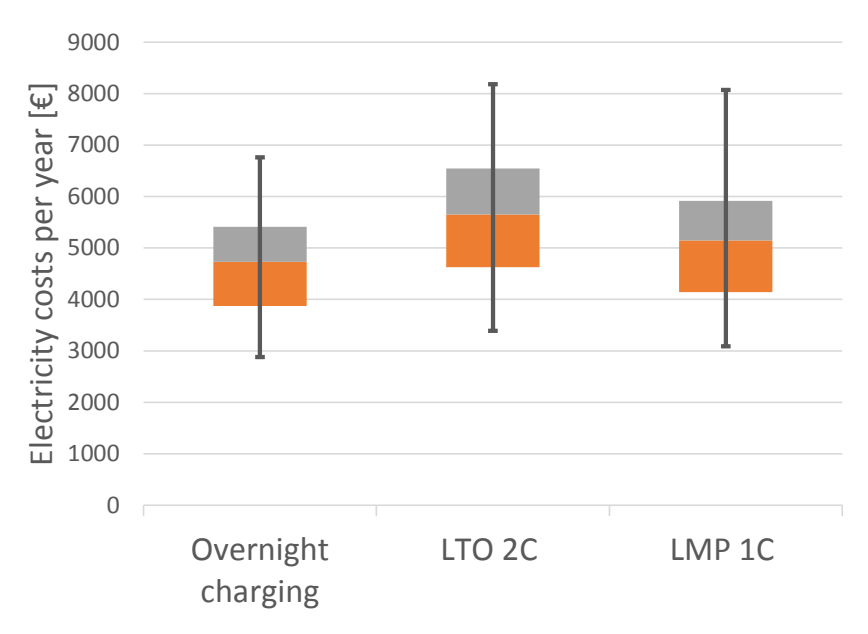


Figure 4.4.3: Energy costs per boat per year, for an energy price between 0.06 and 0.11 € for each concept

COST OF CHARGING STATION

The cost of a Level 3 charging station are reported by [83] between \$30 000 - \$160 000. Variables that are required for a more detailed grid impact calculation are [85]:

- · Sailing patterns / operational profile
- Daily schedules
- Chosen configurations of all involved canal boats
- Charging characteristics
- Charge timing
- Electric canal boat penetration as a factor of total energy usage
- Detailed grid information (peak hours, usage percentage)

This grid impact study could include Vehicle to Grid (V2G) applications as well.

4.4.4. SAFETY

The charging system, whether using overhead wires, metro lines or EV charging stations, must be safe and have at least the following protections [88]:

· Over- and under voltage protection

- Over current protection
- Short circuit protection
- Earth fault protection

If a fault occurs anywhere between the grid and the canal boat the charging station must be switched of directly to ensure safety.

CONCLUSIONS AND RECOMMENDATIONS

This chapter starts with the discussion, giving notable points that arose during the thesis, as well as a critical review of the modelling and results. The reason behind starting with the discussion is that the critical review will be used in the conclusion chapter. The discussion is followed by recommendations to enable future researchers to improve the work. Finally conclusions are presented, giving an extended summary by bringing back the research questions and hypotheses from Chapter 1.2, 'Methodology' and answering them in detail, as well as incorporating the discussion points.

5.1

DISCUSSION

The discussion entails the consideration of notable points, the applicability of the results outside the context of the Amsterdam canals and a critical review of this text that gives remarks and refinements regarding the methods and significance of the models. The recommendations follow, which give an overview how this work can be improved and ideas for further investigation or study.

5.1.1. NOTABLE POINTS

During the creation of this work a few unexpected results and observations surfaced, which will be discussed here.

5.1.1.1. UNEXPECTED RESULTS

- Comparison method: When the Environmental Performance Indicator (EPI) calculation method was conceived, the main research question was difficult to answer. It asks how one could compare a diesel fuel boat and a full electric concept. While keeping in mind that the electricity is generated somewhere, and probably with emissions, this is difficult. During the propagation of the method, a simple and elegant solution came to mind. This was to see what the *minimum* efficiency of the power generation should be if it had to have the same energy consumption as the diesel boat. By doing this, there is no need to analyse losses from power plant fuel to quayside charger in this text. This was not an expected outcome of the creation of the methodology, but answered the main research question, by giving a 'fair' method of comparison. This fairness is achieved by looking at the fossil fuel conversion method for both diesel and power generation. One could argue that the diesel needs to be transported as well, and they would be right. But it is chosen to draw the index boundary at the power plant for electricity, and at the diesel fuel for the diesel boat.
- **Charging strategy:** The charging strategy of the lithium-titanate (LTO) battery was another notable outcome of the simulation that was not expected. 2C charging is more efficient than 4C charging, has less power losses and gives about 20% more state of charge (SOC) over the course of one day. This is a surprising outcome, as one would expect 4C to be the faster charging option with more SOC at the end of the day. More research into the resistance of the batteries has to take place to know the best charging strategy.

5.1.1.2. NOTEWORTHY OUTCOMES

- **Battery model:** The battery model is quite accurate until the SOC becomes smaller than 20%. By using a chemical model, the accuracy over the last 20% could be improved to obtain accurate results for the whole battery SOC range. In this thesis, the solution is to never let the battery reach this SOC, as there is always at least 20% left in the battery. This is only a bypass and a fully functioning method should be implemented.
- **Regulations:** If there was no inflexible regulation about zero emission, the improved manoeuvrability with the use of the bow thruster could also reduce the current diesel energy and power requirements. Hence the reductions here do not only apply to the concepts, but also to the baselines. The diesel is less

126 CHAPTER 5.1. DISCUSSION

efficient in part load operation, but the use of the bow thruster could reduce energy consumption, and could lead to smaller engines.

5.1.2. APPLICABILITY OUTSIDE OF CONTEXT

- **Methodology:** The design methodology presented in this thesis can be applied to the general design of ships varying from small passenger vessels to large crude carriers. Optimizing the ship design by simulating the operational profile in the design phase is a powerful tool that can minimize fuel consumption as well as other emissions. This is useful, as Sulphur Emission Control Areas (SECAS) and NO_x Emission Control Areas (NECAS) will play ever increasing roles in the future shipping industry. However small a canal boat is, the methodology presented in this thesis can be applied to virtually every ship. By defining the operational profile the ship will sail, certain preliminary design choices can already be made. The environmental comparison method is an useful tool that is not only limited to Amsterdam or canal boats. The foundation of the method is universal and applicable on ships, cars, planes and any form of transportation. By looking at discrete operational modes instead of a mean point of operation, accuracy of the design values with respect to the Energy Efficiency Design Index (EEDI) is enhanced.
- **Battery model:** The battery model gives accurate results if the parameters are within a close range of the data from the manufacturer, and if the battery is not discharged over 80%. The model that is used here can be extended to every required application, as it is a 'standalone' model. By changing the parameters according to a manufacturer of choice, simulations can be carried out which give SOC and energy storage size (if required).

5.1.3. FUTURE RESEARCH RECOMMENDATIONS

When the zero emission regulations will be required in 2025, additional research might provide extra insight and design requirements to implement and deploy the electric boats without obstacles. Next some recommendations for further research are outlined, as well as a discussion about the limitations of this research.

- Final configuration: A few remarks about the final configuration and why these results should be used carefully. The main reason that the fixed propeller (FP) scores the lowest energy consumption is because its propeller revolutions per minute (RPM) is much lower than the electric counterparts. However, manoeuvring requirements with a pod drive are lower in terms of energy and power in the 90 degree turns. Pods do have a higher resistance, simply because there is a larger part of the drive train submersed. Combining a lower speed propeller with the manoeuvrability of a pod or steerable thruster, bypassing the gearbox, thus will probably be the most efficient solution. Care must be taken, as there were already boats built with thrusters. These were deployed with limited success, as the thrusters sucked debris through the nozzle and broke down [29]. More research about the possibilities with small electric motors is required.
- **Ship model**: With respect to the modelling of the ship a 1D model is used: only accelerating, steady state sailing and decelerating are included. It is relatively simple to create and gives a general idea of speed, energy consumption and required power of the vessel. 90 degree turns are simulated with SurSim and the power that is required for these configurations is used in this 1D model. Manoeuvring power is averaged and added in the 1D model as well. This lowers the energy consumption at the propeller, as the open water efficiency during manoeuvring and these turns is steady state, and around 30-50% during simulation. This open water efficiency is depending on configuration and concepts, whereas it was calculated in Appendix G.6, 'Manoeuvring' to be more around 20%. This ship model is most useful for ships that do not have a constantly changing operational profile (as is the case here, due to traffic) and do not manoeuvre a lot. The reason that this model is still used is because detailed information about the hydrodynamic coefficients of the canal boats was missing. This lack of data translated into the usage of SurSim to estimate bow thruster application in the tight turns. Without a proper manoeuvring model, containing all the hydrodynamic coefficients, the results have a large spread due to this higher open water efficiency. Although the use of SurSim is questionable, it was the author's view that this was the only applicable option to estimate turn forces and required powers. Future research could include the creation of a shallow water hydrodynamic tool that is able to simulate complex manoeuvres of (small) inland ships.
- Motor types: In this thesis two engine types were modelled, one diesel engine and one electric permanent magnet machine. Electric machines that adopt an axial flux lay-out could be very useful in the

Amsterdam canal boat industry as these motors have large torque capabilities and are still very small. Axial flux motors are a relatively new technology, mostly used in hybrid or full electric cars. These types of motors, coupled with a gearbox, could probably bring down the energy usage some more. The data that is known from literature is however not validated or verified so far, and therefore these motor types have not been analysed. The motor in the pod has been validated with the measurements that were conducted. It is therefore recommended to assess (these) new engine techniques as well and to see if they can be verified and/or validated.

• Legislation: Over the course of this thesis the author has been in contact with all sorts of different parties and stakeholders with regards to the Amsterdam canal and waterway situation. One thing that was striking was the low level of clear communication about legislation between different parties. The recommendation is that all involved parties, the municipality in the form of Waternet, the shipowners and other involved parties set a clear and cohere set of rules with regards to commercial canal boats, based on a mutual understanding of the subject. A revision of the current rules is required. For example the top speed the canal boats must be able to sail as well as noise regulations and battery ventilation and storage rules could use a more modern set of rules.

5.1.4. MODELLING RECOMMENDATIONS

In this section recommendations with respect to the modelling in this thesis will be given. Models will be criticized and further research points are detailed.

- **General:** Keeping in mind the discussed constraints and assumptions the obtained results from this thesis can be applied to the zero emission Amsterdam situation. Looking at accuracy and validation of the different parts of the canal boat, it has been shown that values are compatible with real life situations. The constructed tools provide a helpful hand in designing full electric canal boats, not only for Amsterdam but for cities around the world.
- Battery model charging: Mainly in the case of charging, where only one (lithium metal phosphate (LMP)) or two (LTO) charging curves are available from the manufacturer, it is difficult to model what will happen if charging occurs with a larger or smaller C rating and/or different temperature. More extensive tests and/or more data from the manufacturer can provide a model with higher accuracy for charging. This will in turn provide more detailed efficiency- and discharge values, which are useful to size energy storage and requirements on board.
- **Battery model Temperature dependency**: The temperature model presented in this thesis uses a parametric approach. Individual cell temperature and possible cooling problems or hot spots are not taken into account. Better results will be obtained with a chemical/thermodynamic model of the battery (temperature). The temperature dependency used in this model can then possibly be coupled to a thermal model of the internal battery temperature. This way, thermal hot spots as function of current and SOC can be visualised.
- **Battery model Life cycle**: The method to obtain the remaining lifetime or remaining life of the battery is crude. This is inherent with the manufacturers data, as there is only one discharge curve, at a constant current and constant temperature given. For the LTO case, the provided manufacturer curve is not even complete, as it reaches only 4 000 6 000 cycles out of a theoretically possible of 10 000 or more. Hence, life cycle estimation will need to be improved to give accurate predictions about the life time of the battery. Parameters such as discharge depth, discharge current, temperature, charge current, charge depth, charge time, size of the battery pack all play a role in the lifetime estimation. It is therefore recommended that more insights in the life cycle modelling must be obtained to provide accurate results.
- Hull optimization: In this thesis, no hull optimizations took place except for the inclusion or exclusion of the keel between the concepts. Although the canal boats have been around for years, in coming years a new hull design might prove useful, as space requirements in the boats will change due to the full electric legislation. With recent advancing steps into Computational Fluid Dynamics (CFD) an optimization of hull form could prove advantageous for space optimization and energy consumption.
- **Gearbox and nozzle optimization**: Looking at practical applications, a gearbox coupled with an electric motor can be applied in different ways. A Z-drive or L-drive can have a reduction transmission. When looking at the propeller a nozzle could prove even more energy efficient as it will improve low speed manoeuvrability. Additional research into the topics of the optimal gearbox and nozzle could therefore prove beneficial for the manoeuvring ability of the canal boats. When looking at manoeu-

128 Chapter 5.1. Discussion

vrability, the bow thruster has been mentioned and simulated in Appendix G, 'Propeller optimization'. Additional research into the application of a steerable water jet thruster could improve manoeuvrability and decrease peak powers in the canals and 90 degree turns.

5.2

CONCLUSIONS

The conclusion gives a summary and interpretation of results and a review of the research objectives. Each research question posed will be answered. Furthermore, main outcomes of this work are presented. This chapter will first treat the zero emission concept research questions. Then the first main hypothesis can be analysed, which will lead to an answer of the first main research question. This is succeeded by the analysis of the second set of research questions of this text, the environmental comparison. When these research questions are answered, the main hypothesis is analysed as well and from this the second main research question can be answered.

5.2.1. ZERO EMISSION CONCEPT CONCLUSIONS

Starting with the research questions, as founded in Chapter 1.2.1.1, 'Definition, research questions':

5.2.1.1. DEFINITION, RESEARCH QUESTIONS

What parameters determine energy consumption?

(Ref. Q.1.1)

What is known about the canal boat systems in Amsterdam?

(Ref. Q.1.2)

Typical installations of Amsterdam canal boat systems are known and contain a 80-100 [kW] diesel engine used for main propulsion and a diesel burner with a heating capacity of 20 [kW]. Furthermore, a bow tunnel thruster is sometimes installed with powers ranging between 5 and 10 [kW]. Canal boats cannot be longer or wider than 20 and 4.25 [m] respectively. The minimum required speed they should be able to sail is 11 [km/h] and stopping distance should be less than twice the length of the canal boat at full speed. With regards to required energy per trip, the measured canal boats need about 16 to 18 [kWh] from the energy storage, depending on configuration. By using a higher resistance but optimizing the boat with regards to propulsion the conceptual boats only require about 20 to 26 [kWh] brake energy per trip *including heating*.

How can the baseline be set?

(Ref. Q.1.3)

The baseline is set by measuring two types of canal boats, a diesel and a hybrid boat. By sailing the same trip multiple times, a generalized operational profile with respect to power and energy usage is constructed. Using this operational profile, the vessels can be simulated during a trip and/or full day and compared to the baseline measurements.

What are possible improvement points of the baseline, in terms of energy and power usage? (Ref. Q.1.4)

There are a few improvement points when analysing the measurements that were conducted. A large portion of time and energy is used in the manoeuvring of the canal boats, including sharp turns. Furthermore, there is a large part load operation when using the diesel engine. These points are the main improvement points. By using the bow thruster during manoeuvring, energy consumption and power requirements go down significantly compared to the baselines: From more than 50% energy during manoeuvring per trip down to less

than 40% for the concepts. This reduction is due to the improved manoeuvring as well as simple hull improvement, using the FP baseline hull for the concepts, except for the baseline electric concept. The hulls of these boats differ significantly and, as there is no hull optimization in this graduation project, both hulls are used in the concepts. These hulls underline the need of a small energy storage system, as for a large volume of energy storage an extra keel will have to be constructed underneath the canal boat. This keel increases resistance and hence energy consumption.

The auxiliary energy consumption is also reduced. The capacity is the same, but the electric power required is down to only 6.1 [kW], due to an Coefficient of Performance (COP) of about 3.5. The consequence of the lower energy consumption due to propulsion is a relatively *higher* percentage of energy consumption due to the heating. This energy consumption rises to almost 35% of the total energy discharged by the battery. It therefore becomes an interesting option to optimize even further.

5.2.1.2. CONCEPT, RESEARCH QUESTIONS

What are the considerations, requirements and limitations of the concepts?

(Ref. Q.1.5)

- The concepts must have the same or a larger people transporting capability within the same size boat (≥ 100).
- The concepts must be able to be deployed 365 days per year. This means adequate passenger comfort year-round (sufficient heating).
- The concepts must be able to obtain a minimum speed of 3.3 [m/s] which is the minimum speed that a boat must be able to sail in the centre of Amsterdam with a permit.
- The concepts must have an independent back up propulsion system to safely reach the quay in case of an emergency must be available (see Section 2.3.2.1).

Important points that must be kept in mind, but are not top priority:

- Space in the boat, this is directly linked with the minimum people transporting capacity that must stay the same. If the system is too large, this will require space that could have been used for passengers.
- Cost of components, as this is an conceptual design made for 2025. Cost is included for the battery storage but no full cost/benefit analysis will be conducted.

What are the most viable concept options?

(Ref. Q.1.6)

The most viable concept options are:

- Energy storage: A battery as energy storage, as a fuel cell option is more expensive, requires more volume and the infrastructure is more difficult to create.
- **Electric motor:** A Permanent Magnet Synchronous Machine (PMSM) 55 [kW] electric motor, possibly coupled with a gearbox. This motor is chosen because the specifications and efficiency over the complete operating range is known, see also Appendix C, 'Motor efficiency plot'.
- **Heating:** For heating, two options are viable: A heat pump, and seat heating. Seat heating is only applicable with fixed seats, which is not the case but could be used if the seats are fixed. A normal hot water boiler system is not that efficient (≥78%) and requires a large volume to generate 20 [kW] of heating power. A heat pump with a COP of ≥3.5 is therefore chosen. The required power in case of the 20 [kW] diesel heater is 20 [kW]. In case of the heat pump the required power is only 6.1 [kW], a reduction of 72.5%.

An overview of zero emission possibilities is given in research question Q.1.6. However, due to certain constraints and unique opportunities in the Amsterdam situation, the most suitable components were found to be lithium-ion battery propulsion (LMP or LTO) coupled with a bow thruster and a pod or FP propeller. Concepts are devised that use a 55 [kW] PMSM as main electric motor. Summarizing the results from research question Q.1.6 in one figure:

5.2.1.3. MODEL, RESEARCH QUESTIONS

How can the concepts be modelled?

(Ref. Q.1.7)

The concepts consist of four main parts: Ship, electric motor, energy storage (battery) and heating/auxiliaries (heat pump). Creating the concepts is done by modelling each part in a Matlab/Simulink environment. Three

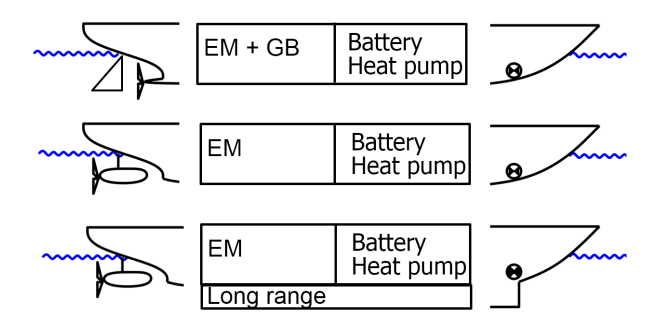


Figure 5.2.1: Schematic view of concepts, EM RF OPT, EM OPT and EM REF respectively

main models are created: 1) A ship model including ship dynamics (inertia) and including an electric motor model, 2) A heat pump model including temperature dependant losses and 3) A battery model, including a current and (ambient) temperature dependency.

DETAILED MODELLING

Detailed modelling is done as follows:

• **Heating:** Auxiliary power exists of two parts: Maritime systems and heating. Focus is on the heating of the canal boat, in the form of the heat pump and seat heating. A heat pump is modelled by taking a typical COP curve of an air-source heat pump. This is coupled to the ventilation and convection losses. The heat energy is calculated by utilizing the COP and the outside temperature to calculate the heat input in the boat. The space in the canal boat heats up and losses will begin to form due to the temperature difference between inside and outside of the boat. The dynamic internal boat temperature can be controlled by setting the heat pump power and hereby setting the required steady state temperature in the boat. This cycle is visualised in Figure 5.2.2. Maritime systems such as Global Positioning System (GPS), heating and lights are modelled as a steady-state power consumption of 600 [W] which is more than sufficient to supply the canal boat.

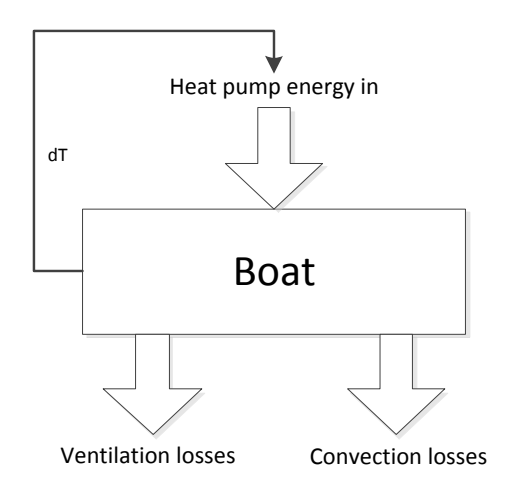


Figure 5.2.2: Schematic view of the input and output streams of the model

- **Ship:** The ship model from Stapersma [34] is adapted to fit the requirements. With the use of the ship model, the energy and power values can be found at each point in the propulsion chain during simulations of the generic profile. The ship model is controlled by a Proportional-Integral (PI) controller which provides feedback about the set and required speed. This set point is fed into the electric motor model, which gives a torque as output. This torque is integrated and this gives a certain advance ratio. This advance ratio is used to calculate the propeller K_t and K_Q values, giving the ship speed dependent on the chosen hull form (resistance curve). See also Figure 5.2.3:
- Battery: The characteristics of Li-ion batteries are taken from the manufacturers. This data is then used in a modified version of the lead-acid battery model from Stapersma [55]. The model is expanded with

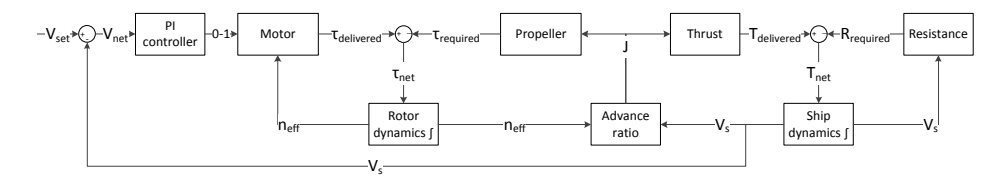


Figure 5.2.3: Ship, motor and propeller modelling

a temperature dependency and a basic lifetime analysis tool. Two different lithium ion battery types are modelled, one LMP and one LTO. There is a characteristic lithium ion voltage drop between 100 and 95% SOC, after which there is a relatively flat discharge voltage curve between 95 and 20% SOC. After 20% SOC the voltage goes exponentially down to the cut-off voltage. To avoid this exponential voltage drop, it is advised to keep the battery above 20% at all times. This is also beneficial for battery lifetime.

How should components be connected to each other?

(Ref. Q.1.8)

The speed setting of the operational profile requires a propeller power. This propeller power asks this required power from the energy storage. The energy storage delivers this requirement together with the requirement from the auxiliary (heat pump). By coupling this way, the resultant battery specifics such as energy storage size and required currents can easily be obtained. The ship model is coupled with the electric motor model. The input in the ship model is the ship required speed, and the output is the ship speed and power. This ship 'required' power goes to the energy storage model which gives an output in the form of voltage, current, SOC, output energy, output power and cycle efficiency (if charging is also applied in the operational profile). See also Figure 5.2.4:

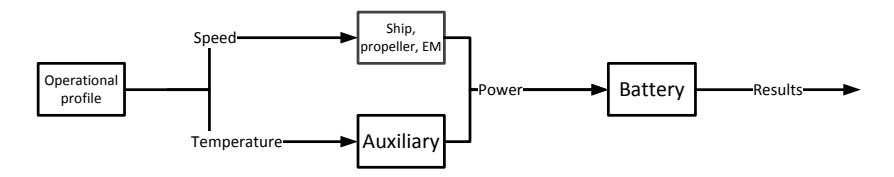


Figure 5.2.4: Integration of the models

What is the simulation strategy?

(Ref. Q.1.9)

The simulation strategy incorporates two main simulations: 1) Verification simulation and 2) Full day simulation. The verification simulation is carried out to check if odd results follow from the model, and to see how the concepts perform. A full day is simulated to obtain the values to size and define the concepts further:

How can the energy storage system be kept in a safe operating condition? (Ref. Q.1.9.1)

This is done by keeping the SOC of the battery above 20% at all times. Different simulations are carried out with and without charging to see how much energy is required for safe and stable operation of the canal boats throughout the day. During all simulations the value of the battery at the end of the day must be above 20% or slightly higher, as the voltage that the battery can deliver drops rapidly with a lower SOC. By incorporating a correct charging strategy intermittent charging will not have a large impact on lifetime. Maximum voltage and currents that the battery is able to handle must be specified to make sure it stays within the correct limits of operation.

Is charging with intervals possible?

(Ref. Q.1.9.2)

Detailed simulations are conducted to see if intermittent charging after each trip is feasible. For lithium- ion, the conclusion is that it is feasible, and it is a smart strategy to do so, as it will decrease the energy storage

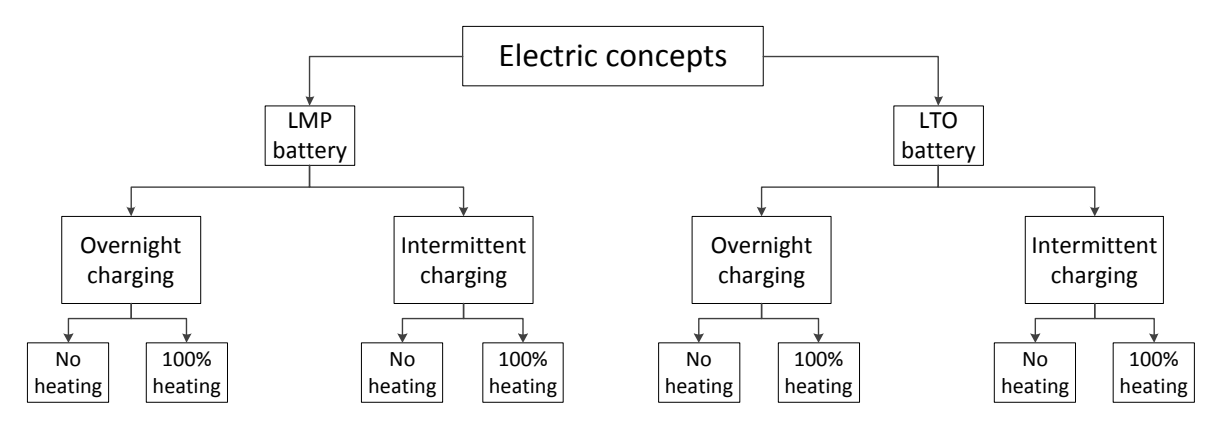


Figure 5.2.5: Electric concepts simulation methodology tree

required on board, hence using less volume and lowering initial costs. It depends on the specific demands from the shipowner if the minimum calculated energy storage sizes are sufficient or if they want a larger range and/or longer lifetime.

Are the obtained model results realistic and do they agree with the baseline?

(Ref. Q.1.10)

Validation can be carried out by comparing the obtained simulation results with the measurement results. The orders of magnitude are equal and the results do not appear to be extreme. The results are furthermore compared with steady-state calculations (the block method) and have a high agreement with the dynamic simulations. For example, when looking at the acceleration time of the modelled and measurement canal boats, it can be seen that they are highly correlated. With respect to the component models, the following verification methods are conducted:

- Ship model: Measurements, static calculations
- Heat pump: Damen Tank Heat Tool, ARKA Systems
- Battery: Manufacturer data, static calculations
- Electric motor: Manufacturer data, efficiency map
- Diesel engine: Manufacturer data, emission curves

What are the lifetime and costs of the energy storage?

(Ref. Q.1.11)

Assuming average costs, and a hull time of 25 years, the cost per year and year pack usage are:

Table 5.2.1: Cost and pack lifetime

	Average cost [€]	Pack lifetime [years]
LMP	11 000	3.6
LTO	6 500	8.3
Lead-acid	12 500	2.2

What infrastructure is necessary to make zero emission possible?

(Ref. Q.1.12)

Quay chargers are required. Possible solutions are tapping electricity from the overhead lines of trams, or using standard car chargers. The impact on the grid should be researched as it is unknown how much extra load the grid in Amsterdam can handle. All canal boats charging simultaneously with a 4C current requires 12 [MW] from the grid, using a charger efficiency of 95%. This is a worst-case scenario.

5.2.1.4. ZERO EMISSION CONCEPT GOAL AND HYPOTHESIS

The first main research goal as defined in Chapter 1.2, 'Methodology':

To design zero emission energy efficient canal boat concept(s)

(Ref. G.1)

A zero emission energy efficient canal boat concept can be designed by using an integrated model of onboard energy consumers that simulates an operational profile

(Ref. H.1)

Three different concepts are analysed and the main conclusion is that it is possible to conceive a full electric canal boat with current battery technology. This conclusion follows from the models, which are used to simulate the concepts and size the energy storage. These simulations are in close cooperation with the conducted measurements and steady-state simulations. The hypothesis can thus be answered positively. All systems in the canal boat, such as heating, propulsion and marine systems are taken into account and are modelled with sufficient detail level. Heating, in the form of a heat pump, is modelled and quantified in Chapter 3.3, 'Auxiliary modelling'. The electric motor used in this work is defined and modelled in Chapter 3.2, 'Ship and system modelling'. Combining these models with the battery model, Chapter 3.4, 'Battery modelling' allows the simulation of the full ship during a given operational profile or mission profile. Energy consumption and storage is minimized where possible, by using the bow thruster during manoeuvring and minimizing energy storage space to be able to remove the 'battery keel'. Within the scope of this thesis, taking into account simplifications, lack of available data and modelling uncertainties, the results are in accordance with measurements conducted on both a diesel and a hybrid canal boat.

Resulting key values are as follows: Brake energy values for a typical boat are between 150 and 200 [kWh] per day. By utilizing tools to optimize the open water efficiency of the propellers and installing an economical heat pump for heating, brake energy consumption for the most favourable concept is reduced to 107 [kWh] including heating when no intermittent charging is taking place. When charging between trips is possible, energy storage can be decreased to less than 65 [kWh] for LMP and 42 [kWh] for LTO. By reducing the resistance and optimizing the open water efficiency and utilising the torque capability of the modelled electric motor to its fullest the required power goes down from 57 [kW] to 45 [kW] at the propulsion shaft. Efficiency from quay to propeller is $\pm 35\%$ for the full electric concepts whereas for the baseline this is 17%.

5.2.2. Environmental comparison conclusions

What are existing methods to rate ships?

(Ref. Q.2.1)

There are a few existing methods to rate ships. These can be categorized in operational methods and design methods.

DESIGN METHODS

- **EEDI:** The EEDI value is based on a point calculation at an installed power measured at 75% Mean Continuous Rating (MCR).
- **CO**₂ **dredging index:** The CO₂ index incorporates auxiliary energy consumption and electric consumers into a design index specifically for dredgers. It can also apply to ships with different missions if the standardized dredging cycle is replaced by the operational profile of the vessel that is analysed.

OPERATIONAL METHODS

- **EEOI:** The Energy Efficiency Operational Indicator (EEOI) is used to evaluate and achieve a reduction of carbon dioxide (CO₂) emissions during operation. This is done by expressing the energy efficiency in CO₂ emitted per unit of transport work.
- **Shipping KPI:** The Shipping Key Performance Indicator (KPI) System uses a hierarchical and mathematical system which includes Shipping Performance Indexes (SPIs), Key Performance Indicators (KPIs) and Performance Indicators (PIs). The CO₂ index is based on the EEOI method and gives the accumulated emitted mass of CO₂ and divides this with the transported work during a set time frame during operations.

How can current rating methods be used to evaluate canal boats?

(Ref. Q.2.2)

The created Amsterdam Environmental Performance Indicator methodology mixes parts of the existing operational and design indices. The emissions and energy efficiency of the concepts and the reference baseline

are rated by conceiving an emissions calculation method that explicitly looks at part load operation and auxiliary energy usage during the design phase of the ship. By setting a discrete cycle of different mission modes, as is done in the CO_2 dredging index, a mean value instead of a point value emerges. This mean cycle can be used for energy and fuel, as well as emissions such as NO_x , something that is not yet applied in the EEDI or dredging index.

Estimations regarding energy storage capacity and environmental footprint can be made by this calculation method, thus aiding in the zero emission future.

How can diesel propulsion be compared with electric propulsion?

(Ref. Q.2.3)

When it is assumed that the electricity from the grid is generated in an environmentally friendly way, there are no emissions for the electric concepts. In order to generate power at an *equal energy efficient level* as the baseline (diesel) boat, a land-based power plant should have an efficiency of at least 43%, from power generation to quay-boat crossing. This way, the chemical conversion from fossil fuels to usable energy is taken into account for both diesel and electricity. This is a fair comparison.

5.2.2.1. Environmental comparison goal and hypothesis

The second main research goal as defined in Chapter 1.2, 'Methodology':

The creation of a calculation method which can quantify emissions, energy and fuel usage and can compare the concept(s) with a baseline. (Ref. G.2)

A fair energy and emission comparison between the baseline and zero emission concepts can be conducted by conceiving an 'Environmental Performance Indicator' methodology (Ref. H.2)

This goal has been achieved as well, by studying existing methods to rate ships based on energy consumption and emissions, and applying these methods to a new extended method based on discrete operational modes emissions and energy or fuel usage can be quantified. This quantification is based on the calculation of the emissions or energy or fuel amount during a set time, and dividing this by the 'benefit of society', in this case defined as 'the amount of people transported x distance sailed'. Due to this, a non dimensional number arises for the energy usage, or Energy Conversion Index (ECI), and the emissions are given in $\lceil g/(kg \cdot km) \rceil$. These obtained values can be compared with the baseline(s), where it must be noted that it depends on the index boundary if the electric boats have emissions or not. Analysing the hypothesis further, it is found that a fair comparison can be made by setting requirements with respect to the power generation efficiency and emission.

6

APPENDICES

The appendices in this thesis consist of attachments that are required for this text, but are not analysed in great detail as in the main body. The appendices are followed by a glossary, bibliography and lists of figures, tables and symbols.



EXAMPLE ENERGY CONVERSIONS

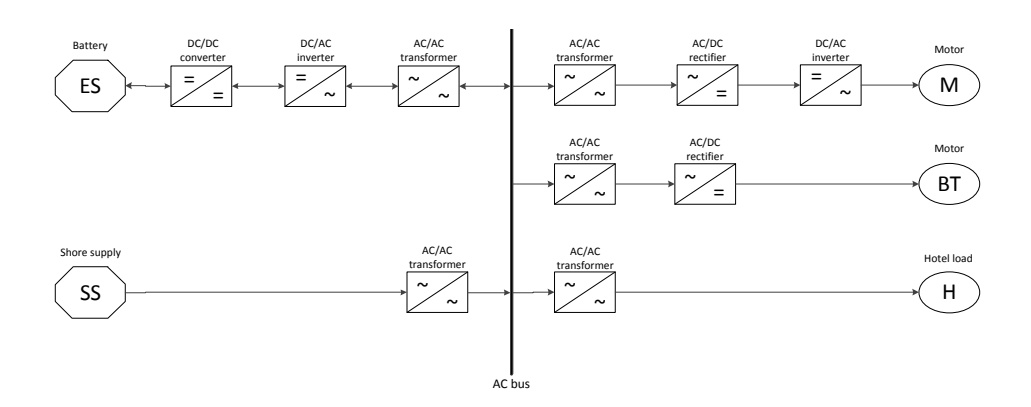


Figure A.1: Typical AC conversion EFD

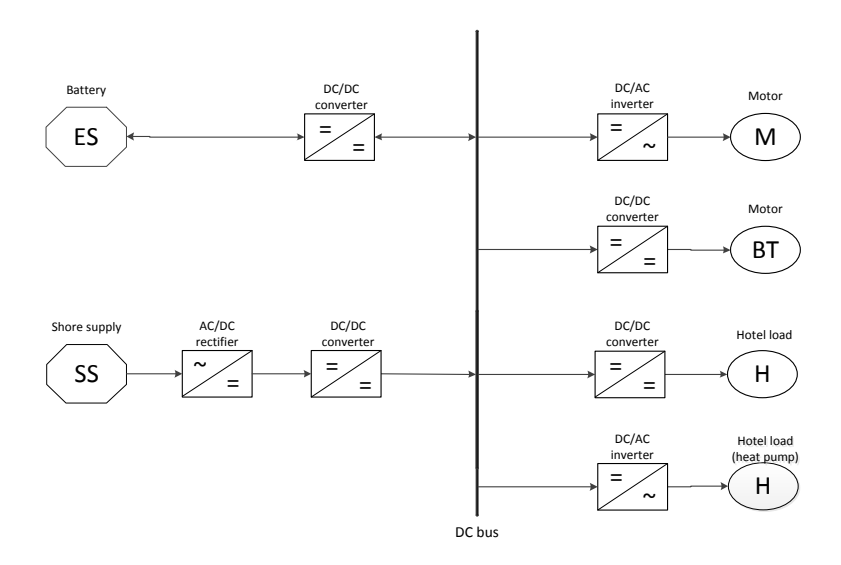


Figure A.2: Typical DC conversion EFD

To give an indication about the consequences of each conversion, an efficiency of 99% for each conversion, inversion or rectification is assumed. Going from energy storage (ES) to motor gives:

- alternating current (AC): $0.99^6 = 0.94$ as conversion efficiency
- direct current (DC): $0.99^2 = 0.98$ as conversion efficiency

As the efficiencies of these conversions are not known for the 40-60 [kW] power range, these conversions will be taken as ideal. However, using a DC network instead of an AC network will clearly have a lower loss as this back of the envelope static calculation example shows.

B

FLYWHEEL AND SUPER CAPACITOR

B.1. FLYWHEEL

A flywheel stores rotational energy. It is a mechanical system enclosed in a semi-vacuum to eliminate air resistance. Often magnetic bearings are used to reduce bearing friction. The advantages of the flywheel are:

- Low noise
- Low charging time
- Power quality improvement

It has disadvantages as well. The largest problem is cost coupled to power density. A 4 [kWh] system costs about 60 000 [ϵ /kWh], 240 000 [ϵ] in total. Furthermore this 4 [kWh] system is 1.2 [m³] which makes it too large for the Amsterdam application, where size is important as the boats have a limited length and width. Because of these very practical reasons, the flywheel is not considered in this text.

B.2. SUPER CAPACITOR

A super capacitor or ultra capacitor is based on capacitor technology and is a zero emission option as well. They can offer thousands of Amperes at a low voltage. The downsides of super capacitors are that they are 1) Expensive, 23 000 [€/kWh] and 2) Offer little energy storage. Super capacitors are built for high peak powers. A 45 [kW] super capacitor will be able to deliver about 1 [kWh] before depleting. The voltage is linearly decreasing when discharging. Because of cost and the low energy density, super capacitors are not analysed in this thesis.



MOTOR EFFICIENCY PLOT

The used 55 [kW] PMSM efficiency plot obtained from the manufacturer is shown in Figure C.1.

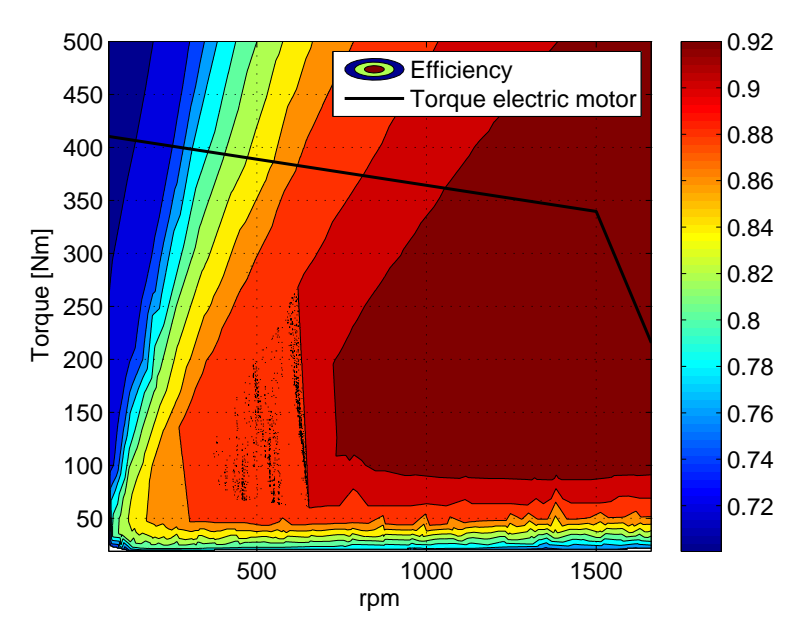


Figure C.1: Torque - rpm - efficiency contour plot



OPENPROP PROPELLER CALCULATION

Using the open source programme OpenProp v3.3.4 Parametric, a parametric optimization is conducted for the propeller at nominal speed [89–92]. These inputs can be found in Table D.1. The results from this examination are further optimized with OpenProp v3.3.4 Single and Propeller Performance v1.1.16. OpenProp is based on moderately-loaded lifting line theory. It calculates the minimum required torque and hence propeller power for a given thrust [90].

Both programs calculate an improved η_o of 1-2%. The difference between the programs is probably due to the method used. OpenProp constructs the blade from discrete sections and calculates the induced velocities using a vortex lattice [89]. Based on the given dimensions, a lower delivered power is calculated in comparison with Propeller Performance. Propeller Performance uses the standard open water diagrams from the Wageningen B series and calculates the coefficients. This is a more generic solution.

Table D.1: Overview of parametric optimization parameters

Range	Min	Increment	Max
Number of blades	3	1	5
Rotation speed [rpm]	280	10	460



ALTERNATIVE PROPULSION MULTIPLE CRITERIA ANALYSIS

Table E.1: Explanation of numbers

- 1 | Very good
- 2 Good
- 3 Average
- 4 Below average
- 5 Poor

Table E.2: Propulsor multiple criteria analysis, lower is better

Туре	Performance 1	Maneuverabili	ty Cost	Relial	oilityMaintenance	Energy consumption	Total
СРР	2	2	4	2	4	1	15
FPP	3	5	1	1	1	3	14
Thruster or	1	1	3	3	4	1	13
pod							
Bowthruster	1	2	4	1	2	2	12
Voith RIM	2	4	4	3	3	3	19
Voith-	2	1	5	5	4	2	19
Schneider							
Cycloidal							
Waterjet	4	3	4	2	2	5	20
Whale tail	4	3	3	5	4	1	20

The whale tail, both Voith propellers and waterjet are omitted in the comparison. This is not only due to the high scores, but also backed up by literature and practice. Waterjets are only efficient at high speeds [22, 23], and have very low efficiency at the speeds of the canal boats. Reliability of whale tail systems is still a challenge [93].

Regarding the Voith propellers, the smallest Voith-Schneider Cycloidal propeller has a blade length of 650 [mm] and a power of 180 [kW] [94]. This makes the unit too powerful for a canal boat, and too deep. The canals are only 1.80 [m] deep where the canal boats are permitted [42]. Placing the Voith-Schneider Cycloidal propeller under the ship (to submerge the blades) with the standard hull draught of 1.25 [m] [16] and a quick calculation reveals that the propeller will run aground. The Voith RIM drive is also omitted. BlueBoat had one of these propulsors installed on the electric canal boat, but it proved unreliable in the

¹Whole profile

Amsterdam environment. This was mostly due to garbage that broke or damaged the blades [19, 29]. The conclusion from this basic comparison is that an fixed pitch propeller (FPP) or pod main propulsion unit coupled with a bow thruster is probably the most efficient and cost effective option.



WATER TEMPERATURE 1990-2010

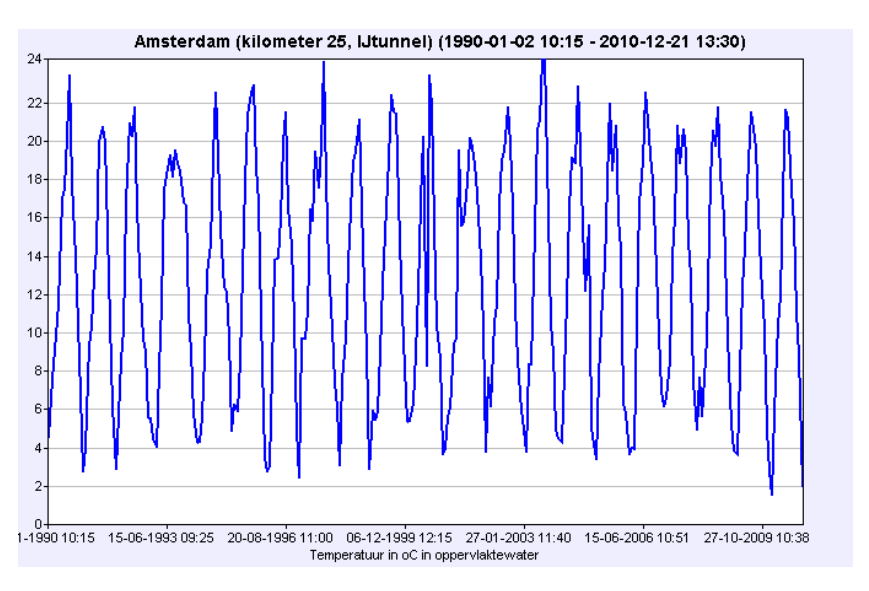


Figure F.1: Water temperature in Amsterdam between 1990-2010)



PROPELLER OPTIMIZATION

G.1. METHODOLOGY

In this appendix, the calculated propeller of the *diesel boat* is calculated for four blocks (nominal speed, high speed, medium speed and manoeuvring speed) and where possible optimized by altering P/D ratio and/or RPM. It is assumed throughout this thesis that the diameter of the propeller is fixed at 0.65 [m] because of water depth. Note that the propeller for the hybrid boat, with the pod propulsion, will not be optimized as the open water efficiency is already theoretically optimized in chapter 3.1.4, 'Hybrid boat resistance'. In every section different propellers are mentioned. Table G.1 gives an overview. This overview can be used as a reference throughout this appendix. QRC stands for Quadratic Resistance Curve. MRC stands for Measured Resistance Curve. Throughout this text, either the number of the propeller or the name in Table G.1 will be used to indicate the propellers.

Table G.1: Overview of used propeller nomenclature

#	Name	Details
1	Reference QRC	Unoptimized propeller using the quadratic resistance assumption, meaning a higher resistance
2	Optimized QRC	Optimized propeller using the quadratic resistance assumption, meaning a higher resistance
3	Reference MRC	Unoptimized, measured propeller (partially loaded canal boat)
4	Optimized MRC	Optimized propeller using the measured resistance (partially loaded canal boat)

When this static analysis is completed, optimization of the 90° turns will take place using the simulation software SurSim. First a validation will be carried out to see if SurSim can be used in this case, see chapter G.8. Following this, a simulation will be conducted for the 90° turns in combination with a bow thruster.

G.2. MEASUREMENT AND THEORETICAL CALCULATIONS

The approach is to calculate the propeller open water efficiency using standard Wageningen B curves and the conducted measurements for each block. An optimization is carried out with the help of computer software programs. Then the energy and power differences for the unoptimized and optimized situations can be derived, after which quick estimations of required energy storage and power will be possible. The propeller that is optimized in the discrete block points can be used in the dynamic model in a later stadium.

G.3. NOMINAL SPEED

The goal of this paragraph is to see whether the open water propeller efficiency can be improved in the nominal working points of this propeller. This is done with use of the program PropellerPerformance. Propeller Performance is based on the Wageningen B series of propellers (four-quadrants). A static analysis is conducted at the nominal speed of the canal boat. First the known data from the reference MRC propeller is used to calculate the P/D ratio. Note that due to limitations of the program, the propeller cannot be calculated

with a lower thrust than 1.5 [kN], so this is slightly more than the value from the measurements, which is 1.45 [kN]. Hand calculations show that this has no significant influence on the η_o . When the reference propeller is fully known, the same pitch is used, but with the higher resistance and higher propeller power to convert it to the reference QRC propeller (Propeller 1 in Table G.2). The open water efficiency goes down compared to the reference MRC (Table G.3, propeller number 3), which is explained by the fact that the propeller is not optimized and has more losses at a higher ship resistance and/or thrust requirement. The next step is to optimize the P/D ratio and RPM of the propeller at nominal speed (Propeller 2 in Table G.2).

Table G.2: Optimization of η_0 as calculated with Propeller Performance, QRC, nominal speed 2.1 [m/s]

Propeller [-]	P _p [kW]	RPM [rpm]		Pitch [m]	P/D ratio [-]	η _ο [-]
1. Reference QRC	8.6	321	2.02	0.82	1.26	0.41
2. Optimized QRC	8.1	450	2.08	0.5	0.76	0.45

To check if the propeller will also have a higher η_0 when the boat is partially loaded the reference and optimized propellers are compared in Table G.3.

Table G.3: Optimization of η_0 as calculated with Propeller Performance, MRC, nominal speed 2.1 [m/s]

Propeller [-]	P _p [kW]	RPM [rpm]		Pitch [m]	P/D ratio [-]	η _ο [-]
3. Reference MRC4. Optimized MRC		300 396	1.56 1.56	0.82 0.5	1.26 0.76	0.46 0.50

G.3.1. OPTIMIZATION RESULTS NOMINAL SPEED

For the optmized QRC propeller, η_0 improves with 3.7% using Equation G.1. See for an overview tables G.2 and G.4. Using Equation G.2 gives the propeller power reduction in [%]. This is equal to almost 6% for the quadratic resistance case.

The open water efficiency for the partially loaded canal boat improves as well. Here the open water improvement is 4.5% and the power reduction is 15%, see Table G.4. The propellers for the canal boats are assumed to be mass produced rather than unique propellers. Hence only standard Wageningen B series solutions have been applied to this case. The results from OpenProp are included for validation in Appendix D, 'Openprop propeller calculation'. It can be noted that when opting for a tailor made solution, open water efficiency can be even higher.

$$\eta_o \text{ reduction } [\%] = \frac{\eta_{o,nom} - \eta_{o,opt}}{\eta_{o,nom}} \cdot 100$$
(G.1)

$$\eta_o \text{ reduction } [\%] = \frac{\eta_{o,nom} - \eta_{o,opt}}{\eta_{o,nom}} \cdot 100 \tag{G.1}$$
 Power reduction $[\%] = \frac{P_{p,nom} - P_{p,opt}}{P_{p,nom}} \cdot 100 \tag{G.2}$

Table G.4: Power reductions at nominal speed for optimized propeller compared to the reference propeller

η_o improvement at QRC propeller	3.7	%
Power reduction at QRC propeller	5.8	%
η_o improvement MRC propeller	4.5	%
Power reduction at MRC propeller	15.0	%

G.4. HIGH SPEED 153

G.4. HIGH SPEED

The goal of this section is to see whether the open water propeller efficiency can be improved in the maximum working point of the propeller as well. This is again done with use of the program PropellerPerformance. The maximum speed a canal boat must be able to sail is 13 [km/h], or 3.6 [m/s] [20]. The propellers will be optimized for this speed.

Using the data from the measurements gives the reference propeller in Table G.5. Note that the P/D ratio is equal to that of the measured propeller at the nominal speed. Again, first the same P/D ratio is taken with the quadratic resistance curve, lowering the η_o (propeller 1 in Table G.5 compared to propeller 3 in Table G.6).

Table G.5: Optimization of η_0 as calculated with Propeller Performance, QRC, maximum speed 3.6 [m/s]

Propeller	P_p	RPM	Thrust	Pitch	P/D ratio	η_o

780

[-] [kW] [rpm] [kN] [m] [-] [-] 571 1. Reference QRC 6.1 0.82 1.26 0.41 45.3

6.1

0.50

0.76

0.46

The partially loaded boat is again used as a check to see if efficiency is higher with the partially loaded boat as well. As can be seen from Table G.6, this is the case. It is found that it uses the same P/D ratio as the optimized propellers from Table G.2.

Table G.6: Optimization of η_0 as calculated with Propeller Performance, MRC, maximum speed 3.6 [m/s]

Propeller [-]	P _p [kW]	RPM [rpm]		Pitch [m]	P/D ratio [-]	η _ο [-]
3. Reference MRC		554	6.0	0.82	1.26	0.42
4. Optimized MRC		772	6.0	0.50	0.76	0.46

G.4.1. OPTIMIZATION RESULTS HIGH SPEED

2. Optimized QRC

40.9

Using equations G.1 and G.2 the improvements in open water efficiency and reductions in maximum power can be calculated. For the QRC propeller, the η_o improves with almost 4.5%, see Table G.7. Power reduction is equal to almost 10% for both resistance cases. See Table G.7.

Table G.7: η_0 and power reductions at nominal speed for optimized propeller compared to the reference propeller

η_o improvement QRC propeller	4.4	%
Power reduction at QRC propeller	9.7	%
η_o improvement MRC propeller	4.5	%
Power reduction at MRC propeller	9.5	%

G.5. MEDIUM SPEED

Using the same methodology as the optimization of the nominal speed, but with the medium speed (2.6 [m/s]), the results are depicted as follows in tables G.8 and G.9.

Table G.8: Optimization of η_0 as calculated with Propeller Performance, QRC, medium speed 2.6 [m/s]

Propeller [-]	P _p [kW]	RPM [rpm]		Pitch [m]	P/D ratio [-]	η _ο [-]
 Reference QRC Optimized QRC 		429 599	3.73 3.73	0.82 0.5	1.26 0.76	0.39 0.43

Propeller [-]	P _p [kW]	RPM [rpm]	Thrust [kN]	Pitch [m]	P/D ratio [-]	η _ο [-]
3. Reference MRC	13.6	378	2.7	0.82	1.26	0.44
4. Optimized MRC	12.5	532	2.7	0.5	0.76	0.48

Table G.9: Optimization of η_o as calculated with Propeller Performance, MRC, medium speed 2.6 [m/s]

G.6. MANOEUVRING

For the manoeuvres the average power is taken. Note that this is an assumption, as the power fluctuates largely in this block. For a general overview however, the average will give an order of magnitude. Using the same methodology as before, the results of the optimization are depicted as follows in tables G.10 and G.11.

Table G.10: Optimization of η_0 as calculated with Propeller Performance, manoeuvring, QRC, speed 1.0 [m/s]

Propeller [-]	<i>P_p</i> [kW]	RPM [rpm]		Pitch [m]	P/D ratio [-]	η _ο [-]
 Reference QRC Optimized QRC 		364 486	3.32 3.32	0.82 0.5	1.26 0.76	0.19 0.21

Table G.11: Optimization of η_0 as calculated with Propeller Performance, manoeuvring, MRC, speed 1.0 [m/s]

Propeller [-]	<i>P_p</i> [kW]		Thrust [kN]	Pitch [m]	P/D ratio [-]	η _ο [-]
3. Reference MRC4. Optimized MRC		345 461	2.96 2.96	0.82 0.5	1.26 0.76	0.19 0.22

G.7. CONCLUSION OF STATIC ANALYSIS

From these four calculated block points (nominal, high, medium and manoeuvring) the power-speed curve can be obtained. Plotting these points in Figure 3.1.6(b) gives Figure G.1. In this figure the difference in the calculated and optimized propeller is displayed.

From these data and the accompanying P/D ratio the open water diagram can be obtained. See Figure G.2(a) for the open water diagram of the reference propeller. In Figure G.2(b) the optimized open water diagram is given. When comparing the η_o values, Figures G.2(a) and G.2(b), it can be seen that for an advance coefficient J smaller than 0.7 the optimized propeller has a higher open water efficiency. As the value of J is \pm 0.6 for the highest speed, it will not exceed 0.7 and hence the optimized propeller will be more efficient throughout the whole speed range. For an explanation of J refer to Chapter 3.2.4, 'Advance coefficient'.

G.8. TURNING 90°

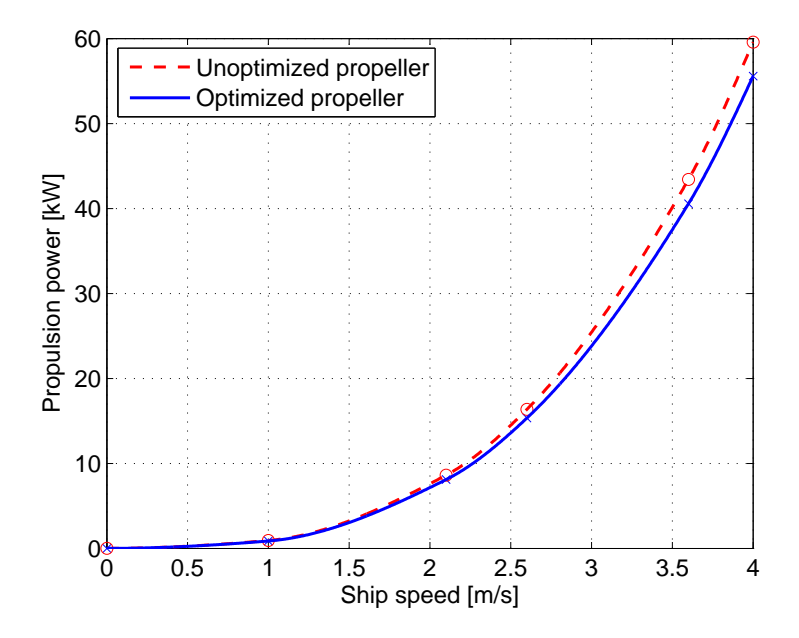


Figure G.1: Difference between calculated cubic propeller law curve and the optimized cubic propeller law curve

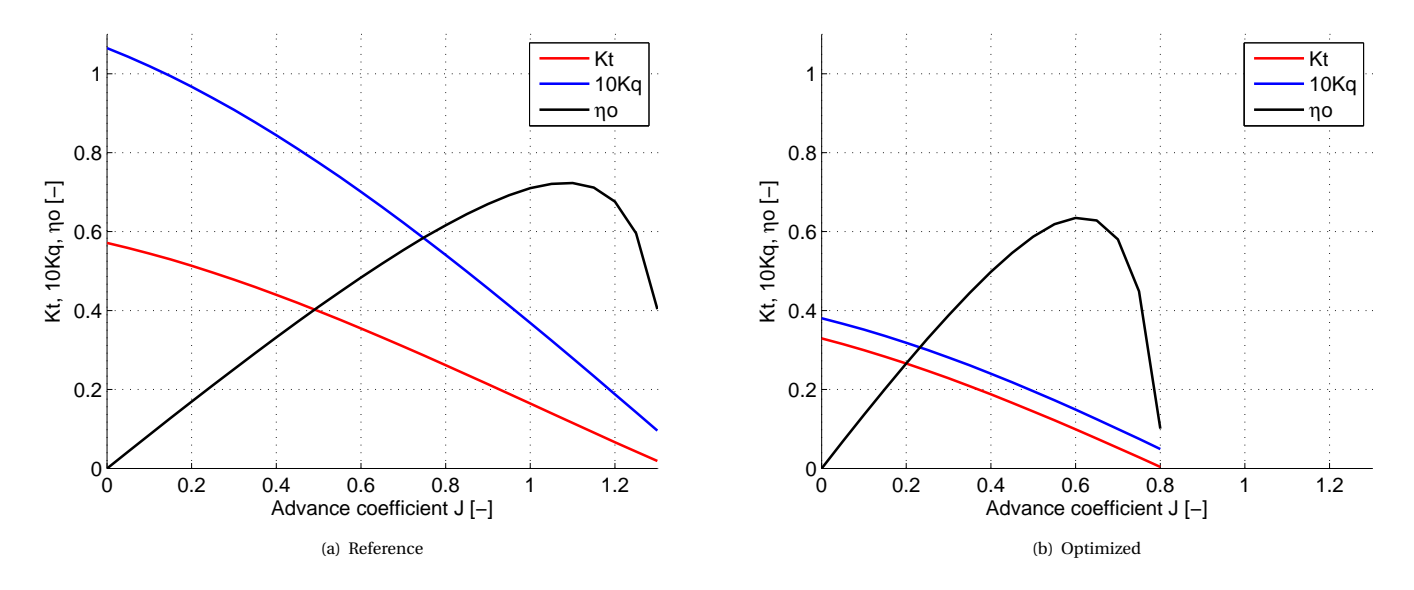


Figure G.2: Open water diagrams for the diesel boat

G.8. TURNING 90°

The computer program SurSim v99.1 is used to calculate dynamic behaviour of the canal boat during a turn. This is important, as the peak power is used during manoeuvring through the narrow corners [16].

G.8.1. Why 90° Turns are important

Only during the 90° turns is the full power of the diesel used. This is because maximum power against the rudder is required to obtain sufficient pressure to turn in a short amount of time. The downside is that this will result in movement forward, hence the thrust will be reversed and maximum power will be directed backwards [11]. This is the most common way to get through the narrow corners. Turning as described here can be more efficient with the help of a bow thruster and/or steerable waterjet, as it will designate the front of the ship directly in the direction of the turn. In theory, this should lower the peak power. This results in a propulsion chain that can be optimized for lower power. Lower power means a smaller engine, and

lower costs. The aim is to be able to take the turns without using more power than is required to obtain the minimum attainable speed (3.6 [m/s]). For the optimized propeller, the power in the turns must stay below 40.9 [kW]. To be able to obtain values for the turns, simulations are conducted with SurSim.

G.8.2. SURSIM BACKGROUND

During sailing important forces influencing manoeuvrability are rudder, propulsion, environmental and hull forces. Rudder and propulsion forces are widely analysed. Hull forces however remain a difficult barrier, especially during (dynamic) manoeuvring. The best way to apprehend these forces is a model scale test. However, this is expensive and not always possible. To be able to predict these hull forces, the Maritime Research Institute Netherlands (MARIN) has developed a computer program that can estimate the forces of seagoing vessels. This program is called SurSim. The theory behind SurSim is based on slender body theory and cross flow drag theory [95]. Different manoeuvres can be simulated in SurSim. For this research, a simulation of the 90° turn will be made.

G.8.3. SURSIM SIMULATION APPROACH

To see if the propeller can be optimized during a turn different simulations with SurSim are carried out. As can be seen from Figure G.3 the measured (reference) data is used as a baseline to see the energy and power requirements in a 90° turn. Furthermore using the same diameter propeller the quadratic resistance data is used to see the difference with the measured data. This is done with and without a bow thruster.

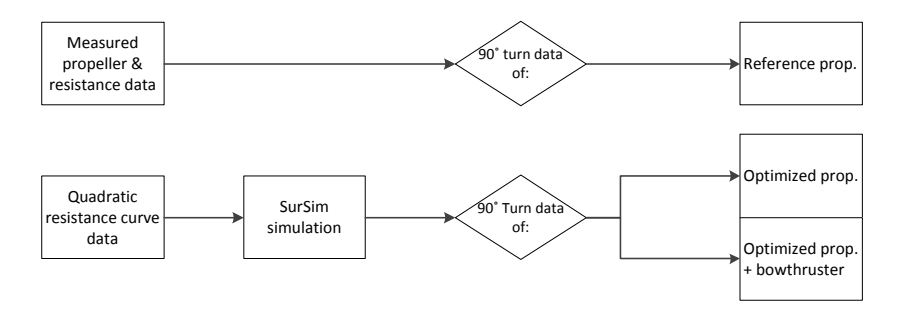


Figure G.3: Schematic lay out of data and simulation methodology

G.8.4. UNDERLYING THEORY OF SURSIM

Based on a linesplan from a harbour canal boat, a simplified hull form is entered in SurSim, see Figure G.4. As it is low detailed, only the rough hull shape is plotted. The hull sections are shown in Table G.12. SurSim uses two-dimensional strip theory to calculate added mass [96, 97]. Strip theory assumes that the longitudinal extent of the ship is divided into sections. For each section, the added mass is calculated, see Equation G.3. By integration of this added mass the lateral forces can be estimated (sway force and yaw moment).

$$m_{yy} = \frac{\rho \cdot \pi}{2} \cdot T^2 \cdot \left(C_1 \exp\left(\frac{C_2 \cdot B}{T} + C_3\right) \right)$$
 (G.3)

Where:

$$C_1 = 0.388 + 0.1485 \cdot C_s - 1.3283 \cdot C_s^4 \tag{G.4}$$

$$C_2 = -0.578 + 0.2 \cdot C_s \tag{G.5}$$

$$C_3 = 0.7529 - 0.4677 \cdot C_s + 1.6148 \cdot C_s^4 \tag{G.6}$$

$$C_{s} = \frac{A_{T}}{R \cdot T} \tag{G.7}$$

In Equation G.3, m_{yy} is the added mass in [kg/m] per section. A_T is the surface of each section in [m²]. For each hull section from appendix G.12, Simplified hull sections the added mass is calculated and used to calculate the hydrodynamic forces.

G.8. TURNING 90°

Ord. [-]	X-location [m]	Draught [m]	Breadth [m]	Area [m ²]	Added mass [kg/m]
0.00	-9.500	0.000	0.000	0.000	0.0
1.00	-8.550	1.250	2.000	2.000	2507.1
2.00	-7.600	1.250	3.500	3.500	2525.2
3.00	-6.650	1.250	4.000	4.000	2529.4
4.00	-5.700	1.250	4.250	4.500	2812.4
5.00	-4.750	1.250	4.250	4.500	2812.4
6.00	-3.800	1.250	4.250	4.500	2812.4
7.00	-2.850	1.250	4.250	4.500	2812.4
8.00	-1.900	1.250	4.250	4.500	2812.4
9.00	-0.950	1.250	4.250	4.500	2812.4
10.00	0.000	1.250	4.250	4.500	2812.4
11.00	0.950	1.250	4.250	4.500	2812.4
12.00	1.900	1.250	4.250	4.500	2812.4
13.00	2.850	1.250	4.250	4.500	2812.4
14.00	3.800	1.250	4.250	4.500	2812.4
15.00	4.750	1.250	4.000	4.000	2529.4
16.00	5.700	1.250	3.800	3.800	2527.8
17.00	6.650	1.250	3.000	3.000	2520.1
18.00	7.600	1.250	2.500	2.800	3004.3
19.00	8.550	1.250	2.000	2.250	2961.9
20.00	9.500	0.000	0.000	0.000	0.0

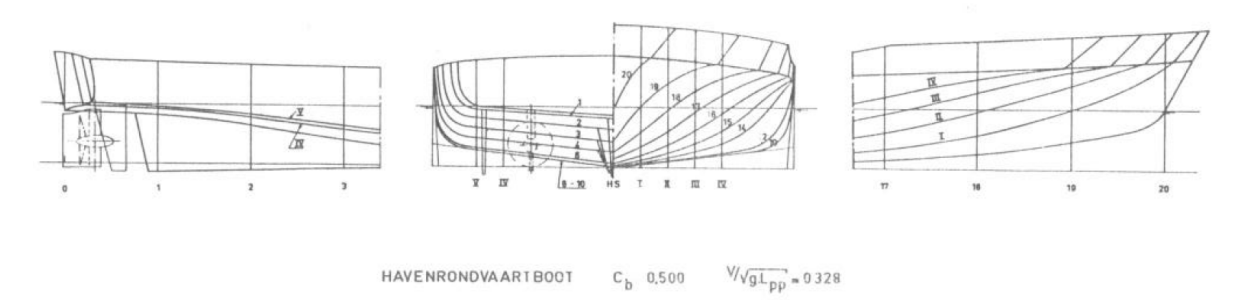


Figure G.4: Linesplan of a harbour tourist boat

G.8.5. RESTRAINTS IN SURSIM USAGE

There are a few important points that one has to keep in mind when using SurSim for the simulations as carried out in this thesis. The strip theory applied in SurSim is two-dimensional, which gives a poor approximation of the bow and stern influences [97]. SurSim can therefore only be used as a rough approximation method. This is reinforced by the knowledge that SurSim was created to simulate sea going vessels, which canal boats are not. Nevertheless, because the resistance of the canal boat calculated using Holtrop & Mennen (also used for seagoing vessels) is in accordance with the quadratic resistance curve (see [16]), the resistance is assumed to be correct. In [97] it is found that SurSim overestimates the turning circle slightly when the entry velocities of the turns are equal. This can be found in the results of this thesis as well, although this could be because of the higher resistance (quadratic curve). The recommendation in [97] is to correct the hydrodynamic coefficients with measured values. This is however not possible without a proper model test. As this is not possible, these coefficients cannot be altered. Therefore, the results will give an indication of possible energy reduction. To validate the usage of SurSim in the Amsterdam canals, a comparative study is conducted between SurSim and the measurements during a turn.

VALIDATION OF SURSIM IN THE AMSTERDAM CANALS

There are some restraints in using SurSim for the canal boat case. In order to know if these restraints are correct, a validation simulation is carried out. The output is detailed in tables G.13 and G.14. The turns that are chosen as reference can be taken without back-and-forth manoeuvring ('steken'). From the tables it can be seen that the SurSim values for time, average speed, average power and X distance are all within 25% of the measured values. Larger deviations exist for the maximum power (61% and 50%) and Y distance (29% and 66%). The reason for the Y distance is that it is difficult to exactly stop the measurement at 90° whereas for the simulation it is possible to do that, hence the large difference. Furthermore, due to the restrictions of manoeuvring in SurSim a turn circle manoeuvre is simulated, and the emphasis in this simulation is to minimize the distances. Maximum power can be explained by the fact that the turn in SurSim becomes steady state after a while, so no excessive power is required. In a real situation it is probable that the captain will give full power when the rudder is fully turned to make the turn faster. As this cannot be ignored, results from the SurSim simulations that require maximum power must entail a spread based on this percentage. An important conclusion however is that the energy between the measured and the simulated turns deviates only 2%.

Type of data X dist. Y dist. **Time** Avg. Avg. Max. Energy Avg. speed power power rpm [m/s][kW] [kW] [kWh] [rpm] [m][m][s]40 48.2 Reference 1.3 18.5 0.21 366 32.2 21.4 SurSim 18.9 0.20 380 37.6 41 1.0 15.9 15.2 23 2 Difference [%] -3 14 61 -4 -17 29

Table G.13: Measurement and SurSim validation results turn #1

Table G.14: Measurement an	d SurSim validation	results turn #2
----------------------------	---------------------	-----------------

Type of data	Time	Avg. speed	Avg.	Max. power	Energy	Avg. rpm	X dist.	Y dist.
	[s]	[m/s]	[kW]	[kW]	[kWh]	[rpm]	[m]	[m]
Reference	40	2.1	14.6	37.8	0.16	321	67.0	47.0
SurSim	32.5	2.1	18.2	18.8	0.16	419	64.6	16.1
Difference [%]	19	0	-25	50	-2	-31	4	66

G.9. SURSIM SIMULATION RESULTS

Simulation

Simulation w/bowthruster

With the data from the SurSim verification in mind, it is time to apply the higher resistance curve to SurSim to simulate the fully loaded canal boat. This quadratic resistance curve (QRC) is applied on propellers two and three in Table G.16. As expected, energy consumption, average power and RPM values go up. This simulation is done with and without a 8 [kW] bow thruster. This power is chosen because it is common for the canal boats. The numerical results can be found in Table G.16 whilst the plotted trajectories can be found in Figure G.5. The simulations use a maximum rudder angle of 50° at a rudder turn rate of $20 \, [deg/s]$, see Table G.15. Environmental effects like current and wind are neglected in the simulation.

Yaw rate [deg/s]	Max. rudder turn rate [deg/s]	Max. rudder angle [deg]
2.6	20	50

50

Table G.15: The used characteristics for the simulations in SurSim

20

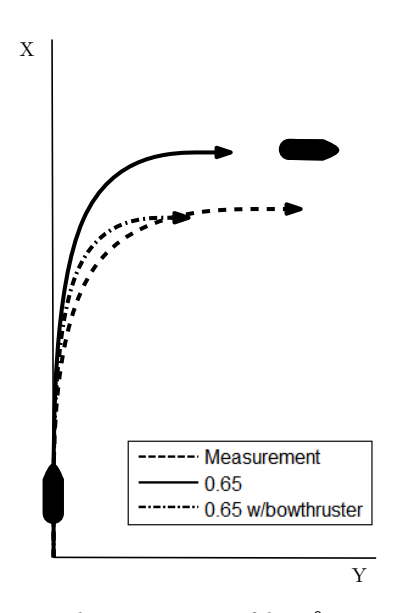


Figure G.5: Schematic overview of the 90° turn (scaled)

G.9.1. SURSIM SIMULATION CONCLUSION

From Table G.16 it can be seen that the simulation, when using the QRC has a higher power and energy consumption. When comparing the simulation with and without the bow thruster, the energy consumption is reduced with 41% (propellers two and three in Table G.16). The turn in an earth fixed reference frame is schematically drawn in Figure G.5.

# [-]	Type of data [-]	Time [s]	Diameter prop. [m]	X dist. [m]	Y dist. [m]
1	Reference, low res.	40	0.65	32.2	21.4
2	Simulation, high res. 1	35.5	0.65	37.0	15.2
3	Sim. w/bowthruster,	33	0.65	31.1	11.8
	high res. ²				

Table G.16: Measurement and simulation results of 90° turn

# [-]	Type of data [-]	Avg. speed [m/s]	Avg. prop. power [kW]	Energy [kWh]	Prop. rpm [rpm]
1	Reference, low res.	1.3	18.5	0.21	366
2	Simulation, high res.	1.1	27.8	0.27	413
3	Sim. w/bowthruster,	1.0	10.7 + 8	0.16	413
	high res.				

G.10. Hybrid boat propeller optimization

The calculated open water diagram for the hybrid propeller can be found in Figure G.6(a). Due to the high rotations (up to 1500 [rpm]) the values for J are relatively small compared to a diesel boat. An optimization is carried out by assuming a gearbox with an unknown ratio. This ratio is then found using the OpenProp software. From this ratio, a new open water diagram can be calculated, this is displayed in Figure G.6(b). Due to the larger required torque the open water efficiency is much higher. The gearbox ratio is found to be around 3, however slight alterations of this ratio do not change performance very much. This has a practical advantage, if for example only gearboxes with a ratio of 3.5 are available.

¹Ouadratic resistance curve

²Quadratic resistance curve

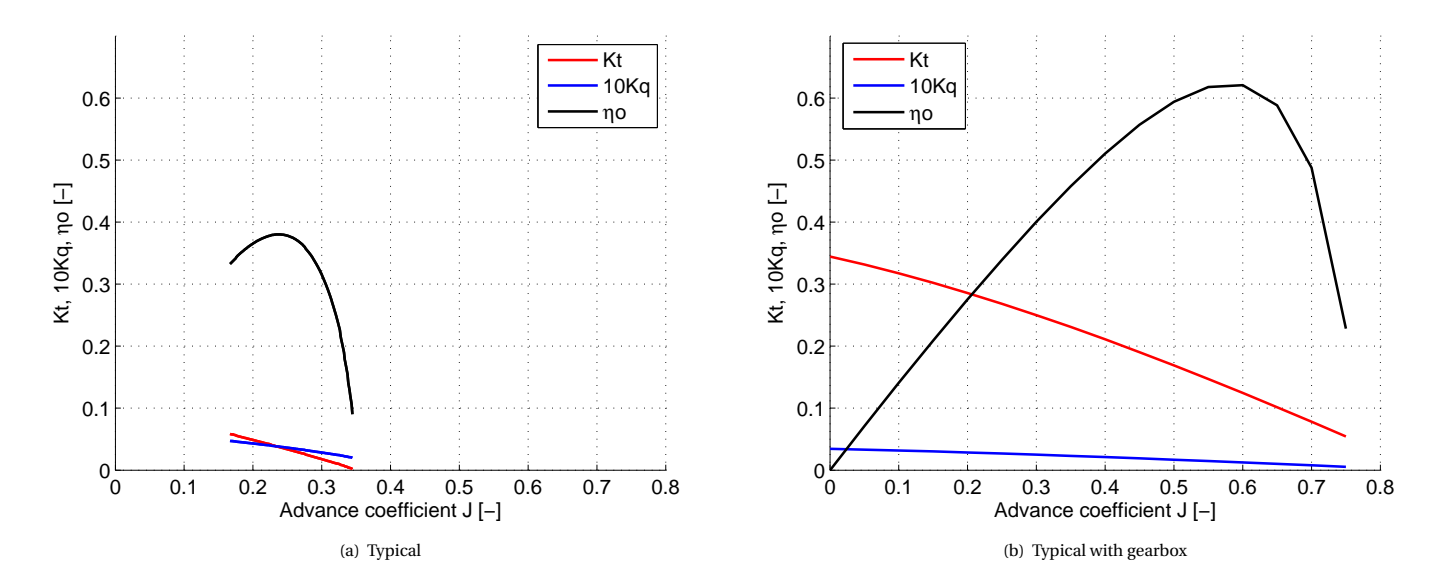


Figure G.6: Open water diagrams for the hybrid boat

H

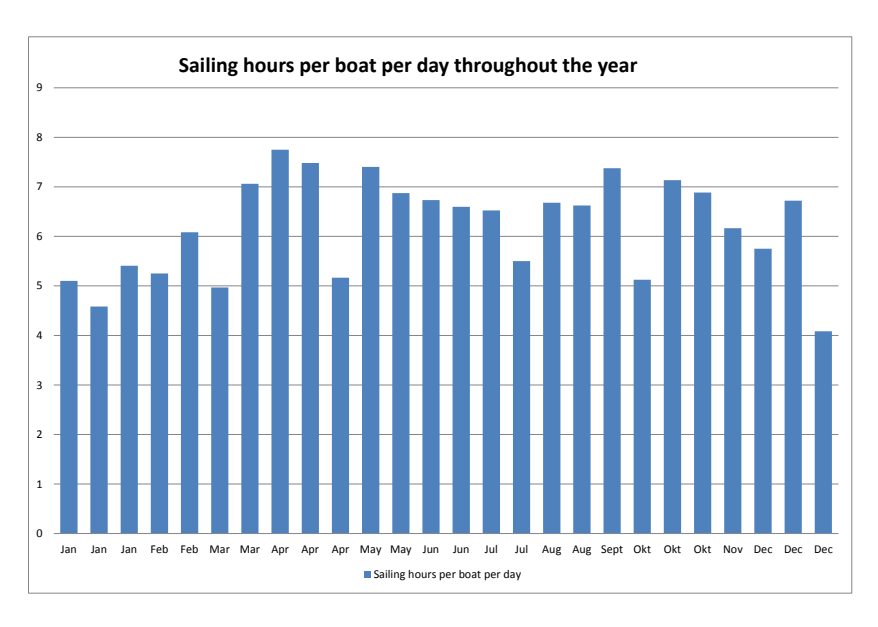
ECI CALCULATION RESULTS FOR CONCEPTS

Table H.1: ECI and minimum efficiencies for the simulations

Baseline, excluding HP: Fpp Pod Baseline, including HP: Pod Concepts including HP: EM RF OPT EM RF OPT	0.076 0.041 0.056	- 0.51 0.51
Fpp Pod Baseline, including HP: Pod Concepts including HP: EM RF OPT EM RF OPT	0.041	
Pod Baseline, including HP: Pod Concepts including HP: EM RF OPT EM RF OPT	0.041	
Baseline, including HP: Pod Concepts including HP: EM RF OPT EM RF OPT	0.056	
Pod Concepts including HP: EM RF OPT EM RF OPT		0.51
Concepts including HP: EM RF OPT EM RF OPT		0.51
EM RF OPT EM RF OPT	0.035	
EM RF OPT	0.035	
		0.43
	0.036	0.44
EM RF OPT	0.037	0.46
EM RF OPT	0.040	0.49
EM RF OPT	0.043	0.53
EM REF	0.051	0.42
EM REF	0.052	0.42
EM REF	0.054	0.44
EM REF	0.059	0.48
EM REF	0.063	0.51
EM OPT	0.041	0.42
EM OPT	0.042	0.43
EM OPT	0.044	0.45
EM OPT	0.048	0.49
EM OPT	0.051	0.52
Concepts excluding HP:		
EM RF OPT	0.023	0.43
EM RF OPT	0.024	0.44
EM RF OPT	0.025	0.46
EM RF OPT	0.026	0.49
EM RF OPT	0.028	0.53
EM REF	0.039	0.42
EM REF	0.040	0.42
EM REF	0.041	0.44
EM REF	0.045	0.48
EM REF	0.048	0.51
EM OPT	0.029	0.42
EM OPT	0.030	0.43
EM OPT	0.031	0.45
EM OPT	0.034	0.49
EM OPT	0.036	0.52

I

SAILING HOURS PER DAY



 $Figure\ I.1:\ Sailing\ hours\ per\ boat\ per\ day\ throughout\ one\ year\ (BlueBoat\ company)$

J

BATTERY PARAMETERS FOR TEMPERATURE FIT

Parameters per ambient temperature line according to an equation of the form:

 $U(T) = f \cdot e^{(g \cdot x)} + h \cdot e^{(i \cdot x)}$ (ref. 3.4.32)

-10° parameters

f = -1.13e-05

g = 0.1479

h = 12.49

i = -0.0004166

0° parameters

f0 = -2.312e-05

g0 = 0.1288

h0 = 12.76

i0 = -0.0003827

 10° parameters

f10 = -3.493e-06

g10 = 0.1349

h10 = 12.98

i10 = -0.0004344

20° parameters

f20 = -1.1e-07

g20 = 0.1693

h20 = 13.09

i20 = -0.0004567

 30° parameters

f30 = -4.422e-09

g30 = 0.199

h30 = 13.16

i30 = -0.0004308

40° parameters

f40 = -1.882e-11

g40 = 0.2517

h40 = 13.21

i40 = -0.0004376

 50° parameters

f50 = -8.535e-12

g50 = 0.2578

h50 = 13.23

i50 = -0.0003962



LIFETIME CALCULATION

Table K.1: Lifetime calculations, for LMP and LTO

LMP: Description	Data source	Variable	Value	Unit
Amount of cycles until 80% capacity remains, 0-100% DOD	Manufacturer	$n_{LC,max}$	2 800	[-]
Maximum capacity of one cycle	Manufacturer	C_{∞}	2 516	[Ah]
Total maximum life time capacity	Installed capacity	$C_{LC,100}$	7 044 800	[Ah]
Remaining life time capacity at 80%	Installed capacity	$C_{LC,80}$	5 635 840	[Ah]
Capacity decrease factor	Equation 3.4.38	f_{cap}	503	[Ah/cycle]
Used cycles	Equation 3.4.39	n_{LC}	2 332	[-]
Available capacity at this number of cycles	Equation 3.4.36	$C_{LC,max}$	5 871 125	[Ah]
Used capacity	Equations 3.4.40 and 3.4.41	Q_{LC}	5868376	[Ah]
Remaining capacity	Q_{LC} minus $C_{LC,max}$		2 748	[Ah]
Remaining capacity	Equations 3.4.35 and 3.4.42	C_{LC}	0^1	[%]
LTO:				
Description	Data source	Variable	Value	Unit
Amount of cycles until 80% capacity remains, 0-100% DOD	Manufacturer	$n_{LC,max}$	5 000	[-]
Maximum capacity of one cycle	Manufacturer	C_{∞}	6 060	[Ah]
Total maximum life time capacity	Installed capacity	$C_{LC,100}$	30 300 000	[Ah]
Remaining life time capacity at 80%	Installed capacity	$C_{LC,80}$	24 240 000	[Ah]
Capacity decrease factor	Equation 3.4.38	f_{cap}	1 212	[Ah/cycle]
Used cycles	Equation 3.4.39	n_{LC}	4 150	[-]
Available capacity at this number of cycles	Equation 3.4.36	$C_{LC,max}$	25 269 697	[Ah]
Used capacity	Equations 3.4.40 and 3.4.41	Q_{LC}	25 151 515	[Ah]
Remaining capacity	Q_{LC} minus $C_{LC,max}$, 200	118 182	[Ah]
O 1 /	LO, musi		02	

¹0% means 80% capacity left

²0% means 80% capacity left



STATIC ENERGY AND POWER CALCULATION

In the previous chapter the required auxiliary energy is calculated. Together with the results obtained from chapter 3.1, 'Resistance modelling' and Appendix G, 'Propeller optimization', a static analysis with respect to the generic operational profile can be conducted. Note that in this chapter only the reference (measured) and optimized propeller with respect to the measurements will be analysed.

L.1. BLOCKS

In Table L.1 an overview from the preceding chapters is given regarding the propeller power required at the different blocks. Combined with the time of each block during one trip of 75 [min], the energy consumption of each block can be calculated. The '+8' in the last column stands for the power of the bow thruster that will

Data [-]	Manoeuvres [kW]	Nom. speed [kW]	Med. speed [kW]	Max. speed [kW]	90° turns [kW]
Diesel reference (measured)	13.1	6.0	13.6	44.0	18.0
Diesel QRC	13.2	8.1	19.0	40.9	10.7+8
Hybrid reference (measured) ¹	12.8	10.7	14.4	30.6	16.2
Hybrid QRC	13.8	13.0	25.5	53.6	7.9+8

Table L.1: Overview of required power

be used in the turns. As can be seen from Table L.1 the QRC configurations are less energy efficient overall. This is due to the higher resistance (boat is assumed fully loaded) instead of empty.

L.1.1. Brake energy comparison

Multiplying the blocks power with the time of the block during one trip, as shown in Equation L.1 gives the static brake energy consumption of the canal boat in Table L.2.

$$E = P \cdot t \tag{L.1}$$

Where P is in [kW], t is in [hr] and E is in [kWh]. The reference cases, as can be found in chapter 2.1, 'Baseline' require for the diesel powered boat 14.5 [kWh] and for the electric powered boat 16.1 [kWh] per trip. Calculating the values for the QRC cases gives an energy value of 16.7 [kWh] for diesel and 17.7 [kWh] for the electric boat.

L.1.2. HEATING ENERGY

Including auxiliary energy usage is delicate. The result for the heat pump modelling from chapter 3.3, 'Auxiliary modelling', indicates that an electrical energy requirement of 6.1 [kW] is needed for a worst-case scenario. However, it is unlikely that this is required all-day long. Therefore, three different scenarios are applied, as described in Table L.3.

¹Assuming 0.9 motor efficiency

Table L.2: Overview of required power

Data [-]	Energy [kWh]
Diesel reference (measured)	14.5
Diesel QRC	16.7
Hybrid reference (measured)	16.1
Hybrid QRC	17.7

Table L.3: Different day scenarios for heat pump usage

Worst case winter condition	Normal winter condition	Summer condition
· Shore heating · 100% of the time heat pump at full power	· Shore heating · 100% of time heat pump at half power	· No heating · No heat pump running

Shore heating means that the heat pump is connected to the quay energy supply during the moored time between trips, hence using no power from the canal boat energy storage. The calculated time to heat the boat is around 15 [min] from 0-20° this should be possible to do before the first passengers arrive each day. Summarizing the three different scenarios with regards to energy usage and power gives Table L.4

Table L.4: Auxiliary energy usage for one trip

Condition [-]	Power [kW]	Energy [kWh]
Worst case winter	≤6.1	7.0
Normal winter	3.1	4.0
Summer	0.0	0.0

L.2. ENERGY REQUIREMENTS PER DAY

From the previous section the energy in different conditions during a steady-state standard trip was found. In this section, the energy requirements for the optimized case are calculated on a per day basis. Total energy for propulsion only, is calculated as 19.9 [kWh] per trip. From Figure I.1 in Appendix I, 'Sailing hours per day', it can be seen that 8 [hr] per day is an upper limit for the daily hours that canal boats need to sail. This upper limit in April is the busiest day for the company, so it is representative for the deployability. The required brake energy capacity can then be calculated with Equations L.2, L.3 and L.4.

$$P_{trip,avg} = \frac{E_{trip}}{t_{trip}} \tag{L.2}$$

$$E_{aux} = E_{systems} + E_{heatpump} \tag{L.3}$$

$$E_{tot,day} = (P_{trip,avg} \cdot t_{sailing,day}) + E_{aux}$$
 (L.4)

In Equation L.3 the auxiliary energy $E_{systems}$ required by the marine systems on board (camera, Automatic Identification System (AIS), lights, Public Announcement (PA) system) is rounded to 0.6 [kWh] per trip.

Energy decomposition for the various systems on board is given in Table L.6 for one sailing day (8 [hr]). Equations L.2, L.3 and L.4 are used to calculate the energy requirements per boat per day as displayed in Table L.6.

From Table L.6 it can be seen that energy usage at the propeller is around 100-110 [kWh] for diesel and electric. Including auxiliary systems and the worst case heat pump scenario the daily energy requirement goes up to about 150-160 [kWh] for both types of propulsion.

Table L.5: Overview of energy requirements for the optimized case, per trip (75 [min] sailing time)

Energy requirements per trip	Diesel	Electric	Unit
Brake energy	16.7	17.7	[kWh]
Auxiliaries, worst case winter	7.0	7.0	[kWh]
Auxiliaries, normal winter	4.0	4.0	[kWh]
Auxiliaries, summer	0.6	0.6	[kWh]

Table L.6: Overview of energy requirements for the optimized case, per day (8 [hr] sailing time)

Energy requirements per day	Diesel	Electric	Unit
Brake energy	100.2	106.2	[kWh]
Marine systems	4.8	4.8	[kWh]
Heating, worst case winter	48.6	48.6	[kWh]
Heating, normal winter	24.4	24.4	[kWh]
Heating, summer	0.0	0.0	[kWh]

L.3. VALIDATION OF ENERGY RESULTS

To see if these results are comparable to a real life situation they are compared to known data from the electric canal boat 'Vossius'. The Vossius is 20 [m] long and has a width of 4.25 [m], comparable to the analysed boat in this thesis. On board is 250 [kWh] of lead-acid batteries. According to [12] it uses around 22 [kWh] during a standard 75 [min] trip. This is without heating, as this is done by a diesel burner. The optimized propeller in this chapter is calculated to have an energy requirement of almost 18 [kWh] during one trip, see Table L.5. Note that this is the requirement at the propulsion shaft, electric losses will need to be added up to know the energy requirement at the batteries. The difference between these values can be explained by the fact that the route sailed in [98] is not known. Furthermore, the amount of traffic in the canals has a large impact on manoeuvring energy. Finally, the Vossius is a different vessel than the measured Barleaus, which could explain the difference. Nevertheless, the numbers are satisfactory in accordance.

M

GLOSSARY

LIST OF ACRONYMS

AC alternating current

ACH air changes per hour

AIS Automatic Identification System

BMS Battery Management System

C Carbon

CCR Centrale Commissie Rijnvaart

CCNR Central Commission for the Navigation of the Rhine

CFD Computational Fluid Dynamics

CI Cost Index

CMS Continuous Monitoring System

CNG Compressed Natural Gas

CO Carbon monoxide

CO₂ carbon dioxide

COP Coefficient of Performance

CRP Contra Rotating Propeller

DE direct current

DE Diesel-Electric

DOD depth of discharge

DWT Deadweight

ECA Emission Control Area

ECI Energy Conversion Index

ECTS European Credit Transfer and Accumulation System

EEDI Energy Efficiency Design Index

EFD Energy Flow Diagram

EEOI Energy Efficiency Operational Indicator

EMI Emission IndexEV Electric VehicleFP fixed propellerI Energy Index

IGBT Insulated Gate Bipolar Transistor

Energy Index
Eml Emission Index

EPA Environmental Protection Agency

EPI Environmental Performance Indicator
EPIs Environmental Performance Indicators

ES energy storage

EU European Union

FC fuel consumption

FI Fuel Index

FTE Full-time Equivalent
FPP fixed pitch propeller

GB gearbox

GHGs Greenhouse Gases

GHG Greenhouse Gas

GPS Global Positioning System

GTL Gas-to-Liquid

HE Hydraulic engine

 $\mathbf{H}_2\mathbf{O}$ Dihydrogen oxide

IMO International Maritime Organization

KPI Key Performance Indicator

KPIs Key Performance Indicators

LHV Lower Heating Value

LMP lithium metal phosphate

LNG Liquid Natural Gas

LTO lithium-titanate

MARIN Maritime Research Institute Netherlands

MARPOL International Convention for the Prevention of Pollution From Ships

MEPC Marine Environment Protection Committee

MCR Mean Continuous Rating

 N_2 Dinitrogen

NECAS NO_x Emission Control Areas

 NO_x Nitrogen oxide

O₂ Dioxygen

PA Public Announcement
PI Proportional-Integral

PID Proportional-Integral-Derivative

PLF part-load capacity
PLF part-load factor
PM Particulate Matter

PMSM Permanent Magnet Synchronous Machine

Pls Performance Indicators

PPM parts per million

PTO power take-off

QRC quadratic resistance curve

RPM revolutions per minute

SECAS Sulphur Emission Control Areas

SFC Specific Fuel Consumption

 SO_x Sulfur oxide SOC state of charge

SOD state of discharge

SPIs Shipping Performance Indexes

SPI Specific Pollutant Index

TI Transport Index

TNO Netherlands Organization for Applied Scientific Research

TSHD trailing suction hopper dredger

TU Technical University

UHC Unburned hydrocarbons

UNESCO United Nations Educational, Scientific and Cultural Organization

V2G Vehicle to Grid

ZE zero emission

176 APPENDIX M. GLOSSARY

LIST OF SYMBOLS

0	degrees	[deg]
a	constant	[-]
A	area	$[m^2]$
C	constant or scale factor	[-]
c	constant	[-]
\mathbf{c}_p	specific heat capacity	[J/kg·K]
D	diameter	[m]
d	distance	[m]
E	energy	[kWh] or [J]
E	source voltage	[V]
FC	fuel consumption	[kg]
g	gravitational acceleration	$[m/s^2]$
hr	hour	[hr]
I	current	[A]
I	inertia	$[kg \cdot m^2]$
i	gearbox ratio	[-]
J	advance ratio	[-]
K	Kelvin	[K]
L	length	[m]
LHV	lower heating value	[kJ/kg]
m	mass	[kg]
M	torque	[Nm]
ṁ	mass flow	[kg/s]
$\dot{\mathbf{m}}_f$	fuel flow	[l/hr]
n	rotational speed	[rpm]
p	amount of passengers	[-]
P	power	[kW]
P	pressure	[Pa]
P/D	pitch diameter ratio	[-]
Q	propeller open water torque	[N]
Q	heat supplied or removed	[kW] or [kJ/s]
R	resistance	[N]

\mathbf{R}^2	accuracy of fit	[-]
SFC	specific fuel consumption	[g/kWh]
T	draft	[m]
T	thrust	[N]
T	temperature	[°C] or [K]
t	time	[s] or [hr]
t	thrust deduction factor	[-]
v	speed	[m/s]
V	speed or volume	$[m/s]$ or $[m^3]$
W	weight	[t]
W	work	[kW] or [kJ/s]
w	wake fraction	[-]
w	gross weight	[N]
x	state of discharge	[-]
y	pseudo state of discharge	[-]
z	amount of propeller blades	[-]

LIST OF GREEK SYMBOLS

α	convective heat transfer coefficient	$[W/(m^2 \cdot K)]$
Δ	displacement	[t]
η	efficiency	[-]
∇	displacement volume	$[m^3]$
ρ	density	[kg/m ³]
τ	torque	[Nm]

LIST OF SUBSCRIPTS

a areaa advanceadm Admiraltyaux auxiliaryavg average

178 APPENDIX M. GLOSSARY

b brake

char characteristic

D delivered

d delivered

e effective

h hull

HP heat pump

i amount

max maximum

min minimum

nom nominal

o open water

p passenger(s)

p propulsion

R relative rotative

s ship

s shaft

t time(step)

tot total

v volume

w weight

 ${f x}$ generic term for emissions (example: NO $_x$ means NO, NO $_2$ and N $_2$ O)

BIBLIOGRAPHY

- [1] Waternet, Regeling Passagiersvervoer te water Amsterdam, Tech. Rep. (Waternet, 2013).
- [2] Amsterdamse Grachtenrondvaart, (2014), www.amsterdam.info/nl/rondvaart.
- [3] Amsterdam Hotspots, (2014), www.amsterdamhotspots.nl/architecture.html.
- [4] Amsterdam Tourist Information, (n.d.), www.worldexecutive.com/locations/europe/netherlands/amsterdam.
- [5] Seventeenth-Century Canal Ring Area of Amsterdam inside the Singelgracht, (2011), whc.unesco.org/en/list/1349.
- [6] B. Baarsma, *Het roer moet om Naar een betere marktordening van bedrijfsmatig passagiersvervoer in de Amsterdamse grachten*, Tech. Rep. (SEO Economisch onderzoek, 2012).
- [7] Zorgvuldig beleid op de Amsterdamse grachten Aanvullingen, correcties, cruciale afwegingen en noodzakelijke nuances in reactie op het SEO rapport, Tech. Rep. (Verenigde Rederijen Amsterdam, 2012).
- [8] Top 50 Dagattracties 2012, (2012), www.nbtc.nl/nl/homepage/cijfersentrends/algemene-cijfers-toerisme.htm.
- [9] Kerncijfers 2013 Gastvrijheidseconomie, (2013), www.nbtc.nl/nl/homepage/cijfersentrends/algemene-cijfers-toerisme.htm.
- [10] E. Regterschot, Inventarisatie rondvaart, (2012).
- [11] H. de Wilde and E. Weijers, *Schone rondvaart Amsterdam Een verkenning van technische en beleidsmatige mogelijkheden*, Tech. Rep. (Energy reseach Centre of the Netherlands, 2008).
- [12] R. Steensma, Elektrisch varen in de Amsterdamse rondvaart bouwsteen voor de Factsheet Elektrische Rondvaart, (2013).
- [13] Over Waternet, (2014), www.waternet.nl/over-waternet/.
- [14] Definitie van "Rondvaartboot", (2014), (Own translation).
- [15] Winter brochure rederij Lovers, (2014), www.lovers.nl/pdf/LC)WinterBrochure_100dpi.pdf.
- [16] F. Jacobs, Study of an Amsterdam canal boat, Tech. Rep. (Technical University Delft, 2014).
- [17] Kabola HR Series Manual, Kabola (2008).
- [18] H. Woud and D. Stapersma, *Design of Propulsion and Electric Power Generation Systems*, IMarEST publications (IMarEST, Institute of Marine Engineering, Science and Technology, 2002) http://books.google.nl/books?id=BzRdAAAACAAJ.
- [19] Personal visit at BlueBoat Company, (2014).
- [20] T. Molkenboer, Wetgeving van toepassing op rondvaartboten van het amsterdamse grachtentype, .
- [21] Future ship powering options exploring alternative methods of ship propulsion, Tech. Rep. (Royal academy of engineering, 2013).
- [22] W. Giles, T. Dinham-Peren, S. Amaratunga, A. Vrijdag, and R. Partridge, *The advanced waterjet: Propulsor performance and effect on ship design*, (2010).
- [23] Wartsila Waterjet Product Guide, Tech. Rep. (Wartsila, 2011).

180 Bibliography

[24] Nota varen in Amsterdam 2.1 - Beleidskader voor het varen en afmeren in en door Amsterdam, voor passagiersvervoer en pleziervaart, (2013).

- [25] http://energy.gov/energysaver/articles/furnaces-and-boilers.
- [26] A. K. Ananes, A. J. Sorensen, and T. Hackman, Essential characteristics of electrical propulsion and thruster drives in dp vessels, in Dynamic Positioning Conference (1997).
- [27] A. K. Adnanes, Maritime electrical installations and diesel electric propulsion, (2003).
- [28] F. Vignola, F. Mavromatakis, and J. Krumsick, Performance of pv inverters, .
- [29] D. Dillema, Persoonlijke correspondentie, (2014), medewerker Werf 't Joppe te Warmond.
- [30] A. Emadi, Handbook of automotive power electronics and motor drives (CRC press, 2005).
- [31] J. Dodge and T. Loder, Latest technology pt igbt vs. power mosfet, Power Electronics, Z1 (2003).
- [32] K. Mazloomi, N. B. Sulaiman, and H. Moayedi, *Electrical efficiency of electrolytic hydrogen production*. International Journal of Electrochemical Science **7** (2012).
- [33] J. Carlton, *Marine Propellers and Propulsion* (Elsevier Science, 2011) http://books.google.nl/books?id=QrLNCxzynU4C.
- [34] D. Stapersma, *Proceedings of the 34th Wegent School: Development in the Design Propulsors and Propulsion Systems, Delft June 19-23, 2000*, edited by P. de Heer, F. of Mechanical Eng., and D. U. o. T. W. Marine technology, Ship Hydrodynamics Laboratory (Delft Technical University, 2000) http://books.google.nl/books?id=-5p3nQEACAAJ.
- [35] J. Holtrop and G. Mennen, An approximate power prediction method, (1982).
- [36] J. Holtrop, *A statistical re-analysis of resistance and propulsion data*, International Shipbuilding Progress **31**, 272 (1984).
- [37] G. Kuiper, Resistance and Propulsion of Ships Technical University Delft Course MT512 (Maritime Research Institute Netherlands, 1995).
- [38] H. Lackenby, Note on the effect of shallow water on ship resistance, BSRA paper (1961).
- [39] M. Araki, *Pid control*, Control systems, robotics and automation **2**, 1 (2002).
- [40] B. Check, http://www.checkcorp.com/seat-heater/products_faqs.asp/Q11.
- [41] Installing Heat Pumps to reduce Energy Consumption, Tech. Rep. (British Waterways, n.d.).
- [42] Uitwerkingsbesluit Doorvaartprofielen (2008).
- [43] E. Silberstein, *Heat Pumps*, HVAC Series (Thomson/Delmar Learning., 2003) http://books.google.nl/books?id=c9Bnjzipj9sC.
- [44] M. Moran, H. Shapiro, D. Boettner, and M. Bailey, *Fundamentals of Engineering Thermodynamics* (Wiley, 2010) http://books.google.nl/books?id=IVPRngEACAAJ.
- [45] D. E. Watkins, *Heating services in buildings* (John Wiley & Sons, 2011).
- [46] A. Hepbasli and Y. Kalinci, *A review of heat pump water heating systems*, Renewable and Sustainable Energy Reviews **13**, 1211 (2009).
- [47] *Heating and Cooling With a Heat Pump*, Tech. Rep. (Natural Resources Canada's Office of Energy Efficiency EnerGuide, 2014).
- [48] D. Jenkins, R. Tucker, M. Ahadzi, and R. Rawlings, *The performance of air-source heat pumps in current and future offices*, Energy and Buildings **40**, 1901 (2008).

BIBLIOGRAPHY 181

[49] H. Henderson, Y. J. Huang, and D. Parker, *Residential equipment part-load curves for use in DOE-2*, LBL Report **42145** (1999).

- [50] A. Handbook, Fundamentals, American Society of Heating, Refrigerating and Air Conditioning Engineers, Atlanta 111 (2001).
- [51] F. P. Incropera, Fundamentals of heat and mass transfer (John Wiley & Sons, 2011).
- [52] G. Pistoia, Lithium-ion Batteries: Advances and Applications (Newnes, 2013).
- [53] J. McDowall, Understanding lithium-ion technology, Battcon, Marco Island, FL, 1 (2008).
- [54] *Valence u27-12xp*, Accessed 01-11-14.
- [55] D. Stapersma, *Theory and model for battery charging and discharging*, Tech. Rep. No. KIM-PFS-98-124 (Royal Netherlands Navel College, 2000).
- [56] E. Versluijs, *Realization and reduction of a dynamic model of a hybrid diesel fuel PEMFC system*, Master's thesis, Delft University of Technology (2010).
- [57] E. van Deursen, *Development of an alternative energy management strategy for controlling hybrid ship drive systems*, Master's thesis, Delft University of Technology (2011).
- [58] D. Linden and T. Reddy, *Handbook Of Batteries*, McGraw-Hill handbooks (McGraw-Hill Education, 2001) http://books.google.nl/books?id=XquySsZp5jsC.
- [59] M. Majima, S. Ujiie, E. Yagasaki, K. Koyama, and S. Inazawa, *Development of long life lithium ion battery for power storage*, Journal of Power Sources **101**, 53 (2001).
- [60] G. Gabrielli and T. von Karman, *What price speed?: specific power required for propulsion of vehicles*, American Society of Mechanical Engineers **72**, 775 (1950).
- [61] R. van de Ketterij, D. Stapersma, H. Kramers, and L. Verheijen, *CO2 Index: Matching the dredging industries needs with IMO legislation*, Ceda dredging days 2009 dredging tools for the future, 1 (2009).
- [62] D. Stapersma and H. Grimmelius, *Trends in propulsion and how they affect environmental sustainability*, (ENSUS, 2002).
- [63] L. Adamson, Mandatory energy efficiency measures for international shipping adopted at IMO environment meeting, (2011), http://www.imo.org/MediaCentre/PressBriefings/Pages/42-mepc-ghg.aspx.
- [64] W. Duursema, M. Verhulst, and J. J. Nieuwenhuis, *A study on a fairer inclusion of small General cargo ships and small Containerships within the EEDI regulatory framework,* (2012).
- [65] Resolution MEPC.203(62), (2011).
- [66] J. Devanney and S. Beach, *EEDI–A Case Study in Indirect Regulation of CO2 Pollution*, Center for Tankship Excellence, Version 1 (2010).
- [67] J. Devanney, EEDI absurdities, Center for Tankship Excellence, USA (2011).
- [68] D. Anink and M. Krikke, *Analysis of the effect of the new EEDI requirements on Dutch build and flagged ships*, Tech. Rep. (Centre for Maritime Technology and Innovation, 2011).
- [69] T. Mundt and M. Kopke, MEPC 62: Energy Efficiency Design Index adopted, Ship & Offshore No. 5 (2011).
- [70] S. Sala, Energy Efficiency and the Shipping Industry, Tech. Rep. (Deltamarin, 2010).
- [71] Ø. Buhaug, J. Corbett, Ø. Endresen, V. Eyring, J. Faber, S. Hanayama, D. Lee, D. Lee, H. Lindstad, A. Markowska, *et al.*, *Second imo ghg study 2009*, International Maritime Organization (IMO) London, UK **20** (2009).
- [72] P. Zachariadis, EEDI explained, Tech. Rep. (Society of Naval Architects and Marine Engineers, 2011).

182 Bibliography

- [73] Resolution MEPC.212(63), (2011).
- [74] Guidelines for the voluntary use of the ship Energy Efficient Operational Indicator (EEOI), MEPC.1/Circ.684 (IMO, 2009).
- [75] The Shipping KPI System V2.2, (2013).
- [76] C. Kontovas and H. Psaraftis, An Online Ship Emissions Calculator as a Decision making Aid and Policy Evaluation Tool. in 13th Congress of Intl. Maritime Assoc. of Mediterranean IMAM (2009) pp. 12–15.
- [77] KPI005: CO2 efficiency, (n.d.), https://www.shipping-kpi.org/book/definition/KPI005.
- [78] Resolution mepc.177(58): Amendments to the technical code on control of emission of nitrogen oxides from marine diesel engines, (2008).
- [79] W. Shi, D. Stapersma, and H. T. Grimmelius, *Comparison study on moving and transportation performance of transportation modes*, International Journal of Energy and Environment **2**, 179 (2008).
- [80] K. Nakahara, R. Nakajima, T. Matsushima, and H. Majima, *Preparation of particulate li-ti having excellent characteristics as an electrode active material for power storage cells*, Journal of Power Sources 117, 131 (2003).
- [81] O. Ito, Emissions from coal fired power generation, (2011).
- [82] C. Botsford and A. Szczepanek, Fast charging vs. slow charging: Pros and cons for the new age of electric vehicles, in International Battery Hybrid Fuel Cell Electric Vehicle Symposium (2009).
- [83] M. Yilmaz and P. T. Krein, Review of charging power levels and infrastructure for plug-in electric and hybrid vehicles, in Electric Vehicle Conference (IEVC), 2012 IEEE International (IEEE, 2012) pp. 1–8.
- [84] Feiten en cijfers over gvb amsterdam, http://over.gvb.nl/feiten-en-cijfers-0.
- [85] S. Habib, M. Kamran, and U. Rashid, *Impact analysis of vehicle-to-grid technology and charging strate-gies of electric vehicles on distribution networks: A review,* Journal of Power Sources **277**, 205 (2015), http://www.sciencedirect.com/science/article/pii/S0378775314020370.
- [86] A. H. Foosnaes, A. N. Jensen, and N. C. Nordentoft, *Report: Case studies of grid impact of fast charging*, Tech. Rep. (EDISON Consortium, 2011).
- [87] Aardgas en elektriciteit, gemiddelde prijzen van eindgebruikers, (2014), http://statline.cbs.nl/StatWeb/publication/?VW=T&DM=SLNL&PA=81309NED&D1=1,3,5,8,11,15&D2=0&D3=1&D4=0-3,5,10-13,15-18,20-23,1&HD=120813-1059&HDR=T&STB=G2,G1,G3.
- [88] P. N. O. G. A. S. Steffen Lind Kristensen, Anders Foosnaes, *Concept study on fast charging station design*, Tech. Rep. (EDISON Consortium, 2011).
- [89] B. Epps, J. Chalfant, R. Kimball, A. Techet, K. Flood, and C. Chryssostomidis, *OpenProp: An open-source parametric design and analysis tool for propellers*, in *Proceedings of the 2009 Grand Challenges in Modeling & Simulation Conference* (Society for Modeling & Simulation International, 2009) pp. 104–111.
- [90] B. Epps and R. Kimball, *Unified Rotor Lifting Line Theory*, Journal of Ship Research 57, 1 (2013).
- [91] B. Epps, OpenProp v2.4 theory document, (2010).
- [92] B. Epps and R. Kimball, OpenProp v3: Open-source software for the design and analysis of marine propellers and horizontal-axis turbines, (2013), http://engineering.dartmouth.edu/epps/openprop.
- [93] O. Levander, Concepts for shipping scenarios 2030, (2010).
- [94] Voith Schneider Propeller Types and Dimensions, (2011).
- [95] E. Rotteveel, *Investigation of inland ship resistance, propulsion and manoeuvring using literature study and potential flow calculations,* (2013).

BIBLIOGRAPHY 183

[96] M. Cornelissen, *Voorspellen van het manoeuvreergedrag van binnenvaartschepen*, Master's thesis, Technical University Delft (2001).

- [97] A. Papanikolaou, *Hydrodynamische Koeffizienten für die linearen Schwingungen von schwimmenden Zylindern* (Techn. Univ., Inst. für Schiffstechnik, Fachgebiet Schiffsentwurf, 1979).
- [98] R. Steensma, Elektrisch varen in de Amsterdamse rondvaart, (2013).

LIST OF FIGURES

1.2.1 Thesis chapters overview	7
1.3.1 Aerial photograph of the Amsterdam canals (Roger Wollstadt, public license)	
1.3.3 Typical canal boat (Tripadvisor.com)	0
2.1.1 Linesplan of a harbour tourist boat	4
2.2.1 Fixed propeller, schematic view	
2.2.2 Energy Flow Diagram of the measured diesel hydraulic vessel	
2.2.3 Pod with four blade propeller under a canal boat	
2.2.4 Energy Flow Diagram of the measured pod/hybrid vessel	
2.2.6 Discrete time and distance distributions	
2.2.7 Energy distributions	
2.2.8 Possible sailing passages in the city centre	
2.3.1 CRP lay out (Wärtsila)	5
2.3.2 Propulsion efficiencies, including waterjets (Boatdesign.net)	
2.3.3 Systems comparison between battery and fuel cell (Mux, Tweakblogs.net)	
2.4.1 Schematic view of concepts, EM RF OPT, EM OPT and EM REF respectively	1
2.4.2 Overview of concepts	
2.4.3 Energy Flow Diagram of the reference diesel boat	2
2.4.4 Energy Flow Diagram of EM RF OPT	
2.4.5 Energy Flow Diagram of EM REF and EM OPT	3
3.1.1 Measured resistance of the diesel/FP canal boat	8
3.1.2 Method of acquiring the quadratic resistance curve	9
$3.1.3 Calculated \ cubic \ propeller \ law \ curve \ for \ the \ quadratic \ resistance \ line \ of \ Figure \ 3.1.2 \ \dots \ . \ . \ . \ 40.0000000000000000000000$	
3.1.4 Measured resistance according to Holtrop and Mennen method	
3.1.5 Resistance for a fully loaded canal boat according to displacement method	
3.1.6 Resulting ship resistance and power curves for a fully loaded hybrid and diesel canal boat 43 3.1.7 Integration of the models	
3.2.1 Model overview	
3.2.2 Ship, motor and propeller modelling	
3.2.4Torque - rpm - efficiency contour plot	
3.2.5 Acceleration comparisons for different ship inertia values	
3.3.1 Model overview	1
3.3.2 Air source heat pump operating principle	3
3.3.3 Part-load empirical efficiency curve for typical heat pumps ([48, 49])	3
3.3.4 Schematic view of the modelled canal boat passenger compartment	
3.3.5 Schematic view of the input and output streams of the model	
3.3.6 Minimum required electric power for different environmental temperatures	6
3.3.7Temperature of the boat, starting at 273 [K] and the heat pump is shut off at 293 [K] for lower energy consumption	6
3 3 8COP values for different environmental temperatures	

186 List of Figures

3.3.9 Time required to heat the boat to 20°C with 6.1 [kW] electric power	. 57
3.4.1 Model overview	. 59
3.4.2 Main components of lithium battery cell (shown ion flows indicate discharging)	
3.4.3 Electrochemical operation of a cell (left: discharge, right: charge) [52]	
3.4.4Battery model macro overview	
3.4.5 Battery model overview	
$3.4.6C_t$ as function of I_{in}	
3.4.7 Resistance as a function of pseudo-discharge state y	
3.4.8 Modelled capacity curves for different C values	
3.4.9 Temperature discharge curves from the manufacturer, as function of capacity and voltage	
3.4.1 Valence and modelled discharge curves for different temperatures	
3.4.1 Modelled capacity curves for different temperature values compared to Equation 3.4.32	
3.4.1 Zemperature discharge curves from the model, dependent on C rate and temperature	
3.4.1 Capacity decrease with respect to applied cycles (Source: Valence)	
3.4.1 Difference factors σ	
3.4.1 Modelled and Valence data for pseudo-discharge state y	
3.4.1 Different curves of Valence, the presented model and the model by Van Deursen compared	
3.4.1 Charge curve comparison between model and Valence	
3.4.1 8) ifference between 0.1, 0.5 and 1C at 23°C	
3.4.1 Modelled curves compared to data from Leclanché	
3.4.2@nternal battery efficiency during discharging and charging for a typical LTO and LMP simulatio	
3.4.2 Visualisation of battery cycle losses during discharging and charging	
	0.5
3.5.1 Definition of system boundary A (upper) and B (lower)	
3.5.2 Definition of different energy flows and efficiencies	. 86
4.1.1 Model overview	. 91
4.1.2 Speed profile used for simulations	
4.1.3 Randomized daily operational profile	
4.1.4 Diesel simulation tree	. 94
4.1.5 Electric concepts simulation methodology tree	
4.2.1 Brake power for the concepts	
4.2.2 Open water efficiency for the electric concepts	
4.2.3 Efficiency of electric motors for the electric concepts	
4.2.4 Energy usage of the electric configurations	
4.2.5 Acceleration from 2.0 to 2.5 [m/s]	. 99
4.3.1 Definition of different energy names	103
4.3.2 Diesel brake power	
4.3.3 Ship speeds obtained during simulation	
4.3.4 Diesel energy conversion efficiency	
$4.3.5 \text{NO}_x$ emission during full day	
4.3.6 Energy results from full day simulation, no charging, full heat pump	
4.3.7 Storage size required per day when only overnight charging and 20% buffer size	
4.3.8Open water efficiency of the concepts	
4.3.9 Required discharge energy from battery for battery types with 1/2 of maximum charging C	
4.3.1 Comparison of battery energy for different charging C rates, for the EM RF OPT concept	
4.3.1 Electric motor efficiency of the concepts	
4.3.1 Breakdown of efficiencies and total chain conversion efficiency during one trip	
4.3.1 Charging strategy for LTO batteries	
4.3.1 Relative difference of the electric configurations (averaged) compared to the diesel (=1) situation	
4.3.1\(\mathbb{E}\) nergy Flow Diagram of the chosen configuration	
4.4.1 Variation study in battery pack initial parameters (cost and lifetime), not including other equipment and/or installation costs	
mem anu/ui iiistaliatiuii custs	. 119

LIST OF FIGURES 187

	2 Typical voltage levels obtained from simulation	
5.2.2 5.2.3 5.2.4	Schematic view of concepts, EM RF OPT, EM OPT and EM REF respectively 2 Schematic view of the input and output streams of the model	131 131 132 132
	Typical AC conversion EFD	
	Typical DC conversion EFD	
C.1	Torque - rpm - efficiency contour plot	143
F.1	Water temperature in Amsterdam between 1990-2010)	149
G.1	Difference between calculated cubic propeller law curve and the optimized cubic propeller law curve	155
G.2	Open water diagrams for the diesel boat	
	Schematic lay out of data and simulation methodology	
	Linesplan of a harbour tourist boat	
	Schematic overview of the 90° turn (scaled)	
	Open water diagrams for the hybrid boat	
I.1	Sailing hours per boat per day throughout one year (BlueBoat company)	163

LIST OF TABLES

1.1.1 Emission regulations according to Waternet [1]	3
2.2.1 Main specifications of the measured boats	16
2.2.2Measured average brake power requirements per block	
2.2.3 Blocks for the route	
2.2.4 Simplified generic operational profile	
2.2.5 Validation of blocks method	
2.2.0 validation of blocks inclined	
2.3.1 Battery types and specifics	28
2.3.2List of functional requirements	
•	
2.4.1 Typical canal boat specifications	32
2.4.2 Overview of concepts	33
3.1.1 Baseline propeller data at nominal speed for an <i>partially loaded</i> canal boat	
3.1.2 Required performance from the propeller, for a fully loaded canal boat	
3.1.3 Calculated data for point of maximum operation	43
3.3.1 Heated seats cost and energy breakdown, worst case scenario	
3.3.2 Overview of modelled segments of the canal boat	
3.3.3 Comparison between the two models	57
3.4.1 Battery overview, values from manufacturer	59
3.4.2 Battery pack data from Valence	
3.4.3 Specific capacities at different c levels	
3.4.4 Calculation example for the Valence battery and 2000 out of 2800 used cycles	
3.4.5 Calculated values and coefficients for LMP battery calculation	
3.4.6 Battery data from Leclanché	
·	
3.4.7 Calculated values and coefficients for LTO battery calculation	
3.4.8 Daily averaged <i>internal</i> battery efficiency	79
4.1.1 Speed profile	92
4.1.2Simplified generic operational profile	
4.1.3 Values used for benefit for society calculation	
4.1.4 Sailing schedule for one day	
4.3.1 Overview of baseline and simulation results per trip, and required energy storage per day	102
4.3.2 Mean value in [g/kWh] emission and fuel results for the diesel daily simulation $\dots \dots \dots$	
4.3.3 One trip energy breakdown for concepts	105
4.3.4 Energy breakdown for the worst case, with heat pump, during the day	105
4.3.5 Overview of required energy	
4.3.6 Size of energy storage (rounded), LMP	109
4.3.7LTO (rounded)	
4.3.8 Mean chain efficiencies for the three methods of energy storage, excluding mooring	
4.3.9 Fuel and emission indices for the diesel baseline	
4.3.1 Minimum mean emission values for land-based power plants	
4.3.1 Emission values for a coal power plant	
4.3.1 % ailing hours	
4.3.1 Requirements, minimal requirements based on measurements and analysis, and used values in	110
the simulations and calculations. LTO 42 [kWh] pack	116

190 List of Tables

	Battery price and cycle variations
5.2.1	Cost and pack lifetime
D.1	Overview of parametric optimization parameters
	Explanation of numbers
G.2	Overview of used propeller nomenclature
G.4 G.5 G.6	Power reductions at nominal speed for optimized propeller compared to the reference propeller 152 Optimization of η_0 as calculated with Propeller Performance, QRC, maximum speed 3.6 [m/s] . 153 Optimization of η_0 as calculated with Propeller Performance, MRC, maximum speed 3.6 [m/s] . 153 η_0 and power reductions at nominal speed for optimized propeller compared to the reference
G.8 G.9	propeller
G.11 G.12	Optimization of η_o as calculated with Propeller Performance, manoeuvring, QRC, speed 1.0 [m/s] 154 Deptimization of η_o as calculated with Propeller Performance, manoeuvring, MRC, speed 1.0 [m/s] 154 Simplified hull sections
G.15	Measurement and SurSim validation results turn #2
H.1	ECI and minimum efficiencies for the simulations
K.1	Lifetime calculations, for LMP and LTO
L.2 L.3	Overview of required power
L.5	Overview of energy requirements for the optimized case, per trip (75 [min] sailing time) 171 Overview of energy requirements for the optimized case, per day (8 [hr] sailing time) 171